TECHNISCHE
UNIVERSITÄT
DARMSTADT

LIGHTWEIGHT INTRUSION DETECTION IN WIRELESS SENSOR NETWORKS

Am Fachbereich Informatik
der Technischen Universität Darmstadt
zur Erlangung des akademischen Grades eines
Doktor-Ingenieurs (Dr.-Ing.)
genehmigte Dissertationsschrift

von

DIPL.-WIRT.-INF. MICHAEL RIECKER

Geboren am 26. März 1982 in Heilbronn, Deutschland

Erstreferent: Prof. Dr.-Ing. Matthias Hollick

Korreferent: Prof. Dr.-Ing. Felix Freiling

Tag der Einreichung: 11. Mai 2015
Tag der Disputation: 22. Juni 2015

Darmstadt, 2015
Hochschulkennziffer D17

ABSTRACT

Wireless sensor networks have become a mature technology. They are increasingly being used in different practical applications. Examples include the monitoring of industrial environments and light adaptation in tunnels. For such applications, attacks are a serious concern. A disrupted sensor network may not only have a financial impact, but could also be safety-critical. Hence, the availability of a wireless sensor network is our key protection goal in this thesis. A special challenge lies in the fact, that sensor nodes typically are physically unprotected. Hence, insider attacks are supposed to occur, e.g., by compromising the nodes and getting in possession of the cryptographic keys, thereby becoming a legitimate member of the network. As a result, mechanisms to detect attacks during operation are necessary.

Traditionally, intrusion detection systems are used to discover network anomalies. Due to severe resource-restrictions, building such a system for wireless sensor networks is challenging; it has to be small in size. Therefore, it is important to reduce the required information for intrusion detection. The majority of these systems designed for wireless sensor networks is working decentralized, i.e., the nodes try to detect the attacks locally, mostly by using some type of collaboration with other nodes. So far, the real-world effects of attacks on wireless sensor networks have not yet been studied widely. Consequently, state-of-the-art intrusion detection systems often need to analyze a large number of metrics for attack detection. The execution frequency of the detection algorithm is mainly periodic or constant. Another problem that needs further research, is the possibility of reducing the detection frequency. We also investigate the feasibility of performing intrusion detection without collaboration, in order to enable the lightweight detection of denial-of-service attacks on wireless sensor networks.

To overcome these shortcomings, in this work we conduct systematic measurements in a real testbed in order to quantify the impact of denial-of-service attacks. This allows us to identify those metrics, which are significantly influenced by an attack, and thus are appropriate for attack detection. We present a fully localized intrusion detection system, in which the nodes do not have to collaborate with each other. Based on these results we propose two architectures, allowing the randomization of the detection frequency. The advantage here is, that an adversary may not predict well in advance, which node is responsible to perform intrusion detection at a certain point in time.

The gathered data from the extensive measurements is analyzed with statistical approaches. The presented intrusion detection systems are evaluated in simulations and prototypical implementations.

ZUSAMMENFASSUNG

Drahtlose Sensornetze werden zunehmend zur Unterstützung von unterschiedlichen, praktischen Anwendungen eingesetzt. Die Einsatzgebiete in der realen Welt, in denen drahtlose Sensornetze eine wichtige Rolle spielen, umfassen beispielsweise die Überwachung von industriellen Anlagen und die Lichtsteuerung in Tunnels. Für diese beispielhaften Anwendungen stellen Angriffe eine große Gefahr dar. Das Ausfallen des Sensornetzes kann neben finanziellen auch sicherheitskritische Auswirkungen haben. Daher ist das wichtigste Schutzziel in dieser Arbeit die Verfügbarkeit des drahtlosen Sensornetzes. Eine besondere Herausforderung beim Gewährleisten der Sicherheit ist durch die oftmals freie Zugänglichkeit zu den Sensorknoten gegeben. Daraus ergibt sich, dass von Insider-Angriffen ausgegangen werden muss, welche z.B. durch Kompromittierung der Knoten im Besitz gültiger kryptographischer Schlüssel und somit legitimer Teil des Netzes sind. Aus diesem Grunde sind Mechanismen zum Erkennen von Angriffen auf das Sensornetz während des laufenden Betriebs nötig.

Traditionell werden Angriffserkennungssysteme zum Aufdecken von Netzwerkanomalien eingesetzt. Aufgrund der starken Ressourcenbeschränkungen ist der Entwurf eines solchen Systems für drahtlose Sensornetze besonders herausfordernd; der Speicherbedarf muss klein sein. Deshalb ist es wichtig, die benötigten Informationen zur Angriffserkennung zu reduzieren. Die überwiegende Mehrheit dieser Systeme für drahtlose Sensornetze arbeitet dezentral, d.h. die Knoten versuchen die Angriffe lokal zu erkennen, wofür meistens eine Form von Kooperation mit anderen Knoten notwendig ist. Bisher wurden die realen Auswirkungen von Angriffen auf Sensornetze unzureichend untersucht, weshalb oft eine Vielzahl an Metriken zur Angriffserkennung herangezogen werden muss. Die Ausführungshäufigkeit des Erkennungsalgorithmus ist vorwiegend periodisch oder konstant. Ebenso lückenhaft erforscht ist die Möglichkeit zur Reduzierung der Ausführungshäufigkeit. Des Weiteren untersuchen wir, ob die Angriffserkennung ohne Kooperation mit anderen Knoten möglich ist, um Angriffe auf die Verfügbarkeit von drahtlosen Sensornetzen leichtgewichtig zu entdecken.

Um diese Lücken zu schließen, werden in dieser Arbeit systematische Messungen in einem realen Testbed durchgeführt, um die Auswirkungen von Angriffen auf die Verfügbarkeit zu quantifizieren. Daraus resultieren Erkenntnisse, welche Metriken besonders von einem Angriff beeinflusst werden und sich somit gut zur Angriffserkennung eignen. Wir stellen ein gänzlich lokal arbeitendes Angriffserkennungssystem vor, das ohne Kooperation mit anderen Knoten auskommt. Aufbauend auf den erhaltenen Ergebnissen werden zwei Architekturen vorgeschlagen, welche die Ausführungshäufigkeit des Angriffserkennnungsmechanismus randomisieren. Dadurch ist es für einen Angreifer schwerer vorherzusehen, welcher Knoten zu welchem Zeitpunkt Angriffe erkennen soll.

Die gewonnenen Daten aus den umfangreichen Messungen werden mittels statistischer Verfahren untersucht. Die vorgestellten Angriffserkennungssysteme werden in Simulationen und prototypischen Implementierungen evaluiert.

ACKNOWLEDGMENTS

First of all, I would like to thank Prof. Matthias Hollick for giving me the opportunity to work in his group. Without his constant support, this thesis would not have been possible. I also thank Prof. Felix Freiling for being my co-referee and for having motivated me to do research in IT security. Additionally, I would like to thank Prof. Stefan Katzenbeisser, Prof. Alejandro Buchmann, and Prof. Max Mühlhäuser for their contributions as members of my committee.

I would like to express my gratitude for the support to all the people I have worked with, especially Dingwen Yuan, Sebastian Biedermann, Rachid El Bansarkhani, and Sascha Hauke. I also want to thank my students for the productive cooperation, and our sometimes very long discussions. Thanks to my past and present colleagues at the *Secure Mobile Networking Lab* as well as the *Center for Advanced Security Research Darmstadt*, it was a pleasure to work with you!

Finally, I would like to thank my wife Daria, my family and friends for believing in me.

Darmstadt, 2015 Michael

CONTENTS

LIST OF TABLES

PREVIOUSLY PUBLISHED MATERIAL

Various material is included in this thesis, which has previously been published in peer-reviewed conferences and journals, but also in technical reports. To meet the regulations of the Computer Science department at TU Darmstadt, in what follows we list the chapters that include verbatim fragments from these publications.

Chapters 2 and 3 build upon "A Survey on Intrusion Detection in Wireless Sensor Networks" by Michael Riecker and Matthias Hollick. In *Technical Report, TU Darmstadt*, 2011.

Chapter 4 builds upon "Measuring the Impact of Denial-of-Service Attacks on Wireless Sensor Networks" by Michael Riecker, Daniel Thies and Matthias Hollick. In *Proceedings of the 39th IEEE Conference on Local Computer Networks (LCN)*, 2014. Besides, it contains data obtained in a Master's thesis [Alm15], out of which a technical report has been published [RAH15]. Additional data has been obtained in another Master's thesis [Thi12], and in a Bachelor's thesis [Ban14].

Chapter 5 builds upon "Patrolling Wireless Sensor Networks: Randomized Intrusion Detection" by Michael Riecker, Dingwen Yuan, Rachid El Bansarkhani and Matthias Hollick. In *Proceedings of the 10th ACM International Symposium on QoS and Security for Wireless and Mobile Networks (Q2SWinet)*, 2014.

Chapter 6 builds upon "Lightweight Energy Consumption Based Intrusion Detection System for Wireless Sensor Networks" by Michael Riecker, Sebastian Biedermann and Matthias Hollick. In *Proceedings of the 28th ACM Symposium On Applied Computing (SAC)*, 2013. An extended version has been published in the *International Journal of Information Security, Volume 14, Issue 2, pages 155–167*, 2015.

1 INTRODUCTION

> Well begun is half done.
>
> Aristotle

1.1 MOTIVATION

In the early 1990's, Mark Weiser introduced a vision called ubiquitous computing, a vision of how we will live and interact with future computing environments [Wei91]. He believed that computers would become almost invisible in use and envisioned the installation of hundreds of wireless computing devices per person. A clear trend in computing is observable: a decrease in size is accompanied by an increase in the number of devices. At the beginning of the computing era, there was one computer, a mainframe, for many people. Later there was one computer, a so-called personal computer, for everyone. Currently, we see that everyone uses *multiple* computing devices, such as tablets, mobile phones, and notebooks. This development has been made possible by the invention of small, lightweight, cheap, and mobile processors that are used (1) in everyday objects (embedded computing [Wol12]), (2) on the human body (wearable computing [Man97]), and (3) embedded in the environment (ambient intelligence [RAS08]). We also notice a shift in networking paradigms. Recently, smart things form networks, an example being wireless sensor networks. These networks bridge the gap between the real and the physical world by monitoring the environment with a variety of sensors, such as temperature, humidity, speed, etc. Hence, they show a context-sensitive behavior and are able to remember pertinent events since they have a memory. The single devices communicate over the wireless channel. According to Marc Langheinrich [Lan05], one of the important drivers for ubiquitous computing is Moore's Law, which states that the processing speed and storage capacity double every 18 months. However, Moore's Law does not apply to batteries. The capacity of a battery hardly increased over the past 30 years. Since wireless sensor nodes are typically battery-powered, energy consumption is a critical issue in all WSN applications.

Wireless sensor networks have become a technology, that may have a significant business impact over the next five years [Pre14]. The sensor nodes are envisioned to be connected in the Internet of Things [AIM10], allowing new business opportunities, even though many future applications are still unclear. According to Gartner's forecast [Pre14], the number of sensors will increase dramatically to more than 26 billion units by 2020. The year 2014 has already been labelled "The Year of the Sensor" [Pre14].

From tracking industrial operations such as leakage detection and pipe pressure measurement [SBR10] to determining the occupancy and sleep patterns in a home with the intention to reduce the energy consumption needed for heating, ventilation and cooling [LSS+10], there is a wide range of real-life applications in which WSNs

play an important role. Guaranteeing security in such prominent applications is an issue.

Apart from attacks on the integrity and confidentiality of data, we also have to defend against threats to the availability of the WSN, such as denial-of-service (DoS) attacks. Wireless sensor networks are especially susceptible to denial-of-service attacks due to the resource-constrained nature of sensor nodes. In this thesis, the availability is our key protection goal. Most of the security solutions proposed rely on cryptography, for instance, when securing the routing protocol and providing data confidentiality. Cryptography helps to provide a first level of security. However, often an attacker has physical access to a node and can obtain the key material, thereby becoming a legitimate member of the network. As a result, a WSN must be able to detect insider attacks, which is difficult without an intrusion detection system (IDS). Building such a system is challenging, given the characteristics of wireless sensor nodes with low processing power and a small amount of storage. Since an IDS must run together with the regular application, it has to be small in size. Therefore, it is crucial to reduce the required information for intrusion detection to the most useful one. Additionally, the operation of the IDS ideally is limited and not performed continuously or periodically. The main advantage is that an attacker cannot know well in advance, which node in which part of the network will perform attack detection.

1.2 GOALS

As highlighted in our survey on intrusion detection in wireless sensor networks in Chapter 3, the practical effects of denial-of-service attacks have not yet been studied widely. As a consequence, the decision on which features are relevant for intrusion detection is rather arbitrary. Most existing solutions rely on different features without proper reasoning. Furthermore, the current state-of-the-art intrusion detection systems are still resource-intensive. They typically require (1) to install an IDS on the nodes permanently, (2) to constantly perform intrusion detection possibly analyzing a large number of metrics, and (3) to collaborate with other nodes in order to identify an attack.

To overcome these shortcomings, the key objective of this thesis is to investigate the effects of denial-of-service attacks and to design lightweight IDSs based on the obtained results, reducing the load of the nodes. In particular, the following goals are addressed in this thesis:

- To develop a systematic approach for measuring the impact of denial-of-service attacks
- To show the feasibility of building lightweight IDSs for sensor networks
- To evaluate the designed systems with respect to common metrics

1.3 CONTRIBUTIONS

With the aim to overcome the identified shortcomings, the contributions we have made aligned to our research goals can can be summarized as follows.

1.3.1 *Measuring the Impact of Denial-of-Service Attacks*

We follow a systematic approach to analyze the impact of denial-of-service attacks on the network behavior; therefore, we first identify a large number of metrics easily obtained and calculated without incurring too much overhead. Next, we statistically test these metrics to assess whether they exhibit significantly different values under attack when compared to those of the baseline operation. The metrics look into different aspects of the nodes and the network, for example, microcontroller and radio activities, network traffic statistics, and routing related information. Then, to show the applicability of the metrics to different WSNs, we vary several parameters, such as traffic intensity and transmission power. We consider the most common topologies in wireless sensor networks such as central data collection and meshed multi-hop networks by using the collection tree and the mesh protocol. Finally, the metrics are grouped according to their capability of distinction into different classes. In this work, we focus on jamming and blackhole attacks. Our experiments reveal that certain metrics are able to detect a jamming attack on all nodes in the testbed, irrespective of the parameter combination, and at the highest significance value. This knowledge allows us to build intrusion detection systems, that only focus on the most useful features for attack detection. After having obtained these initial results, we study the combination of several metrics with regard to intrusion detection, applying a logistic regression. The created regression models are then used to implement a fully localized intrusion detection system requiring no collaboration, showing that the models can be generalized to different networks.

1.3.2 *Token-based Intrusion Detection*

Due to the resource-constraints of the nodes, it is desirable to reduce the tasks of each node to a minimum. We claim that even critical security functions such as intrusion detection can be performed by means of randomizing the detection frequency with the goal of making it more lightweight. To this end, we present Patrol, a system which distributes the load caused by various tasks across the network. Patrol makes use of tokens that are exchanged between nodes and activate a certain functionality, such as intrusion detection, temporarily. As a proof-of-concept, we design and implement within Patrol a lightweight intrusion detection algorithm based on the energy consumption of the nodes. We show that by analyzing the energy consumption, flooding attacks can be detected reliably. To illustrate these facts, we use a real-world testbed consisting of the widely-employed TelosB nodes.

1.3.3 *Mobile Agent-based Intrusion Detection*

Similar to Patrol, we again strive to randomize the detection frequency. However, in the system presented now we send the whole IDS routine through the network. In particular, we propose a lightweight, energy-efficient system which makes use of mobile agents to detect intrusions based on the energy consumption of the sensor nodes as a metric. A linear regression model is applied to predict the energy consumption. Simulation results indicate that denial-of-service attacks such as flooding

and blackhole can be detected with high accuracy, while keeping the number of false-positives very low.

1.4 OUTLINE

The remainder of this thesis is structured as follows:

Chapter 2 "*Foundations*" presents a detailed introduction to wireless sensor networks. We specially cover security aspects and discuss challenges in guaranteeing security.

Chapter 3 "*Related Work*" summarizes related work to the fields of performance monitoring and intrusion detection in wireless sensor networks. Besides, the shortcomings of existing approaches are portrayed. We also reformulate the identified shortcomings into research questions, that we are going to address throughout this thesis.

Chapter 4 "*Measuring the Impact of Denial-of-Service Attacks*" describes a systematic way to analyze the real-world effects of attacks and presents the results we obtained through our evaluation. Futhermore, we design a fully localized intrusion detection system.

Chapter 5 "*Token-based Intrusion Detection*" introduces an intrusion detection system that makes use of tokens instructing the nodes to activate a specified functionality.

Chapter 6 "*Mobile Agent-based Intrusion Detection*" complements the randomized intrusion detection systems proposed within this thesis by applying mobile agents that transfer themselves and the audit data from node to node.

Chapter 7 "*Conclusions and Outlook*" gives the conclusion to this thesis, summarizing our contributions and discussing possible future work.

2 FOUNDATIONS

> Start where you are. Use what you have.
> Do what you can.
>
> A. Ashe

This chapter presents an introduction to wireless sensor networks, the hardware and application scenarios in Section 2.1. Next, Section 2.2 is devoted to discussing security in wireless sensor networks. In particular, we present common adversaries and attacks that we typically have to defend against.

2.1 WIRELESS SENSOR NETWORKS

Typically, wireless networks are based on infrastructure, such as GSM, UMTS, etc. But what if no infrastructure is available or if it is too expensive to set up? In these cases, the solution is to use wireless ad hoc networks [Toh02]. They establish a network without any infrastructure, solely using networking abilities of the devices. The challenges associated with ad hoc networks are, among others, the lack of central organization, the limited range of wireless communication, and the device mobility. In particular, the access to the medium must be decided in a distributed fashion, and routes need to be established. For many scenarios, the communication is multi-hop, because a sender cannot communicate directly with an intended receiver. Sometimes, mobility is an requirement which leads to a constantly changing topology. Wireless sensor networks can be considered a subtype of wireless ad hoc networks, that focus on interacting with the environment.

2.1.1 *Basics of Wireless Sensor Networks*

About a decade ago, the era of small sensor nodes which are low-cost, low-power, and multifunctional has begun. The tiny nodes, also called motes, are deployed for monitoring real-world phenomena. As shown in Figure 2.1, they typically consist of a microcontroller, memory, radio chip, power unit, and one or more sensors for measuring the environment. It is either possible to directly deploy them to specific positions, e.g., inside the phenomenon, or to randomly distribute them in inaccessible terrain, e.g., via aerial scattering. As a consequence, the position of a node may not be known in advance. After deployment, the nodes form a self-organized network and identify neighboring nodes. Usually, all data is flowing towards a central node, called the sink or base station. In order to reach this sink, the messages likely have to be forwarded via multi-hop routing, since the radio chip is not powerful enough to communicate directly with the sink when the node is too distant.

The protocol stack used by the WSN is similar to the seven layers specified in the OSI model, but does not adhere strictly to it. It consists of the application layer, transport layer, network layer, data link layer, and the physical layer. Because of

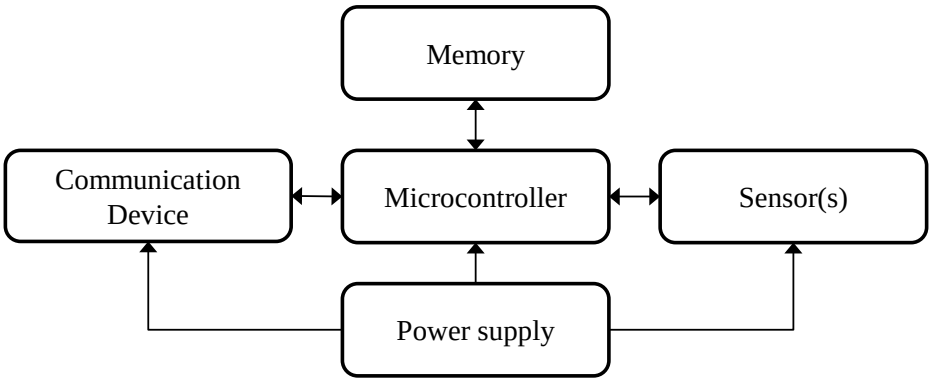

Figure 2.1: Common structure of a sensor node

the resource-constraints, the main design goal of the protocols developed for sensor networks is energy-efficiency. We briefly describe the purpose of each layer [ASSC02]:

- Physical layer – responsible for modulation, transmission and receiving techniques
- Data link layer – responsible for medium access and ensuring reliable connections
- Network layer – responsible for routing the data supplied by the transport layer
- Transport layer – responsible for providing data to be transferred
- Application layer – responsible for specifying how the data will be provided

2.1.2 *Hardware*

The microcontroller is the core of a sensor node and has access to all modules. It is a general purpose processor with a low power consumption. Typical examples are the Texas Instruments MSP430 and the Atmel ATMega. While the first has a 16-bit architecture, the latter is a slower 8-bit microcontroller, but offers a larger memory. A widely used sensor node is the Telos node, which has been developed at the University of California, Berkeley [PSC05]. It has a MSP430F1611 microcontroller, 48 KB ROM and 10 KB RAM. As a radio chip, the CC2420 operating according to the IEEE 802.15.4 standard is used. The radio operates in the 2.4 GHz band, providing data rates of up to 250 kbps. The low power consumption is achieved by sleeping most of the time. At the moment, these characteristics are common for default node platforms.

2.1.3 *Application Scenarios*

The above mentioned characteristics of sensor nodes allow their use in a plethora of application scenarios. For example, Mao et al. [MMH+12] deploy a sensor network for monitoring the CO2 emission in an urban area covering around 100 square kilometers. In order to establish connectivity among this wide area, relay nodes are necessary. The collection tree protocol (CTP) [GFJ+09] is used as routing protocol. Together with GreenOrbs [LHL+11] (also using CTP) it is an example of a large-scale WSN consisting

of thousands of nodes. GreenOrbs is deployed in a chinese forest for evaluating the carbon sequestration ability, which is an opposite of carbon emissions.

In the logistics domain, Bijwaard et al. [BvKH+11] apply sensor networks in order to monitor the cold chain of perishable goods such as fruits and pharmaceuticals.

Sen et al. [SMR+12] present a system to monitor road traffic queues in real-time. It is able to classify the traffic states by measuring metrics such as signal strength and packet reception rate in the communication between a transmitter-receiver pair.

Lu et al. [LSS+10] use sensors to determine the occupancy and sleep patterns in a home with the intention to reduce the energy consumption needed for heating, ventilation and cooling.

Ceriotti et al. [CCD+11] describe a WSN which is a part of a closed-loop control system. The WSN monitors the light conditions in a tunnel and sends the readings to a control station dynamically adjusting the lamps intensity for improving tunnel safety and reducing power consumption.

Recently, Wang et al. [WAL+14] take a new perspective on WSNs by modeling social networks, such as twitter, as sensor networks where a human can be considered a sensor node.

2.2 SECURITY IN WIRELESS SENSOR NETWORKS

In this section, we present the definitions of important terms used in this work. Furthermore, we discuss important security goals. We also present typical adversaries and attacks in wireless sensor networks. Finally, we mention challenges associated with providing security.

2.2.1 *Terminology*

Throughout this thesis, we adapt the following definitions:

- Confidentiality – information must be kept secret from anyone but those who are authorized [MOV96].
- Integrity – information should not be alterable by unauthorized or unknown means [MOV96].
- Availability – systems have to work promptly, and service to authorized users is not denied [SB12].
- Authentication – corroboration of the identity of an entity (e.g., a node) or corroborating the source of information (message authentication) [MOV96].
- Attack, intrusion – any attempt to access a service, resource, or information in an unauthorized way; it also applies to attempts at compromising confidentiality, integrity, or availability [WS04].
- Attacker, adversary – these terms are used synonymously to represent the originator of an attack [WS04].

- ▷ Denial-of-service – the result of an adversary intentionally and successfully preventing any part of a WSN from functioning correctly or in a timely manner [WS04].

2.2.2 *Security Goals*

Clearly, in the mentioned applications in Section 2.1.3, security can be considered a baseline requirement. They require reliable data, i.e., an attacker shall not be able to change the measured data of the sensor nodes. Otherwise, the systems are not working as intended. It is also necessary to protect the WSNs from denial-of-service. This is especially important in safety-critical applications such as the lighting control in tunnels [CCD+11], where an adversary may disable switching on the light by disrupting the network. Depending on the scenario, also confidentiality may be desired. Mechanisms on how to provide these goals are described in what follows.

Confidentiality

As data is transmitted over the air, and not through a cable, listening to traffic is very easy. A straightforward countermeasure is to use cryptography. Symmetric algorithms such as AES are very resource-efficient and can be executed on sensor nodes without incurring too much overhead. However, especially in dense networks key distribution is a big issue [CA07]. Typically, in-network data processing to reduce the amount of transmitted data is favorable [KEW02]. Hence, all nodes along a path need to share a key at least with their direct neighbors. A single key for the whole network is inappropriate due to security reasons [ZSJ06]. A common assumption is that nodes are not tamper-proof because of cost-constraints, and therefore an adversary can gain access to the key material by physically compromising a node [WS04, WAR06]. Even though asymmetric algorithms such as RSA and ECC have become feasible on resource-constrained nodes, their execution time is still much higher than that of symmetric algorithms [GKS05, LN08].

Integrity

Packets sent over the air can also easily be modified by an attacker. To combat this, methods such as message authentication codes or digital signatures can be applied [MOV96]. The same problems as with protecting confidentiality arise here as well. Since the data is the most valuable asset in a sensor network, integrity needs to be ensured in all deployments.

Availability

The resource-constraints make wireless sensor networks highly susceptible to attacks, which render the network unavailable. These attacks are often referred to as denial-of-service attacks [WAR06]. In some cases, cryptographic protection can be exploited to cause denial-of-service, by letting the nodes perform expensive operations extensively. For example, Wang et al. [WDN07] tackle a specific problem related to public-key cryptography in WSNs. Since these operations are computionally expensive, an attacker could abuse broadcast authentication schemes using asymmetric cryptography

to cause denial-of-service. This can be achieved by broadcasting fake messages, whose signatures have to be checked by the nodes to exhaust the energy. The authors design a scheme that is a trade-off between two standard defense strategies, i.e., (1) forwarding the message without authentication, and (2) verifying the message before forwarding. The principle of their approach is as follows. As soon as a node is receiving a lot of faked incoming broadcast messages, it will shift to defense strategy 2. Otherwise, it will stick to the first strategy. The goal is to restrict the influence of DoS attacks to small parts of the network by dropping fake messages as soon as possible, while at the same time keeping the delay of the successful reception of legitimate messages small. The scheme is evaluated in simulations.

Taking into account the fact that the focus of wireless sensor networks is to interact with the environment, the question arises whether one or more security goals are more important than others. As an exemplary scenario, we consider WSNs used in industrial settings to automate processes, as presented in the work of Suriyachai et al. [SBR10]. The WSN described is deployed at an oil refinery in order to monitor the environment, such as pipe pressure and temperature. Based on the measurements of the sensor nodes, actions can be taken with the assistance of actuator systems in case of safety-critical situations. For instance, shut-off valves are used in the pipes to stop operation. Hence, it is crucial that the sensed data arrives timely and unaltered at the sink, and that the availability of the WSN is very high. In particular, a potential threat is that an adversary maliciously changes the sensor data in order to cause a negative effect with respect to the goal of the deployed WSN. Going back to the example of industrial automation, false data may lead to defective products or even the destruction of machines. Similar issues apply to all other scenarios, impacting the purpose of the WSN. These requirements shift the focus of the classical security goals from confidentiality, integrity and availability to the latter two. However, the majority of research to provide security in WSNs is concentrated on methods to guarantee confidentiality, such as key management schemes [EG02, ZSJ06] and crypto implementations [GKS05, SOS+08, LN08].

2.2.3 *Classes of Adversaries*

The adversaries wireless sensor networks are exposed to are—until now—very different from Internet adversaries. First of all, attackers on the Internet do not need to be in physical proximity. They can possibly attack with a large number of malicious nodes from different locations. Since very often standard applications are used, well-known vulnerabilities might be exploited, e.g., with the assistance of security testing tools. In contrast to that, the applications running on sensor nodes are typically tailor-made.

In what follows, we group adversaries in different categories. The grouping of Karlof and Wagner [KW03] can be extended by the notion of passive and active attackers:

- Outsider versus insider attacks – outsider attacks are performed by nodes which are not part of the WSN; insider attacks are carried out by legitimate nodes of the WSN which behave against their specification.

- Passive versus active attacks – passive attacks are typically not noticeable by the victim network, since they do not involve actions that affect the network. Exam-

ples include eavesdropping, i.e., listening to communication of other nodes, and traffic analysis. In contrast to that, active attacks intentionally lead to changes in the target network. Examples include changing messages of others (manipulation, but also replaying), pretending to be someone else (impersonation), denying a communication (repudiation) and denial-of-service. Hence, it is easier to detect active attacks, whereas passive attacks mainly remain undetected.

- Mote-class versus laptop-class attacks – a mote-class attacker uses devices with similar capabilities to the sensor nodes for attacking the WSN; an adversary with laptop-class capabilities will attack the WSN with more powerful devices with regard to bandwidth, processing power, memory, transmission range and energy, as compared to the sensor nodes.

2.2.4 *Attacks on Wireless Sensor Networks*

Many of the traditional attacks in computer networks are also applicable to WSNs. Yet, the inherent characteristics of wireless sensor networks make them especially prone to attacks. As data is transmitted over the air, it is extremely easy for an adversary to sniff traffic. Having to meet stringent budget requirements, sensor nodes tend not to be tamper-proof and as such offering no protection against node compromise. Unless in traditional wired networks, there is often no firewall available.

The majority of attacks that current intrusion detection systems try to detect affect the network layer. Nevertheless, sensor networks can be attacked on all available layers. In what follows, we present common attacks in WSNs with respect to the protocol stack described in Section 2.1.1 [KW03]. The majority of them are denial-of-service attacks.

Physical layer

Physical layer attacks mostly interfere with the sending, receiving, or broadcasting of packets on the lowest level. With jamming, physical node compromise, and cloning we describe three severe attacks.

- Jamming

  Jamming can occur at different layers. At the physical layer, it refers to the interruption of wireless communication by emitting radio signals that fill a wireless channel [WSS03]. To combat this attack, techniques such as channel hopping can be used [XTZ07].

- Node compromise

  A very powerful physical attack is the node compromise. Since sensor nodes are likely to be placed in outside, unprotected environments, it is possible to capture them, alter their memory, or in the worst case they can even be destroyed. Hence, an adversary might, for example, get access to the cryptographic keys, and become a legitimate member of the WSN. Furthermore, the attacker can also reprogram a node to behave in a different way. Benenson et al. [BCF08] describe in detail the ways how a node can physically be captured. To protect against node compromise attacks one could, e.g., use a tamper-proof case. However, this

would increase the costs dramatically and therefore is commonly considered impractical [WS04]. Instead, it is necessary to detect attacks during operation.

▷ Cloning

The replication of a compromised sensor node is referred to as cloning [CPMM11]. Conti et al. [CPMM11] take a decentralized approach to clone detection, requiring a number of assumptions: (1) nodes are relatively stationary, (2) are aware of their own location, (3) are time-synchronized, and (4) use an ID-based public key cryptosystem. Nodes continously identify clones and exclude them from network operation. In each run of the protocol, two steps are executed. First, a random value is broadcasted by a centralized mechanism to all nodes. Second, each node signs and broadcasts a message containing its ID and geographic location. Upon reception of such a message, it is forwarded with a certain probability to multiple pseudorandomly selected locations. After verifying the signature and ensuring the message freshness, the destination checks for IDs with incoherent locations indicating a cloning attack. The authors consider an adversary able to compromise a certain fixed number of nodes, replicating at least one into several clones. In addition, they assume that the adversary tries to prevent its detection by circumventing the detection protocol. The strongest adversary assumed can compromise nodes independent of their position, leveraging information obtained about the detection protocol to compromise those nodes, that give a high probability to remain undetected clones. The scheme is evaluated in simulations, showing that it is effective in attack detection given an adversary selectively dropping messages. Besides, it is shown that the algorithm outperforms the similar approach proposed earlier by Parno et al. [PPG05] with respect to efficiency and effectiveness.

Link layer

The link layer manages the medium access control, which is a frequent target of an attacker. In this section, we consider eavesdropping and jamming attacks. Other attacks related to fairness issues are covered in [WAR06].

▷ Eavesdropping

The wireless communication medium allows to passively capture traffic without exposing an identity. Detection of such an eavesdropper is difficult. Hence, data should be encrypted.

▷ Jamming

When jamming occurs at the link layer, the adversary sends packets without following the carrier sense access rules of the medium access control. The effects of this attack are different. In some cases, the nodes will not sense a free channel, and therefore are not able to transmit packets. In other cases, the ongoing communication is interrupted, e.g., by causing collisions [WAR06]. Typically, the adversary is able to prevent communication over the wireless medium. There are different attacker models, which are described in detail in Section 4.1.3. Jamming is also very energy-intensive for the attacker, which is the reason why devices other than sensor nodes are commonly used for attacking,

also allowing to transmit at a higher power. Similar to jamming at the physical layer, countermeasures include, for example, frequency hopping.

Network layer

The network layer is essential for routing data, and hence is susceptible to a variety of attacks. Data often has to be transferred using multi-hop routing. This mechanism assumes that the forwarding nodes are honest. However, if an attacker controls a node, he can change its behavior.

- Selective forwarding

  In a selective forwarding attack, certain data packets are discarded by the malicious node instead of forwarding them. Neighboring nodes of the attacker can possibly detect this attack by monitoring the traffic flow, and consequently avoid the route via the compromised node.

- Message flooding

  An attacker may inject packets at a very high rate at the network layer. The analysis of network traffic statistics can discover a message flooding attack.

- Sinkhole

  In a sinkhole attack, traffic gets attracted by the attacker through a compromised node. This may be exploited to enable further attacks, like selective forwarding. In general, the goal is to have an attacking node look like an ideal node with respect to the routing metrics. Methods for attracting traffic include announcing a low hop-count or a high link quality to all destinations. In some cases the link quality is indeed very high, for instance, if the attacker is using a powerful radio. If the link quality is low, the attacker may spoof it. This increases the chances of the attacker to be part of the routing paths of its neighbors. An intrusion detection approach for detecting sinkholes is described in [NLL06].

- Greyhole / Blackhole

  A combination of selective forwarding and the sinkhole attack is called greyhole. Packets received by the attacker get dropped randomly. In case that all incoming data packets are discarded, this attack is referred to as blackhole. An approach to detect blackhole attacks is presented by Krontiris et al. [KDF07].

- Wormhole

  The attacker tunnels messages from one part of the network and replays them in another part via a low-latency link. Thus, two nodes might believe that they are neighbors, even though they are multiple hops distant. Or, the wormhole convinces nodes far away from the base station, that the route via the attacker is just one or two hops away, effectively creating a sinkhole. An approach to detect wormholes is described in [DG10].

- Sybil

  A sybil attack occurs, if an adversary represents multiple identities with only one physical device. For example, the attacker may compromise routing or voting algorithms. One solution to prevent sybil attacks are authentication mechanisms.

Transport layer

The purpose of the transport layer is to manage end-to-end connections [ASSC02]. With flooding and desynchronization, we present two transport layer attacks [WAR06].

- Connection flooding

  If a protocol has to maintain the state of a connection, it becomes vulnerable to denial-of-service attacks. An attacker can cause resource exhaustion by repeatedly making new connection requests. As a consequence, legitimate nodes cannot successfully establish a connection. A countermeasure against this attack is to use client puzzles, i.e., the entity requesting the connection has to solve a puzzle in order to demonstrate its commitment to the connection. The intuition behind that is, that a connecting client does not spend energy for creating unnecessary connections.

- Desynchronization

  When an existing connection is disrupted, this is called a desynchronization attack. For example, an adversary may claim in the name of a victim node to have missed some packets, causing the other honest node to retransmit the messages. The usage of packet authentication prevents such an attack.

Application layer

The application layer manages the application-related operations and gathers the sensor readings. The considered attacks are path-based denial-of-service and malicious sensor stimuli [RM08].

- Path-based Denial-of-Service

  Usually, sensor nodes honestly forward the packets they receive to the base station. An attacker injecting a large amount of data traffic leads to a waste of the network bandwidth, and will also drain energy of the nodes on the paths. A combination of packet authentication and anti-replay protection is able to prevent this attack [RM08].

- Sensor stimuli

  When a detected event results in communication, an attacker may trigger false events by physically stimulating the sensors, e.g., by using a lighter, in order to overwhelm the network with messages. Mechanisms such as rate-limiting can reduce the effects of this attack [RM08].

2.2.5 *Challenges*

Some of the security goals can be achieved by using cryptography, for instance, when securing the communication against eavesdropping. However, certain characteristics unique to wireless networks require the usage of intrusion detection systems, monitoring the network during operation. Nodes may be deployed in unattended environments, where they could be physically captured and cryptographic material compromised. As a result, an insider attacker can bypass cryptographic mechanisms.

Besides, due to the wireless medium, it is difficult to prevent denial-of-service attacks such as jamming [PIK11]. This is another factor that motivates the need for intrusion detection systems.

Intrusion detection, and providing security in general, is a challenging task in a WSN for several reasons. First of all, the communication is multi-hop, i.e., nodes are required to forward traffic from their neighbors, which implies a notion of trust. The topology of the network is very often not known a priori and subject to regular changes, allowing an attacker to insert his own nodes, but also creating routing errors when no adversary is present, e.g., due to node failure or mobility. Many frequently used nodes have severe constraints in CPU, memory, bandwidth, and energy. Due to these resource limitations, traditional techniques used in wired networks cannot be applied without modifications. For example, the amount of audit data is restricted by low storage, and complex computation is impossible. Another issue is the wireless communication, information can be retrieved or inserted easily by an attacker. There is no central point (except for the base station) which receives all traffic directly with no hops in-between, rendering classic IDS architecture (network-based [MHL94] and host-based [WS02]) unsuitable. In addition, transmitting data is very costly in terms of energy for the sensor nodes and thus should be minimzed. These factors altogether require intrusion detection systems specifically tailored to wireless sensor networks.

Even when confidentiality and integrity is guaranteed, a WSN cannot fulfill its task if it suffers from denial-of-service, and thus is not available to authorized users [WS04]. Because denial-of-service attacks may severely reduce the value of a WSN, and in some scenarios also threaten the health and safety of people, we focus on this type of attack.

2.3 SUMMARY

Wireless sensor networks have become an indispensable technology in many application areas. Within this chapter, we have highlighted their unique characteristics that have to be taken into account when designing security solutions for them. We also discussed common security threats that we have to defend against. In particular, we identify denial-of-service attacks to be a major concern.

3 RELATED WORK AND PROBLEM STATEMENT

> All things are the same except for the differences, and different except for the similarities.
>
> T. Sowell

After having outlined the threats wireless sensor networks are exposed to and motivating the need for IDSs to detect attacks during operation, we examine the current state-of-the-art approaches in this field. We present an IDS taxonomy to compare different solutions. In this thesis, we focus on systems specifically developed for wireless sensor networks.

Firstly, we address the field of intrusion detection in Sections 3.1 and 3.2. We then turn our attention to the problem of measuring the impact of attacks on network operation in Section 3.3. Related work which is specific to our contributions will be discussed subsequently in each corresponding chapter.

3.1 INTRUSION DETECTION SYSTEMS

The field of intrusion detection in computer systems was mainly influenced by the seminal works in [And80, Den87]. Wireless sensor networks differ greatly from traditional networks. For that reason, IDSs tailored to wireless sensor networks have been introduced, which are now the focus of our survey. This work is an extended version of [RH11].

A taxonomy allows to compare different intrusion detection systems. Each system considers a special type of attacker with possibly different capabilities. The system may be dedicated to a specific attack or could be applicable to multiple attacks. The architecture allows detecting the attacks using some type of detection technique at a given detection frequency. For the decision on whether there is an attack or not, often a type of collaboration is needed. The IDS has certain requirements regarding the wireless sensor network. The analyzed intrusion detection systems are evaluated in simulations and/or implementations. Therefore, we believe that an intuitive taxonomy should answer the following questions:

- ▷ Who is the attacker?
- ▷ What is the attacker capable to do?
- ▷ What type of attacks can be detected?
- ▷ What is the architecture of the IDS?
- ▷ Is collaboration needed?
- ▷ How are attacks detected?

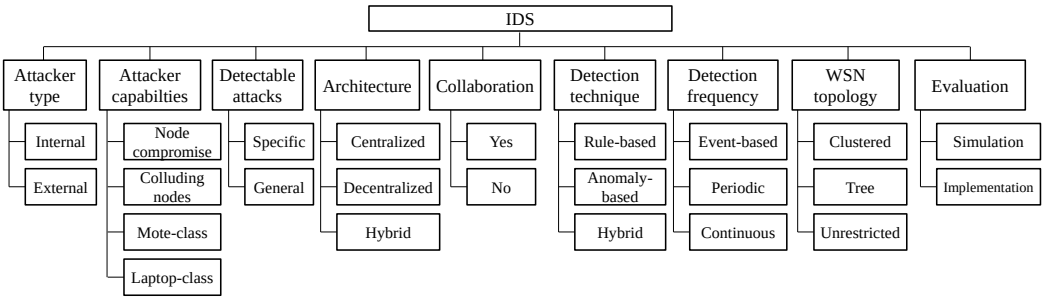

Figure 3.1: IDS taxonomy (adapted from [BMS14])

- ▷ At which frequency is intrusion detection performed?
- ▷ What type of WSNs can run the IDS?
- ▷ How is the IDS evaluated?

The IDS taxonomy to answer these questions is shown in Figure 3.1. It is similar to related work [BMS14], however, we believe that it is important to include the attacker capabilities an IDS is designed for, as well as the attacks the IDS can defend against. Note that the presented taxonomy is not fixed; new categories may be added, depending on the future development in this area. We now describe the individual elements in detail.

3.1.1 *Attacker Type*

A main dimension to characterize an attacker is the *internal* versus *external* distinction. External attacks are performed by nodes which are not part of the WSN, whereas internal attacks are carried out by legitimate nodes of the WSN which behave against their specification. Typically, internal attacks are harder to detect.

3.1.2 *Attacker Capabilities*

A mote-class attacker uses devices with similar capabilities to the sensor nodes for attacking the WSN; an adversary with laptop-class capabilities will attack the WSN with more powerful devices with regard to bandwidth, processing power, memory, transmission range and energy, as compared to the sensor nodes.

In most of the proposed IDSs it is assumed that an attacker may compromise a node and gain access to the cryptographic material. Sometimes it is possible that multiple nodes collude in performing the attack. However, a common assumption is that the majority of nodes is well behaving.

3.1.3 *Detectable Attacks*

The purpose of an IDS is per definition the detection of an attack. Some systems are targeted to detect a particular attack, while others try to identify general malicious

behavior. In the latter case the challenge is to distinguish truly malicious behavior from temporal anomalies or from unknown behavior.

3.1.4 *Architecture*

Intrusion detection systems can be classified according to their architecture into *centralized* and *decentralized*, as well as *hybrid* systems, each of which has specific advantages/disadvantages.

As the term decentralized implies, intrusions are detected locally by the sensor nodes. The nodes are equipped with an IDS and monitor their environment. Having an incomplete picture of what is going on in the network, decentralized solutions might be unable to detect certain attacks. In addition, the nodes cannot apply powerful statistical analysis methods and the amount of audit data is limited, due to the resource restrictions. However, if those systems are designed in a lightweight fashion (e.g., low communication overhead), decentralized IDSs are suitable for WSNs. Besides, the decentralized architecture is more resilient in case of an attack.

In a centralized system, all information relevant for intrusion detection has to be transferred to a single point, typically the base station. Intrusion detection is only performed at the base station, which is assumed to be more powerful in terms of memory and processing power than sensor nodes and thus allowing for more sophisticated detection methods. Centralized systems have a global view of the network, offering the possibility to detect attacks that would have remained undiscovered in other architectures. However, the amount of control/reporting traffic is increased. A challenge is to find a trade-off between reporting frequency and detection accuracy. Besides, a centralized architecture creates a single point of failure and is of special interest to an attacker.

Hybrid IDSs are a combination of centralized and decentralized IDSs, i.e., in this architecture, intrusion detection is performed both locally and globally. In our opinion, hybrid IDSs are a promising avenue for further research. They can exploit advantages of both approaches while at the same time minimizing the disadvantages.

3.1.5 *Collaboration*

While in some approaches nodes need to collaborate with their neighbors to spot the attacker, others are capable of that without cooperation. Cooperating with other nodes and using several monitoring nodes enables to cope with malicious motes that try to hide from detection and give wrong intrusion alerts. In our definition, the term collaboration comprises (1) the need for cooperating with other nodes, e.g., for identifying the attacker; (2) monitoring the communication of other nodes; or (3) analyzing exchanged information in the network which is not purely node-centric, such as routing information. In addition, centralized systems are assumed to always use collaboration, because the data from various nodes is analyzed.

3.1.6 *Detection Technique*

There are two predominant approaches an intrusion detection system can follow. The first approach is *rule-based detection* [IKP95], where signatures containing typical attack characteristics are used to detect *known* attacks. Thus, it works in a similar way as virus detection using signatures. The big advantage of this approach is, that it can detect known attacks with an accuracy of 100%. However, novel attacks cannot be detected at all. The second approach to intrusion detection is called *anomaly detection* [GDMV09]. A profile of the normal network behavior is created, and deviations of this behavior (anomalies) will be detected. Anomaly detection techniques are based on the assumption that regular behavior in a sensor network is the usual case, and attacks occur only with low frequency. An *anomaly* or *outlier* is an observation that differs from the majority. It can be identified by analyzing either the sensor data itself or traffic within the network. Clearly, this approach is much more flexible than rule-based detection, as it may detect new types of attacks. This advantage comes at the cost of possible false alarms. False alarms might arise from the fact, that the normal operation changed slightly or the regular behavior has not been covered completely, such that supposed anomalies are also adhering to system specification.

3.1.7 *Detection Frequency*

The frequency at which intrusion detection is performed influences how much overhead is introduced on the responsible nodes. In our survey, we identify four different detection frequencies:

- Event-based: the algorithm is activated when a certain event is triggered, e.g., packet reception
- Periodic: after a concrete time interval has passed, the IDS functionality is executed
- Continuous: in this case, intrusion detection is performed without interruption
- Random: a node is selected in random intervals to perform attack detection

From an energy consumption perspective, continous monitoring is the most expensive. The energy consumption of the remaining three options depends on the settings and the specific WSN application.

3.1.8 *WSN Topology*

An IDS may require a particular topology. In our survey, we describe works that either need a clustered WSN, a tree topology, or are not limited to a specific topology.

3.1.9 *Evaluation*

The proposed IDS can be evaluated in simulation, implementation, or a combination of both. Whereas simulations are very useful to analyze scalability issues, implementations can better assess the actual behavior in real-world.

Table 3.1: Overview of existing intrusion detection systems for wireless sensor networks

Paper	Year	Detectable attacks	Architecture [1]	Collaboration	Detection technique	Detection frequency	WSN Topology [2]	Evaluation [3]
[OM05]	2005	Specific	D	Yes	Anomaly-based	Event-based	U	S
[dSMR+05]	2005	Specific	D	Yes	Rule-based	Periodic	U	S
[RZL06]	2006	n/a	D	Yes	n/a	n/a	U	n/a
[LNLP06]	2006	Specific	D	Yes	Anomaly-based	Periodic	U	S
[NLL06]	2006	Specific	C	Yes	Anomaly-based	Periodic	U	S
[KDF07]	2007	Specific	D	Yes	Rule-based	Periodic	U	S
[SCK07]	2007	Specific	D	Yes	Rule-based	Periodic	C	S
[LCC07]	2007	General	D	Yes	Anomaly-based	Periodic	U	S
[LKP07]	2007	Specific	D	Yes	Anomaly-based	Periodic	U	None
[GZC07]	2007	General	C	Yes	Anomaly-based	Periodic	U	I
[KDGM08]	2008	Specific	D	Yes	Rule-based	Periodic	U	S + I
[YT08]	2008	General	D	Yes	Anomaly-based	not specified	U	None
[KBG+09]	2009	n/a	D	Yes	n/a	n/a	U	S + I
[WFK+09]	2009	Specific	C	Yes	Rule-based	Periodic	T	S
[DG10]	2010	Specific	D	No	Rule-based	Event-based	U	S + I
[HHJ10]	2010	Specific	D	Yes	Rule-based	Continuous	C	S
[VJU+12]	2012	General	D	Yes	Rule-based	Periodic	C	I
[RWV13]	2013	General	H	Yes	Hybrid	Periodic	U	I
[KE14]	2014	Specific	D	Yes	Rule-based	Continuous	C	S

Abbreviations:

[1] C = Centralized, D = Decentralized, H = Hybrid
[2] U = Unrestricted, C = Clustered, T = Tree
[3] S = Simulation, I = Implementation

3.2 STATE-OF-THE-ART INTRUSION DETECTION SYSTEMS

We have grouped important IDSs proposed for wireless sensor networks according to our taxonomy and present them in what follows. For an overview of the analyzed intrusion detection systems, please refer to Table 3.1.

3.2.1 *Decentralized IDSs*

Onat and Miri [OM05] follow a cooperation-based approach to intrusion detection, assuming static nodes and a tree-based routing protocol. The nodes identify abnormal behavior of their neighbors with regard to two features, the *average receive power* (in dBm) and the *average packet arrival rate* (in packets/unitTime). In their algorithm, they define a main packet buffer length N, and only the last N packets received from each neighbor are used to calculate the statistics to describe the normal behavior. Deviations from normal behavior are then identified as intrusions. The approach is able to detect node impersonation and resource depletion attacks. The algorithm proposed by

Onat and Miri, however, needs a training phase in which the normal behavior of a node is learned. During this phase, no intrusions can be detected. In evaluating the results for the packet arrival rate, Onat and Miri state that the mechanism only works for networks with uniform traffic patterns, where, e.g., nodes measure a certain phenomenon in fixed intervals. If, however, only the changes in the phenomenon are observed and reported, this mechanism might fail. As an example let us consider a sensor that observes changes to the temperature and reports them to the sink. During the day, the temperature might not change at all, but in the morning and evening, the changes are bigger. Thus, the method would not work as there is no homogeneous traffic pattern.

Another decentralized approach to intrusion detection tailored to wireless sensor networks is proposed by da Silva et al. [dSMR+05]. Special monitor nodes are responsible for intrusion detection, however, the authors provide no guidance on where to place these monitor nodes, and on the optimal number. It also remains unclear, when a monitor node is activated. Their algorithm consists of three phases: data acquisition, rule application, and intrusion detection. In the data acquisition phase, the monitor node overhears messages and stores important information to be used for analysis in the following phase. Information is considered important, if it is useful for the rule application. The rule application phase evaluates the stored information according to predefined rules. A message failing one of the rules results in the incrementation of a failure counter. Besides, this specific message is no longer subject to evaluation of other rules because of resource restrictions. The authors argue, that this strategy reduces the detection latency. As they mention, there is a trade-off between accuracy, processing cost, and runnnig time. The smaller the buffer size (no. of messages processed during rule application), the larger is the number of false-positives. Finally, in the last phase, an attack is detected if the number of failures is greater than an expected value. The expected value is based on a failure history (expected amount of occasional failues) for each node in the neighborhood, which is kept by the monitor node.

In [RZL06], Roman et al. introduce a technique for monitoring neighbors, called *spontaneous watchdogs*. The authors propose a general IDS architecture for static sensor networks, consisting of *local agents* and *global agents*. Local agents monitor only local activities and the packets sent and received by the node itself. Global agents overhear the communication of their neighbors, and can also behave as watchdogs. Since the operation of global agents is more costly in terms of energy, the global agent is activated only with a probability of $\frac{1}{n}$, where n is the number of nodes fulfilling certain requirements (*spontaneous watchdog*). In case a local or global agent detects a possible intrusion, an alert is sent to the base station. They do not a provide an evaluation of their approach, no implementation or simulation exists.

Loo et al. [LNLP06] present a method to detect routing attacks in sensor networks. They use a clustering algorithm to build a model of normal traffic behaviour, which in turn is applied to detect abnormal traffic. Thus, this approach is able to detect unseen attacks, as it is not based on rules. Their intrusion detection scheme does not require communication between sensor nodes, which significantly reduces the power consumption. A wide range of routing attacks can be detected. In their approach, each node is equipped with an IDS which should work independently and detect intrusions locally. The only information used is the node's own routing table, and all packets

the node received. They identified a set of twelve features to detect routing anomalies in a variety of routing protocols. These features are listed in Table 3.2. Feature 1 is used to detect anomalies in data traffic, which could be signs for a denial-of-service attack. Features 2,3, and 4 can be used to detect sinkhole attacks, as sinkholes may require the nodes to request routes. In a similar way, features 5, 6, and 7 indicate a sinkhole attack due to the manipulation of the routing protocol. Route error attacks can be detected using features 8 and 9. The last three features recognize path changes of the nodes to the base station, again to detect sinkhole attacks.

Table 3.2: Features used for intrusion detection [LNLP06]

No.	Feature Description	Attack
1	No. of Data Packets Received	DoS
2	No. of Route Requests Received	Sinkhole
3	No. of Route Requests Sent	Sinkhole
4	No. of Route Requests Dropped	Sinkhole
5	No. of Route Request Replies Received	Sinkhole
6	No. of Route Request Replies Forwarded	Sinkhole
7	No. of Route Request Replies Sent	Sinkhole
8	No. of Route Errors Received	DoS
9	No. of Route Errors Sent	DoS
10	No. of Updates on Route to Base Station	Sinkhole
11	Mean of Hop Count to Base Station	Sinkhole
12	Standard Deviation of Hop Count to Base Station	Sinkhole

Krontiris et al. [KDF07] design an IDS to detect the blackhole and the selective forwarding attack using only partial and localized information. Every node monitors its neighborhood, i.e., it promiscuously listens to the channel and temporally buffers the overheard packets. Within a defined window of time, the monitor node checks whether the overheard packets have been forwarded or not. Collaboration with its nearest neighbors is required to detect the attacker. They follow a rule-based approach (rate of messages dropped above a certain threshold) to detect deviations from normal behavior; the attacker node is identified, if more than half of the watchdog nodes raise an alert for this node. This approach is extended in [KDGM08], in order to detect sinkhole attacks. It is specifically designed to work with the MintRoute [WTC03] protocol of TinyOS [HSW+00], having link quality estimates as the routing cost metric. The architecture remains the same as in [KDF07], i.e., every node has its own IDS client which communicates with others in order to reach a conclusion on an intrusion event. A difference in detecting sinkhole attacks now is, that the nodes do not have to store overheard packets or any other information in their memory, as the rules of the IDS client are applied to temporarily buffered packets. In this paper, they introduce rules to detect the sinkhole attack. A node checks for each overheard route update packet, if the sender field is different from its own node ID and if it is the ID of one of its neighbors. When this is not the case, an alert is produced, as route update packets should only originate from a legitimate sender. If a rule is satisfied, it is possible to conclude that the attacker is a neighboring node, since the route update packets are only broadcasted locally. To identify the attacker, nodes must cooperate, as the sender field is altered. Nodes broadcast a list with the IDs of their neighbors as an alert

message. Upon receiving this message, a node removes all node IDs from the list of potential attackers, that are not part of its own neighbors. Thus, its own neighbor list and the list of node IDs in the alert message are intersected. This process continues, as the result is stored and used for the intersection with the next alert the node receives. As soon as there is only one node left in the result, this node will be identified as the attacker. Depending on the topology, it might be the case that the attacker cannot be identified. This is referred to as *false-negative*. In their experiments, the false-negative rate decreases with the network density.

The collaboration of sensor nodes is more generalized in [KBG+09], in which the approach does not focus on specific attacks, but rather on cooperative techniques. The problem of intrusion detection is formally defined and necessary and sufficient conditions on the solvability of the cooperative intrusion detection are identified. However, they only investigated the case of a *single* attacker. Their implementation demonstrates, that the algorithm is lightweight enough to run on sensor nodes.

Su et al. [SCK07] propose a security system called eHIP which combines intrusion prevention and intrusion detection. They assume a time-synchronized, static cluster-based WSN, in which data is routed through the cluster heads to the sink. To prevent intrusions, they use two authentication mechanisms, one for control messages (such as routing messages) and one for sensed data. The reason for this approach is to conserve energy efficiently, as from a security point of view these types of messages are of different importance. As control messages should be highly secured, a keyed-hashing message authentication code (HMAC) is applied to them on the basis of hop-by-hop security. That means, each intermediate node has to verify a control message by checking the HMAC code and re-generating a new one for the verified control message until it arrives at the destination node. Regarding the delivery of sensed data, each intermediate node needs to authenticate the data sender. Otherwise, an attacker could send bogus data which would be forwarded and thus deplete energy. The HMAC computation and transmission consumes much time and energy, but as they assume sensed data is not as sensitive, they use an energy-efficient one-time key chain to authenticate the sender. As a second line of defense they implement a collaboration-based intrusion detection system monitoring cluster heads as well as member nodes. A cluster head aggregates the data from other nodes and thus requires more security. In cluster head monitoring, the member nodes cooperate to detect misbehavior, whereas the cluster head is responsible for monitoring the member nodes. The authors claim that attacks like packet dropping, packet duplicating, and packet jamming can be detected, but no details are given. Their simulation focuses on energy-efficieny and makes no statements about detection accuracy.

An insider attacker detection algorithm using only localized information is presented by Liu et al. [LCC07]. It explores the spatial correlation existent among the networking behaviors of sensors in close proximity. In a typical sensor network, neighboring sensors should have similar communication and computation workloads. Deviations from these characterics thus indicate a malicious behavior. In their approach, each sensor monitors the behavior of its immediate neighbors. The algorithm considers multiple attributes simultaneously in node behavior evaluation, without requiring prior knowledge of what normal/abnormal behavior is. A node is considered malicious, if its behaviour is significantly different from that of nodes in the same neighborhood. In that case, a report is generated and sent to the base station.

Generally, the algorithm consists of four phases: first local information is collected, second the collected data is filtered, third initial outliers using Mahalanobis distances are identified, and fourth the majority vote to obtain a final list of outlying sensors is applied. Filtering the data is necessary to remove falsified information by an attacker. This is achieved by assigning a trust value to each neighbor in the range [0,1], where a value closer to 1 indicates a higher possibility that the node is a normal sensor. The trust value is computed according to the degree of the node's deviation from the neighborhood activities.

In [LKP07], Li et al. use monitoring nodes, observing the quantity of packets which are erroneously received. The approach requires a training phase, in which the monitor node learns the number of "regular" collisions, i.e., collisions during normal operation without attack. The detection algorithm uses Wald's Sequential Probability Test (SPRT) [Wal04] to conclude from a given set of observed samples (collision/no collision) whether there is indication for a jamming attack or not. An evaluation of the approach is missing.

Yu and Tsai [YT08] develop a framework of a machine learning based intrusion detection system. Their system is not limited to particular attacks. Each node runs an intrusion detection agent and overhears the traffic of its neighbors. The first component of the intrusion detection agent is called Local Intrusion Detection Component (LIDC) and detects if the node itself is attacked by analyzing local features. The Packet based Intrusion Detection Component (PIDC) monitors the neighbor nodes to find the attacker. To build the detection model, they apply a rule-learner called SLIPPER [CS99] which is then used to classify observed traffic into *normal* and *abnormal* traffic. Whereas a single rule for itself might not have a high detection accuracy, the accuracy based on the complete set of rules is very high. The detection model has been evaluated on a dataset that was constructed from raw TCP data for a wired local area network. No evaluation is given for the proposed framework for WSNs.

The proposed decentralized algorithm by Dimitriou and Giannetsos [DG10] is investigating connectivity information to find evidence that no attack is being conducted. If, after the start-up has finished, a node overhears packets that include the IDs of unknown nodes, these nodes are put in a list of suspected nodes. The individual nodes then have to check whether the suspected nodes are legitimate and should be included in the neighborhood information or not. This is done by finding a short path to a suspected node which excludes all other suspected nodes. The existence of such an alternative path proves that no wormhole is present and that the suspected node can be added to the neighborhood list. Otherwise, the suspected node is removed from the neighborhood. However, in rare cases the algorithm may not be able to find a short path to legitimate nodes and hence treat them as attacked nodes. It is shown that the algorithm always prevents the wormhole attack.

The decentralized approach proposed by Hai et al. [HHJ10] concentrates on *clustered* sensor networks and is able to detect several routing attacks, based on neighbor knowledge and routing rules. In their architecture, every node has an IDS agent and belongs to a single cluster. There are two intrusion modules, a local and a global IDS agent. The local agent monitors sent and received packets by the node. In addition, a list about malicious nodes in the network (blacklist) is kept. The global agent monitors the communication of the neighboring nodes. In order to detect anomalies, the overheard communication is checked using pre-defined rules (similar to those in

[dSMR+05]) and two-hop neighbor knowledge. Alerts are sent to the cluster head, who decides if there is an attack or not. An anomalous event is considered an attack, if the number of alerts concerning a specific node is greater than a certain threshold. In that case, the attacker is isolated from the cluster by sending a blacklist update to the nodes. The used pre-defined rules detect selective forwarding, sinkhole, hello flood, and wormhole attacks. Nodes with a low trust value cannot take part in intrusion detection.

Regarding detectable attacks, research focused so far on developing specific solutions to defend against individual attacks [VJU+12]. To overcome this limitation, Valero et al. [VJU+12] present a security framework called Di-Sec that only applies to clustered heterogeneous WSNs consisting of low-end nodes together with high-end nodes serving as cluster heads. It works similar to virus detection engines: illegitimate behavior is specified in so-called Detection and Defense Modules (DDMs) and checked against the actual behavior observed through the Monitoring-Core (M-Core) [VUV+12]. The default DDMs supplied with Di-Sec can detect jamming, sybil, selective forwarding, and internal attacks aiming at modifying the sensed values. A domain specific language can be used to develop own defense mechanisms. The M-Core is *constantly* given all information a node has or receives. This includes, for instance, the numbers of received and lost packets, the neighbors, and even all incoming packets not necessarily addressed to the node.

Karapistoli and Economides [KE14] design an IDS for ultra-wideband (UWB) sensor networks. In their approach, the WSN is divided into clusters which are re-organized each round by assigning new cluster heads. Nodes are assigned a trust value; untrustworthy nodes cannot be elected a cluster head. Cluster heads are supposed to monitor the cluster members, while three cluster members are in charge of monitoring the cluster head. The monitoring nodes need to store each collected/overheard packet and evaluate it against pre-defined rules. When a node is found to be malicious, the location is obtained by invoking an UWB ranging-based localization algorithm.

3.2.2 *Centralized IDSs*

Ngai et al. [NLL06] propose an algorithm to detect sinkhole attacks, even in presence of colluding nodes. The first step consists of estimating the attacked area and thus finding a list of suspected nodes. They assume, that the base station has a rough understanding on the location of nodes, e.g., obtained through various localization mechanisms. The base station can detect data inconsistencies using the following statistical method. Let $X_1, ..., X_n$ be the sensing data collected in a sliding window, and $\overline{X}$ be their mean. Define $f(X_j)$ as

$$f(X_j) = \sqrt{\left(\frac{(X_j - \overline{X})^2}{\overline{X}}\right)}$$

Then a node is suspected, if $f(X_j)$ is greater than a certain threshold, because the data from this node is different from others in the same area. Hereafter, the base station can estimate the position of the sinkhole and circle a potentially *attacked area* containing all suspected nodes. The radius of the circle is chosen to cover all suspected nodes. In a second step, the intruder will be identified. This is accomplished by analyzing the routing pattern in the affected area. In detail, the base station broadcasts

a request message containing the IDs of all affected nodes. The request includes a timestamp to prevent replay attacks and is signed with the private key of the base station. On receiving the request, the affected node replies with its own ID, the ID of the next-hop node and the routing cost (e.g., hop-count) to that node. The reply message is sent along the reverse path in the broadcast, as the next-hop and routing cost could already be affected by the attack. At the base station, the routing pattern is then analyzed by constructing a tree using the next-hop information. In a sinkhole attack, all network traffic flows towards the same destination which reveals the identity of the intruder. With some adjustments, the authors are able to deal with multiple malicious nodes. As a first measure, symmetric encryption is used to avoid alteration of packets during transmission. Every node has an individual key shared with the base station. In addition, path redundancy is introduced by forwarding reply messages to a certain number of neighbors. Multiple malicious nodes may collaborate and provide incorrect routing information like hop-count in order to expose a non-malicious node as intruder. However, the base station can detect this inconsistency by calculating the difference between the hop-count which is supplied by a node and the count of edges from the node to the current root.

Gupta et al. [GZC07] design a centralized IDS which collects and analyzes application data as well as management information. The latter information is collected through a separate routing protocol either periodically or event-based, in case an anomaly has already been detected from application data. A decision tree is applied to identify attacks from the collected data.

Wang et al. [WFK+09] propose a scheme to detect packet droppers and modifiers in wireless sensor networks. They require tree-based routing towards the sink with changing topology from round to round. Each node adds special bits to messages in order to allow the sink to calculate the individual packet dropping rate, having to be aware of the topology and the parents of all nodes. Besides, each packet needs to be encrypted. Three different algorithms can then identify the packet dropping nodes. Existing en-route filtering schemes [YLLZ04, ZSJN04] can be integrated to detect packet modifiers. The scheme is evaluated only in simulations.

3.2.3 *Hybrid IDSs*

Raza et al. [RWV13] design an IDS specifically for the Internet of Things, i.e., internet-connected 6LoWPAN networks. Processing-intensive IDS modules run on the 6LoWPAN Border Router (6BR), which connects 6LoWPAN networks with the Internet. In addition, the corresponding lightweight modules are executed on the nodes. Apart from IDS functionality, a distributed mini-firewall is provided. Three main modules run on the 6BR: a module collecting information about the network (parent and neighbor information for each node as well as information to reconstruct the destination oriented directed acyclic graph used in the routing protocol [RWV13]), an intrusion detection module, and a firewall module. Similary, two corresponding lightweight modules are installed on the nodes: a module to map information to the 6BR, and a module for the centralized firewall. The authors present algorithms to detect inconsistencies in the routing graph, selective forwarding, and sinkhole attacks. The firewall can block manually specified external hosts as well as hosts that are found to be malicious by the nodes in real-time.

3.3 PERFORMANCE AND SECURITY METRICS

The research area quality of service in wireless sensor networks is a very active one. Much attention is paid to metrics such as delay, throughput, and duty cycle. However, the systematic quantification of the effects of denial-of-service attacks on WSNs has been neglected in the field literature.

Several works investigate link quality metrics, for example, to combat interference or to improve the quality of service. Liu et al. [LC11] introduced a link estimator based on machine learning techniques. Their models can predict the link quality by using a combination of PHY parameters (Signal to Noise Ratio (SNR), Link Quality Indicator (LQI), and Received Signal Strength Indicator) and the Packet Reception Rate (PRR) as input. Boano et al. [BZV+10] investigate the combination of PRR, SNR and LQI into a single, more robust metric to estimate the link quality. Boano et al. [BVN+11] also developed JamLab, a system to generate accurate interference, and analyzed the impact of interference on the packet reception rate. All these works are not concerned with attack detection.

Dong et al. [DLHZ13] conduct a study on the packet delivery performance in a large-scale WSN, and identify the underlying causes of the losses with the packet drops due to an exceeded retransmission threshold being the most relevant. They note that the link quality is greatly affected by the environment, e.g., temperature and humidity. Hence, this behavior has to be taken into account when designing intrusion detection algorithms.

Marfievici et al. [MMP+13] present a case study on the impact of environmental factors on outdoor wireless sensor networks. In particular, the effects of the vegetation as well as seasonal and daily variations on the packet delivery rate are studied. Wennerström et al. [WHR+13] conduct a similar study analyzing the influence of meteorological conditions on the packet reception ratio and the signal strength of outdoor wireless sensor networks.

Also Zhao et al. [ZG03] conducted a study on packet delivery performance in dense wireless sensor networks. Even though they take into account interfering transmissions at the MAC layer occuring during normal operation, an intended attack is not considered. Another work dealing with packet delivery performance was presented in [HHW09]. Hauer et al. evaluated the effects of WLAN interference on packet delivery performance in IEEE 802.15.4 body area networks.

Xu et al. [XTZW05] analyzed several detection approaches for jamming attacks. They used three different metrics to distinguish between jamming and normal or congested traffic: (1) the averaged received signal strength indicator (RSSI), (2) the carrier sense time, and (3) the packet delivery ratio (PDR). The authors concluded that the combination of PDR and RSSI is able to detect jamming attacks reliably. These same authors extended their work on jamming attacks in [XTZ07], and examined the impact of jamming attacks on the packet delivery ratio as well as implemented channel surfing techniques to cope with interference.

Recently, Lu et al. [LWW11] introduced a system to detect jamming attacks in time-critical networks. They proposed a new metric for performance quantification called the message invalidation ratio. Eventually, a message is regarded as invalid if the message delay is greater than a certain threshold. They studied the impact of jamming attacks on this particular metric.

Despite some of these works address the impact of jamming attacks on packet delivery performance, they lack a comprehensive analysis of other mote-level metrics, such as energy consumption or routing-related information. In addition, they are not concerned with different classes of denial-of-service attacks, such as blackhole attacks.

3.4 SUMMARY AND PROBLEM STATEMENT

Relying only on intrusion detection systems in securing systems is not sufficient. Security sometimes is regarded as a standalone component within the whole system, providing security in a separate module. However, this approach is considered a flawed approach in establishing network security. Instead, to build a secure system, security needs to be integrated into each component. Otherwise, the unprotected components become an attack vector [PSW04].

Several works are concerned with intrusion prevention. Sun et al. [SLX+09] design a secure network access control system, restricting network access only to eligible sensor nodes. Luk et al. [LMPG07] present a system to secure the communication of sensor nodes. While jamming is commonly considered an attack, Martinovic et al. [MPS09] use it as security primitive to prevent sensor nodes from receiving fake data. Wood et al. [WSZ07] focus on a mote-class adversary mounting four different types of jamming attacks. To combat these attacks and to allow the network to operate while the attack is ongoing, they propose four countermeasures. The general idea behind them is to hide messages from the jammer.

Using technologies such as 6LoWPAN [HC08] it is possible to connect sensor networks to the internet. Hence, these devices will also face security threats that are typically defended against with firewalls. To the best of our knowledge, Hossain and Raghunathan [HR10] present the first firewall system for wireless sensor networks. This system is a stateless, rule-based firewall similar to a traditional packet-filter firewall. Firewall policies can be created using a rule definition language. For energy saving reasons, the rules are transformed into executable binary code.

The research area of monitoring and debugging wireless sensor networks is a very active one. Even though the majority of works do not focus on attack detection, they can help preventing bugs, and thus hinder an attacker from exploiting them. Sundaram et al. [SEZ10] present a technique for debugging WSN applications by encoding and recording the control-flow. Upon fault detection, the recorded trace may be sent to the base station for analysis and reproducing the fault. This work focuses on node-level faults. Recently, Sundaram and Eugster [SE13] develop a solution supporting distributed diagnosis of complex failures that are the result from node interaction. Another distributed system is presented by Liu et al. [LMZL11], where nodes collaborate in diagnosis tasks. A hardware-software approach that requires no modification to the application or the operating system was proposed by Tancreti et al. [THBR11]. Systems that monitor the health of WSNs are able to identify, e.g., node failures, isolated nodes, and traffic anomalies [KBT13, RRV07, RB06, RM09]. A secure network monitoring system with randomly selected monitoring nodes whose identity is not exposed is presented by Yu and Li [YL08].

o

During the last years, a couple of intrusion detection systems have been proposed, which are targeted at WSNs. In this chapter, we have surveyed the most important

contributions in this area. The majority of them are decentralized solutions, in which the sensor nodes are responsible for detecting intrusions. A first unsolved challenge remains in finding suitable features to build the detection model upon. Those features should be able to discriminate well between normal and abnormal behavior. Secondly, the proposed systems are still rather heavyweight: a variety of features needs to be analyzed in a mostly periodic or continuous fashion. Besides, the large majority of current intrusion detection systems require some type of collaboration. To the best of our knowledge, the only exception is the IDS proposed by Dimitriou et al. [DG10]. However, this system is limited to detect wormhole attacks.

We now discuss both shortcomings and formulate the arising research questions we are going to address in this thesis.

3.4.1 *Systematic Methodology for Measuring the Impact of Denial-of-Service Attacks*

As our survey on related work in the field of performance and security monitoring has shown, the main research interest until now was on the behavior of quality of service metrics during normal operation of the sensor network. Intended attacks are mostly not considered at all. Besides, these works lack a comprehensive analysis of other metrics provided by the nodes, which could possibly be helpful in identifying attacks.

What is missing so far, is an understanding of the real-world effects of denial-of-service attacks on wireless sensor networks. It is this understanding that would allow us to build effective intrusion detection systems by analyzing the behavior of the WSN with regard to those metrics, that are significantly influenced by attacks. We strive to base the decision of an intrusion detection system whether the network faces an attack or not on the most discriminating metrics for efficiency reasons.

Thus, we identify two main research questions:

- How can the impact of attacks be measured in a systematic fashion?
- Which metrics are the most influenced and thus the most appropriate for attack detection?

Addressing these questions paves the way to practical lightweight intrusion detection systems, taking only the most appropriate metrics into account. As detailed in Chapter 4, we answer the aforementioned research questions by presenting a systematic approach for measuring the impact of denial-of-service attacks.

3.4.2 *Novel Lightweight Intrusion Detection Systems*

Furthermore, the current state-of-the-art intrusion detection systems are still rather heavyweight:

- A large number of different metrics needs to be analyzed in order to detect an attack.
- Typically, it is required to install an IDS on the nodes permanently, and to constantly perform intrusion detection.

- ▷ Nodes rely on collaboration for attack detection.

The following open issues are to be resolved:

- ▷ Are lightweight IDSs feasible? How can the load of the nodes be reduced? Is collaboration always required?
- ▷ Which performance can be achieved?

Answering these questions is essential in enabling lightweight IDSs. In Chapters 5 and 6 we present two novel IDSs investigating the trade-off between detection frequency and detection time, the first system using a randomly activatived, pre-deployed attack detection algorithm while the latter applies mobile agents. Furthermore, in Chapter 4, we propose a fully localized IDS that does not need collaboration at all.

The literature review we have conducted in this chapter served as the basis for the definition of our problem statement. It is specified along two key research directions. Firstly, we aim at establishing a methodology that can be used universally to asses the quality of metrics for identifying an attack. Secondly, our objective is to design lightweight IDSs. The contributions of this thesis are aligned to the identified research questions and will subsequently present answers to the questions mentioned in this chapter, which are refinements of the goals of this thesis as mentioned in Section 1.2.

4 MEASURING THE IMPACT OF DENIAL-OF-SERVICE ATTACKS

> Measurement is the first step that leads to control and eventually to improvement. If you cannot measure something, you cannot understand it. If you cannot understand it, you cannot control it. If you cannot control it, you cannot improve it.
>
> H. Harrington

The decision on which features are relevant for intrusion detection is crucial. To identify the most pertinent features, we need to develop an understanding of the real-world effects of attacks on WSNs. In this chapter, we describe a systematic way to analyze these effects in a testbed consisting of TelosB motes, which has been published in [RTH14], but has been extended in this thesis. For this purpose, we collect a large number of local metrics under various combinations of parameters, such as topology and traffic intensity. The jamming and blackhole attacks we carry out are two benchmark denial-of-service attacks, which operate on the link and the network layer, respectively. By using statistical tests, we identify those metrics deviating significantly in an attacking scenario as compared to normal working conditions. The metrics are classified according to their distinction capabilities.

Our work contributes to evaluate the effects of attacks against WSNs in a systematic way. Particularly, (1) in the case of denial-of-service attacks, we identify metrics which are able to differentiate between attacking and non-attacking scenarios. (2) Our results lay the foundation for developing lightweight intrusion detection systems for WSNs, focusing on the most suitable metrics. (3) Using logistic regression models, we implement a fully localized intrusion detection system.

The remainder of this chapter is organized as follows. In Section 4.1, we present our system design. Section 4.2 is devoted to describe our exhaustive scheme to analyze whether a metric is appropriate to detect an attack. In Sections 4.3 and 4.4, we assess our procedure, and thus we classify metrics according to their response to attack detection. The proposed IDS is presented in Section 4.5, before discussing the work of this chapter in Section 4.6. Related work is mentioned in Section 4.7. Finally, some concluding remarks are given in Section 4.8.

4.1 DESIGN

A number of factors might influence a WSN under attack. For example, in a dense WSN the attack effects should propagate faster. In a systematic fashion, we control the topology, the intensity of the normal data traffic in a WSN, and the transmission power in order to understand the impact of these factors on the metrics, and thus on attack detection. We consider two DoS attacks, one prohibiting other communication (jamming) and one misdirecting the traffic (blackhole).

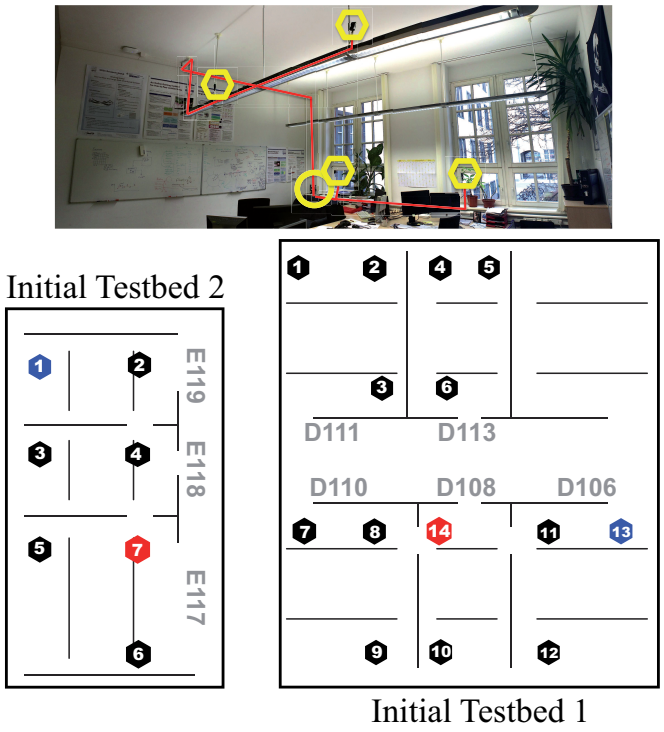

Figure 4.1: Mote placement at the computer science building and sample deployment in one office (image source: http://www.tudunet.tu-darmstadt.de)

In what follows, we describe in detail the testbeds we use, the underlying protocols, attack implementations and the metrics we analyze.

4.1.1 *Testbeds*

Our measurements are carried out in the TUDμNET[1], a federation of wireless sensor network testbeds deployed at various buildings of the Technische Universität Darmstadt. We performed initial tests to pre-test our assumption that a large number of metrics is significantly influenced by denial-of-service attacks in two small testbeds, followed by measurements in two larger testbeds, thereby considering additional attacker models. Subsequently we present the test setups.

Initial Tests

We have selected two different initial testbeds, i.e., subgroups of TelosB motes within the TUDμNET (Figure 4.1 is showing the mote placement in the corresponding offices; the attacker has node ID 14 in initial testbed 1 and node ID 7 in initial testbed 2). These motes provide a MSP430 MCU and a CC2420 radio chip. We run the operating system Contiki [DGV04] using ContikiMAC. The first initial testbed contains 14 motes, located in neighboring office rooms of the computer science building. The second initial testbed is located at a different place of the TUDμNET to compensate for environmental influences or interferences, and to show the applicability of the analyzed metrics to other WSNs. This second initial testbed consists of 7 sensor nodes.

1 http://www.tudunet.tu-darmstadt.de

The main difference between the two initial testbeds is the environment influencing the networks. While one initial testbed is located in office rooms with few people, the second is, among others, located in a pool room with frequently moving people and other interference resulting in a more challenging environment with respect to factors such as link quality. We vary a number of parameters such as:

- ▷ *Topology (mesh/collect)* - With the mesh and the collection tree protocol[2] [GFJ+09], we consider two of the most widely-used protocols in WSNs.
- ▷ *Traffic (high/low)* - We want to analyze the impact of different traffic intensities on the detection capabilities of the metrics.
- ▷ *Transmission power (high/low)* - To vary the average node degree, we use two different transmission power settings.
- ▷ *Attack (jamming/blackhole/no attack)* - The influence of two different DoS attacks on the metrics is analyzed, and compared to an attack free scenario.

To generate data traffic in the mesh network, messages containing a timestamp are exchanged between a random source and destination node on a regular basis. The nodes in the collect network periodically transmit messages to the base station. The intervals between the transmissions are set to 4 (for high traffic) and 10 seconds (for low traffic). Thus, each node either generates 6 or 15 packets per minute. Each packet has a message size of 6 bytes.

The varied transmission power leads to new topologies with changing network density. The CC2420 radio chip allows to set it to a value in the range of 1 (minimum) to 31 (maximum). For the first testbed, the transmission power is set to 10 (-11 dBm) for the "low power" setting, and to 16 (-6 dBm) for the "high power" setting. In the second testbed, the configuration is set to 8 (-13 dBm) and 16 (-6 dBm), because the second WSN is smaller and the distance between nodes is reduced.

During the series of measurements, each node periodically collects local metrics and makes them available through its serial port. The local collecting cycle time is set to 4 seconds which corresponds to the high traffic setting. Note that all metric values are measured for the duration of the collecting cycle and then reset. The TUDμNET allows collecting all serial outputs in one centralized SQL database. This approach offers the advantage that all the metrics are collected over an out-of-band communication channel. Thus, the artificial traffic and our measurement collection do not interfere with each other.

Figures 4.2 and 4.3 depict the topologies of the two testbeds depending on the transmission power. Nodes are labeled with an ID number. Each arc connecting two nodes is labeled with the minimum transmission power value required to establish a path between both nodes. In the first collect testbed, node 13 is the base station. In the second collect testbed, the base station is located at node 1. When running the mesh protocol, base stations are not needed. The adversaries are placed close to the inner nodes of the two testbeds. To compensate for specific measurement errors or temporary anomalies, we perform three different test-runs at different daytimes for each combination of the testbed parameters *topology*, *traffic flow*, *transmission power*

2 In the remainder of this document we use the terms collect protocol as well as collection tree protocol interchangeably.

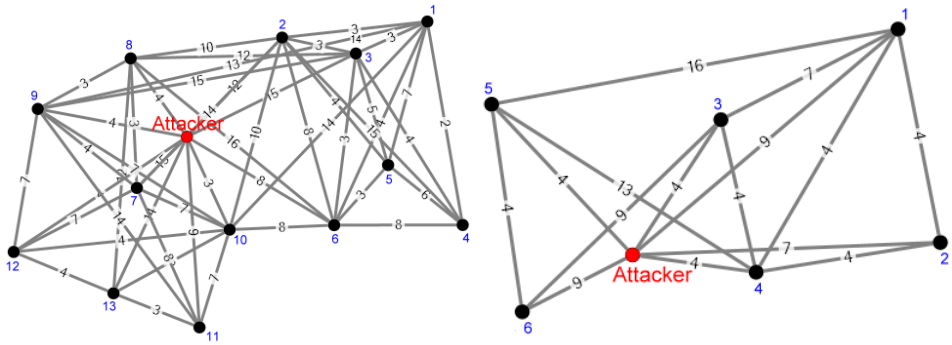

Figure 4.2: Topologies of the two initial testbeds with high transmission power (each arc connecting two nodes is labeled with the minimum transmission power value required to establish a path between both nodes) [Thi12]

and *attack*. Each test-run has a duration of 15 minutes. We have chosen the test-run duration after assessing the time the network requires to reach steady state, which is about 1 minute. Overall, there are 144 measurement test-runs performed in both testbeds, providing about 3 million data samples.

Final Tests

For the final tests, we have selected two larger independent testbeds consisting of TelosB motes. The first testbed (referred to as final testbed 1) is located in neighboring office rooms of the computer science building, containing 37 motes in total (see Figure 4.4). The second testbed (referred to as final testbed 2) is located at a different building to take environmental influences or interferences into account. Besides, we are able to show that the analyzed metrics are applicable to different WSNs. This second testbed consists of 35 sensor nodes (see Figure 4.5). The main difference between the two testbeds is the environment in which they are deployed, having an impact on the networks. The first testbed faces a challenging environment with a lot of interference and poor link quality, since it is deployed in a large number of office rooms separated through doors and walls, and a pool room with frequently moving people. In contrast to that, the second testbed is deployed in a large rectangular hall.

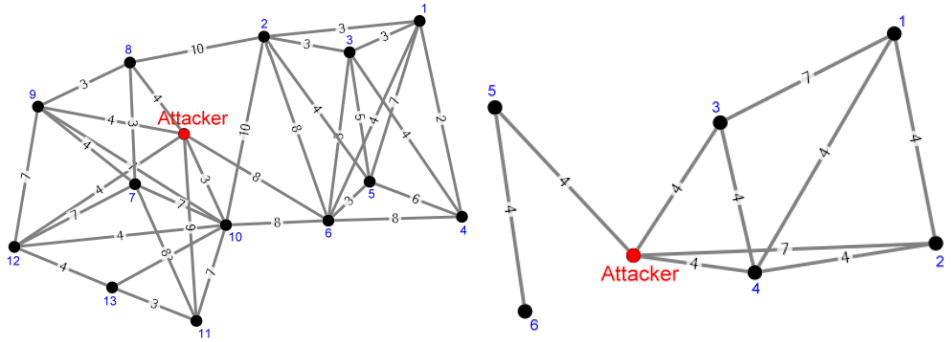

Figure 4.3: Topologies of the two initial testbeds with low transmission power (each arc connecting two nodes is labeled with the minimum transmission power value required to establish a path between both nodes) [Thi12]

Common problems such as unidirectional links and a constantly changing topology are observed in our testbeds. Hence, many challenges of real-world deployments are addressed. Besides the parameters considered in the initial tests, we now also vary:

- ▷ *Attack (constant jamming/random jamming/reactive jamming/blackhole/blackhole with random jamming/blackhole with reactive jamming/no attack)* - In general, we consider two different DoS attacks, namely jamming and blackhole. Three different jammers are implemented. Also, we analyze the combination of both attacks.
- ▷ *Attacker location (inner/outer and inner)* - The location and the number of attackers influence the metrics.
- ▷ *Attack delay (no delay/delay)* - Depending on when the attack starts, the metrics are influenced differently.

To resemble a real deployment, we again generate artificial data traffic. The intervals between the transmissions are set to 3 (for high traffic) and 10 seconds (for low traffic). Thus, the artificial traffic varies between 6 and 20 transmitted packets per minute in each node. Each packet has a message size of 100 bytes, including the header. We have chosen the packet size according to [SMR+12]. For the final testbed 1, the transmission power is set to 9 (-12 dBm) for the "low power" setting, and to 15 (-7 dBm) for the "high power" setting. In the final testbed 2, the configuration is set to 4 (-21 dBm) and 8 (-13 dBm). In Figures 4.4 and 4.5, the base stations are marked in blue, while the attackers are marked in red.

Figure 4.6 shows heatmaps of the nodes in the final testbed 1 representing the required power to reach a specific neighbor under various transmission powers. Grey areas are not reachable by the node. The respective heatmaps for the final testbed 2 are given in Figure 4.7.

The attacker location parameter can be set to *inner*, which means the attacker is placed near the sink in the CTP or near the center of the WSN in mesh networks. Hence, the attacker can reach a large number of neighbors and heavily influence the network. If the parameter is set to *both*, then two attackers are placed in the testbed, the first having the same position as in the inner setting, the second being placed on the outer limits of the networks. For the combined attackers, the blackhole will always be placed near the sink/center.

Regarding the attack delay, when using *no delay*, the adversary will immediately attack when the test-run starts. The *delay* setting, in contrast, allows the network to establish its operation without attack. Then, 7.5 minutes after the start of the test-run, the attacking begins. Note that the attacking nodes remain silent until they start their attacks, and do not take part in the WSN operation. Otherwise, this would lead to different metric values.

Each test-run is repeated two times and has a duration of 20 minutes, out of which 15 minutes are actually used for measuring. As the initial test-runs have shown, the actual starting time of a job can be slightly different for the individual nodes. The reason is that flashing the nodes lasts for a varying amount of time.

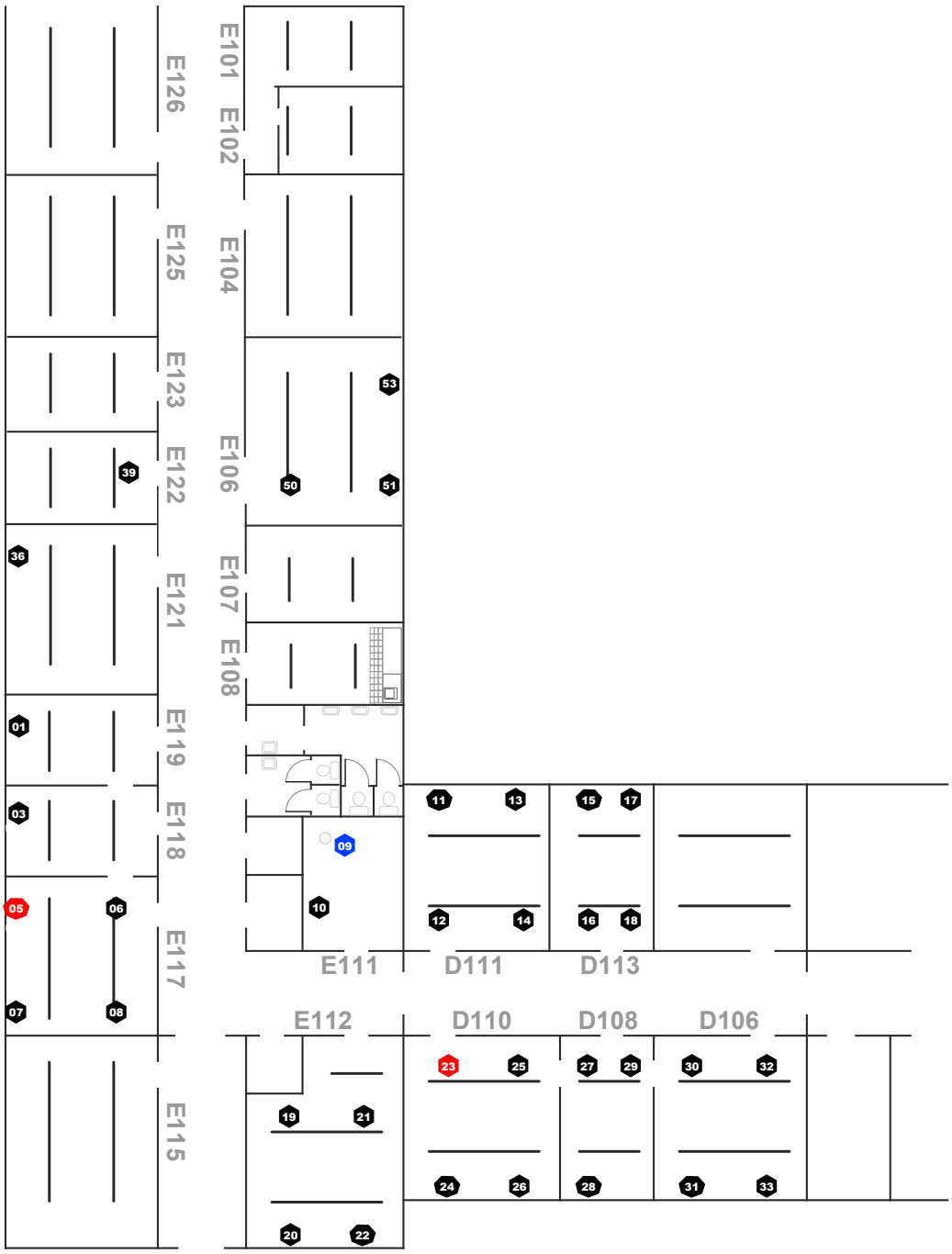

Figure 4.4: Mote placement final testbed 1 [Alm15]

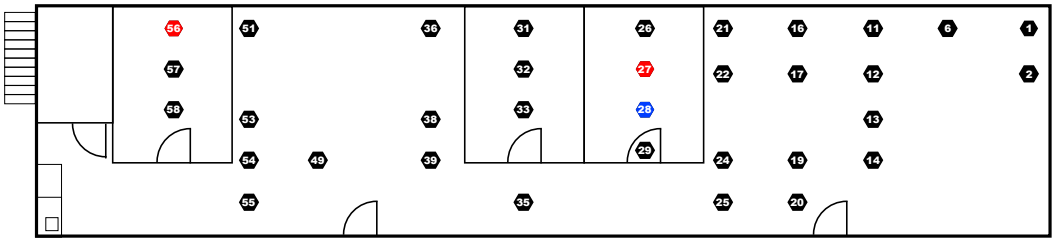

Figure 4.5: Mote placement final testbed 2 [Alm15]

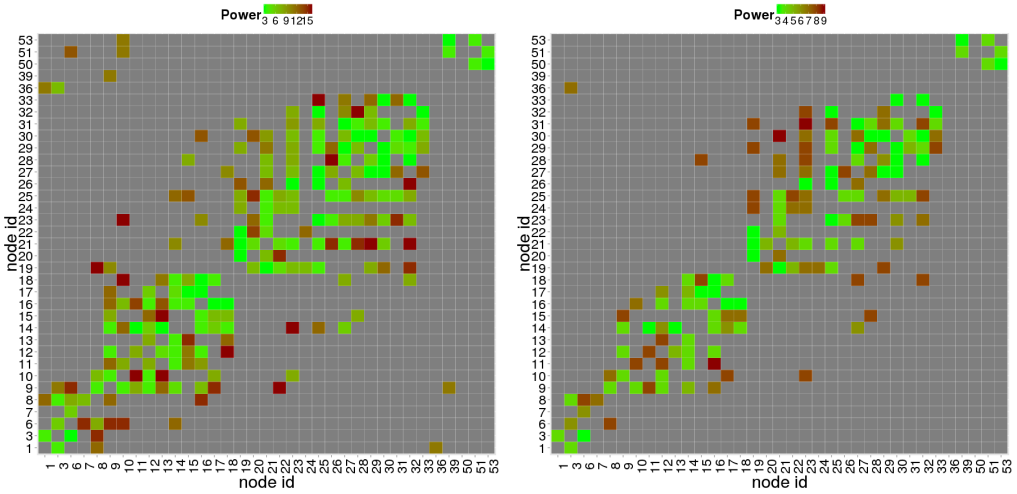

Figure 4.6: Final testbed 1 power table for high (left) and low (right) power [Alm15]

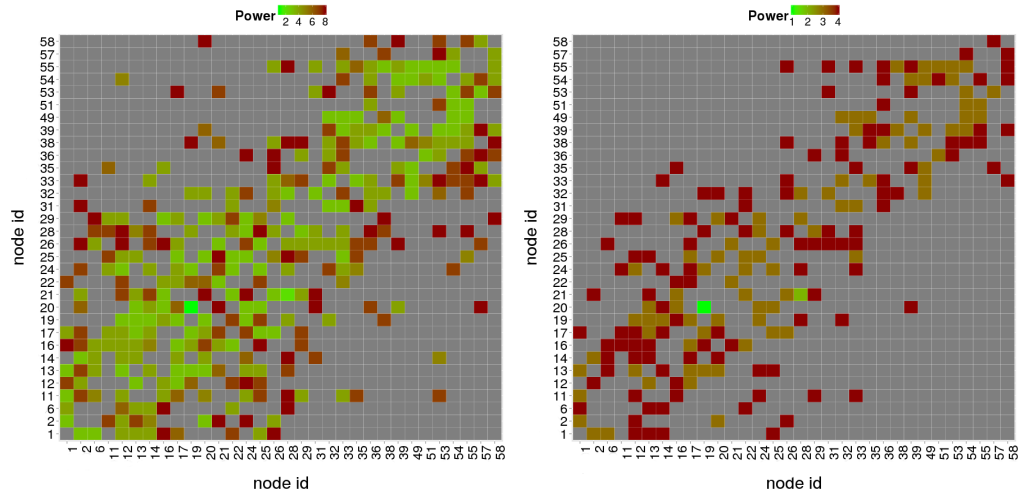

Figure 4.7: Final testbed 2 power table for high (left) and low (right) power [Alm15]

4.1.2 *Protocols Employed*

We have chosen the mesh and collection tree protocol topologies, because they are among the most relevant protocols in WSNs. They are common for a lot of practical deployments [LHL+11, CCD+11], and are used in scenarios such as central data collection and meshed multi-hop networks.

Collect Protocol

The collect protocol [GFJ+09] is used in data collection scenarios and provides mechanisms for building up a tree-based topology within the WSN. It also yields reliable hop-by-hop data packet forwarding to the base station at the root. Therefore, the collect protocol has desirable properties such as tracking network information and message delivery state, for example, packet successful reception. Furthermore, it has built-in methods for collecting statistical network data, which we use as protocol specific metrics in our analysis.

With the progress of IPv6 as a communication standard for wireless sensor networks [VD10], new routing protocols such as RPL [WTt12] may become the standard in wireless sensor networks. Our methodology can then be applied to analyze the impact of attacks on this technology as well.

Mesh Protocol

The mesh protocol is implemented by Contiki's Rime stack and allows sending messages using multi-hop routing to specific destinations in the WSN. For finding the best route to the destination, each node manages an own routing table containing the next-hop neighbor for a specific receiver. However, the multi-hop forwarding mechanism cannot ensure packet delivery, since no acknowledgement packets are sent at the reception of data. Hence, the mesh protocol provides support for less metrics than the collect protocol.

4.1.3 *Attack Implementations*

An analysis of the literature reveals that the question of security has been mainly tackled from the cryptographic point of view, with a focus on data integrity and confidentiality. For instance, besides standard symmetric algorithms which run very efficiently on the resource-constrained nodes, also public-key cryptography has become feasible [WGE+05, LN08]. Still, given the often unattended nature of sensor nodes, it is reasonable to assume an attacker physically compromising the nodes and gaining access to the cryptographic key material. Therefore, defense mechanisms against threats to the availability of the WSN, such as denial-of-service (DoS) attacks, and mechanisms to provide operational security are needed. Hence, we consider two (standard) denial-of-service attacks, operating on layer 1 and layer 3. First, we analyze a physical layer jamming as it is a simple but still powerful attack. Then, we evaluate a blackhole attack. We implement both attacks in the collection tree and mesh protocol, respectively.

The jamming attack is carried out in three different ways: constantly, randomly, and reactively. The *constant jammer* is the simplest attack model, in which the attacker uses

the radio communication to constantly keep sending packet after packet. This results in the radio channel being blocked for all neighboring nodes.

The *random jammer* operates in a similar way, except that the intervals between jamming and sleeping are chosen randomly. The size of those intervals influences the network disturbance, which can range from light to heavy.

The *reactive jammer* is the most sophisticated attacker model we consider. Rather than proactively flooding the channel, this attacker will jam certain packets reactively upon sensing traffic.

The implemented jammers are independent of the network protocols used in the WSN.

Constant Jamming

Jamming is a denial-of-service attack on the availability of the communication channel. One of the most simple jammers is the constant jammer. This type of attacker constantly sends packets on the used channel. Every regular node in range of the jammer's signal will postpone sending data until the jammer stops. The reason for this is, that collisions occur with two concurrent transmitters. These collisions make it impossible to correctly reconstruct the sent information because of the overlapping signals. Hence, the regular nodes do not send when the channel is busy. As a consequence, all nodes in transmission range of the jammer are effectively rendered out-of-service.

In our implementation on the TelosB motes, we directly access the physical layer transmitting method provided via the radio chip. Using this method, the jamming node directly transmits the jamming packets to the environment. In our initial tests, only this type of jammer is evaluated.

Random Jamming

The constant jammer is the basis for the random jammer, the only difference being that the intervals between jamming and non-jamming are random. Hence, the regular nodes can successfully transfer messages from time to time, until the jamming blocks the communication again.

Reactive Jamming

A reactive jammer becomes active upon sensing a packet on the channel, trying to cause packet collision. For that purpose, it constantly listens to the channel. If the attacker senses that a packet is being transmitted he will instantly start sending a pre-defined packet. If this is done fast enough, this single packet will cause a collision on the network layer. The node whose transmission is being targeted will sense this collision and try to send the packet again, leading to another counter-packet sent from the reactive jammer. This process will continue until the maximum number of retransmissions on the regular node is reached, or the reactive jammer does not send its packet fast enough. The repeated retransmissions of the packet will increase the battery consumption.

We expect this attack to be hard to detect, since the jammer is active only occasionally. With no ongoing traffic, the attacker is silent. In addition, a successful collision will

hide the jammer because of the channel being inaccessible. However, if the jammer fails to send its packet fast enough, its transmission can be observed.

Contiki Modifications

Contiki employs various mechanisms in order to ensure a fair and robust network performance. Hence, certain features have to be disabled or modified to allow the jammers to operate. We have made changes to the following parts:

- Watchdog
- CC2420 network stack
- Clear channel assessment (CCA)
- Energysaving

Watchdog: The watchdog regularly checks all running processes for loops causing constant CPU consumption. Upon finding such a process stuck in a loop, the mote gets rebooted by the watchdog. The constant listening to the radio channel, as performed by all jammers, leads to the watchdog rebooting the mote repeatably every 2 to 3 seconds. Disabling the watchdog prevents this behavior.

CC2420 network stack: By default, the CC2420 network stack does not support jamming, because turning off the radio is considered beneficial. Hence, this function is disabled in order to allow a constantly listening jammer. Besides, the sending process had to be realized in an efficient way. Since the jammer always uses the same packet to cause denial-of-service, continuously removing and allocating a new packet is not necessary. Instead, just one packet is allocated on start-up which is used repeatedly for transmission, and never changed or freed. This is especially necessary for the reactive jammer, because allocating a new packet would consume too much time before it could be sent.

Clear channel assessment: If sending a packet would lead a collision, the CCA prevents the transmission. With the assistance of the CCA, a mote can detect an ongoing transmission, and pause its own transmission until the channel is free again. However, this behavior is the opposite to the intended behavior of the jammer, and therefore the CCA is disabled.

Energysaving: As motes are often battery-powered, decreasing the energy consumption is crucial. Contiki's default energysaving routines cause the mote to sleep regularly. In order to keep the jammer always active, this feature is deactivated.

Blackhole

A blackhole node tries to attract all the neighborhood traffic. Instead of forwarding this traffic to the destination, it discards all incoming data packets. The implementations of this attack on the routing protocol need to be specifically adapted to mesh and collect networks. In the case of a mesh network, the blackhole node advertises route announcements with the best routing metric to all destinations and also replies to route requests by handling the incoming requests as the desired final destination and replying on behalf of it. The collect protocol also requires some modifications for attracting the traffic. The blackhole node periodically broadcasts announcement

messages with routing information which are used for selecting the parent node. In particular, it sets its own announcement routing metric to one in order to trick the other nodes into selecting it as parent. Since the base station has announcement value zero, a blackhole setting this value to zero would be suspicious. The routing metric is not only announced directly, but is also piggybacked onto outgoing data or acknowledgement packets. In addition, the blackhole will modify the routing information sent by other nodes, setting its costs again to one.

Containing blackhole attacks is possible by using secure routing protocols [WFSH06], but preventing jamming attacks is difficult. Taking into account the characteristics of jamming and blackhole attacks in both collect and mesh networks, it is possible to develop specific detection approaches. However, we are interested in the actual impact of these attacks on real wireless sensor networks.

4.1.4 *Metrics*

We identify an exhaustive list of metrics that have been selected based on two main criteria. First, we focus on metrics that are already provided by the node or the used protocols. Second, the metrics should be calculatable in a lightweight manner. These choices stem from efficiency reasons, as we envision the metrics to be used in lightweight IDSs. In our experiments, metrics can be divided into three categories: basic metrics, collection tree specific metrics, and mesh network specific metrics. Due to the lack of acknowledgments in the mesh protocol, metrics such as the packet delivery rate are missing for this type of network. In the following, we describe our metrics that were directly provided by Rimestats/Energest in detail.

Basic Metrics

All sensor nodes can obtain basic metrics, independently of the underlying protocol.

- *B01 - Received Signal Strength Indicator (RSSI):* RSSI represents the current radio signal power measured at the receiver and is typically expressed in dBm.
- *B02/B03 - Transmit/Listen time:* It represents the amount of time the radio chip is in transmitting/listening mode during a specific time period. We measure the time with a timer of 8192 Hz.
- *B04/B05 - Transmit/Listen duty cycle:* It depicts the usage of the transmit and listen time as percentage values with respect to the entire measurement period.
- *B06/B07 - Transmitted/Received packets on network layer:* The packet rate metrics at the network layer contain counters for all outgoing and incoming packets.
- *B08/B09 - Transmitted/Received packets on MAC layer:* It counts the outgoing and incoming packets on the MAC layer.
- *B10 - Packets with invalid CRC checksum:* It counts, how often a received packet is discarded because of an invalid CRC checksum.
- *B11 - Energy consumption by radio activities:* It is calculated as

$$\mathrm{energy}_r = (l \cdot 18.8 + t \cdot 17.4 + i \cdot 0.426) \cdot v$$

where $energy_r$ is the current energy consumption of the radio activities, l is the listen time, t is the transmit time, i is the idle time, and v is the current operating voltage. The specific values are taken from the CC2420 manual.

- *B12 - Radio load percentage:* This metric also represents the uptime of the radio. It is given as the percentage value of the uptime with respect to the entire measurement period.
- *B13 - Energy consumption by MCU activities:* It is calculated as

$$power_{MCU} = m \cdot 0.5 \cdot v$$

where $power_{MCU}$ is the current energy consumption of the MCU, m is the MCU uptime, and v is the current operating voltage. The specific values are taken from the MSP430 manual.

- *B14 - MCU load percentage:* This metric represents the percentage value of the MCU uptime with respect to the entire measurement period.
- *B15 - Contention drop:* This metric counts the number of times the node fails to send a packet due to a busy channel.
- *B16 - Pending packets:* This is a boolean metric indicating whether the node has unprocessed packets in the incoming packet buffer.
- *B17 - Too short packets:* When received packets are shorter than the footer (also called trailer) plus the checksum, this counter is increased.
- *B18 - Too long packets*: Similar to "Too short Packets", this metric counts all received packets that have a greater size than specified in the packet header.

Metrics of the Collection Tree Protocol

The collection tree protocol provides additional routing statistic measurements which can be used as possible detection metrics:

- *CTP01/CTP02 - Transmitted/Received data packets:* These counters represent the amount of transmitted/received data packets using the collection tree protocol.
- *CTP03/CTP04 - Transmitted/Received acknowledgement packets:* It counts the amount of transmitted and received ACK packets.
- *CTP05- Received duplicate packets:* It describes the amount of received duplicate data packets.
- *CTP06 - Dropped packets by queue overload:* If the queue buffer for incoming data packets is overloaded, the next arriving packets will be discarded. This metric counts the occurrences of this event.
- *CTP07 - Packet delivery rates (PDR):* The PDR describes the fraction of successfully transmitted data packets.

- ▷ *CTP08 - Changing parent node:* If a sensor node is not able to communicate directly with the base station, it will connect to a parent node which then forwards its data traffic. The amount of changes is counted by this metric.
- ▷ *CTP09 - Parent congestion*: It counts the number of occurences the parent was congested and had to be changed.
- ▷ *CTP10 - Link estimation of best neighbor:* A node defines its parent node by choosing the neighbor with the lowest routing costs. The routing costs are calculated by either the link estimation or by the header information of incoming packets. This metric estimates the link quality to the best neighboring node.
- ▷ *CTP11 - Best neighbor*: It represents the current best neighboring node based on its CTP routing score (rtmetric).
- ▷ *CTP12 - Number of neighboring nodes:* This value represents the number of reachable nodes in the neighborhood.

Metrics of the Mesh Protocol

The mesh protocol used in the testbed is based on a simple broadcasting of normal data messages. The following metrics are derived:

- ▷ *M01 - Number of direct neighbors in the routing table:* It represents the number of reachable nodes in the neighborhood. It is identified by those routing table entries having the same value for the next hop and the destination.
- ▷ *M02 - Number of entries in the routing table:* This metric contains the number of all entries in the routing table, and not only the direct neighbors as in the previous metric.

Having detailed the metrics we study under two different denial-of-service attacks, we will now illustrate a systematic way to assess the metric behavior. This assessment can also be applied for evaluating additional metrics in arbitrary protocols. Note that the metrics *B18 - Too long packets*, *CTP09 - Parent congestion*, and *CTP11 - Best neighbor* have not been analyzed in the initial tests.

4.2 METHODOLOGY

In this chapter, we quantify the effects of denial-of-service attacks in WSNs on a variety of metrics. Our work aims at establishing a comprehensive scheme to find out if there are metrics more susceptible to exhibit an altered behavior under attack than others. Also, we want to rank a set of metrics fitting typical WSNs according to their response in case of attack. This will be further applied to develop an intrusion detection system in Section 4.5.

To determine whether the metric measured values under attack deviate significantly from those in an attack-free scenario, we perform statistical tests. We inspect the cumulative distribution function and perform the Kolmogorov-Smirnov test at a significance level of $\alpha = 0.05$ to check for normality. Both analyses show that there is evidence enough to assume the data not to be normally distributed and, hence, we

carry out a non-parametric test. We have chosen the so-called Wilcoxon-Mann-Whitney test [UKK+12] to contrast whether there are statistically significant differences between *attack* and *attack-free* scenarios. The Wilcoxon-Mann-Whitney test is the analogue of the t-test without the assumption of normality. We use the open-source statistic tool *R*[3] for all tests.

Before starting the evaluation process, we first have to preprocess the collected data. We introduce a binary label (attack/no attack) to distinguish between values in an attack/normal scenario. Furthermore, we have to remove the first minute of each test-run, since the WSN is unbalanced during start-up, leading to wrong metric values. For instance, the PDR (computed over intervals of 4 seconds) in the collect protocol cannot be calculated, as no packets have been sent yet. Next, we group the obtained information during the test-runs according to every combination of parameters separately for each metric and for each node. With a significance level of $\alpha = 0.05$ we test the null hypothesis that the attack values and the normal values have identical data distributions, and note the corresponding p-values. Therefore, if the p-value is less than the significance value, we reject the null hypothesis. The lower the p-values are, the more differ attack values from normal values. We also calculate for each run and for each node the arithmetic mean and standard deviation of the different metrics. Note that for the final tests, we test with a significance level of $\alpha = 0.01$.

Using the Wilcoxon-Mann-Whitney test, we are able to detect significant changes in *individual* metrics. However, the combination of several metrics might also be helpful in detecting attacks. For example, the detection capability of the transmit duty cycle metric is higher in wireless sensor networks with high traffic, as shown in Section 4.4. In contrast to that, the listen duty cycle metric has a better distinction capability in low traffic WSNs. Thus, the combination of these two metrics might be a relevant metric as well. Therefore, we apply a logistic regression to study such effects.

The sequence of the analysis we conduct is given by:

1. Model creation
2. Estimation of the logistic regression function
3. Assessing the model fit
4. Interpretation of the regression coefficients

First, we create the models using the AIC criterion [Aka72], which proved to provide reliable models that do not suffer from overfitting [SH06]. The models describe the relationship between the independent metrics and the dependent variable indicating the presence of an attack. Our goal is the reduction of the number of independent metrics during model creation. Therefore, we start with the null model containing only the constant term. For each metric we now perform a univariate logistic regression. The metric with the smallest AIC value is added to the model. Simultaneously, we check whether removing a metric from the current model leads to a reduction of the AIC value. The final model has the smallest deviation and, hence, the best explanatory power. For every combination of the varied parameters, the models in the

3 http://www.r-project.org

initial testbeds have been created for each node individually, as well as for all nodes combined together. In our final testbeds, we also consider models that only take the data of the direct neighbors of the attacker into account.

The result of our logistic regression analysis are those metrics that best represent the observed data. With the likelihood-ratio test we check the statistical significance of the chosen metrics as a group, i.e., we check whether the metrics can distinguish between attack and no attack. Then, we perform an analysis of variance (also called ANOVA) in order to assess how well the specified models represent the observed data. Finally, we assess the model fit of each model with the assistance of McFaddens-R^2 [LHSoo] which allows to compare the quality of all models.

4.3 METRIC ASSESSMENT

In order to assess the quality of a metric for distinguishing between attack and no attack, we classify them into four categories, namely A, B, C, and D metrics. This is done independently for the collect and mesh protocol, as they provide different metrics. As explained before, the p-values are determined by performing the Wilcoxon-Mann-Whitney test. The classification is performed for each attack in the following way:

- Class A - These metrics are able to detect the attack in both traffic intensities, both transmit power settings, on all nodes in both testbeds, and with highest significance value (minimum and maximum p-values are lower than $2.2 \cdot 10^{-16}$, which indicates that the null hypothesis is rejected at all possible significant values $\alpha = 0.1, 0.05, 0.01, ...$).
- Class B - Metrics which can detect the attack in both traffic intensities, both transmit power settings, and having a minimum significance level lower than $2.2 \cdot 10^{-16}$ in both testbeds.
- Class C - Metrics that identify an attack in both traffic intensities, and both transmit power settings.
- Class D - All remaining metrics that are capable to disclose the attack.

This classification allows us to identify widely applicable metrics for attack detection (Class A), while others are only suited for specific scenarios or specific nodes (Classes B, C, and D). We admit that our classification is biased towards globally effective attacks and is dependent on the network size as well as on the strength of the attack. Thus, in a larger network there might be no Class A metrics at all, which is true for our final testbeds. Still, it gives us a more fine-grained view on the impact of the implemented attacks on our inital testbeds. Regarding the results of the final testbeds, we assess the quality of the metrics in a different way. In this case, we present the detection rates of each metric, i.e., in how many cases the metric showed significantly different values under attack.

Table 4.1: Classification of the analyzed metrics for the different scenarios in the initial testbeds. Sc. 1: Jamming (Collect), Sc. 2: Jamming (Mesh), Sc. 3: Blackhole (Collect), Sc. 4: Blackhole (Mesh)

ID	Metric	Class			
		Sc. 1	Sc. 2	Sc. 3	Sc. 4
B01	RSSI	B	B	C	C
B02	Transmit time	B	B	C	C
B03	Listen time	A	A	C	D
B04	Transmit duty cycle	B	B	C	C
B05	Listen duty cycle	B	B	B	C
B06	NET Sent pkts	B	B	B	C
B07	NET Received pkts	B	B	B	C
B08	MAC Sent pkts	B	B	B	D
B09	MAC Received pkts	B	B	B	C
B10	Invalid CRC	C	C	C	D
B11	Radio energy	B	B	B	C
B12	Radio load	B	B	B	C
B13	MCU energy	B	B	B	C
B14	MCU load	B	B	B	C
B15	Contention drop	D	D	D	D
B16	Pending pkts	C	D	-	-
B17	Too short pkts	D	-	-	-
CTP01	Sent data pkts	B	N/A	B	N/A
CTP02	Received data pkts	B	N/A	B	N/A
CTP03	Sent ACK pkts	B	N/A	B	N/A
CTP04	Received ACK pkts	B	N/A	-	N/A
CTP05	Received duplicates	C	N/A	C	N/A
CTP06	Dropped pkts	D	N/A	D	N/A
CTP07	Packet delivery rate	A	N/A	B	N/A
CTP08	Changing parent	D	N/A	D	N/A
CTP10	Link estimation	B	N/A	B	N/A
CTP12/M01	No. of neighbors	A	A	B	C
M02	No. of routing entries	N/A	A	N/A	C

4.4 RESULTS

In this section we present the evaluation results for our initial tests in the smaller testbeds, as well as for our final tests in the larger testbeds. We particularly investigate the influence of the network density and the traffic intensity on the metric behavior.

4.4.1 *Initial Tests*

We find that several metrics are well-suited to detect the implemented attacks. From Table 4.1 we observe that the metrics in the collect topology constantly perform as good as the metrics in the mesh topology, and in some cases better (an entry in the table marked with "-" indicates there is not enough evidence to reject the null hypothesis; an entry marked with "N/A" signifies that the corresponding metric is not available in this protocol). In the collection tree protocol setting, the implemented

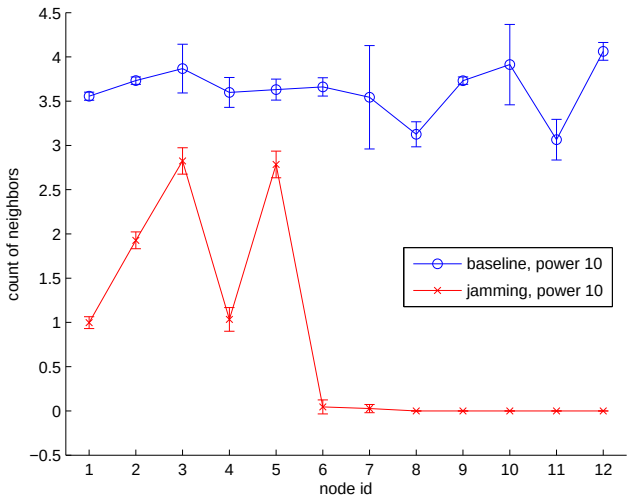

Figure 4.8: Jamming attack in a mesh WSN with low traffic and low transmission power (initial testbed 1); the neighbor count is shown for every node

traffic is more deterministic because all traffic is destined to the sink, whereas in the mesh protocol we use broadcast messages to different destinations. Thus, metrics related to network traffic statistics perform better in the collection tree protocol.

The main finding is that jamming attacks have a more significant global influence on the metrics than blackhole attacks, which tend to be locally restricted. Class A metrics are only available for jamming attacks. For example, the number of neighbors is significantly reduced. The most affected nodes are in the direct neighborhood of the jammer, having a neighbor count of zero whenever the WSN is jammed, as shown in Figure 4.8 (in all subsequent figures the error bars show the standard deviation of the metric values). While this metric can be obtained in both collect and mesh networks, another metric which is only available for collect networks also reaches class A quality,

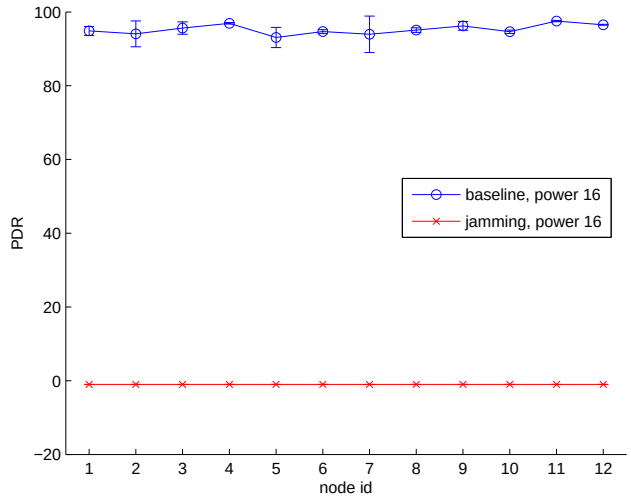

Figure 4.9: Jamming attack in a collect WSN with low traffic and high transmission power (initial testbed 1); the PDR is shown for every node

namely the packet delivery rate. As shown in Figure 4.9, in an attack-free scenario the PDR is almost 100% for all nodes. In contrast, under a jamming attack, the PDR drops to zero, i.e., no packets can be transferred successfully. In a wireless sensor network with higher traffic, the average PDR in a normal scenario is reduced due to the higher amount of collisions. Besides, the PDR is also able to detect blackhole attacks, but in this case the effects of the attack are more local. The PDR is especially reduced for nodes that are not the direct neighbors of the base station and hence have to route their data via other nodes. In such a situation, the blackhole is effectively causing denial-of-service by dropping packets.

There is also a large number of Class B metrics that are heavily influenced by the attacks. Unsurprisingly, metrics covering traffic related information such as the number of sent/received packets are helpful in detecting the attack. However, not all nodes in the testbeds are affected in the same significant way, as some are more distant from the attack. Next, we want to give insights on the impact of selected parameters on the metrics' attack detection capability.

Influence of the Network Density

We now investigate the influence of the network density on the metric distinction capabilities between an attacking scenario and the normal operation. Therefore, we describe the behavior of those metrics that are able to identify the attack in one network density setting, but fail to do so in the other density setting. We perform this analysis separately for the different network protocols and the different attacks. From now on, we call a network using the high transmission power a *dense* network. A network operating with the low transmision power setting is called a *sparse* network. An overview of the results is presented in Table 4.2, in which we list the minimum *p-value* we calculated across all nodes in both testbeds, if we were able to reject the null hypothesis that the attack and the normal values of this metric have identical data distributions. Otherwise, p is greater than 0.05, which means that the metric in this density setting cannot differentiate between attack and normal operation.

JAMMING We start with analyzing the influence of the network density under a jamming attack on the metrics in the collect topology. If we compare the dense to the sparse WSN, we notice four differences. First, the jamming attack affects the sparse WSN stronger and thus causes parent changing events (rows d1 and d4). The effects of the jamming on the routing metric are more severe and influence the reachability of nodes. Second, the dense WSN is subject to a greater message dropping due to contention, because there is higher traffic than in a sparse network (row d2). Third, in a sparse network the count of invalid packets because of short packet size is higher (row d3). The jamming attack has a greater chance to corrupt messages because a sparse network does not suffer as much from contention as a dense WSN. The same reasoning explains the last difference. In a sparse wireless sensor network, there are no dropped packets due to queue overload in an attack-free scenario, since the overall traffic is lower. Consequently, packet dropping indicates the presence of jamming attacks (row d5).

Regarding the mesh topology, the results are similar: in a dense network, the number of messages dropped due to contention (row d11) and the number of pending packets (row d10) is higher.

Table 4.2: Influence of the network density on the initial testbeds

Row	Metric	Topology	Traffic	Attack	p for Sparse WSN	p for Dense WSN
d1	Parent change	Collect	Low	Jamming	$p < 1.6 \cdot 10^{-10}$	$p > 0.05$
d2	Contention	Collect	Low	Jamming	$p > 0.05$	$p < 3.9 \cdot 10^{-6}$
d3	Too short pkts	Collect	High	Jamming	$p < 6 \cdot 10^{-4}$	$p > 0.05$
d4	Parent change	Collect	High	Jamming	$p < 7.3 \cdot 10^{-15}$	$p > 0.05$
d5	Dropped pkts	Collect	High	Jamming	$p < 2.2 \cdot 10^{-16}$	$p > 0.05$
d6	Parent change	Collect	Low	Blackhole	$p < 1.2 \cdot 10^{-6}$	$p > 0.05$
d7	Parent change	Collect	High	Blackhole	$p < 5.1 \cdot 10^{-7}$	$p > 0.05$
d8	Contention	Collect	High	Blackhole	$p > 0.05$	$p < 1 \cdot 10^{-6}$
d9	Dropped pkts	Collect	High	Blackhole	$p < 2.2 \cdot 10^{-16}$	$p > 0.05$
d10	Pending pkts	Mesh	Low	Jamming	$p > 0.05$	$p < 2.2 \cdot 10^{-16}$
d11	Contention	Mesh	Low	Jamming	$p > 0.05$	$p < 6.4 \cdot 10^{-5}$
d12	Contention	Mesh	Low	Blackhole	$p > 0.05$	$p < 6 \cdot 10^{-5}$
d13	Listen time	Mesh	Low	Blackhole	$p < 5.4 \cdot 10^{-5}$	$p > 0.05$
d14	MAC Sent pkts	Mesh	Low	Blackhole	$p < 7.7 \cdot 10^{-5}$	$p > 0.05$
d15	Contention	Mesh	High	Blackhole	$p < 3.6 \cdot 10^{-12}$	$p > 0.05$

BLACKHOLE Concerning the collect protocol, the blackhole causes a higher number of parent changing events in the sparse network due to the lower number of possible parents (rows d6 and d7). As Figure 4.10 shows, nodes that are not direct neighbors of the blackhole (node IDs 1-6) exchange their parent ID with the attacker. We also find that in an attack-free sparse network there is a low number of dropped messages caused by queue overload. A blackhole increases this count in a sparse network by

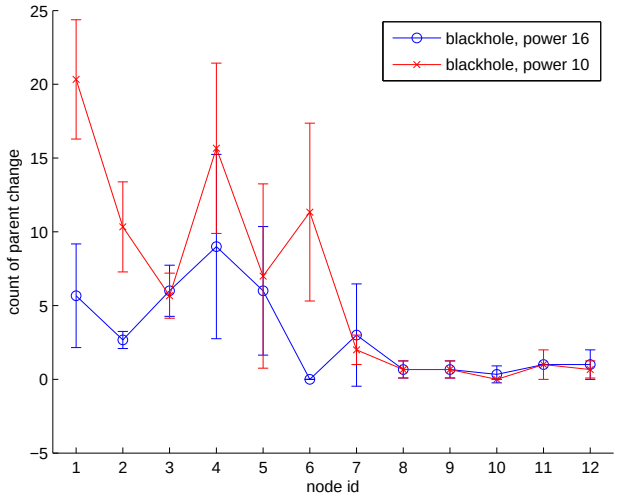

Figure 4.10: Comparison of the effects of a blackhole attack in a low traffic collect WSN, depending on the density (initial testbed 1); the count of parent changing events is shown for every node

Table 4.3: Influence of the traffic intensity on the initial testbeds

Row	Metric	Topology	Density	Attack	p for Low Traffic	p for High Traffic
i1	Too short pkts	Collect	Sparse	Jamming	$p > 0.05$	$p < 6.7 \cdot 10^{-4}$
i2	Contention	Collect	Sparse	Jamming	$p > 0.05$	$p < 1.3 \cdot 10^{-11}$
i3	Dropped pkts	Collect	Sparse	Jamming	$p > 0.05$	$p < 2.2 \cdot 10^{-16}$
i4	Contention	Collect	Sparse	Blackhole	$p < 5.6 \cdot 10^{-7}$	$p > 0.05$
i5	Dropped pkts	Collect	Sparse	Blackhole	$p > 0.05$	$p < 2.2 \cdot 10^{-16}$
i6	Contention	Mesh	Sparse	Jamming	$p > 0.05$	$p < 6.9 \cdot 10^{-5}$
i7	Pending pkts	Mesh	Dense	Jamming	$p < 2.2 \cdot 10^{-16}$	$p > 0.05$
i8	Contention	Mesh	Sparse	Blackhole	$p > 0.05$	$p < 3.6 \cdot 10^{-12}$
i9	Invalid CRC	Mesh	Sparse	Blackhole	$p > 0.05$	$p < 4.7 \cdot 10^{-5}$
i10	Listen time	Mesh	Dense	Blackhole	$p > 0.05$	$p < 7.1 \cdot 10^{-11}$
i11	MAC Sent pkts	Mesh	Dense	Blackhole	$p > 0.05$	$p < 2.2 \cdot 10^{-14}$
i12	Invalid CRC	Mesh	Dense	Blackhole	$p > 0.05$	$p < 1.3 \cdot 10^{-5}$
i13	Contention	Mesh	Dense	Blackhole	$p < 6 \cdot 10^{-5}$	$p > 0.05$

actively advertising routes very often (row d9). In addition, a blackhole attack in a dense network provokes more message dropping at certain nodes due to contention (row d8).

For the mesh network we make the following observations. The number of contention drops is in general higher in a dense network with high traffic and is therefore not a significant metric for detecting blackhole attacks. However, an increase in this contention dropping rate is significant in a sparse network (row d15). In particular, we notice that the direct neighbor of the attacker in the second testbed (node ID 6) has a highly increased number of packets dropped due to contention. In a sparse network, traffic is flowing to the blackhole over fewer nodes, provoking an increased number of messages dropped due to contention at the direct neighbors of the blackhole. This behavior cannot be observed in the tree-structured collect protocol and is weakened in a low traffic scenario, where the corresponding metric is not significant in a sparse network, as opposed to a dense network (row d12). Further, we note that when a blackhole is active, the listen time for nodes on the route to the blackhole is increased in a sparse network, as more messages have to be transferred over those nodes (row d13). Similarly, the number of sent packets on the MAC layer is significantly reduced in a sparse network because messages are not forwarded by the blackhole (row d14).

Influence of the Traffic Intensity

Equal to the analysis of the network density, in what follows we evaluate the impact of the traffic intensity on the metrics. For an overview of the results, please refer to Table 4.3. Again, for significant metrics we give the minimum *p-value* we calculated across all nodes in both testbeds; otherwise p is greater than 0.05.

JAMMING Investigating the metric behavior in the collect protocol, we remark three observations in a high traffic setting: (1) there is higher packet dropping due to

contention (row i2) and (2) due to queue overload (row i3), and (3) the number of too short messages is higher (row i1). Thus, the jamming attack has a more severe negative effect on these three metrics, since more messages flow through the network.

Correspondingly, also the mesh protocol exhibits a higher packet dropping rate due to contention under high traffic (row i6). Besides, with low traffic and under normal operation, no pending packets are observed. A jamming attack increases the number of pending messages (row i7). In a high traffic wireless sensor network, this metric is not significant, as we also have pending packets without attack.

BLACKHOLE Focussing on the collect protocol, a high traffic results in more messages dropped due to queue overload (row i5), since a higher count of messages has to be transferred over fewer links. When the traffic is low, the number of messages dropped due to contention is significantly increased during a blackhole attack because of the malicious node blocking the channel with its route announcements (row i4).

Again, we observe similar results in the mesh protocol. In a high traffic setting, the number of packets dropped due to contention (row i8) and the number of packets with bad CRC checksum (row i9) is higher. This holds for nodes on the route to the blackhole, which experience an increased traffic flow. In contrast to the sparse network, the number of packets dropped due to contention is not significant in a dense high traffic WSN. Also without attack this number is relatively high, as opposed to the low traffic WSN experiencing a significant increase under a blackhole attack (row i13). Given high traffic, the number of packets with bad CRC checksum (row i12) and the count of sent packets on the MAC layer (row i11) is higher when compared to the low traffic WSN. Besides, in a high traffic WSN the listen time is reduced for nodes that are exposed to the blackhole dropping packets, while with low traffic there is no significant difference (row i10).

Logistic Regression

The results of the logistic regression analysis lay the foundation for a simple, lightweight intrusion detection system. The general process of attack detection contains the following steps:

Given: Regression coefficients $\beta_0, \ldots, \beta_k$ and

data set $x_1, \ldots, x_k$

Step 1: Creation of the logit model

$$\eta = \beta_0 + \beta_1 \cdot x_1 + \cdot + \beta_k \cdot x_k$$

Step 2: Calculation of the logit η

Step 3: Calculation of the logistic function

$$\hat{\Pi}_i = \frac{1}{1+e^{-\eta}}$$

Step 4: Decision

$$\text{If } \hat{\Pi}_i > 0.5 \longrightarrow \text{ Attack detected}$$

The single steps of this algorithm will be explained in the next subsection using a simple example. For better readability, the values of the regression coefficients are not shown in the following results.

JAMMING RESULTS To begin, we focus on the initial testbed 1. Table 4.4 represents the relation between the factors in the logistic regression model and the associated metrics in the collection tree protocol. It serves as the basis for all subsequently presented results.

Table 4.4: Factors and associated metrics for the collection tree protocol

Factor	**Metric**
β_1	B01 - RSSI
β_2	B03 - Listen time
β_3	B02 - Transmit time
β_4	B16 - Pending pkts
β_5	B06 - NET sent pkts
β_6	B07 - NET received pkts
β_7	B08 - MAC sent pkts
β_8	B09 - MAC received pkts
β_9	B18 - Too long pkts
β_{10}	B17 - Too short pkts
β_{11}	B15 - Contention drop
β_{12}	B10 - Invalid CRC
β_{13}	B11 - Radio energy
β_{14}	B13 - MCU energy
β_{15}	CTP12 - No. of neighbors
β_{16}	CTP11 - Best neighbor
β_{17}	CTP10 - Link estimation
β_{18}	CTP09 - Parent congestion
β_{19}	CTP08 - Changing parent
β_{20}	CTP03 - Sent ACK pkts
β_{21}	CTP01 - Sent data pkts
β_{22}	CTP02 - Received data pkts
β_{23}	CTP04 - Received ACK pkts
β_{24}	CTP05 - Received duplicates
β_{25}	CTP06 - Dropped pkts
β_{26}	CTP07 - Packet delivery rate
β_{27}	B14 - MCU load
β_{28}	B04 - Transmit duty cycle
β_{29}	B05 - Listen duty cycle
β_{30}	B12 - Radio load

Table 4.5 shows the significant factors as well as the model quality for the jamming attack in a CTP network with low power and low traffic intensity. The models have been created per node, and including all nodes simultaneously, as can be seen in the last row. The second column contains those metrics, that have been used in the logit model. They are labelled as β_i; the corresponding names can be found

Table 4.5: CTP, initial testbed 1, low power, low traffic, jamming

Node	Factors	Analysis of variance	LR-test	R^2
11	β_{15}	$1,25e-8 < 1179,31$	$764,83 > 3,84$	1
13	β_{26}	$4,41e-8 < 1176,20$	$762,77 > 3,84$	1
14	β_{15}	$1,25e-7 < 1175,17$	$762,11 > 3,84$	1
15	β_{15}	$6,38e-8 < 1176,20$	$762,82 > 3,84$	1
16	β_{15}	$2,01e-8 < 1178,27$	$764,16 > 3,84$	1
17	β_{15}	$3,02e-8 < 1175,17$	$762,11 > 3,84$	1
23	β_{26}	$6,71e-9 < 1178,27$	$764,11 > 3,84$	1
25	β_{26}	$7,10e-9 < 1178,27$	$764,11 > 3,84$	1
26	β_{26}	$7,27e-9 < 1178,27$	$764,16 > 3,84$	1
28	β_{17}	$7,16e-8 < 1175,17$	$762,11 > 3,84$	1
30	β_{17}	$6,39e-9 < 1176,20$	$762,82 > 3,84$	1
31	β_{17}	$6,39e-9 < 1177,24$	$763,49 > 3,84$	1
all nodes	β_{15}	$1,27e-6 < 13486,47$	$9159,60 > 3,84$	1

in Table 4.4. The analysis of variance is presented in the third column, comparing the -2 log likelihood value (first term) to the value of the chi-squared distribution (second term). The relation $<$ indicates, that we cannot reject the null hypothesis, and hence the model is perfectly fit. Otherwise, the relation $\not<$ leads to the rejection of the null hypothesis. The fourth column contains the results of the likelihood-ratio test, assessing the significance of the chosen regression coefficients when separating the two groups. The first term represents the value of the reduced, i.e., the chosen model, whereas the second term is the chi-squared value. If the null hypothesis is rejected (first term $<$ than the second term), the chosen metrics are significant for the separation of the groups. Details on these tests can be found in [Meno2]. The fifth column shows the quality criterion McFaddens-R^2, indicating how well the model fits the observed data. A value greater than 0.2 leads to an acceptable model fit, and a value greater than 0.4 to a perfect model fit [LHS00]. These boundaries are common in statistics. In the following, we use the term model fit synonomously for the analysis of variance, the likelihood-ratio test, and the McFaddens-R^2.

From Table 4.5 we observe that in this setting only single metrics are needed for attack detection. The metrics are all specific to the CTP. The most often used metric is the number of neighbors metric, followed by the packet delivery rate and the link estimation.

We now describe the attack detection examplarily for node 23, given the general process as outlined before.

Input: $\beta_0 = 26.0131, \beta_{26} = -0.5215, x_{26} = -1$

Step 1: Regression model $\eta = \beta_0 + \beta_{26} \cdot x_{26}$

Step 2: Logit $\eta = 26.0131 - 0.5215 \cdot (-1) = 26.5346$

Step 3: Logistic regression function $\hat{\Pi}_i = \frac{1}{1+e^{-\eta}}$

$$\hat{\Pi}_i = \frac{1}{1+e^{-26.5346}} = 1$$

Step 4: Decision $1 > 0.5 \longrightarrow$ Attack detected

Table 4.6: CTP, initial testbed 1, high power, low traffic, jamming

Node	Factors	Analysis of variance	LR-test	R^2
11	β_{15}	$1,24e-8 < 1147,21$	$743,75 > 3,84$	1
13	β_{26}	$7,82e-9 < 1146,18$	$743,05 > 3,84$	1
14	β_{26}	$8,05e-9 < 1148,25$	$744,44 > 3,84$	1
15	β_{26}	$1,81e-8 < 1033,19$	$661,09 > 3,84$	1
16	β_{15}	$2,59e-8 < 1145,14$	$742,36 > 3,84$	1
17	β_{15}	$1,63e-8 < 1147,21$	$743,75 > 3,84$	1
23	β_{26}	$6,72e-9 < 1147,40$	$743,75 > 3,84$	1
25	β_{26}	$9,90e-9 < 1146,18$	$743,05 > 3,84$	1
26	β_{17}	$1,25e-8 < 1147,21$	$743,75 > 3,84$	1
28	β_{17}	$6,22e-9 < 1146,18$	$743,05 > 3,84$	1
30	β_{17}	$6,22e-9 < 1147,21$	$743,75 > 3,84$	1
31	β_3, β_{17}	$1,52e-8 < 1145,14$	$743,05 > 3,84$	1
all nodes	$\beta_8, \beta_{13}, \beta_{15}$	$9,06e-6 < 13019,86$	$8844,85 > 3,84$	1

With high power and low traffic, the significant metrics (number of neighbors, packet delivery rate, link estimation) remain the same in most cases, as can be seen in Table 4.6. Exceptions are node 31 as well as the analysis over all nodes, requiring two and three metrics per model, respectively.

Given low power and high traffic, we see that the packet delivery rate and the number of neighbors are the most often used metrics (Table 4.7). Moreover, the basic metric MAC received pkts is able to detect an attack on node 31.

Similar results are obtained for the high power in combination with high traffic intensity. The packet delivery rate and the link estimation occur very often in the generated models as shown in Table 4.8.

To summarize, in about 96 percent of the cases, a single metric is sufficient for successful attack detection in the inital testbed 1. Regarding the used metrics, the CTP specific metrics link estimation, number of neighbors, and packet delivery rate are the most significant metrics. Besides, integrating the number of received packets on the MAC layer into the model helps achieving better results in some cases. Throughout all parameter combinations we achieve a perfect model fit, and the chosen metrics are significant for the separation of the groups.

Next, we turn our attention to the initial testbed 2. In this setup, the number of received packets on the MAC layer is most frequently used in the models. In addition, the packet delivery rate is a highly significant metric, as it was in the initial testbed 1. However, the number of neighbors and the link estimation do not appear as often as before, they are only relevant in a setting with low power and low traffic intensity. The results are shown in Appendix A.1.1.

In summary, ordered descendingly according to the number of occurences, the most relevant metrics across both initial testbeds for detecting the jamming attack using the CTP are:

- ▷ Packet delivery rate

Table 4.7: CTP, initial testbed 1, low power, high traffic, jamming

Node	Factors	Analysis of variance	LR-test	R^2
11	β_{15}	$6,62e-8 < 1147,21$	$743,75 > 3,84$	1
13	β_{15}	$3,07e-8 < 1145,14$	$742,36 > 3,84$	1
14	β_{15}	$2,17e-8 < 1144,10$	$741,67 > 3,84$	1
15	β_{15}	$1,88e-8 < 1145,14$	$742,36 > 3,84$	1
16	β_{15}	$2,99e-8 < 1146,18$	$743,05 > 3,84$	1
17	β_3, β_{15}	$3,91e-8 < 1146,18$	$743,75 > 5,99$	1
23	β_{26}	$6,45e-9 < 1148,25$	$744,44 > 3,84$	1
25	β_{26}	$6,45e-9 < 1148,25$	$744,44 > 3,84$	1
26	β_{26}	$6,45e-9 < 1148,25$	$744,44 > 3,84$	1
28	β_{26}	$5,18e-9 < 960,51$	$600,51 > 3,84$	1
30	β_{26}	$6,22e-9 < 1147,21$	$743,75 > 3,84$	1
31	β_8	$1,35e-8 < 1146,18$	$743,05 > 3,84$	1
all nodes	$\beta_1, \beta_8, \beta_{15}$	$7,28e-5 < 12946,10$	$8793,23 > 7,81$	1

Table 4.8: CTP, initial testbed 1, high power, high traffic, jamming

Node	Factors	Analysis of variance	LR-test	R^2
11	β_{26}	$7,56e-9 < 1148,25$	$744,44 > 3,84$	1
13	$\beta_4, \beta_{10}, \beta_{17}, \beta_{19}$	$8,23e-9 < 1145,14$	$744,44 > 9,84$	1
14	β_{26}	$6,63e-9 < 1146,18$	$743,05 > 3,84$	1
15	β_{26}	$9,67e-9 < 1147,21$	$743,75 > 3,84$	1
16	β_{26}	$1,80e-6 < 1148,25$	$744,44 > 3,84$	1
17	β_{17}	$1,17e-8 < 1148,25$	$744,44 > 3,84$	1
23	β_{17}	$8,38e-9 < 1147,21$	$743,75 > 3,84$	1
25	β_{17}	$6,29e-9 < 1147,21$	$743,75 > 3,84$	1
26	β_{17}	$6,30e-9 < 1147,21$	$743,75 > 3,84$	1
28	β_{17}	$6,23e-9 < 1148,25$	$744,44 > 3,84$	1
30	β_{17}	$6,22e-9 < 1146,18$	$743,05 > 3,84$	1
31	β_{26}	$6,54e-9 < 1147,21$	$743,75 > 3,84$	1
all nodes	β_{15}	$1,25e-6 < 13141,09$	$8927,04 > 3,84$	1

- ▷ Link estimation
- ▷ Number of neighbors
- ▷ MAC received pkts
- ▷ NET received pkts
- ▷ Transmit time

Hence, the results of the logistic regression analysis are similar to those of the Wilcoxon-Mann-Whitney test.

For interpreting the results of the jamming attack in the mesh protocol, Table 4.9 relates metrics to factors. In general, the number of metrics in each model is increased,

Table 4.9: Factors in the mesh protocol

Factor	Metric
β_1	B01 - RSSI
β_2	B03 - Listen time
β_3	B02 - Transmit time
β_4	B16 - Pending pkts
β_5	B06 - NET Sent pkts
β_6	B07 - NET Received pkts
β_7	B08 - MAC Sent pkts
β_8	B09 - MAC Received pkts
β_9	B18 - Too long pkts
β_{10}	B17 - Too short pkts
β_{11}	B15 - Contention drop
β_{12}	B10 - Invalid CRC
β_{13}	M01 - No. of neighbors
β_{14}	M02 - No. of routing entries
β_{15}	B11 - Radio energy
β_{16}	B13 - MCU energy
β_{17}	B14 - MCU load
β_{18}	B04 - Transmit duty cycle
β_{19}	B05 - Listen duty cycle
β_{20}	B12 - Radio load

compared to the CTP setting. The relevant metrics are similar, and include the following, ordered decreasingly:

- ▷ MAC received pkts
- ▷ Number of routing entries
- ▷ NET received pkts
- ▷ Number of neighbors
- ▷ Radio energy

The detailed results are presented in Appendix A.1.1.

BLACKHOLE RESULTS The models created for the blackhole attack require more metrics, and hence are more specific. Besides, the model quality is worse than for the jamming attack. This holds for both initial testbeds and both protocols. We examplarily show the results for the initial testbed 1 using the CTP with low traffic intensity and low power (see Table 4.10). Further results are given in the Appendix A.1.1. In this example, the CTP specific metrics link estimation, packet delivery rate, and the number of neighbors are among the most relevant metrics. At least one of these metrics is included in each model. Regarding the basic metrics, the number of received packets on the network layer as well as the number of sent packets on the MAC layer are significant.

Table 4.10: CTP, initial testbed 1, low power, low traffic, blackhole

Node	Factors	Analysis of variance	LR-test	R^2
11	$\beta_8, \beta_{13} : \beta_{15}, \beta_{17}, \beta_{19}, \beta_{21}, \beta_{23}, \beta_{25} : \beta_{29}$	$60,20 < 1166,88$	$734,73 > 22,36$	0,96
13	$\beta_2, \beta_3, \beta_5 : \beta_8, \beta_{11}, \beta_{13}, \beta_{14}, \beta_{17}, \beta_{20}, \beta_{23}, \beta_{26} : \beta_{29}$	$453,12 < 1159,64$	$536,21 > 27,59$	0,70
14	$\beta_1, \beta_6 : \beta_8, \beta_{11}, \beta_{15}, \beta_{17}, \beta_{18}, \beta_{25}, \beta_{26}, \beta_{29}, \beta_{30}$	$716,19 < 1161,71$	$403,29 > 22,36$	0,52
15	β_{15}, β_{26}	$2,01e-6 < 1173,10$	$761,39 > 5,99$	1
16	β_{17}, β_{26}	$5,00e-6 < 1177,24$	$764,16 > 5,99$	1
17	$\beta_1 : \beta_3, \beta_6, \beta_7, \beta_{11}, \beta_{15}, \beta_{17}, \beta_{18}, \beta_{21}, \beta_{25}, \beta_{26}, \beta_{28}, \beta_{29}$	$400,49 < 1160,67$	$764,16 > 24,99$	0,74
23	$\beta_1, \beta_3, \beta_4, \beta_6, \beta_7, \beta_{11}, \beta_{14}, \beta_{15}, \beta_{17} : \beta_{21}, \beta_{23}, \beta_{26} : \beta_{28}, \beta_{30}$	$6,56e-4 < 1160,67$	$764,11 > 28,87$	1
25	$\beta_7, \beta_{17}, \beta_{19}, \beta_{20}, \beta_{26}, \beta_{27}, \beta_{30},$	$4,70e-6 < 1172,06$	$764,11 > 14,07$	1
26	β_{17}	$6,48e-8 < 1178,27$	$764,16 > 3,84$	1
28	$\beta_1, \beta_2, \beta_4 : \beta_{10}, \beta_{12}, \beta_{13} : \beta_{15}, \beta_{17}, \beta_{23} : \beta_{26}, \beta_{28}, \beta_{29}$	$505,01 < 1156,53$	$510,32 > 31,41$	0,67
30	$\beta_1, \beta_3 : \beta_8, \beta_{13} : \beta_{15}, \beta_{17}, \beta_{19} : \beta_{21}, \beta_{23}, \beta_{26}, \beta_{28}$	$641,27 < 1159,64$	$442,14 > 27,59$	0,57
31	$\beta_1, \beta_6 : \beta_8, \beta_{14}, \beta_{15}, \beta_{17}, \beta_{20}, \beta_{23}, \beta_{26}, \beta_{29}$	$261,01 < 1164,81$	$662,99 > 22,36$	0,83
all nodes	$\beta_1, \beta_4 : \beta_8, \beta_{11} : \beta_{13}, \beta_{15}, \beta_{17} : \beta_{21}, \beta_{23}, \beta_{26} : \beta_{30}$	$11492 < 13463,34$	$3412,26 > 33,92$	0,37

4.4.2 *Final Tests*

In this section we analyze the metrics in the larger final testbeds. We start with evaluating the Wilcoxon-Mann-Whitney tests before creating the logistic regression models.

Basic Metrics

The overall performance of the basic metrics can be seen in Table 4.11, showing the detection rate aggregated for all attacks, scenarios and nodes. The detection rate is defined as the sum of all significant Wilcoxon-Mann-Whitney tests that could detect the six different attacker models for each single metric. The most influenced metrics relate to the number of sent and received packets, as well as energy consumption.

Table 4.12 takes a closer look at how well the better metrics performed in detecting the specific attacks. In this case, we define an attack to be successfully detected if more than 75% of all the calculated Wilcoxon-Mann-Whitney tests for this attack have been significant. An interesting observation is the last metric NET sent packets, which did not have a detection rate of more than 75% in Table 4.11. Instead, the detection rate was only 66%. However, it is well-suited to detect the constant and the random jammers. In contrast to that, the similar overall performing metric transmit time is not listed in Table 4.12. This indicates that the metric NET sent packets performs very

Table 4.11: Overall performance - basic metrics - final testbeds

Metric	Detection rate
B09 - MAC received pkts	0.84
B11 - Radio energy	0.83
B07 - NET received pkts	0.83
B12 - Radio load	0.83
B08 - MAC sent pkts	0.80
B13 - MCU energy	0.80
B14 - MCU load	0.79
B05 - Listen duty cycle	0.79
B01 - RSSI	0.78
B04 - Transmit duty cycle	0.76
B02 - Transmit time	0.67
B06 - NET sent pkts	0.66
B03 - Listen time	0.57
B10 - Invalid CRC	0.39
B15 - Contention drop	0.37
B16 - Pending pkts	0.22
B18 - Too long pkts	0.22
B17 - Too short pkts	0.00

Table 4.12: Basic metrics with attack detection over 0.75 in the final testbeds

Metric	**Constant jammer**	**Random jammer**	**Blackhole + Random jammer**	**Blackhole + Reactive jammer**	**Blackhole**	**Reactive jammer**
B09 - MAC received pkts	✓	✓	✓	✓	✓	✓
B11 - Radio energy	✓	✓	✓	✓	✓	✓
B07 - NET received pkts	✓	✓	✓	✓	✓	✓
B12 - Radio load	✓	✓	✓	✓	✓	✓
B13 - MCU energy	✓	✓	✓	✓	✓	✓
B14 - MCU load	✓	✓	✓	✓	✓	-
B01 - RSSI	✓	✓	✓	✓	✓	-
B08 - MAC sent pkts	✓	✓	✓	✓	-	-
B04 - Transmit duty cycle	✓	✓	✓	✓	-	-
B05 - Listen duty cycle	✓	✓	✓	-	-	-
B06 - NET sent pkts	✓	✓	-	-	-	-

good in two cases, while the metric transmit time has a more constant detection rate, but is of lower quality for each attack.

Table 4.13: Overall performance - basic + CTP metrics - final testbeds

Metric	Detection rate
CTP12 - Number of neighbors	0.89
B09 - MAC received pkts	0.86
CTP10 - Link estimation	0.85
B05 - Listen duty cycle	0.85
B11 - Radio energy	0.84
CTP07 - Packet delivery rate	0.84
B07 - NET received pkts	0.84
CTP11 - Best neighbor	0.84
B12 - Radio load	0.84
B08 - MAC sent pkts	0.83
B13 - MCU energy	0.83
B14 - MCU load	0.82
B06 - NET sent pkts	0.81
B04 - Transmit duty cycle	0.79
B01 - RSSI	0.77
CTP04 - Received ACK pkts	0.75
CTP01 - Sent data pkts	0.73
CTP09 - Parent congestion	0.73
CTP02 - Received data pkts	0.69
CTP03 - Sent ACK pkts	0.69
B02 - Transmit time	0.68
B03 - Listen time	0.63
CTP06 - Dropped pkts	0.49
B15 - Contention drop	0.45
B10 - Invalid CRC	0.43
B18 - Too long pkts	0.32
CTP05 - Received duplicates	0.25
CTP08 - Changing parent	0.23
B16 - Pending pkts	0.22
B17 - Too short pkts	0.00

The constant jammer and the random jammer are the two most often detected attacks. They affect the majority of metrics. The combined attacker models with the blackhole attack and the random or reactive jammer are also detected by a large number of metrics. Finally, the blackhole attack and the reactive jammer showed the least amount of metrics suitable for detection. Regarding the blackhole attack, this is consistent with the results obtained in our initial tests. The reactive jammer is difficult to detect globally.

CTP Metrics

Table 4.13 shows the overall performance of the basic metrics together with the CTP specific metrics.

The CTP metric number of neighbors shows the best performance, having a detection rate of 0.89. Regarding the detected attacks, there are 18 metrics which can identify

an attack over all nodes with a probability of $p > 0.75$ (Table 4.14 shows the results averaged over both final testbeds). Note that the performance of many basic metrics obtained using the CTP has increased. In detail, these are NET sent packets, transmit duty cycle, MAC sent packets, MCU load and listen duty cycle. This is due to the ability of the CTP to notify a sender whether a packet has successfully arrived or not, leading to a performance increase for metrics related to packet transmission.

Table 4.14: Basic + CTP metrics with attack detection over 0.75 in the final testbeds

Metric	Constant jammer	Random jammer	Blackhole + Random jammer	Blackhole + Reactive jammer	Blackhole	Reactive jammer
CTP12 - Number of neighbors	✓	✓	✓	✓	✓	✓
B09 - MAC received pkts	✓	✓	✓	✓	✓	✓
CTP10 - Link estimation	✓	✓	✓	✓	✓	✓
B05 - Listen duty cycle	✓	✓	✓	✓	✓	✓
B11 - Radio energy	✓	✓	✓	✓	✓	✓
CTP07 - Packet delivery rate	✓	✓	✓	✓	✓	✓
B07 - NET received pkts	✓	✓	✓	✓	✓	✓
CTP11 - Best neighbor	✓	✓	✓	✓	✓	✓
B12 - Radio load	✓	✓	✓	✓	✓	✓
B13 - MCU energy	✓	✓	✓	✓	✓	✓
B14 - MCU load	✓	✓	✓	✓	✓	✓
B08 - MAC sent pkts	✓	✓	✓	✓	-	✓
B04 - Transmit duty cycle	✓	✓	✓	✓	✓	-
B06 - NET sent pkts	✓	✓	✓	✓	-	-
CTP01 - Sent data pkts	✓	✓	✓	-	-	-
CTP04 - Received ACK pkts	✓	✓	✓	-	-	-
B01 - RSSI	✓	✓	✓	-	-	-
CTP09 - Parent congestion	-	-	✓	✓	-	-

Mesh Metrics

As the mesh protocol only provides two additional network metrics and is lacking the advanced features of the CTP, the mesh metrics perform similar to the basic metrics. The results can be found in Appendix A.1.2.

Influence of the Testbed

The data in our final tests has been obtained in two physically separated locations. In this section, we analyze the influence of this parameter on the detection capabilities. Examplarily, we show the results for the CTP metrics in the final testbed 1 (Table 4.15) and in the final testbed 2 (Table 4.16). Further results are presented in Appendix A.1.2.

We observe the trend that a denser network like the final testbed 2 improves the detection. This is especially true for the constant jammer, the best metric having a detection rate of 0.99. In contrast to that, the detection of the blackhole attack remains mainly unchanged (even a slight tendency for better detection in the sparser final testbed 1 is noticeable). The reason for these results is given by the attack characteristics. Jamming can create more damage, if the network is denser, by rendering more nodes unavailable. Regarding the blackhole attack, changes to the topology (caused by the attacker) can be observed better, if the network is sparser.

Table 4.15: Detection rates CTP metrics - final testbed 1

Metric	Constant jammer	Random jammer	Reactive jammer	Blackhole	Blackhole + Random jammer	Blackhole + Reactive jammer
CTP12 - Number of neighbors	0.87	0.85	0.83	0.88	0.90	0.87
CTP07 - Packet delivery rate	0.87	0.80	0.80	0.84	0.78	0.83
CTP10 - Link estimation	0.74	0.76	0.78	0.78	0.88	0.88
CTP11 - Best neighbor	0.78	0.77	0.79	0.78	0.86	0.84
CTP09 - Parent congestion	0.70	0.63	0.66	0.65	0.78	0.75
CTP04 - Received ACK pkts	0.74	0.64	0.62	0.64	0.77	0.74
CTP03 - Sent ACK pkts	0.65	0.64	0.66	0.65	0.70	0.73
CTP02 - Received data pkts	0.65	0.64	0.66	0.65	0.70	0.73
CTP01 - Sent data pkts	0.74	0.65	0.57	0.62	0.72	0.71
CTP06 - Dropped pkts	0.43	0.43	0.47	0.42	0.48	0.46
CTP05 - Received duplicates	0.27	0.19	0.18	0.24	0.24	0.31
CTP08 - Changing parent	0.20	0.16	0.13	0.16	0.22	0.19

Influence of the Density

The density within a specific testbed has only a minor influence on the metrics. The results can be found in Appendix A.1.2.

Influence of the Traffic Intensity

The traffic intensity may have different effects on the metrics, depending on the specific attack. For example, the blackhole is highly dependent on the number of packets sent by other nodes. The results can be found in Appendix A.1.2. We notice that the detection rates mainly increase for all attacks when more traffic is sent. This is expected, as an attacker can stronger influence the network given higher traffic.

Table 4.16: Detection rates CTP metrics - final testbed 2

Metric	Constant jammer	Random jammer	Reactive jammer	Blackhole	Blackhole + Random jammer	Blackhole + Reactive jammer
CTP12 - Number of neighbors	0.99	0.86	0.78	0.83	0.87	0.81
CTP10 - Link estimation	0.93	0.83	0.81	0.84	0.85	0.81
CTP11 - Best neighbor	0.86	0.83	0.79	0.80	0.83	0.81
CTP07 - Packet delivery rate	0.92	0.79	0.80	0.76	0.79	0.80
CTP04 - Received ACK pkts	0.92	0.85	0.64	0.67	0.84	0.67
CTP01 - Sent data pkts	0.97	0.87	0.59	0.60	0.85	0.65
CTP09 - Parent congestion	0.74	0.73	0.71	0.71	0.73	0.73
CTP03 - Sent ACK pkts	0.73	0.69	0.65	0.63	0.69	0.64
CTP02 - Received data pkts	0.73	0.69	0.65	0.63	0.69	0.64
CTP06 - Dropped pkts	0.51	0.50	0.50	0.48	0.50	0.49
CTP08 - Changing parent	0.40	0.32	0.20	0.22	0.29	0.23
CTP05 - Received duplicates	0.42	0.21	0.20	0.23	0.29	0.17

Influence of the Attacker Location and Start

In general, two attackers increase the detection rates, which is expected. The start of the attack, however, did not show significant differences in detection rates. Even though in the setting with no delay, an attacker has higher chances to prevent a WSN from operating, the attack effects are still strong enough when starting the attack in the middle of the test-run. In other settings, different from our setup, this behavior may change. The results are presented in Appendix A.1.2.

Comparison to the Initial Tests

The results obtained with the larger testbeds are similar to those of the smaller testbeds. The large majority of metrics, that reach at least class B quality in the initial tests, are also among the best metrics with attack detection over 0.75 in the final tests (see Table 4.17). Minor differences occur due to the size of the networks, some metrics are only influenced significantly if they are direct neighbors of the attacker. Metrics marked as N/A have not been analyzed in the initial tests. Hence, we have shown that our identified metrics are widely applicable for attack detection.

Logistic Regression

In our final tests, there are three different groups of models that have been created and evaluated using a logistic regression:

Table 4.17: Comparison between the initial and the final tests: metrics of good quality for attack detection

Final Tests	**Initial Tests**
Best neighbor	N/A
Link estimation	Link estimation
Listen duty cycle	Listen duty cycle
-	Listen time
MAC received pkts	MAC received pkts
MAC sent pkts	MAC sent pkts
MCU energy	MCU energy
MCU load	MCU load
NET received pkts	NET received pkts
NET sent pkts	NET sent pkts
No. of neighbors	No. of neighbors
Packet delivery rate	Packet delivery rate
Parent congestion	N/A
Radio energy	Radio energy
Radio load	Radio load
Received ACK pkts	Received ACK pkts
-	Received data pkts
RSSI	RSSI
-	Sent ACK pkts
Sent data pkts	Sent data pkts
Transmit duty cycle	Transmit duty cycle
-	Transmit time

- Single nodes:
  This analysis is the similar to the Wilcoxon-Mann-Whitney evaluation, because a logistic regression model is created for each single node.

- All nodes:
  In an attempt to create generally applicable models, we used the data of all nodes as input.

- All neighboring nodes:
  The last group consists of models, that only take the data of the direct neighbors of the attacker into account.

For assessing the model fit, we now concentrate on McFaddens-R^2, because it is considered the most appropriate for logistic regression [Meno2]. The calculated McFaddens-R^2 classifies the models in three categories:

- **Bad models:** returned a McFaddens-R^2 of < 0.2

- **Acceptable models:** a McFaddens-R^2 in the interval $[0.2 - 0.4]$ indicates an acceptable model fit

- **Perfect models:** a value of > 0.4 for the McFaddens-R^2 represents a perfect model fit

Our analysis showed that the models created for all nodes do not perform well, because there are nodes too distant from the attacker to be influenced significantly (see Appendix A.1.3). Hence, in the following we concentrate on the single and neighboring nodes. For each of the remaining two groups an overview is given about the model quality for the specific attacks. In addition, the metrics are ranked according to the number of occurences in the models. Finally, we show how many metrics are included per model. A high count of metrics indicates that the models are very specific, and detection in different settings may be difficult.

Single Nodes

Using the data of individual nodes as input, we create separate logistic regression models for each node.

Table 4.18: Model quality - single nodes - basic metrics - final testbeds

		Mesh		CTP	
		Count	Percent	Count	Percent
JammingCnst	Bad model	59	0.056	33	0.032
	Acceptable model	106	0.100	118	0.115
	Perfect model	891	0.844	873	0.853
	Sum usable models	997	0.944	991	0.968
JammingRnd	Bad model	37	0.035	39	0.038
	Acceptable model	160	0.152	172	0.168
	Perfect model	859	0.813	813	0.794
	Sum usable models	1019	0.965	985	0.962
JammingReact	Bad model	191	0.181	148	0.145
	Acceptable model	281	0.266	315	0.308
	Perfect model	584	0.553	561	0.548
	Sum usable models	865	0.819	876	0.855
SingleBlackhole	Bad model	174	0.165	125	0.122
	Acceptable model	311	0.295	298	0.291
	Perfect model	571	0.541	601	0.587
	Sum usable models	882	0.835	899	0.878
BlackholeReactJamming	Bad model	132	0.250	46	0.090
	Acceptable model	209	0.396	156	0.305
	Perfect model	187	0.354	310	0.605
	Sum usable models	396	0.750	466	0.910
BlackholeRndJamming	Bad model	34	0.064	22	0.043
	Acceptable model	107	0.203	102	0.199
	Perfect model	387	0.733	388	0.758
	Sum usable models	494	0.936	490	0.957

BASIC METRICS Table 4.18 shows the results when using only the basic metrics in the CTP and mesh setting. A usable model is defined as a model of at least acceptable quality. The basic metrics obtained from the CTP runs show a mean percentage of about 0.92 usable models, while this rate is reduced to about 0.87 in the mesh runs.

Table 4.19 presents the most frequently used basic metrics in the regression models. The results are similar to the Wilcoxon-Mann-Whitney test, especially metrics related to network traffic are very useful.

Table 4.19: Most often used basic metrics in all single node models - final testbeds

Metric	Occurences (%)
B06 - NET sent pkts	84.4
B07 - NET received pkts	80.5
B01 - RSSI	67.5
B08 - MAC sent pkts	64.9
B13 - MCU energy	57.1
B09 - MAC received pkts	56.5
B11 - Radio energy	53.2
B04 - Transmit duty cycle	51.9
B05 - Listen duty cycle	46.7
B03 - Listen time	37.6
B10 - Invalid CRC	36.6
B02 - Transmit time	36.3
B12 - Radio load	32.4
B14 - MCU load	31.1
B15 - Contention drop	30.9
B18 - Too long pkts	23.8
B16 - Pending pkts	12.9
B17 - Too short pkts	6.4

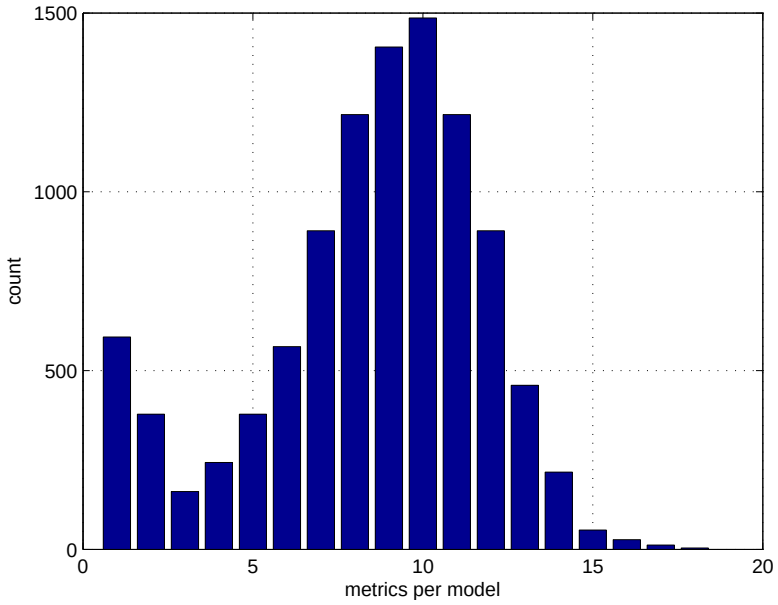

Figure 4.11: Count of metrics used in each model created for single nodes using basic metrics - final testbeds

We now analyze how many metrics are included in each generated model. Figure 4.11 shows the distribution, the majority of models do not need more than 10 metrics. There are also models requiring only one metric and having at least an acceptable model fit. The metric no. of sent packets on the MAC layer occurs in almost 400 models as a single metric, and thus is well-suited to differentiate between attack

and no-attack. In addition, the metrics MCU energy and radio energy appear as single metrics in a smaller number of models (about 25 models in total). Taking a closer look at which attacks can be detected by solely using the no. of sent packets on the MAC layer as metric, we find that it can detect a constant jammer reliably.

Table 4.20: Model quality - single nodes - protocol specific metrics - final testbeds

		Mesh		CTP	
		Count	Percent	Count	Percent
JammingCnst	Bad model	92	0.087	1	0.001
	Acceptable model	121	0.115	9	0.009
	Perfect model	843	0.798	1014	0.990
	Sum usable models	964	0.913	1023	0.999
JammingRnd	Bad model	104	0.098	1	0.001
	Acceptable model	280	0.265	22	0.021
	Perfect model	672	0.636	1001	0.978
	Sum usable models	952	0.902	1023	0.999
JammingReact	Bad model	310	0.294	6	0.006
	Acceptable model	430	0.407	42	0.041
	Perfect model	316	0.299	976	0.953
	Sum usable models	746	0.706	1018	0.994
SingleBlackhole	Bad model	269	0.255	6	0.006
	Acceptable model	463	0.438	41	0.040
	Perfect model	324	0.307	977	0.954
	Sum usable models	787	0.745	1018	0.994
BlackholeReactJamming	Bad model	121	0.229	1	0.002
	Acceptable model	194	0.367	8	0.016
	Perfect model	213	0.403	503	0.982
	Sum usable models	407	0.771	511	0.998
BlackholeRndJamming	Bad model	29	0.055	0	0.000
	Acceptable model	99	0.188	5	0.010
	Perfect model	400	0.758	507	0.990
	Sum usable models	499	0.945	512	1.000

PROTOCOL METRICS From Table 4.20 we observe that using the CTP metrics, a large number of usable models can be created for all tested attacks. The metrics of the mesh protocol have more difficulties to detect the reactive jammer, the blackhole, as well as a combination of both. The results of the Wilcoxon-Mann-Whitney tests also using single nodes as input are similar.

Table 4.21 shows the relevant metrics using the CTP. Out of the CTP specific metrics, the number of neighbors and the packet delivery rate appear in many models.

An interesting finding is, that the metric sent ACK pkts is never included in the logistic regression models, but it had a detection rate of 0.69 according to the Wilcoxon-Mann-Whitney test. This means that other metrics capture the effects of this metric as well.

Including the CTP metrics during model creation leads to a large number of models containing only one metric, as can be seen in Figure 4.12. Metrics such as the packet delivery rate have the ability to detect attacks without further metrics.

Table 4.21: Most often used CTP metrics in all single node models - final testbeds

Metric	Occurences (%)
B06 - NET sent pkts	59.3
B07 - NET received pkts	57.9
B01 - RSSI	49.6
B08 - MAC sent pkts	44.8
B13 - MCU energy	42.7
B11 - Radio energy	40.6
B09 - MAC received pkts	40.0
B04 - Transmit duty cycle	35.8
B05 - Listen duty cycle	34.4
CTP12 - Number of neighbors	31.7
CTP07 - Packet delivery rate	28.9
B12 - Radio load	28.2
B10 - Invalid CRC	27.5
B14 - MCU load	26.2
B03 - Listen time	26.0
B02 - Transmit time	25.8
CTP11 - Best neighbor	24.8
B15 - Contention drop	22.0
CTP10 - Link estimation	19.3
B18 - Too long pkts	15.8
CTP09 - Parent congestion	15.5
CTP02 - Received data pkts	11.7
CTP04 - Received ACK pkts	11.6
CTP01 - Sent data pkts	9.6
B16 - Pending pkts	8.2
CTP08 - Changing parent	5.5
CTP06 - Dropped pkts	5.3
B17 - Too short pkts	4.1
CTP05 - Received duplicates	4.0
CTP03 - Sent ACK pkts	0.2

Regarding the mesh metrics, their overall performance is very similar to those of the basic metrics (see Table 4.22). The two mesh metrics are frequently used in the models, but the basic metrics transmitted and received packets on the network layer are more significant.

Comparing the number of metrics per model to the CTP setting, we notice that the amount of models using only one metric is significantly reduced (see Figure 4.13). This is because also the basic metrics are influenced by the higher level checks of the CTP for packet successful reception. Using the mesh protocol, the positive influence of these mechanisms is lacking.

All Neighboring Nodes

The models created for single nodes turned out to be very good. The only drawback is, that they are very node specific. To solve this problem and to obtain more generally usable metrics, the logistic regression function was given the aggregated data of all

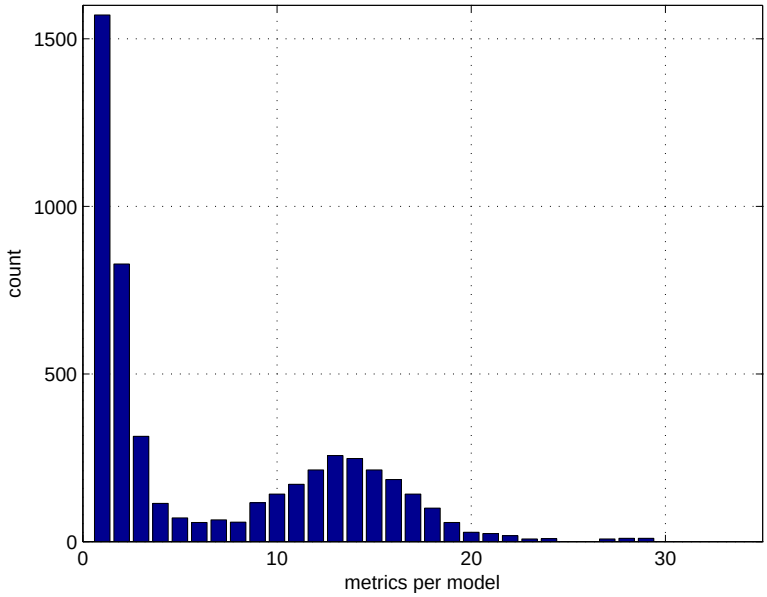

Figure 4.12: Count of metrics used in each model created for single nodes using CTP metrics - final testbeds

Table 4.22: Most often used mesh metrics in all single node models - final testbeds

Metric	Occurences (%)
B06 - NET sent pkts	59.4
B07 - NET received pkts	58.1
B01 - RSSI	50.0
B08 - MAC sent pkts	44.5
B13 - MCU energy	41.8
B11 - Radio energy	40.5
B09 - MAC received pkts	39.1
M02 - No. of routing entries	37.8
B04 - Transmit duty cycle	35.1
M01 - No. of direct neighbors	34.9
B05 - Listen duty cycle	33.7
B12 - Radio load	28.3
B10 - Invalid CRC	27.9
B14 - MCU load	25.9
B03 - Listen time	25.7
B02 - Transmit time	25.3
B15 - Contention drop	21.6
B18 - Too long pkts	16.2
B16 - Pending pkts	8.1
B17 - Too short pkts	4.0

nodes as input. However, the model quality turned out to be bad because of the range of the attack on the network. Whereas the direct neighbors of the attacker exhibit significant changes in their metrics when under attack, the very distant nodes may not

Figure 4.13: Count of metrics used in each model created for single nodes using mesh metrics - final testbeds

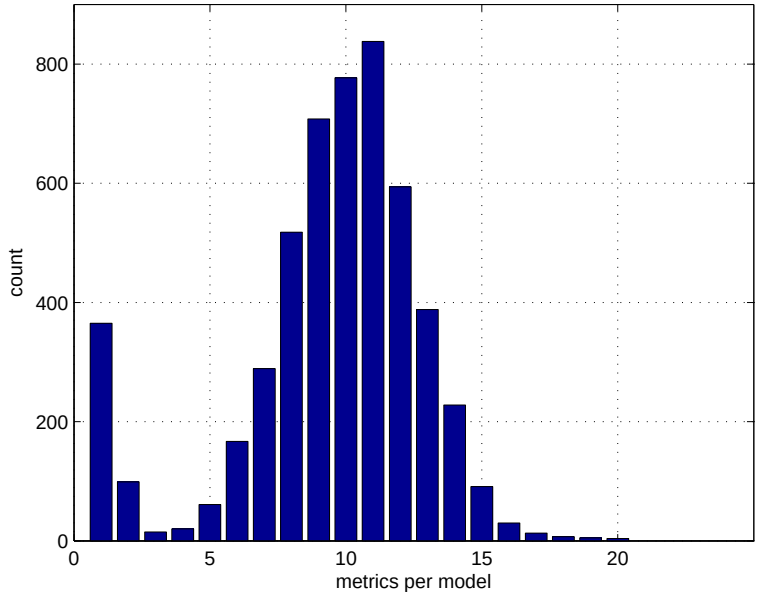

detect any changes in the network at all. Including these distant nodes in the model creation phase proved to be a disadvantage, as can be seen in Appendix A.1.3.

Therefore, in this section we analyze the logistic regression models created taking only the neighboring nodes of the attacker into account. Table 4.23 shows all the nodes which are one-hop away from an attacker.

The most often used metrics in the models created for neighboring nodes are similar to the single node setting. However, they typically require more metrics per model. This holds for basic, CTP, as well as mesh metrics. The corresponding results are shown in Appendix A.1.4. The most promising models are obtained when using protocol-specific metrics, especially CTP metrics. Figure A.5 reveals that several models using the CTP require less than 6 metrics per model and thus outperform the mesh metrics as shown in Figure A.6.

BASIC METRICS The amount of usable models for detecting an attack, when focussing on the basic metrics, is shown in Table 4.24. Except for the models created for the constant as well as the random jamming, the amount of usable models is reduced compared to the models created for single nodes.

PROTOCOL METRICS Table 4.25 shows that the CTP produces perfect models more often than using the mesh. Even though also the mesh protocol is able to detect the jammers, the amount of usable models for blackhole and combined blackhole attackers is low. These results are in line with the initial tests, showing that the mesh protocol metrics cannot offer a good blackhole detection, even when using a combination of multiple metrics.

Table 4.23: Attacker neighbors

Final testbed 1

Node	Attacker
6	5
7	5
10	23
14	23
16	23
19	23
20	23
21	23
24	23
25	23
26	23
27	23
28	23
29	23
30	23
31	23
32	23

Final testbed 2

Node	Attacker
11	27
12	27
17	27
19	27
20	27
21	27
22	27
25	27
26	27
28	27
29	56
32	56
33	56
35	56
36	27
38	56
49	56
51	56
53	56
54	56
57	56
58	56

4.5 IDS

We now describe the fully localized IDS, which does not rely on collaboration. Therefore, we present the system, its storage requirements, its computation time, and its energy consumption in Section 4.5.1. Next, we discuss the models selected for intrusion detection in Section 4.5.2. Finally, we evaluate the IDS in Section 4.5.3.

4.5.1 *Implementation*

In this section, we implement an IDS on the nodes based on the usage of the previously created logistic regression models. Hence, we do not calculate the models on the nodes, but let them evaluate the existing models using the steps already presented in Section 4.4.1:

Table 4.24: Model quality - neighboring nodes - basic metrics - final testbeds

		Mesh Count	Mesh Percent	CTP Count	CTP Percent
JammingCnst	Bad model	0	0.000	0	0.000
	Acceptable model	0	0.000	0	0.000
	Perfect model	32	1.000	32	1.000
	Sum usable models	32	1.000	32	1.000
JammingRnd	Bad model	5	0.156	5	0.156
	Acceptable model	20	0.625	18	0.563
	Perfect model	7	0.219	9	0.281
	Sum usable models	27	0.844	27	0.844
JammingReact	Bad model	21	0.656	25	0.781
	Acceptable model	7	0.219	3	0.094
	Perfect model	4	0.125	4	0.125
	Sum usable models	11	0.344	7	0.219
SingleBlackhole	Bad model	26	0.813	19	0.594
	Acceptable model	5	0.156	10	0.313
	Perfect model	1	0.031	3	0.094
	Sum usable models	6	0.188	13	0.406
BlackholeReactJamming	Bad model	16	1.000	9	0.563
	Acceptable model	0	0.000	7	0.438
	Perfect model	0	0.000	0	0.000
	Sum usable models	0	0.000	7	0.438
BlackholeRndJamming	Bad model	8	0.500	11	0.688
	Acceptable model	0	0.000	5	0.313
	Perfect model	8	0.500	0	0.000
	Sum usable models	8	0.500	5	0.313

Given: Regression coefficients $\beta_0, \ldots, \beta_k$ and

data set $x_1, \ldots, x_k$

Step 1: Creation of the logit model

$$\eta = \beta_0 + \beta_1 \cdot x_1 + \cdot + \beta_k \cdot x_k$$

Step 2: Calculation of the logit η

Step 3: Calculation of the logistic function

$$\hat{\Pi}_i = \frac{1}{1+e^{-\eta}}$$

Step 4: Decision

If $\hat{\Pi}_i > 0.5 \longrightarrow$ Attack detected

Implementing these steps requires only a single funtion, resulting in few lines of code. This function is given the current metric readings. A `for` loop iterating over all metric readings is needed in order to calculate the logit model. Calculating the logistic function is performed in three steps. The first step involves inverting the sign of the

Table 4.25: Model quality - neighboring nodes - protocol specific metrics - final testbeds

		Mesh		CTP	
		Count	Percent	Count	Percent
JammingCnst	Bad model	0	0.000	0	0.000
	Acceptable model	0	0.000	0	0.000
	Perfect model	32	1.000	32	1.000
	Sum usable models	32	1.000	32	1.000
JammingRnd	Bad model	2	0.063	0	0.000
	Acceptable model	20	0.625	12	0.375
	Perfect model	10	0.313	20	0.625
	Sum usable models	30	0.938	32	1.000
JammingReact	Bad model	22	0.688	15	0.469
	Acceptable model	6	0.188	9	0.281
	Perfect model	4	0.125	8	0.250
	Sum usable models	10	0.313	17	0.531
SingleBlackhole	Bad model	28	0.875	9	0.281
	Acceptable model	3	0.094	6	0.188
	Perfect model	1	0.031	17	0.531
	Sum usable models	4	0.125	23	0.719
BlackholeReactJamming	Bad model	16	1.000	4	0.250
	Acceptable model	0	0.000	5	0.313
	Perfect model	0	0.000	7	0.438
	Sum usable models	0	0.000	12	0.750
BlackholeRndJamming	Bad model	8	0.500	3	0.188
	Acceptable model	0	0.000	5	0.313
	Perfect model	8	0.500	8	0.500
	Sum usable models	8	0.500	13	0.813

logit model, before $e^{-\eta}$ is calculated. For that purpose, an extra math library has to be loaded in Contiki for providing floating point arithmetics. Finally, the logistic function is calculated and evaluated by an if-condition.

ROM and RAM Usage

One key aspect of the developed IDS is to be lightweight. Hence, the additional ROM and RAM consumption which is introduced by the IDS is measured in this section. Table 4.26 compares the ROM and RAM consumption of the baseline Contiki without IDS to the IDS used with a different amount of metrics.

The increase of about 8056 bytes when adding the IDS is mainly due to the needed math libraries for floating point arithmetic. Every metric which is added leads to an increase of about 20 to 38 bytes. This increase per metric is slightly different, because the applied compiler parameters and optimizations affect the firmware image size. Per metric, the RAM usage increases by 4 bytes, which corresponds to the needed amount for one variable of the type double. Given that the required math library is not already loaded, an IDS image which makes use of one metric leads to an increase of the firmware size by about 26 % as compared to the baseline image. However, an option is to import only the code for the `powf()` function instead of the whole library.

Table 4.26: IDS ROM and RAM usage

Image	ROM in bytes	RAM in bytes
Contiki without IDS	30164	6848
IDS with 1 metric	38220	6852
IDS with 2 metrics	38280	6856
IDS with 3 metrics	38320	6860
IDS with 5 metrics	38382	6868
IDS with 10 metrics	38586	6888
IDS with 15 metrics	38776	6908
IDS with 20 metrics	38956	6928
IDS with 25 metrics	39088	6948

Each added metric increases the image slightly by about 0.1%. In our setting, the node started to refuse to boot with an amount of 700 metrics.

IDS Computation Time and Energy Consumption

We measure the clock ticks needed for the IDS function call, using between 1 and 25 different metrics. It takes four to five clock ticks to perform this task, which is between about 31 ms and 39 ms. The most expensive computation is the floating point arithmetic to exponentiate using `powf()`. Next, we measure the additional energy consumption of the IDS. The lowest energy consumption was obtained for one metric, resulting in about 330 µJ per IDS function call. If 25 metrics are used, the energy consumption is about 463 µJ. In cases when the result of the calculated logit model was largely negative, the `powf()` call simply returned the value 0 without actually calculating. In such situations, the energy consumption highly decreased to about 100 µJ.

4.5.2 *Selected Model*

In order to evaluate the applicability of different models for attack detection, we have chosen them according to the number of metrics used and the resulting model quality. We expect models with few metrics to perform better in a similar, but different testing environment than the environment they have been created for. The main performance metrics are the false-positive as well as the detection rates. In addition, we analyze the time it takes to detect the attack. The scenario we investigate has the following properties:

- ▷ **Testbed:** Final testbed 1
- ▷ **Protocol:** CTP
- ▷ **Transmission power:** High
- ▷ **Traffic intensity:** Low

This testbed was chosen because the environment is more challenging, and therefore the attack detection is harder. With the CTP, we expect to be able to detect the blackhole attack better than with the mesh protocol.

We concentrate on detecting the constant jammer, the blackhole, as well as the combination of blackhole and random jammer. For each of these attacker models, we focus on logistic regression models that have been created by analyzing the data of the direct neighbors of the attacker.

Constant Jammer

As we can observe from Table 4.27, two out of the four available models involve just one metric for attack detection, while at the same time they achieve a perfect model quality. These single metrics are respresented by the packet delivery rate and the number of sent packets on the MAC layer, respectively. The packet delivery rate exhibits significantly different values when the attack occurs. However, there is a high variation for each node, which is not the case for the number of sent packets on the MAC layer. Hence, we choose the bold printed model in Table 4.27 for evaluation.

Table 4.27: Constant jammer models

Parameter	Model quality	Count of used metrics
Inner attacker, no delay	0.99	1: CTP07 - Packet delivery ratio
Inner attacker, delay	**0.99**	**1: B08 - MAC sent pkts**
Both attackers, no delay	0.94	18
Both attackers, delay	0.84	24

Blackhole

For the blackhole attack, we again selected a model with a perfect model quality, this time using more than one metric. This bold printed model is shown in Table 4.28.

Blackhole and Random Jammer

The number of available models is reduced to two when using the combined attackers. While both models require a similar amount of metrics, only the first model has a perfect model quality. The details of the selected bold printed model are shown in Table 4.29.

Table 4.28: Blackhole models

Parameter	Model quality	Count of used metrics
Inner attacker, no delay	**0.99**	**6**
Both attackers, no delay	0.73	22
Inner attacker, delay	0.51	16
Both attackers,delay	0.28	21

Table 4.29: Blackhole and random jammer models

Parameter	Model quality	Count of used metrics
Both attackers, no delay	**0.47**	**20**
Both attackers, delay	0.07	21

4.5.3 *Evaluation*

Figure 4.14: Mote placement in the IDS evaluation testbed

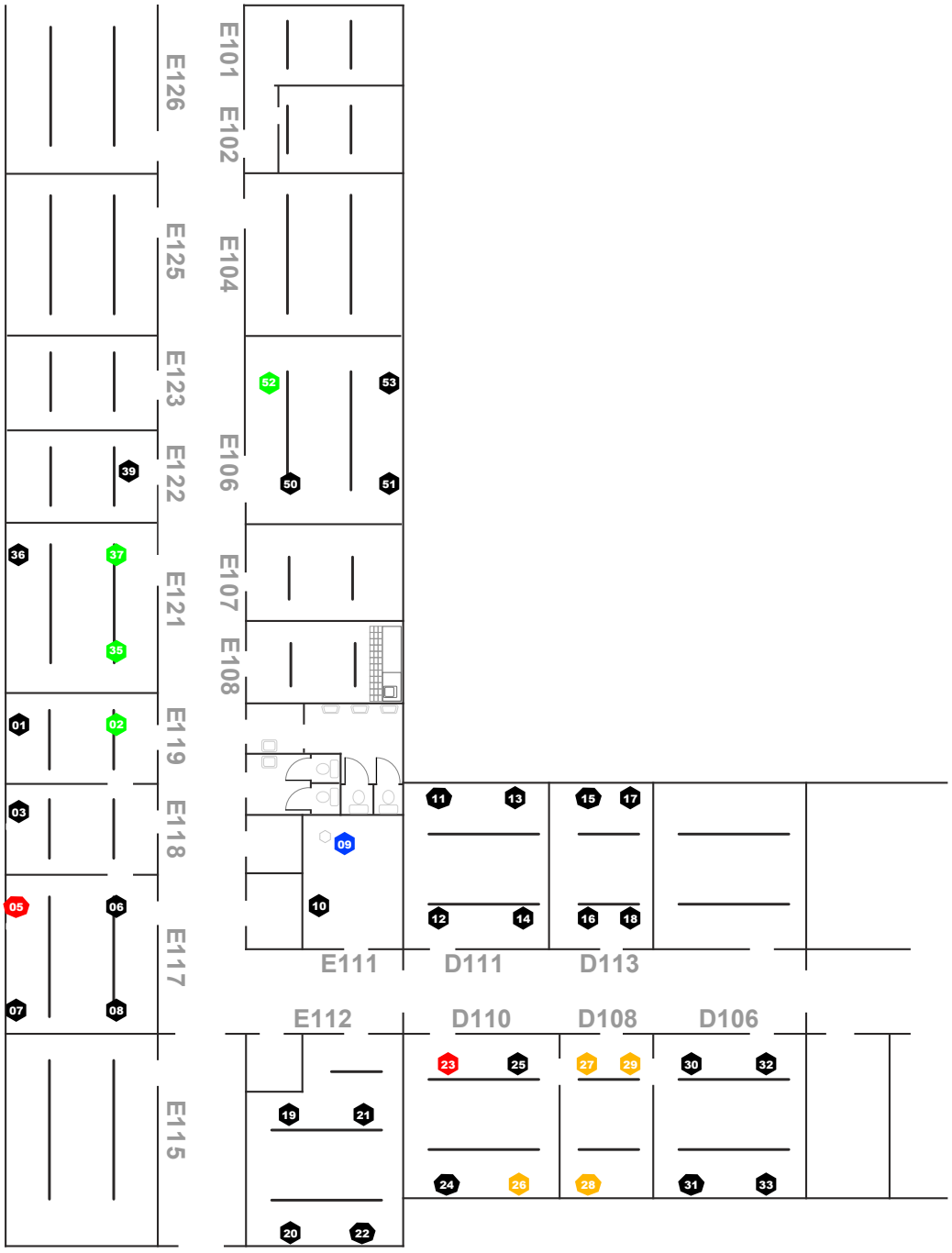

Next, we deploy the selected models to real sensor nodes. We use a similar, but different (see below for a description) testbed for our experiments. The testbed parameters for evaluating the IDS models are as follows:

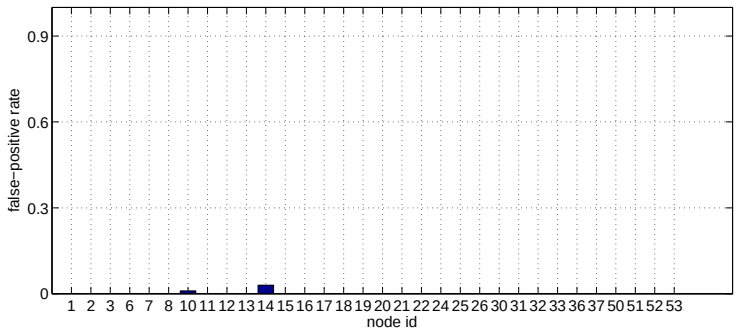

Figure 4.15: False-positives for model 1 (constant jammer)

- ▷ **Testbed:** Similar to final testbed 1
- ▷ **Protocol:** CTP
- ▷ **Transmission power:** High
- ▷ **Traffic:** Low
- ▷ **Attacker location:** Outer and inner
- ▷ **Attack delay:** No delay
- ▷ **Repetitions**: 5

Note that the evaluated models partly have been created with different parameters. There is also a change in the network topology, because four nodes have been replaced, as shown in Figure 4.14. Nodes marked in green have been added, while nodes marked in orange have been removed, as compared to the final testbed 1. The attacking nodes remain the same. We start the evaluation with running the IDS in a setting without attackers, in order to determine the false-positive rates. The detection function is always called after a node has updated its metrics, i.e., every 4 seconds. Each test-run has a duration of 15 minutes and is repeated five times for each scenario.

Neutral Runs

The false-positive rate for each model is tracked directly from the start of the test-run, including the initialization phase where the network is established. Since there is no attacker present, no attack should be detected.

MODEL 1 - CONSTANT JAMMER - FALSE-POSITIVES The false-positive rate for the constant jammer detection model is depicted in Figure 4.15. For most of the nodes we achieve a false-positive rate of 0%.

MODEL 2 - BLACKHOLE - FALSE-POSITIVES Although only a few good regression models have been created for the blackhole attack, the false-positive rate is in general low (see Figure 4.16). Recall that the blackhole was one of the attacks that are difficult to detect with the Wilcoxon-Mann-Whitney test.

MODEL 3 - BLACKHOLE + RANDOM JAMMER - FALSE-POSITIVES The model resulting from the combination of blackhole and random jammer included 20 metrics. Still, the false-positive rate shown in Figure 4.17 is rather low.

Attack Runs

This section is devoted to describe the evaluation of the the attack runs, with a present attacker. The detection rate is defined as percentage of correctly identified attacks, given the periodic metric measurements, and is averaged over the 5 different test-runs. Nodes marked with a "*" are neighbors of an attacker.

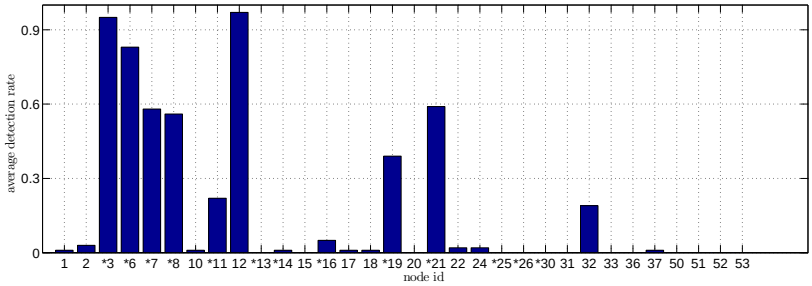

Figure 4.18: Model 1 - constant jammer - detection rate

ATTACK DETECTION - MODEL 1 - CONSTANT JAMMER The constant jammer can reliably be detected on certain nodes, as can be seen in Figure 4.18. The outer attacker at node 5 influenced its neighbors significantly, while the attacker at node 23 was difficult to detect. The density around node 5 is lower, indicating that the model is able to better identify the attacker if fewer normal traffic is observed. The detection time of the neighboring node 3 is about one minute, measured from the start of the test-run. After the network has stabilized (which takes about one minute), the attack is almost instantly detected.

ATTACK DETECTION - MODEL 2 - BLACKHOLE The detection of the blackhole attack performs quite well, a large number of nodes detect the attack as shown in Figure 4.19. This is especially true for the neighboring nodes of the attacker, but also some non-neighbors identified the attack. The detection time is very similar to the

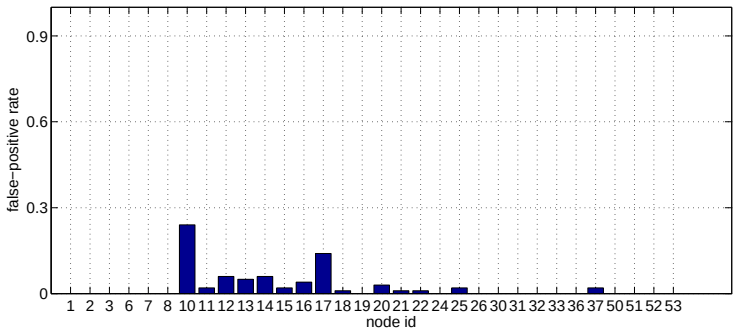

Figure 4.16: False-positives for model 2 (blackhole)

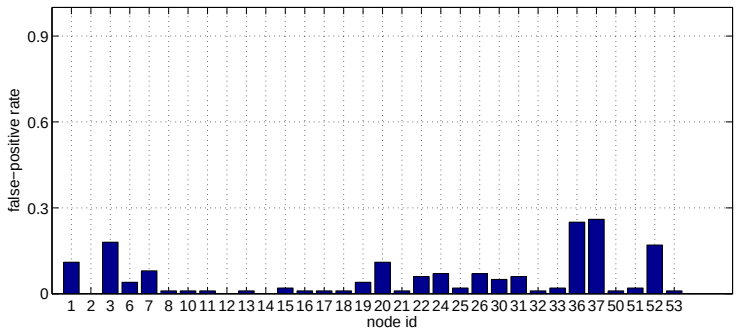

Figure 4.17: False-positives for model 3 (blackhole + random jammer)

constant jammer. During the first minute, the detection alternates between true and false, and then stabilizes.

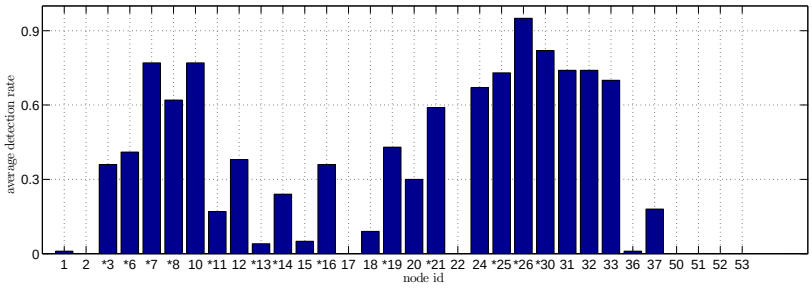

Figure 4.19: Model 2 - blackhole - detection rate

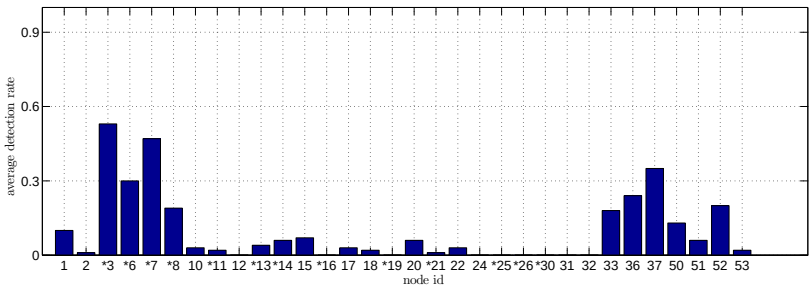

Figure 4.20: Model 3 - blackhole and random jammer - detection rate

ATTACK DETECTION - MODEL 3 - BLACKHOLE AND RANDOM JAMMER The detection rates for the combination of blackhole and random jammer are very low. This is due to the large number of metrics that are needed in the model, it cannot be generalized to other wireless sensor networks. Yet, the nodes near the random jammer at node 5 did detect the attack, as shown in Figure 4.20. In contrast to that, the blackhole at node 23 has not been detected.

4.6 DISCUSSION

Except for the metric dealing with too short packets, all other metrics we tested with the Wilcoxon-Mann-Whitney test are at least able to detect the jamming attack. The distinction capabilities in the case of a blackhole attack are a little worse, as the metric classification exhibits. The reason for these results is the different types of attacks. Jamming targets the physical or low layer communication medium, while the blackhole is an attack on the routing algorithms at higher layers. Therefore, it is difficult to find indications for a blackhole at the lower layers. One of the best blackhole metrics in the collect network is the link estimation, which measures the link quality to the neighbors with expected transmissions to the sink as cost metric. Routing algorithms make use of these values on higher layers. Therefore, the link estimation provides information about network anomalies with regard to manipulated values. For this reason, the metric might also have detection capabilities for sinkholes and wormholes, being also based on the same traffic attracting scheme.

The received packet rate on the MAC layer, counting all received regular packets using the radio chip, is another metric that can detect jamming attacks. The implemented attacker uses regular packets for the jamming, which is the reason for the highly increased values in the jamming scenarios. If a jammer uses a random signal without any packet structure, this metric might be unsuitable for jamming detection.

Regarding the results of the IDS using logistic regression models, we have shown that some models are general enough to detect attacks in different networks than they have been created for. We want to emphasize that the same IDS image was uploaded to all nodes, which has been created taking into account the data of the neighbors of the attacker. If a node-specific model would have been used in the same testbed the data has been gathered with, we expect even better results with regard to false-positives and detection rates. However, it may be limited to very similar networks.

As we have seen, in the final tests it was necessary to change the metric classification that has been originally applied in the initial tests. In larger testbeds, depending on the attack, there are nodes that are too distant from the attacker, and hence their metrics are not influenced significantly. For the same reason, including such nodes in the model generation of the logistic regression is a disadvantage. It was further shown, that in many cases the combination of metrics leads to better results with regard to attack detection. However, in certain scenarios, e.g., using the CTP, a single metric can effectively differentiate between attack and no attack. If many metrics are included in a model, there is a higher probability that it is overfitted to the training data. From the above mentioned observations we can derive guidelines on how to design the IDS: (1) when building the model, the focus should be on nodes that are close to the attacker, and (2) models with fewer metrics should be preferred over models with a better statistical model quality, but with a larger number of metrics, if it is desired to create a model that can be applied to slightly different networks.

4.7 RELATED WORK

Apart from the works mentioned in Chapter 3, the closest approach to ours has recently been presented in [PAS+14]. The authors detect jamming attacks in IEEE

802.11 networks with the assistance of a machine learning algorithm. Similar to us, they analyze the impact of jamming attacks on the system performance by investigating six metrics that are either directly influenced by the attacks, or that support the attack decision. However, the paper does not focus on identifying the most significant metrics for attack detection. In a training phase, data is collected and then provided to the machine learning algorithms for model creation. The authors focus on a classifier called Random Forests, which is based on decision trees. The detection accuracy is improved by including all metrics in the learning process instead of a single metric. Deploying the created models to the devices allows an on-the-fly jamming detection.

4.8 SUMMARY

In this chapter, the effects of DoS attacks on a large number of distinct performance and network metrics in WSNs are studied in a systematic way. We identify widely applicable metrics and verify that they show a significantly different behavior under attack when compared to the baseline operation. The local metrics are able to detect jamming and blackhole attacks in a lightweight and practical way, since they are easily obtained without incurring too much overhead. Most of the metrics are already calculated by the lower network layers. Hence, it is possible to directly implement the intrusion detection mechanisms in the operating system of the sensor nodes to locally detect network anomalies. Unlike our proposed intrusion detection systems in Chapters 5 and 6, this system is immediately working and does not require a start-up phase. There is no need for communication with other nodes, it is fully localized. Using models with few metrics proved to be more accurate than using models with multiple metrics. While the overhead of the IDS is very low, attackers can be detected reliably. We have shown that some of the created logistic regression models generalize to WSNs with similar, but different topologies and setups.

We identify the packet delivery rate as a decisive metric to distinguish between attacking and normal scenario. Other highly significant metrics for jamming detection are the listen time and the number of neighbors; both can detect the attack on all nodes in the initial testbeds, and across all combinations of parameters. The effects of the blackhole attack are more locally restricted, yet we find several highly significant metrics that are able to detect the attack on selected nodes. Examples include the number of sent/received data packets, the link estimation of the best neighbor, and the radio energy consumption.

We focused on lightweight detection of two denial-of-service attacks, however, our approach to identify the quality of the metrics will also work to identify attacks other than DoS, thus paving the way to practical lightweight IDSs in wireless sensor networks.

5 TOKEN-BASED INTRUSION DETECTION

> Without deviation from the norm,
> progress is not possible.
>
> F. Zappa

After having identified useful features for intrusion detection in wireless sensor networks in Chapter 4, in the following two chapters we focus on novel IDS architectures.

Recently, applications such as distributed data mining [FCG10] or volcanic earthquake timing using wireless sensor networks [LTZ+13] have been introduced that require the execution of resource-intensive algorithms. As a consequence, the energy remaining for performing intrusion detection is reduced. Our work in this chapter is based on [RYBH14] and aims at reducing the workload of the nodes by adding randomization to the execution of tasks. For example, heavyweight operations are only carried out upon special triggering. For that purpose we introduce Patrol, a system based on tokens passed around the network, which instruct the nodes to execute special tasks. After visiting a node, the token continues its walk through the network. As a proof-of-concept, we develop a lightweight, decentralized intrusion detection algorithm, analyzing a single metric which proved to be useful in detecting denial-of-service attacks such as blackhole and flooding. In detail, a profile of the normal energy consumption of each node is calculated. We show that even with randomized intrusion detection, flooding and blackhole attacks can be detected very fast. Using Patrol, the nodes only temporally perform intrusion detection, reducing computational effort and distributing load across nodes.

The remainder of this chapter is organized as follows. In Section 5.1, we present the system overview. Section 5.2 is devoted to describing Patrol in detail. Therefore, we show our basic setup, the security mechanisms we have implemented, and the token communication. We then analyze the token distribution from a mathematical point of view in Section 5.3. Next, in Section 5.4, we propose an efficient intrusion detection algorithm and show that the energy consumption can be used as a sole metric for the detection of flooding attacks. In Section 5.5, we evaluate the Patrol architecture and the intrusion detection system. Directly related work is discussed in Section 5.6. Finally, some concluding remarks are outlined in Section 5.7.

5.1 SYSTEM OVERVIEW

This section is devoted to the presentation of the network and attacker models, the assumptions and requirements, and the brief description of Patrol.

5.1.1 *Network Model*

Our system design is suited for arbitrary wireless sensor networks, we do not impose any restrictions on node capabilities, topology, or routing protocols. Each node has to

be aware of its neighbors. We consider a network in which each node can eventually be reached, i.e., all nodes need to be connected. The base station is required for the token management.

5.1.2 *General Attacker Model*

We assume that an attacker can delete tokens from the network, which would prevent the execution of the desired functionality. It is also possible that the adversary replays tokens in order to cause DoS by letting the nodes perform the specified tasks exhaustively. We further assume that the base station cannot be compromised.

5.1.3 *Specific Assumptions and Requirements*

Leveraging tokens, we have specific assumptions and requirements. At the system start-up, a node can hold an arbitrary number of tokens. Every token has a unique name. Thus, we are able to differentiate between tokens. This allows the use of multiple tokens possibly activating different functionalities.

As a proof-of-concept application, we introduce a novel and lightweight IDS intended to detect DoS attacks such as jamming and blackhole. The primary goal is to minimize the computations for intrusion detection. Similarly, the communication overhead must be kept at a reasonable level, i.e., we transmit audit data only to the direct neighborhood of each node. We assume that the power consumption is relatively constant, and that an adversary can mount attacks influencing the power consumption. Therefore, our IDS is not applicable for each WSN scenario. It is most appropriate for environmental monitoring settings with regular measurement and transmitting patterns as in [TPS+05]. However, it may not be suited for area surveillance, where intensive event-based activity may trigger false detection.

Furthermore, we assume that the attacker may compromise a node and is able to alter its energy readings. However, he cannot change the transmitted data of other nodes without physically capturing them. We also assume that the majority of nodes is well-behaving. The attacker can employ multiple, possibly colluding malicious nodes at different locations and may also change their positions. Note that Patrol can be extended with other intrusion detection algorithms that cover different types of attacks. The assumptions and requirements outlined above are specific to the proof-of-concept application.

5.1.4 *Patrol Overview*

Patrol relies on tokens being exchanged between nodes. Upon receiving a token, a node will activate a pre-deployed algorithm. In the remainder of this chapter we focus on activating IDS functionality, however, Patrol is not limited to security tasks. Our design has several advantages:

- Each node may perform intrusion detection, we do not require dedicated security nodes.
- The load is distributed across all nodes in the network.

- ▷ Multiple intrusion detection algorithms can be activated via different tokens, allowing a very flexible configuration of desired functionalities.
- ▷ The token authorizes a node for attack detection.

All messages are authenticated and integrity-protected. Further information about the security mechanisms are given in Section 5.2.2. Patrol has been implemented on Contiki [DGV04].

5.2 PATROL ARCHITECTURE

We now present Patrol in detail. Therefore, after showing the basic setup, we describe the lightweight security mechanisms used to protect Patrol. Finally, we explain the implementation of the token communication.

5.2.1 *Basic Setup*

Tokens are assigned to the nodes by the base station. We assume that each node has at least one neighbor and at least one node holds a token. When a user-defined delay has passed, the token is transmitted to a random node. However, different forwarding strategies can be applied as well (see Section 5.5.2). Our architecture allows one or more tokens to be used at the same time. The underlying application we use for testing our architecture relies on (1) broadcasting the energy consumption to all direct neighbors of a node (required for our intrusion detection algorithm), and (2) broadcasting regular dummy traffic to resemble a real deployment (unicasting would make no difference). The messages sent are protected, details are given in what follows.

5.2.2 *Security Mechanisms*

The messages of the nodes are authenticated and integrity-protected using hash chains, which automatically renew themselves. Every node knows all the hash chain anchors (h_0) of its direct neighbors, which can be used to authenticate them. Every protected message has a prepended initialization vector (IV) of 8 bytes and an appended hash chain value of 20 bytes. The data itself and the hash chain value are encrypted using Salsa20/20 [Ber08] (256 bit key) to ensure integrity (through inherent diffusion of the algorithm) and authentication (through hash chain value). The message secrecy is also guaranteed through Salsa20/20, but is of minor importance in our system. The individual pseudo-random IV for every message consists of the message type and a pseudo-random number. We use SHA-1 as the hash algorithm. The Salsa20/20 routines consume about 5454 bytes, while SHA-1 requires about 2690 bytes. En-/Decrypting 64 bytes with Salsa20/20 takes about 6 ms on the TelosB motes. Approximately the same amount of time is needed for hashing 20 bytes with SHA-1. We choose Salsa20/20 for efficiency reasons, the AES implementation on the TelosB mote needs more ROM and is consistently slower than Salsa20/20 [Ber08].

The keys and hash chain anchors are initially distributed by the nodes at the start-up. We assume that this distribution is secure and that the nodes are aware of their potential neighbors, e.g., by using common protocols such as the collection tree [GFJ+09]

and the mesh protocol, or by relying on the routing information provided by the employed application. Alternatively, the keys/hash chains can be predeployed, which would further reduce the code size. The integration of standard key management schemes such as LEAP+ [ZSJ06] is also possible.

We propose the following mechanisms as countermeasures to an attacker deleting and replaying tokens. A node sends an authenticated status message to the sink indicating that it received a token. Whenever a system-defined threshold is passed without seeing such a status message, a new token has to be generated by the base station. Hence, it is not possible to remove all tokens without being detected, given that an adversary cannot compromise the whole network. Less overhead would be introduced, if instead of sending status messages, each token would be assigned a time to live mechanism. When a token reaches the end of its lifetime, it simply stops forwarding itself and a new token is created by the base station. To protect against replay attacks, sequence numbers are used. Besides, each node only accepts a well-defined number of tokens within a given period.

5.2.3 *Token Communication*

In our architecture, it is necessary to define one or more nodes that hold tokens initially before the start-up. These nodes act as token distributors and send the tokens to one of their direct neighbors. Currently, we choose this neighbor randomly. If an attacker compromises a node holding the token and does not forward it, this would be detected by Patrol since we expect a status message from each node upon token reception.

As we test our system in a real-world testbed, we are facing the problem of unidirectional links, e.g., A can reach B, but the opposite link is not functional. Therefore, in our sample application presented in Section 5.4, we maintain a neighbor list created from the broadcast messages each node overhears. Tokens are only accepted if they are sent by a node in the neighbor list, which is maintained independently from the routing protocol and updated frequently. The node must receive a message from the neighbor regularly, otherwise the neighbor is removed from the list. However, in our initial tests, not all tokens could be transmitted successfully due to the unidirectional link.

To compensate for this and other interference, we add two mechanisms. First, we unicast the token with the highest transmission power provided by the CC2420 radio chip (0 dBm). Second, after sending the token we wait for acknowledgment. In case that the acknowledgment does not arrive, we repeat the token sending for at most two times. If the whole process of token sending fails, we instruct the initial receiver to drop the token—if it was received— by sending so-called token-cancel packets for at most three times. Then we try to pass the token on to another node.

The adding of token-cancel packets achieves a higher probability that both communication sides share the same token state, given a unidirectional link. For example, consider node A sending a token to node B. When the link is unidirectional and we do not use token-cancel packets, it is possible that node B actually received the token while node A considers it is not accepted. Since links are bursty, given the token is transferred successfully, it is also very likely that the token-cancel packets are received successfully. Hence, both sides will have the consensus that the token should not be

transferred over this link. Besides, a node checks if it has a specific token already. When that is the case, it will reject the token. As a consequence, intrusion detection is not performed consecutively on one node.

Patrol with CTP

When adapting Patrol to be used with the collection tree protocol, there are some challenges caused by the characteristics of CTP which will be covered in what follows.

Patrol and the sample application are based on broadcasting and unicasting. In detail, the topology is highly connected due to the broadcasted messages and this implies a rather large neighborhood. The token distribution relies on the neighborhood table, to be precise, the node holding the token chooses a node in its neighborhood and sends the token via unicast. Compared to such a large neighborhood, CTP tries to build up a topology which is minimally connected, this means that the perfect topology is achieved if every node is reachable by at most one link. Hence, the problem is that a node's nighborhood consists of only one other node, which is its parent. Thus, the token can only be sent to the parent and finally it will reach the base station, in other words, a dead end.

The main issue to solve is a node's lack of information regarding the neighborhood. A possible solution is to propagate information about the topology. This can be done at lower layers, for example, the network layer, or at higher layers by establishing a communication channel and providing neighborhood information via messages. We have chosen the latter one, since we did not want to change the original CTP code for compatibility reasons.

In our implementation, the first step is to change Patrol's original communications, which are based on broadcasting, to the unicast-based CTP, therefore resulting in CTP forming the network.

The next step is to generate a node's neighborhood table to look up the possible recipients of the token. This neighborhood table has to be updated with addresses of the node's parent and children. The addresses of the children can be obtained if a child reports its address to the parent. This is realized in the following way:

- ▷ Establish a new communication channel based on unicast
- ▷ Look up the parent's address
- ▷ Send the own address to the parent

Afterwards, the parent node will receive the addresses of all children and can add them to the neighborhood table.

5.3 TOKEN DISTRIBUTION

We start this section by presenting a proper mathematical framework in order to model the token distribution induced by our proposal. Due to the structure of wireless sensor networks and the fact, that the WSN topology can be modeled by a directed graph, we adopt the Markov Chain model. In particular, we denote a directed graph by $G = (V, E)$ consisting of a finite set of states $V = \{N_i \mid i \in \mathbb{N}\}$, $|V| = d < \infty$ each associated to a single sensor node in the sensor network. Two nodes N_i and N_j are

said to be neighbors, if there exists at least one directed edge $e_{i,j} \in E$ defining a link between two of them.

According to our token-based approach, as indicated above, any sensor node $N_i \in V$ in the network that holds a token is required to forward it after some fixed time period to a neighbor N_j. The Markov Chain model is applied for selecting the next neighbor, which receives the token in the next transition. More specifically, each neighbor obtains the token with probability $p_{i,j}$, where $p_{i,j} = P(X_t = N_j \mid X_{t-1} = N_i)$ denotes the transition probability of transmitting the token from node N_i to N_j. In order to keep track of the token, we introduce the random variable X_t, which points to the position of the token after the t-th move. As a consequence of the Markov property (memoryless property), we have $P(X_{t+1} = N_{i_j} \mid X_t = N_{i_{j-1}}) = P(X_{t+1} = N_{i_j} \mid X_t = N_{i_{j-1}}, \ldots, X_0 = N_{i_0})$, which particularly states that the transition probability of any move depends only on the actual state and not on previous moves. In many mathematical applications one considers the so-called transition matrix $\mathbf{P}$ containing all transition probabilities, with zeros on the diagonal because forwarding the token to oneself is prohibited. The row i of matrix $\mathbf{P}$ is filled with the transition probabilities $p_{i,1 \leqslant j \leqslant d}$ from state N_i to any neighbor N_j represented by column j:

$$\mathbf{P} = \begin{bmatrix} p_{1,1} & \cdots & p_{1,d} \\ \vdots & \ddots & \vdots \\ p_{d,1} & \cdots & p_{d,d} \end{bmatrix}.$$

The dimension d of the matrix is equal to the number of nodes. Furthermore, the entries within a row sum up to 1. The initial state at the beginning of the algorithm is chosen uniformly at random over the set of states V with $p_{0,j} = 1/d$. As a result, we obtain the initial vector $\vec{v}^{(0)} = (v_0^{(0)}, \ldots, v_d^{(0)}) = (\frac{1}{d}, \ldots, \frac{1}{d})$ that is filled at position $1 \leqslant j \leqslant d$ with the probability for the state N_j to be selected in the initial phase. In general, $\vec{v}^{(n)}$ is filled with the probabilities of any state to be chosen after the n-th move. This vector can efficiently be determined via

$$\vec{v}^{(n)} = \mathbf{P} \cdot \vec{v}^{(n-1)} = \mathbf{P}^n \cdot \vec{v}^{(0)}.$$

Hence, the quantity $\vec{v}_j^{(n)}$ represents the probability of node N_j receiving the token after the n-th transition. In this work, we also wish to determine the minimum number of steps expected to move from state N_i to N_j. We start by defining mathematical objects known from statistics. Thus, let $H^j = \inf\{t \in \mathbb{N} : X_t = N_j\}$ denote the hitting time of the state N_j and

$$h_i^j = P(H^j < \infty \mid X_0 = N_i)$$

denote the probability of hitting N_j when starting from N_i. From this, one can deduce the expected number of steps (hitting time)

$$t_i^j = \mathbb{E}(H^j \mid X_0 = N_i)$$

from N_i to N_j. The hitting probability is obtained by solving the following system of equations

$$h_i^j = \begin{cases} 1 & \text{for } N_i = N_j \\ \sum_{N_l \in S} h_l^j \cdot p_{i,l} & \text{for } N_i \neq N_j. \end{cases} \tag{5.1}$$

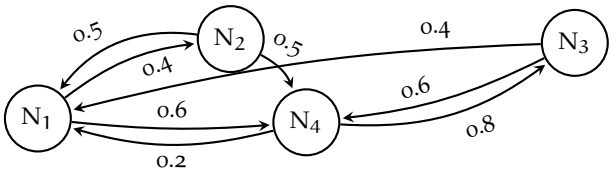

Figure 5.1: Sample states with transition probabilities

As for the expected hitting time, it is required to solve

$$t_i^j = \begin{cases} 0 & \text{for } N_i = N_j \\ 1 + \sum\limits_{N_l \in S} t_l^j \cdot p_{i,l} & \text{for } N_i \neq N_j\,. \end{cases} \tag{5.2}$$

To illustrate this approach exemplarily, consider the graph depicted in Figure 5.1. The indicated numbers correspond to the different hitting probabilities.

For instance, in order to determine the hitting time and hitting probability of the state N_3, we have to build the systems of equations according to 5.1 and 5.2 using the abbreviations $h_i := h_i^3$ and $t_i := t_i^3$, which gives us:

$$\begin{aligned} h_3 &= 1 & t_3 &= 0 \\ h_1 &= 0.4 \cdot h_2 + 0.6 \cdot h_4 & t_1 &= 1 + 0.4 \cdot t_2 + 0.6 \cdot t_4 \\ h_2 &= 0.5 \cdot h_1 + 0.5 \cdot h_4 & t_2 &= 1 + 0.5 \cdot t_1 + 0.5 \cdot t_4 \\ h_4 &= 0.8 \cdot h_3 + 0.2 \cdot h_1 & t_4 &= 1 + 0.8 \cdot t_3 + 0.2 \cdot t_1 \end{aligned}$$

A solution to these equations reveals the hitting probabilities h_i and hitting times t_i for $1 \leqslant i \leqslant 4$ from state N_i to state N_3. The complexity to solve such a system of equations is bounded by $O(d^2)$, where d denotes the dimension of the matrix. Following this, the overall complexity raises to $O(d^3)$ when computing the corresponding quantities for all nodes in V. Based on this method, the base station can compute the expected number of steps to reach a certain state after each move of the token. We note that due to changing links in a WSN, the corresponding quantities need to be recomputed over time.

5.4 PROOF-OF-CONCEPT APPLICATION: ENERGY-BASED IDS

Common for many of the proposed intrusion detection systems for WSNs is the large number of features that need to be analyzed in order to detect an attack. For example, Liu et al. [LCC07] present an insider attacker detection algorithm using localized information, relying on the spatial correlation among networking behaviors of sensors in close proximity. In their approach, each sensor monitors the behavior of its immediate neighbors with respect to the packet dropping rate, the packet sending rate, the forwarding delay time, and the actual sensor readings. Based on our results obtained in Chapter 4, we keep attack detection lightweight by focusing examplarily on the energy consumption as a single metric in order to detect denial-of-service attacks.

Using the Patrol architecture, we develop an IDS which lets the nodes periodically collect the energy that has been consumed by the radio component for sending

and receiving packets. The radio energy consumption is obtained using Energest, the software-based power profiling of Contiki [DGV04]. Each node independently stores and broadcasts its energy consumption in a certain time interval to the direct neighbors of the node. Thus, we take into account that the load is not distributed evenly across nodes, for example, nodes close to the base station often receive and forward comparatively more messages.

To determine what a normal power consumption rate is for each node, we require a training phase (called *warm-up* phase) in which we assume that no attacker is present. In this phase, we collect all broadcasted energy values for each node and calculate the mean μ_t. Besides, the standard deviation σ_t is computed. Hence, we have a profile of the normal power consumption of each node. After the warm-up phase, we calculate the actual μ_a out of the last n energy values received. We call n the window size. We check whether μ_a falls within the range of $\mu_t \pm k \times \frac{\sigma_t}{\sqrt{n}}$, where k is the parameter defining how big the interval is for values considered as normal (we call k the detection tolerance; a larger k is more conservative in detection). If it is not, we consider the value to be an outlier. Table 5.1 presents the costs of Patrol and the proof-of-concept application in terms of storage. We observe that the security mechanisms add ROM overhead of 9066 bytes and RAM overhead of 1504 bytes. Still, the required amount of ROM and RAM are easily provided by state-of-the-art sensor nodes.

To illustrate the influence of flooding attacks on the nodes' energy consumption, we perform a 45 minutes test-run in which node 22 is the attacker (the description of the testbed is given in Section 5.5). Figure 5.2 shows the energy consumption of two different nodes, one being close to the attacker, the other being distant. While the attack has no impact on the distant node 15, the increase in energy consumption is significant for node 21. These results confirm that analyzing the energy consumption is helpful for detecting denial-of-service attacks.

5.5 EVALUATION

In this section we evaluate Patrol and its IDS implementation with respect to the main metrics: the detection and hitting times. First, we provide details about the testbed used. Next, we introduce a different token forwarding strategy, *uniform sending*, aimed at a more evenly distributed token visit frequency. We then describe the influence of critical parameters of the intrusion detection system on the detection and hitting times. A discussion on the energy consumption of the IDS concludes the evaluation.

Table 5.1: Patrol ROM and RAM footprint (bytes)

Type	**ROM**	**ΔROM**	**RAM**	**ΔRAM**
Contiki + Patrol	24894	-	6978	-
Contiki + Patrol w/Security	33960	9066	8482	1504

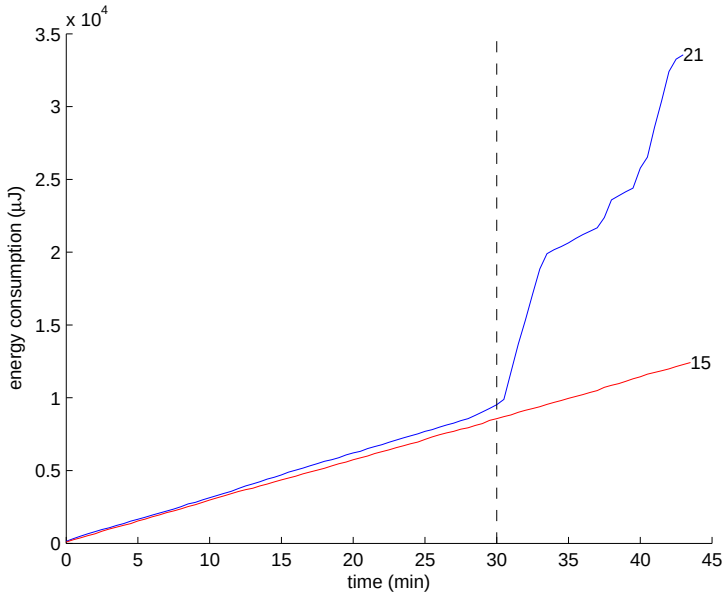

Figure 5.2: Energy consumption of nodes 21 (direct neighbor of the attacking node 22) and 15 (very distant from the attacker); the attack is started after 30 minutes

5.5.1 *Testbed*

We use the TUDμNET [GGSB13] for our measurements, a federation of wireless sensor network testbeds deployed at various buildings of the Technische Universität Darmstadt. We have selected one testbed at the computer science building, with TelosB motes running the operating system Contiki [DGV04] (Figure 5.3 is showing the mote placement in the corresponding offices). These motes have a MSP430 MCU and a CC2420 radio chip. The testbed contains 20 motes, out of which 15 motes are well-behaving nodes and 5 are potential attackers.

The setup for the experiments is as follows. Each node generates dummy traffic consisting of packets of 10 bytes sent every 60 seconds with the transmission power set to level 11, which equals $-10\,\mathrm{dBm}$. A randomly selected attacker is triggered after 30 minutes, broadcasting messages of 90 bytes at the rate of 1 packet/s with a transmission power of $0\,\mathrm{dBm}$ using level 31. The aggressiveness of the attacker influences the detection time. The warm-up phase requires 30 energy samples to be collected before calculating μ and σ. Beginning at the system's start-up, we immediately send tokens at the highest transmission power ($0\,\mathrm{dBm}$). In test-runs using only one token, node 25 is the initial token holder. When we use two tokens, nodes 25 and 15 are in posession of the tokens. The delay between token sendings is set to 60 seconds.

5.5.2 *Different Token Forwarding Strategies*

We first provide an analysis of the random sending followed by the introduction of another sending strategy. Let $G = (V, E)$ be a connected graph which has n nodes and m edges. When starting a random walk on G at node v_0, we visit its next neighbor with probability $1/d(v_0)$, where $d(v_0)$ is the degree of v_0. Given the fact that the

transition from one node to another is independent of the preceding and succeeding transitions, we can assume a Markov chain. For this Markov chain, let $M = (p_{ij})_{i,j \in V}$ be the matrix of transition probabilities from i to j with

$$p_{ij} = \begin{cases} 1/d(i) & \text{if } i,j \in E \\ 0 & \text{otherwise} \end{cases} \tag{5.3}$$

As shown in Equation 5.3, every edge is passed through with the same frequency, i.e. $2m$, since $\pi(i)p_{ij} = 1/(2m)$ for $i,j \in E$, given a stationary distribution [Lov96]. Yet we find that in the real testbed this condition is not always true because of unmodeled effects such as contention, unidirectional links, and varying link quality. In a 12-hour test-run we investigate the relationship between the mean neighbor count and the number of received tokens. From Figure 5.4 we conclude that a higher number of neighbors generally leads to a higher amount of received tokens. The correlation coefficient is about 0.59, hence, nodes with very low degrees, such as nodes 20 and 24, are unprivileged by tokens. For example, node 25 receives the token approx. 50 times more often than node 24. However, even though node 28 has almost twice the amount of neighbors than node 30, it receives a token about half as often. To compensate for this uneven number of visits, we modify the random forwarding strategy to achieve a more evenly distributed visit frequency for all nodes. Let the neighbors of a node be denoted by $n_i, i = 1, ..., L$. Since we know the degree of all neighbors (the neighbor

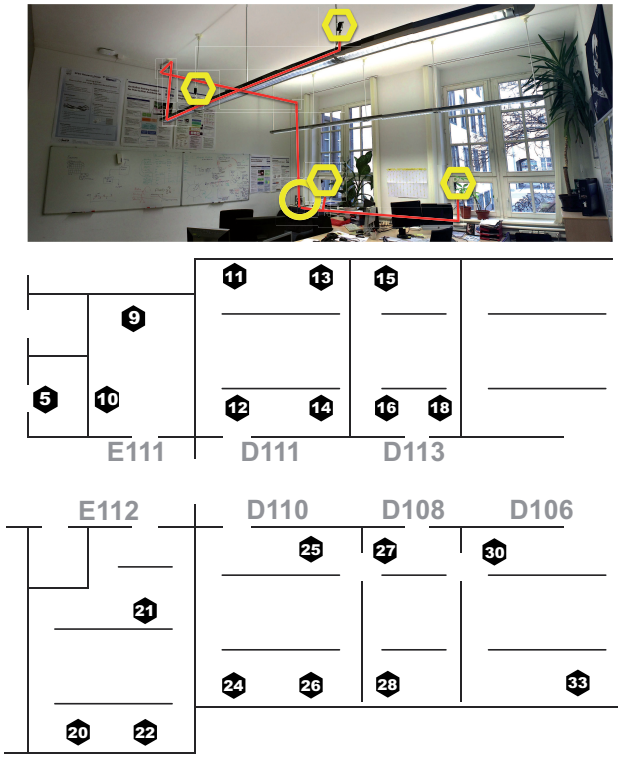

Figure 5.3: Mote placement at the computer science building and sample deployment in one office (Image source: http://www.tudunet.tu-darmstadt.de)

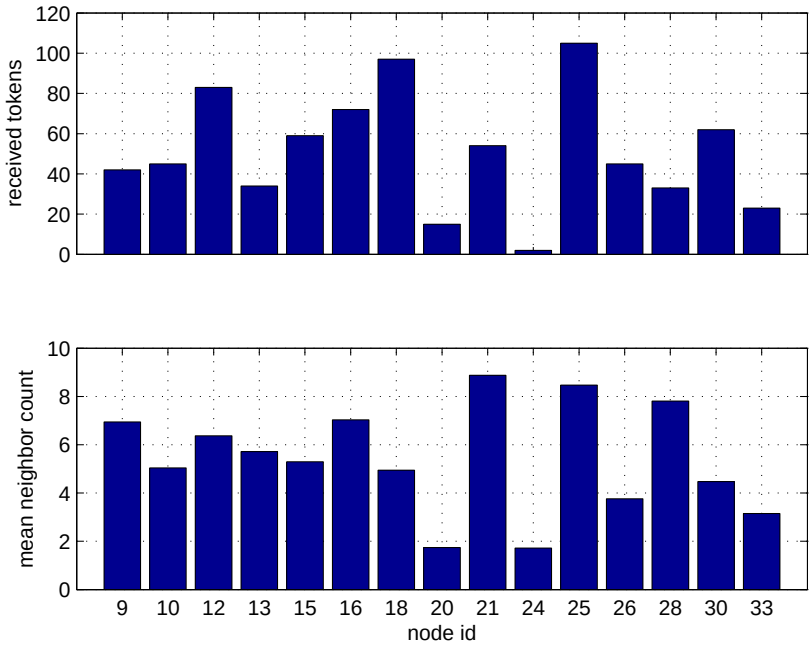

Figure 5.4: Received tokens and mean neighbor count (random sending), correlation coefficient 0.59

count is included in every broadcasted energy message), we can select n_i as next token destination according to the probability

$$p = \frac{1}{d(n_i)\sum_{j=1}^{L}\frac{1}{d(n_j)}}$$

assigning each node a similar chance to get the token. This forwarding strategy is called *uniform sending*. Figure 5.5 shows that this strategy achieves a slightly better token visit distribution. The correlation coefficient is reduced to about 0.40. Even though in the new test-run the mean neighbor count of node 24 is reduced from about 1.7 to about 0.9 when compared to random sending, it receives a token three times more often. Nevertheless, we could not achieve a truly uniform sending due to the conditions of the communication channel, especially because of the bad link quality. We leave the detailed analysis of other forwarding strategies for future work.

5.5.3 *Detection Time*

We now investigate how long our system takes to detect the flooding attack. The used parameters are listed in Table 5.2. We vary the detection tolerance k, the *window size*, the *forwarding strategy*, and the *number of tokens*.

Initially we start with experiments having a window size of 30 and random sending of one token. Each experiment has a duration of 60 minutes and is repeated five times with a randomly selected attacker. The first parameter we vary is the detection tolerance k. As expected, reducing k from two to one improves the detection time

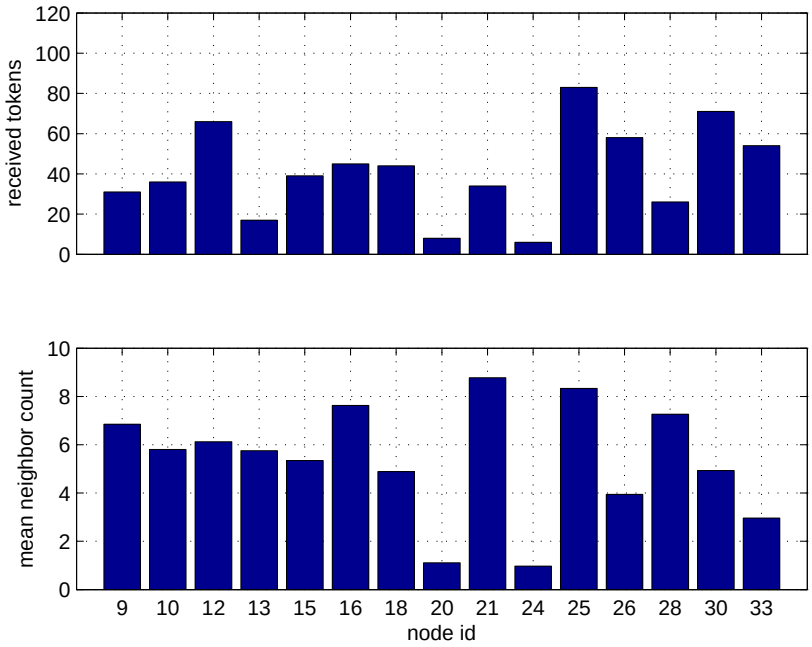

Figure 5.5: Received tokens and mean neighbor count (uniform sending), correlation coefficient 0.40

(on average 136 seconds for $k = 1$, random sending), while a higher k value leads to detection times that are about 20 seconds higher. Thus, we keep k fixed to one in all future experiments. Table 5.3 compares the detection times with regard to the two different forwarding strategies and different number of tokens. A higher number of tokens could improve the detection time by performing intrusion detection more often at different nodes. We observe that the use of uniform sending improves the detection time on average by about 20%. It achieves significantly better results when the attacker is located at corner positions and is flooding nodes that have a low degree, since the token is sent more often into such areas as compared to random sending. Otherwise,

Table 5.2: Experimental setup

Parameter	**Value**
No. of nodes	15
Initial token holder(s)	Node 25 (15)
Warm-up phase	30 samples
Window size	10, 20, 30 samples
Detection tolerance k	1, 2
Start token sending	immediately
Token sending delay	60 sec
Forwarding strategy	random, uniform
Start flooding	after 30 min

the detection time is similar to random sending. Even though there is a relatively large variance in the results induced by the randomness of token sending, the usage of two tokens significantly reduces the detection times. The corresponding confidence intervals do not overlap. However, the drawback of using two tokens is an increase in energy consumption. While the average total energy consumption of the WSN over all nodes and covering a period of 45 minutes is about 19 Joule with one token, this number increases to about 24 Joule with two tokens. Due to interference and a very poor link quality in the testbed, the tokens need to be retransmitted multiple times, resulting in an increased energy consumption. Similar results are obtained for random sending.

In all test-runs, multiple nodes detect the flooding attack. Uniform sending has a positive effect on the number of detector nodes: while a randomly sent token leads to about 6 nodes that can detect the intrusion, on average about 8 nodes can do so with a uniformly sent token. No false-positives occured over all settings.

The effects of the window size on the detection accuracy and detection time when sending one token randomly are studied in the following. Figure 5.6 illustrates the results. By reducing the window size from 30 to 10, we achieve on average a detection time of about 98 seconds in the latter case. However, this improvement comes at the cost of a false-positive rate of 40%.

Finally, we analyze the trade-off between our proposed random intrusion detection and constant detection. Therefore, we compare the implemented outlier detection algorithm when it is activated *without* tokens. This means, whenever a node receives an energy message, given that the warm-up phase ended, it will perform intrusion detection. The mean detection time in this setup is reduced to about 55 seconds, which is slightly better than sending two tokens uniformly.

Blackhole Attack

With the same setup described before, we have also tested Patrol using the CTP and mesh protocol, and performing a blackhole attack. Again, each experiment has a duration of 60 minutes and is repeated five times with a randomly selected attacker. The attack implementation remains the same as described in Section 4.1.3.

The general trends observed for the flooding attack are also true in sensor networks running the CTP and mesh protocol: uniform sending performs better than random sending, and the usage of two tokens reduces the detection time. Table 5.4 shows the results for the CTP and mesh protocol, respectively. While the detection times of the blackhole attack in a mesh WSN are similar to those of a flooding attack as presented

Table 5.3: Detection times for the flooding attack, depending on the forwarding strategy and the number of tokens

No. of Tokens	Attack	Forwarding	Avg. Detection Time (sec)
1	Flooding	Random	136
1	Flooding	Uniform	110
2	Flooding	Random	82
2	Flooding	Uniform	66

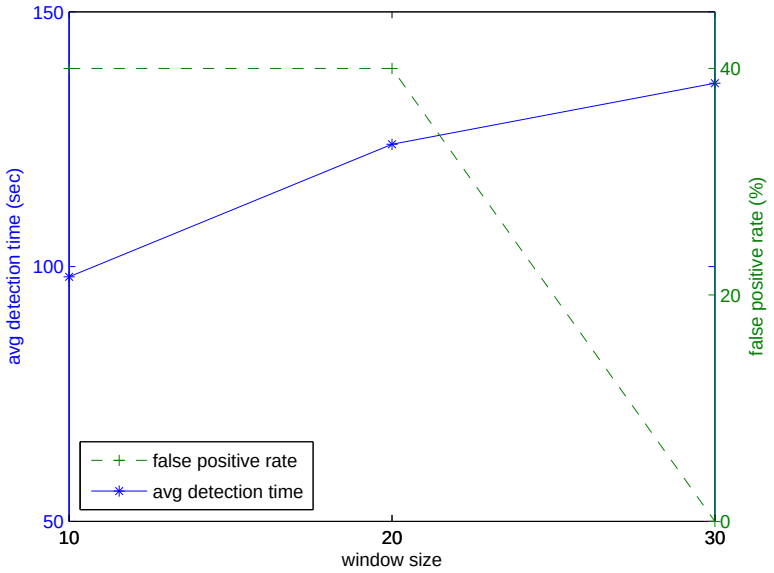

Figure 5.6: Detection times and false-positive rates for different window sizes (one token, random sending)

before, the detection times of the blackhole attack when using the CTP are about twice as high compared to the mesh setting. This is because in the collection tree protocol setting, the implemented traffic is more deterministic since all traffic is destined to the sink. Hence, also the energy consumption is more deterministic and the blackhole attack does not influence it as much as in the mesh protocol.

5.5.4 *Hitting Time*

As explained in Section 5.3, the hitting time is defined as the timespan between two consecutive token receptions at the same node. We investigate the influence of the forwarding strategy on hitting times. The two test-runs each last for 12 hours during

Table 5.4: Detection times for the blackhole attack, depending on the forwarding strategy and the number of tokens

No. of Tokens	Attack	Forwarding	Avg. Detection Time (sec)
1	Blackhole (Mesh)	Random	111
1	Blackhole (Mesh)	Uniform	94
2	Blackhole (Mesh)	Random	82
2	Blackhole (Mesh)	Uniform	71
1	Blackhole (CTP)	Random	276
1	Blackhole (CTP)	Uniform	203
2	Blackhole (CTP)	Random	227
2	Blackhole (CTP)	Uniform	166

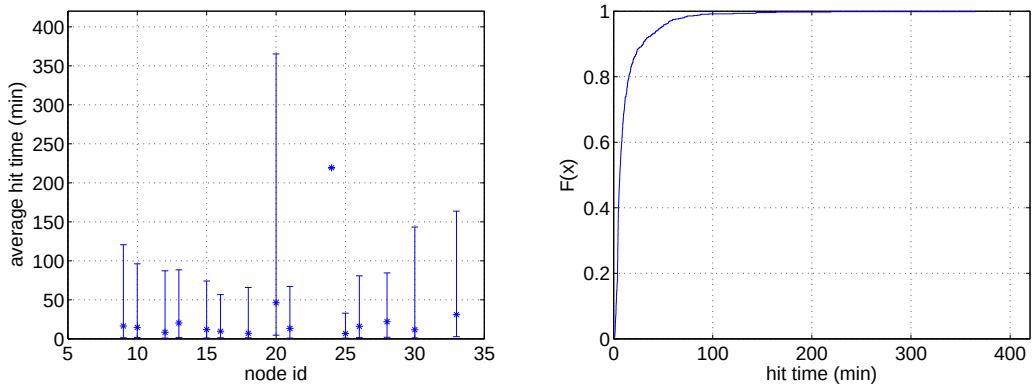

Figure 5.7: Average hitting times and CDFs for the random sending (1 token)

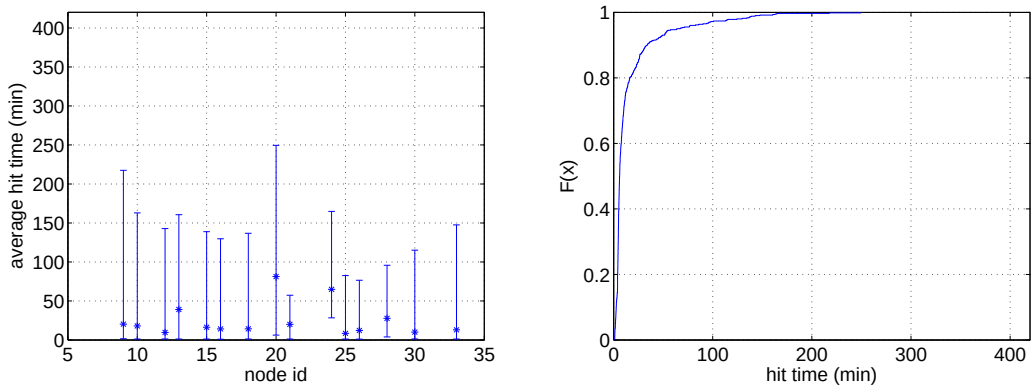

Figure 5.8: Average hitting times and CDFs for the uniform sending (1 token)

which no attacker is present. Figures 5.7 and 5.8 show the average hitting time and the corresponding CDF with one token sent randomly and uniformly. If there is no visible hitting time for a node, it means that this node was not active in our tests.

While the average hitting time for 90% of the nodes is similar for the two forwarding strategies, the maximum hitting time for nodes with a low degree (node IDs 20, 24, 33) is reduced when sending uniformly. Besides, node 24 is visited five times by a token sent uniformly, but only once by a token sent randomly. Hence, we achieve a slightly better connected network with regard to tokens. Similar results are obtained with two tokens being used, as shown in Appendix A.2. Again, we observe that uniform sending outperforms random sending with regard to nodes with a low degree, because those nodes are visited more often within shorter time. In addition, the use of two tokens instead of just one decreases the average hitting time. Since we are interested in the frequency of performing intrusion detection, we do not differentiate between a token visiting a node twice, and two different tokens visiting a node.

We argue that our system is scalable to the number of nodes in the network, since we can increase the number of tokens proportional to the network size. In WSNs consisting of a larger number of nodes, this could achieve that all areas are included in intrusion detection.

5.5.5 *Energy Consumption*

We designed our system to be energy-efficient. In the following, we elaborate on the energy consumption of the intrusion detection system.

Regarding the communication overhead, the application layer payload of a token is 30 bytes, and that of an energy packet is 35 bytes, both including security mechanisms. The actual energy consumption depends on the chosen settings. This includes, e.g., the transmission power, the number of tokens, the delay between token forwarding, and the delay between sending energy messages. All communication is restricted to the local neighborhood.

The execution time of the outlier detection algorithm is in the order of µs. Therefore, this energy consumption is negligible. However, computationally more expensive algorithms may be applied within Patrol as well, since we are able to randomize the detection process.

In summary, the introduced overhead is tolerable in resource-constrained WSNs.

5.5.6 *Discussion*

In Chapter 6, we study the application of mobile agents for intrusion detection [RBH13]. The agents contain the code for intrusion detection and move through the network, carrying the energy status of the nodes and estimating the expected power consumption with the assistance of a linear regression model. This approach is not as scalable as the token-based approach proposed in this chapter. The size of the agent reaches about 1 KB in a 12-node network because not only code, but also all required energy readings have to be transferred through the whole WSN, creating a much larger communication overhead. In contrast to that, Patrol transfers small token messages and limits the transmission of energy readings to the direct neighbors of a node. Besides, we significantly reduce the detection time.

However, there are also advantages of using mobile agents instead of the token-based approach. Since the agent does not need to be stored permanently, storage can be saved, e.g., for a larger amount of application data. Similarly, the agent can be changed more easily, without the need for reprogramming the nodes.

Compared to the state-of-the-art intrusion detection systems presented in Chapter 3, our randomized solutions cannot easily be evaded by an attacker. He cannot predict well in advance and at exactly which point in time a node will perform intrusion detection. In addition, an advantage lies in the flexibility our approaches offer with respect to changes during operation, and to the requirements of the WSN. The topology is completely irrelevant, as opposed to IDSs only working with clustered or tree-structured wireless sensor networks. In our case, randomizing the detection frequency leads to a small increase of the detection time. However, the main challenge our proposed IDSs face is the communication overhead.

5.6 RELATED WORK

Patrol allows randomizing the execution of the sensor nodes' tasks. In this thesis we focus on attack detection by developing a lightweight intrusion detection algorithm based on the nodes' energy consumption. Multiple authors have already used energy

consumption as a metric for intrusion detection. However, there is little related work in the area of sensor networks. Nash et al. [NMHH05] analyze several parameters in their IDS such as CPU load and disk access for estimating the power consumption of mobile computers with the assistance of a linear regression model. Therefore, the complexity of the applied linear regression is quite high.

Buennemeyer et al. [BNC+08] also focus on mobile devices, and take a power profiling approach for intrusion detection. Given a dynamically adapting threshold value, their system generates an alert in case of abnormal current changes. The fact that battery readings need to be transmitted to a central point renders the system not applicable for wireless sensor networks, due to the significant communication overhead. Moreover, the amount of data that needs to be analyzed in order to create a reliable profile is high. Finally, at the central server, attack traffic is correlated with Snort alerts. As a result, the combination of anomaly detection with a rule-based IDS leads to a high complexity.

Furthermore, a plethora of intrusion detection systems have been presented in the last years. However, as our survey on intrusion detection in Chapter 3 has shown, no approach directly related to wireless sensor networks is concerned with randomization, and existing systems have strong requirements. In [dC14], a different type of randomization as compared to our intrusion detection systems is investigated for the case of mesh networks.

5.7 SUMMARY

In this chapter we present Patrol, a flexible system for WSNs aimed at reducing the load of nodes. Patrol allows to randomize the execution of tasks, even those of security-critical functions. It relies on tokens which are exchanged in the network. Upon receiving a token, a node performs a specified task. Otherwise, the node does not have to spend energy for possibly heavyweight operations. As proof-of-concept, we propose and implement a lightweight intrusion detection algorithm analyzing the energy consumption of the network within Patrol. It can detect flooding and blackhole attacks on a large number of nodes in the testbed, within a reasonable detection time. Two different strategies for forwarding the token are presented and compared: random and uniform sending. The latter achieves better detection times by assigning each node a similar chance to get a token. We analytically and experimentally investigate the frequency of performing intrusion detection, showing the feasibility of reducing it.

6 MOBILE AGENT-BASED INTRUSION DETECTION

> A person does not grow from the ground like a vine or a tree, one is not part of a plot of land. Mankind has legs so it can wander.
>
> R. Payne

As we have seen in Chapter 3, the existing intrusion detection systems differ not only in architecture, but in applied detection techniques and detectable attacks. Some are not limited to particular malicious behavior, while others can only detect specific attacks like sinkholes or wormholes. In the approach of Liu et al. [LCC07], each sensor monitors the behavior of its immediate neighbors, identifies outliers using Mahalanobis distances, and applies a majority vote to create the final list of outlying sensors. Consequently, this approach requires significant computational effort which can be too heavyweight in certain situations. Valero et al. [VJU+12] present a security framework which analyzes all information a node has or receives. This includes, for instance, the numbers of received and lost packets, the neighbors, and even all incoming packets not necessarily addressed to the node. This variety of analyzed features is common for many of the proposed IDSs.

In Chapter 5, we show the feasibility of randomizing the attack detection process, using a pre-installed intrusion detection algorithm. Hence, the storage costs are fixed. If it is desired to reduce these costs, an alternative is to send the IDS routine through the network. This approach is investigated in what follows. The proposed intrusion detection system in this chapter is characterized by a mobile agent, which moves from node to node, carrying the battery status of the nodes. The battery status is used to estimate the expected power consumption based on past observations, with the assistance of a linear regression model. This work is based on [RBH13] and [RBBH14].

The remainder of this chapter is organized as follows. We first present our system, its requirements and assumptions in Section 6.1. Then, the usage of mobile agents in wireless sensor networks is discussed in Section 6.2. After reporting simulation results in Section 6.3, we summarize directly related work in Section 6.4. Finally, Section 6.5 concludes the chapter.

6.1 SYSTEM OVERVIEW

This section presents our system, states the assumptions, and describes the method applied for intrusion detection.

6.1.1 *Mobile Agents used for Intrusion Detection*

As it was shown in Chapter 3, one possible classification of current intrusion detection systems for WSNs is according to their architectural design (1) decentralized, (2)

centralized, and (3) hybrid systems. The majority of IDSs work in a decentralized fashion, where intrusions are detected locally by the sensor nodes. Therefore, the nodes must install an IDS such as *Di-Sec* [VJU+12], which consumes about 13 KB out of 48 KB ROM provided by a default node platform such as TelosB. In some approaches nodes need to collaborate and overhear each other's communication, spending a significant amount of energy. Another drawback is that decentralized solutions might be unable to detect certain attacks, as a single node has only local knowledge (including its direct neighborhood).

In a centralized system, all information relevant for intrusion detection has to be transferred to a single point, typically the base station. This can create a large communication overhead and is subject to a single point of failure.

Hybrid IDSs are a combination of centralized and decentralized IDSs. However, they are still in their infancy for wireless sensor networks.

In the following, we propose a new IDS architecture based on mobile agents. Our design has features that respect the unique requirements of sensor networks:

- ▷ Efficiency: The mobile agent must not be stored permanently by a node. It carries only necessary data and may delete obsolete information.
- ▷ Flexibility: Instead of reprogramming all sensor nodes, a mobile agent is easily changed. Multiple agents can be used with different IDS functionality.

Compared to our token-based approach presented in Chapter 5, the difference is that we do not store the IDS functionality permanently on each node. Even though also Patrol allows the execution of different intrusion detection algorithms, they need to be pre-deployed.

6.1.2 *Attacker Model, Assumptions, and Requirements*

We require our IDS to be very lightweight and energy-efficient. To achieve this goal, different design alternatives are possible. In this chapter, we focus on reducing the permanent storage costs needed for the IDS, whereas in Chapter 5 we reduce the communication overhead. Besides, both systems randomize the detection frequency. Complex computations for attack detection should be avoided. Instead of analyzing multiple features, we again focus examplarily on the energy consumption as a single metric capable of detecting many types of DoS attacks. We further require the mobile agent itself and the data it carries to be of reasonable size. For this purpose, the number of energy readings needed to decide whether a node is under attack is minimized. Similarly, the data representation has to be chosen appropriately.

We assume an adversary mounting attacks that influence the power consumption, which is supposed to be relatively constant under normal conditions. We also assume that the attacker may compromise a node and alter its readings, but he cannot change those of other nodes without physically capturing them. Deviations from normal power consumption must be strong enough to be detectable. For example, the attacker might launch a flooding attack, causing a large number of additional messages to be transferred. Even though an attacker might try to evade detection by flooding at a very low rate, we argue that in a DoS scenario an aggressive attacker is more realistic.

We further assume that agents are transmitted as regular messages and can be executed on the nodes. In order not to create new attack vectors, we assume means

to ensure the integrity of the mobile agents and the carried data. For instance, the messages of the nodes can be authenticated and integrity-protected using automatically renewing hash chains, as implemented and described in Chapter 5. As a result, every protected message has a prepended initialization vector of 8 bytes and an appended hash chain value of 20 bytes.

Another assumption is that an attacker cannot remove a mobile agent without evidence, i.e., missing agents can be detected by the sensor network for example with the assistance of beacon messages. A node sends an authenticated status message to the sink indicating that it received a mobile agent. Whenever a system-defined threshold passed without seeing such a status message, a new mobile agent has to be generated. In our simulations, the usage of beacon messages proved to provide reliable results (this is again similar to Patrol).

In the case of an attack, a warning should be generated and transmitted to the base station. As we focus on intrusion detection, this part is beyond the scope of this thesis.

6.1.3 *Energy-based Intrusion Detection*

In Chapter 4, we propose a systematic way to analyze the impacts of flooding and blackhole attacks on the network behavior. We statistically test a large number of metrics to assess whether their values under attack are significantly different from non-attack values. In our experiments we find several metrics appropriate for attack detection, one of them being the energy consumption, which is the basis of this system.

Instead of sending data to other nodes and/or the base station for intrusion analysis, our proposed IDS is based on mobile agents that visit nodes and collect their energy statuses. Our system thus exchanges the overhead of installing a local IDS with the overhead of sending/receiving an agent. We then use a linear regression model to predict the normal energy consumption for each node independently, i.e., we take into account that the energy consumption varies across nodes, e.g., nodes near the base station often exhibit higher load. If a node's energy consumption is deviating significantly, i.e., it consumes either too much or too little energy, a warning is generated. The idea of analyzing the energy consumption is similar to the sample IDS developed within Patrol. However, in the statistics-based approach in Chapter 5, we calculate a range of the normal energy consumption. Now, we attempt to predict the changes in the energy consumption. We want to emphasize that our system is not limited to the energy as metric for intrusion detection; other metrics such as the packet delivery rate might be applied as well.

Linear Regression

To determine a range in which the energy consumption of a node should fall, we apply a linear regression model. The mobile agent produces a data set denoted

$$D = \{(x_{ij}, y_{ij}) | i = 1, 2, ...; j = 1, 2, ..., M\}$$

Each x_{ij} corresponds to the energy status of node j at the ith visit, and y_{ij} corresponds to the energy status predicted at the $(i-1)$th visit. For each node j, we learn a target

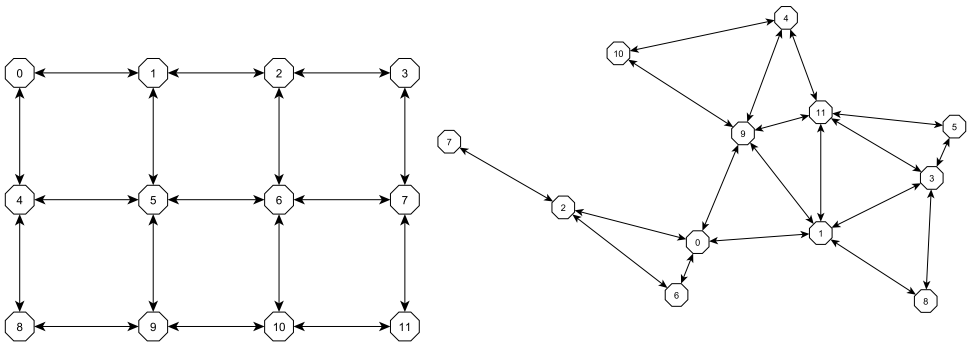

(a) WSN with 12 nodes and mesh topology

(b) WSN with 12 nodes and random topology

Figure 6.1: Mesh and random topologies of a WSN with 12 nodes

function f_j which maps the observations x into the prediction y. As we assume a linear relation between x and y, we can write the general form of the regression equation as

$$f_j(x) = b_j + a_j x = y \tag{6.1}$$

In Equation 6.1, the parameter b_j is the y intercept of the linear model, and a_j is the slope. We minimize the sum of the squares of the differences between the predicted and the actual values. At the ith visit, b_j and a_j are calculated using the last K pairs of (x,y). The slope is calculated as

$$a_j = \frac{K \sum_{t=i+1-K}^{i} x_{tj} y_{tj} - \sum_{t=i+1-K}^{i} x_{tj} * \sum_{t=i+1-K}^{i} y_{tj}}{K \sum_{t=i+1-K}^{i} x_{tj}^2 - (\sum_{t=i+1-K}^{i} x_{tj})^2}$$

The intercept is then given by

$$b_j = \frac{\sum_{t=i+1-K}^{i} y_{tj} - \sum_{t=i+1-K}^{i} a_j x_{tj}}{K}$$

This linear regression with ordinary least squares has a time complexity of $O(MK)$. The effect of the size of K (called *history size*) on the detection time is studied in Section 6.3.

6.2 PRACTICAL CONSIDERATIONS OF A MOBILE AGENT-BASED IDS

We now analyze the usage of mobile agents in a sensor network in terms of energy consumption and agent movement.

6.2.1 *Energy Consumption*

To show that mobile agents can be used in sensor networks, we analyze their energy consumption.

As pointed out by Piotrowski et al. [PLP06], a TelosB node has about 6750 J of usable energy. If we assume the agent to be 1 KB of size and using the power consumption

per bit as presented in [PLP06], we conclude that receiving one agent needs 1851 µJ, while sending one agent consumes at most 1712 µJ at highest transmission speed and 0 dBm transmit power. These costs only involve the radio energy.

Regarding an implementation of our IDS on real sensor nodes, certain aspects need to be considered. Apart from the mobile agent code itself, the energy values have to be transmitted alongside. In order to distinguish the agent code from regular data, e.g., sensor readings, the virtual channel concept of Contiki's Rime communication stack can be exploited. Packets containing the agent and the collected data may be tagged with a special identifier, that allows the receiving node to determine if it received a regular packet or an agent packet. A 4 bytes field for the total energy consumption and an index to identify specific readings can be used. The index field can also have a length of 4 bytes, leading to a total memory amount of 8 bytes for one energy reading. The security mechanisms will add an additional overhead of 28 bytes, as described in Section 6.1.2. That means, if the history size is set to 3, the data section of the mobile agent reaches 1296 bytes in a 12-node network. Therefore, fragmentation is needed, and the environmental conditions should guarantee a high packet delivery rate. Otherwise, this system may not be very efficient, and approaches such as Patrol could be advantageous.

6.2.2 *Agent Movement*

One crucial design decision in a mobile agent based system is the agent movement. By default, the agent in our system performs a random walk, but we also analyze different movement strategies which are more sophisticated. To start, we present basic facts and simulation results about how often a node is visited by the mobile agent in different topologies when walking randomly.

Random Walk

A random walking agent is similar to a token forwarded randomly, and hence, the analytical considerations in Section 5.3 apply here as well.

In our experiments, we simulate a network with 12 sensor nodes arranged (1) in a mesh and (2) in a random topology, an example is shown in Figure 6.1a and Figure 6.1b, respectively. The arrows indicate a link between two nodes, i.e., the nodes being in transmission range of each other. From Figure 6.2 we observe the influence of the node degree; for instance, node 1 is visited approx. twice as often by the mobile agent as node 2 in the random topology. This is due to the higher degree of node 1. Similar results are obtained for the mesh topology, in which a node at the border (like node 8) is not visited as regularly as a node in the center (like node 5). As a consequence, an attack started by a node with a low degree is likely to take more time to be detected. However, nodes with many links are more attractive to an attacker, as the effects of an attack propagate faster.

Other Walking Strategies

Since the random walk is favouring nodes with a high node degree, we want to analyze modified walking strategies with more evenly distributed node visits. Again, we take two different topologies into account, the mesh topology as shown in Figure 6.3

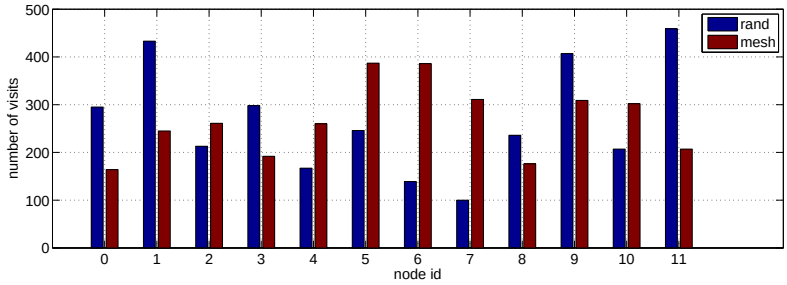

Figure 6.2: Average distribution of visits of a random walking agent

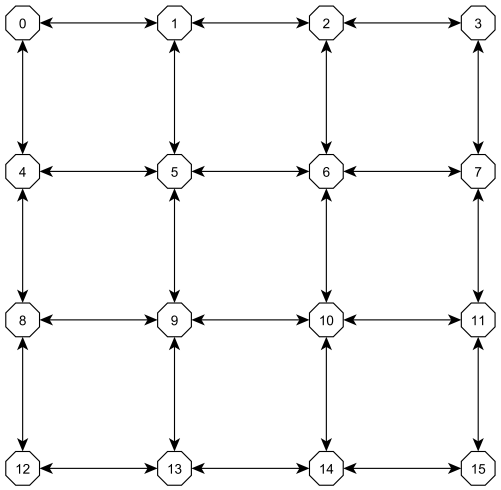

Figure 6.3: WSN with 16 nodes and mesh topology

and the random topology in Figure 6.4. Both topologies consist of 16 nodes. First, we increased the probability of visiting a node with a low degree (degree 2 in our simulated topologies) to 0.75. We found that this modification leads to a drastic disadvantage for nodes with a higher node degree, which are visited very rarely by the agent. In contrast, nodes with low degree such as node 12, are visited often. Therefore, we change the visit probabilities p for the mesh topology as follows: $p = 0.44$ for choosing a node with two links, $p = 0.33$ for three links, and $p = 0.23$ for four links. This setup yields a more even visit distribution of all nodes, as can be seen in Figure 6.5 which shows how often each node is visited in the three different

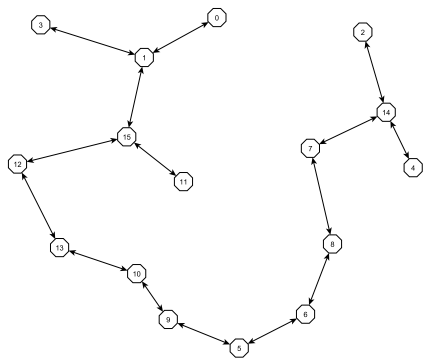

Figure 6.4: WSN with 16 nodes and random topology

walking strategies. The visit probabilities for the random topology have to be adjusted in the following way to achieve similar results as in the mesh topology: $p = 0.38$ for choosing a node with one link, $p = 0.26$ for two links, $p = 0.24$ for three links, and $p = 0.12$ for four links. The corresponding visit frequency dependent on the walking strategy for the random topology is presented in Figure 6.6. This modified (also called *biased*) random walk assures that the degree influence on the visit frequency is reduced. In Patrol, the same idea is realized by forwarding the token uniformly.

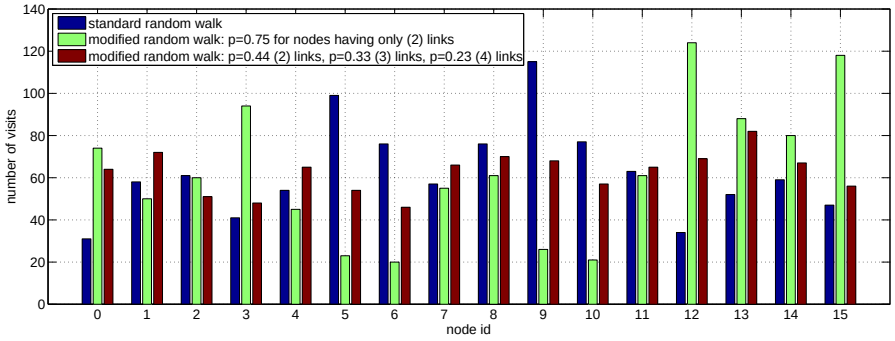

Figure 6.5: Average distribution of visits of an agent walking with three different walking strategies in a mesh topology

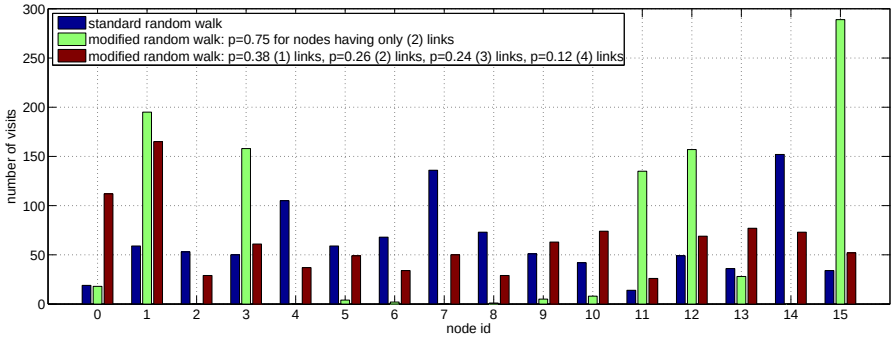

Figure 6.6: Average distribution of visits of an agent walking with three different walking strategies in a random topology

6.3 SIMULATION STUDY

We now describe our simulation-based evaluation. First, we show the feasibility of our approach. Then we describe the determination of optimal values for the critical parameters of our simulation, namely *migration time*, *slope*, and *history size*. Furthermore, we evaluate the proposed detection algorithm with regard to detection accuracy in a scenario with a flooding and a blackhole attack. We also study the influence of the history size and the walking strategies on the detection time. Finally, the limitations of our system are discussed. We summarize our findings in Table 6.1.

For all simulations, we extended an existing WSN simulator, designed for the STEF scheme [KSBE07] and developed in Java, to be used with mobile agents. The simulation platform is a standard ThinkPad W500 laptop with 4 GB RAM and an

Table 6.1: A summary of the major simulation results of this chapter

Objective	**Section**	**Conclusion**
Feasibility	6.3.1	By launching a flooding attack we show that the energy consumption is a feasible metric for detecting intrusions.
Parameters	6.3.2	We determine optimal parameters for our simulated network. They are unique for each WSN.
Detection Accuracy	6.3.3	Flooding and blackhole attacks can be detected with a low false-positive rate.
History Size	6.3.4	Larger history sizes increase the detection time.
Walking Strategy	6.3.5	A biased random walk can improve the detection time.

Intel Core 2 Duo T9600. The simulated sensor nodes correspond to TelosB nodes; their energy consumption rates were obtained from [PSC05]. Currently, we only simulate the energy consumption of the radio chip CC2420 as this is the largest energy driver in a WSN. As routing protocol we implement AODV, which is a reactive routing protocol and therefore is challenging for the IDS, because the energy consumption may fluctuate. As a consequence, this could lead to false-positive detection results. The agent has a size of 1 KB.

6.3.1 *Initial Demonstration*

Simulations were performed to analyze the influence of a flooding attack on the energy consumption of all nodes in the network. The goal is to detect attacks based on the energy consumption on either the malicious node itself or indirectly on its neighbors. The simulated WSN consists of 12 nodes arranged in a mesh topology (see Figure 6.1a; the arrows indicate a link between two nodes, i.e., the nodes being in transmission range of each other) with each node sending one random message per minute. After 128 minutes, node 3 starts an attack by flooding an additional message with a random destination to the WSN every minute.

Figure 6.7 shows the energy consumption (averaged over four test-runs) of each node. A very important finding is that this attack does not only influence the energy consumption of the malicious node itself, but it also affects all other nodes. The increase in energy consumption is especially significant for the direct neighbors of the attacking node, namely nodes 2 and 7. Those nodes receive a considerably higher number of messages than before launching the attack. Thus, the performed flooding attack can be detected not only by analyzing the energy slope of the malicious node itself, but also by monitoring other nodes in the WSN which have abnormal energy consumptions. This is important, as the attacker is likely to report fake data to the mobile agent.

6.3.2 *Determination of Parameters*

To reliably detect attacks, we need to determine meaningful values for the parameters used in our approach, in particular the *warm-up phase* and the *slope limit*, which should not be exceeded without triggering an alert.

Before calculating the energy slopes, we need a warm-up phase expressed as the number of agent migrations, in which the mobile agent collects multiple energy values from each visited node. The warm-up phase should guarantee that the agent collects as many energy readings of each node as required by the history size. Because the agent moves randomly, the number of migrations has to be higher than the number of nodes multiplied by the size of the history. Additionally, as shown in Section 6.2.2, the visit frequency depends on the node degree. To account for this, we need another multiplier k. In our simulations, $k = 2$ led to a high probability of collecting sufficient energy values from all nodes, and is therefore used in the rest of this chapter. Thus, we calculate the number of agent migrations needed before starting the detection mechanism following Equation 6.2.

$$warmup_{migrations} = number_{nodes} \times size_{history} \times k \tag{6.2}$$

Next, we have to determine a value for the slope limit, which is divided into *upper* and *lower* slope limit to also take attacks into account causing a lower energy consumption by, e.g., discarding packets. Exceeding or falling below those limits is regarded an anomaly. For this purpose, we performed additional simulations. The simulated sensor network consists of 12 randomly placed nodes. Each node injects one random message per minute into the network. Every minute, the agent migrates randomly from node to node. The history size is set to three, which means the agent carries the measured energy values of the last three visits of each node.

Figure 6.8 shows the current slopes of the collected energy values calculated by our randomly migrating agent (averaged over four test-runs). Immediately after the start, the WSN is not balanced, and there are relatively high slopes in the energy consumption due to the nature of the managing phase of the underlying routing protocol. Since we use AODV, the nodes need to establish routes and create routing tables after the start-up, resulting in a message overhead.

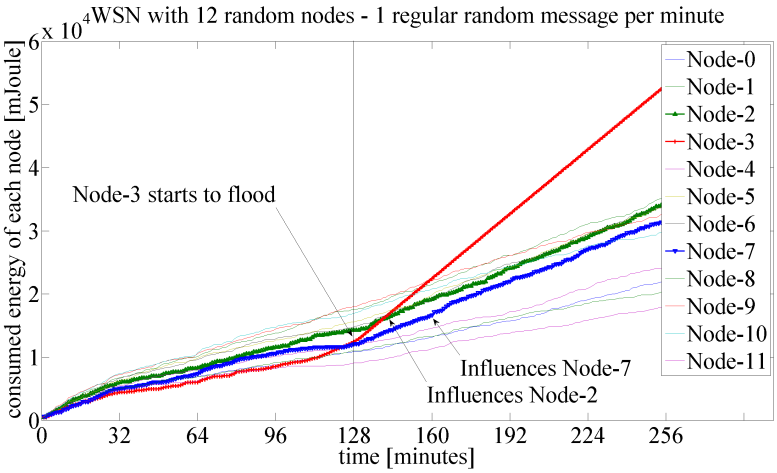

Figure 6.7: Measured energy of a WSN with 12 nodes arranged in a mesh

After the warm-up phase, which lasts for 72 migrations following Equation 6.2, the WSN becomes more balanced and the average slope of all nodes is stabilizing. Considering the results of Figure 6.8, we choose a value of 0.3 for the upper slope limit, i.e., the limit that applies to attacks increasing the energy consumption. Furthermore, we use a lower slope limit of 0.02, i.e., the minimal slope each node should have; otherwise an attack might be underway. Such an attack resulting in an abnormal low energy consumption could be a blackhole attack (see Section 6.3.3). It is possible to reduce the slope range, however, this could lead to an increased number of false-positives.

6.3.3 *Detection Accuracy*

To evaluate the effectiveness of our approach, we measure the detection accuracy when performing a flooding and a blackhole attack. The false-positive rate is therefore tracked and we determine the average number of migrations until detection. As a false-positive in the flooding attack scenario, we count all cases in which a node that is not the attacking node itself or a direct neighbor is reported as anomalous. Therefore, the false-positive rate is rather pessimistic, as effects of the attack might also propagate to 2-hop neighbors. Regarding the blackhole attack, a false-positive is reported whenever a node other than the attacker is wrongly identified as suspicious. Throughout all simulations in both attacking scenarios we were always able to detect the attack, i.e., the true-positive rate is 100%.

In our simulations, we vary the number of nodes from 8 to 16. Another parameter we vary is the migration time of the agent.

Flooding Attack

We performed a flooding attack in WSNs with 8 and 16 nodes arranged in a random topology; an example topology is shown in Figure 6.1b in Section 6.2.2. Each node is transmitting one message per minute. The parameters used are listed in Table 6.2.

Immediately after the warm-up phase, a randomly selected node starts a flooding attack by unicasting an additional random message every minute. Our agent uses

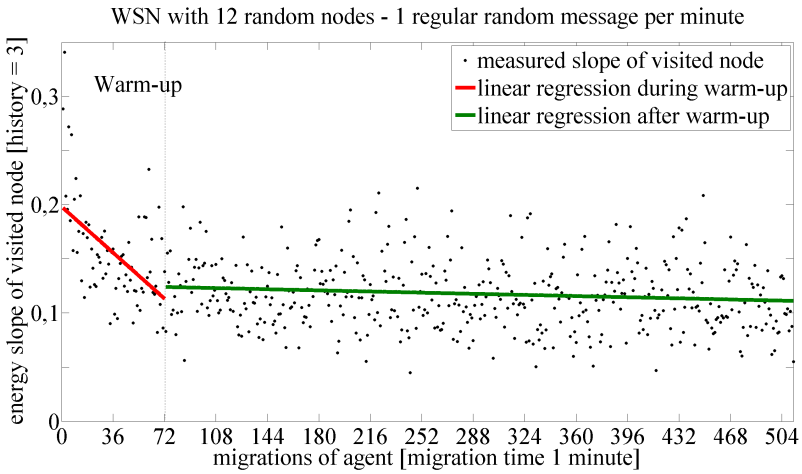

Figure 6.8: Energy slopes in a WSN with 12 nodes and random topology

Table 6.2: Values used for attack simulation

No. of nodes	Warm-up	History size	Slope limit
8	48 migrations	3	0.3
16	96 migrations	3	0.3

different migration times of 30s, 60s, and 90s. Moreover, the false-positive rate is tracked. Figure 6.9 shows the averaged results of the simulations (for each network size and for each migration time we performed 12 different test-runs). The false-positive rate can be observed in Table 6.3.

In our initial tests (not shown here), we found that a high migration rate led to a higher false-positive rate. This was due to the fact that the mobile agent needs comparatively more energy for its own operation, thereby interfering with the normal energy consumption of the wireless sensor network. To compensate for this, we let the agent subtract its own energy consumption from the nodes' energy readings. Therefore, the agent keeps track of the number of visits of each node, as the nodes themselves do not consider the agent's energy consumption. Table 6.3 and Figure 6.9 show that in all configurations a low false-positive rate in combination with a useful detection time is achieved. For instance, with a migration time of 30s, it takes about 5 migrations in a 8-node network until detection while at the same time the false-positive

Table 6.3: False-positive rate for the flooding attack

No. of nodes	30s	60s	90s
8	8.3%	8.3%	8.3%
16	8.3%	8.3%	0%

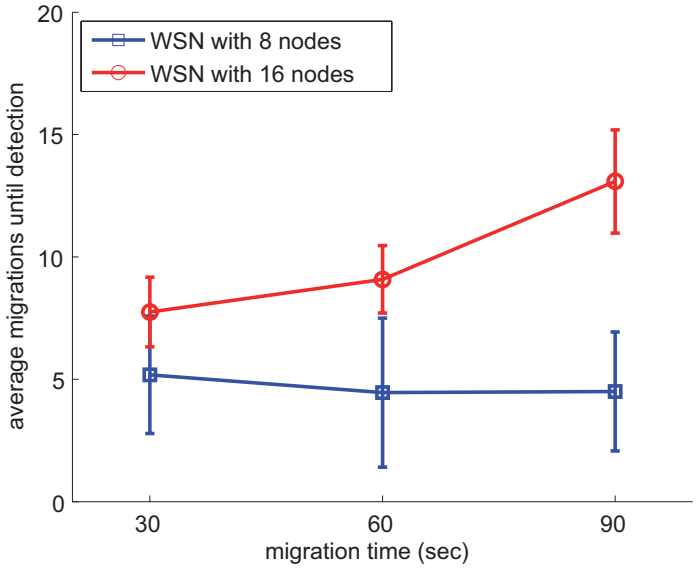

Figure 6.9: Average migrations until detection of a flooding attack

rate reaches 8.3%. The number of migrations needed to detect the flooding attack increases linearly with the number of nodes.

Blackhole Attack

The flooding simulation setup presented above was also used to evaluate the detection of a blackhole attack. Hence, the parameters of Table 6.2 remain mostly unchanged. The only difference is that the slope limit is now set to 0.02, as the blackhole attack should decrease the energy consumption (of the destination nodes and the nodes not on a path to the attacker) due to dropped packets. Figure 6.10 shows the results of the simulations. Again, for each network size and for each migration time we performed 12 test-runs. Compared to the results of the flooding attack, the agent needs more migrations until detection. This is because the blackhole attack does not influence the energy consumption of the attacker's neighbouring nodes as significantly as the flooding attack.

In a blackhole attack, the regular nodes have to be inactive, i.e., not receiving packets for a certain period of time until the slope drops. This epoch is fixed and therefore a higher migration speed cannot compensate the effect of the increasing number of migrations until detection. The 95% confidence intervals also show that the variation of the average migrations until detection is higher than for the flooding attack. Depending on the location of the attacker, it takes longer to detect the attack in a larger network. This is also true for the flooding attack.

Regarding the false-positive rate (Table 6.4), we achieve slightly worse results than with the flooding attack. The lowest false-positive rate is 8.3% for a migration time of 30s in a 16-node network.

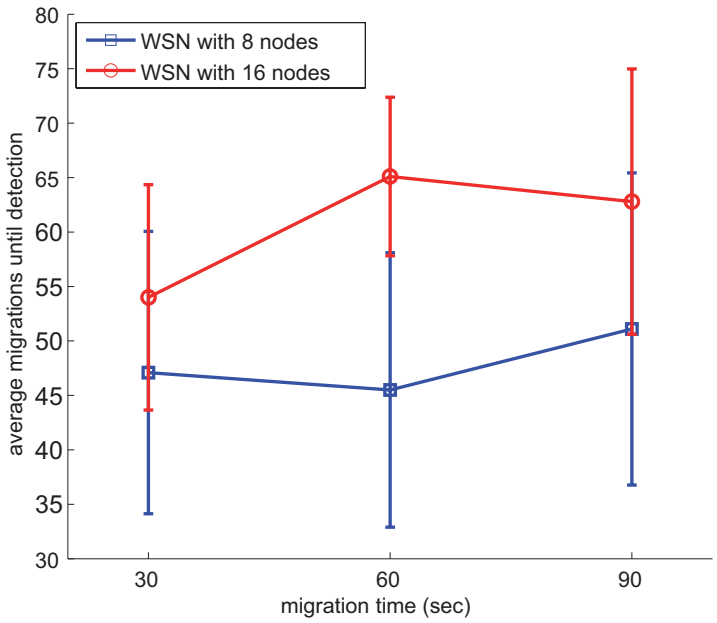

Figure 6.10: Average migrations until detection of a blackhole attack

Table 6.4: False-positive rate for the blackhole attack

No. of nodes	30s	60s	90s
8	16.6%	16.6%	16.6%
16	8.3%	16.6%	16.6%

6.3.4 *Influence of the History Size*

One way to optimize our IDS and keep it as lightweight as possible, is to change the history size, i.e., the number of readings needed from each node to predict the energy consumption. In simulations for a 12-node WSN we varied the history size from 2 to 3 and 4, while performing a flooding attack. Figure 6.11 presents the results showing that the average number of migrations until detection increases with the history size. A smaller history size is able to reflect the change in the energy consumption more quickly, thereby generating an anomaly alert faster than a larger history size. The drawback is a higher false-positive rate (see Table 6.5).

6.3.5 *Influence of the Walking Strategy*

Attacks that affect nodes with a low degree could potentially take more time to be detected by a random walking agent as compared to different walking strategies. Therefore, we now investigate the influence of the walking strategy on the detection time.

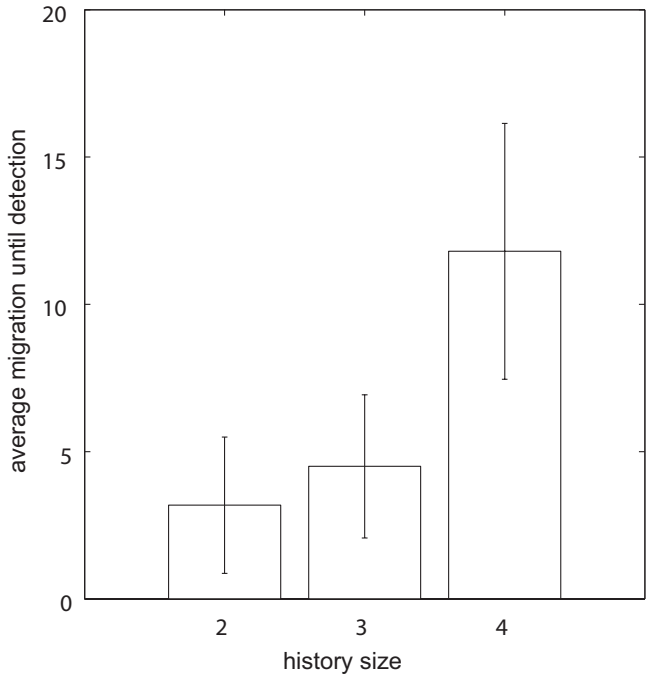

Figure 6.11: Influence of the history size (WSN with 12 nodes in a random topology and a flooding attack)

Table 6.5: False-positive rate for the flooding attack, depending on the history size, migration time = 90s

History size	False-positive rate
2	33.3 %
3	8.3%
4	0%

Table 6.6: Detection, false positive (FP) and false negative (FN) rates for the flooding attack

Topology	Walking strategy	Migrations	FP	FN
Mesh	Random	86	18.75%	6.25%
Mesh	Biased Random	37	6.25%	0%

The setup for the simulations evaluating different walking strategies is as follows. The mesh wireless sensor network consists of 16 nodes, the topology of which is the same as shown in Figure 6.3 in Section 6.2.2. Each node is transmitting one message every two minutes, the agent migrates every 30 seconds, the slope limit is 1.0, and the history size is set to three. The warm-up phase lasts for 256 migrations, after 320 migrations we start the flooding by letting node 0 send one additional message every minute. If an intrusion was detected during the period the warm-up phase ended and before the attack started, we count this event as false-positive. Cases, in which a node that is neither a direct neighbor of the attacker nor the attacker itself was found to be suspicious, also count as false-positive. If we did not detect an intrusion within 576 migrations, this event is counted as false-negative (see also Figure 6.12). The probabilities for the biased random walk were defined as $p = 0.44$ for choosing a node with two links, $p = 0.33$ for three links, and $p = 0.23$ for four links. Each experiment is repeated 16 times.

The results can be found in Table 6.6. In such a setting, having a more isolated node be the attacker, the biased random walk achieves significantly better results, given a mesh topology. The average number of migrations needed to detect the attack is reduced by about 43%. Besides, we were always able to detect the attack within 576 migrations. We achieve similar results for a random topology.

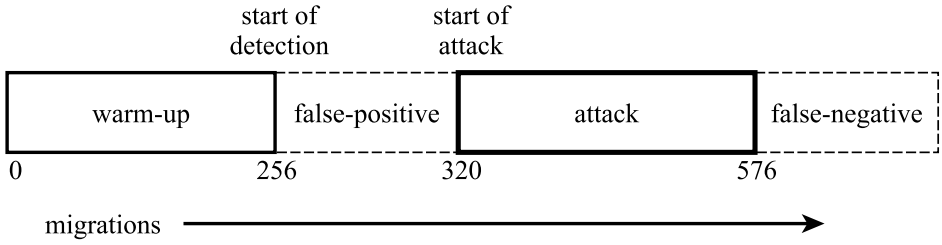

Figure 6.12: Evaluation setup

6.3.6 *Discussion*

In this chapter we show that mobile agents can be used in WSNs to detect intrusions reliably. However, our proposed approach has some limitations which we discuss in the following:

- The system presented herein is not suited for every WSN scenario. While it works very well in environmental monitoring settings with regular measurement and transmitting patterns as in [TPS+05], the opposite is true for example in area surveillance scenarios, where a detected event is resulting in intense activity.
- The assumption of the linearity of the energy consumption may not always hold in a real-world testbed, in which we face problems with unreliable and bursty links. As a consequence, such behavior could result in an increased false-positive rate.
- An attacker with physical access could change the agent and let nodes execute his own code. Since we assume that nodes can be physically compromised, a trusted base station is required to prevent such an attack. One possibility to do so is by using public-key cryptography, which has become feasible in wireless sensor networks [LN08]. The base station signs the agent code with its private key. As per assumption all sensor nodes know the public key of the base station, they can verify that the code has not been changed.
- The low amount of storage available on today's standard nodes limits the applicability of our system to comparatively small WSNs.
- Transferring huge agents requires a large amount of energy. Hence, reducing the size of the agent by using middleware such as Agilla [FRL05] is a promising direction.
- Our approach is not supposed to be a general security framework capable of defending against all types of attacks, such as sybil or data manipulation attacks. Attacks that have no influence on the energy consumption remain undetected.

6.4 RELATED WORK

Our work covers several aspects: (1) the mobile agent paradigm, (2) the usage of mobile agents to detect intrusions, and (3) the energy consumption as a possible metric for attacks. The combination of these techniques is unique in wireless sensor networks. In this section we discuss related work for these aspects.

Mobile Agents in WSNs

With *Agilla*, a middleware for wireless sensor networks was presented by Fok et al. [FRL05] which allows the development and usage of mobile agents. Instead of deploying pre-installed applications, mobile agents perform the desired tasks. They model each agent as an autonomous entity, but provide inter-agent communication.

The mobile agent-based computing model has been evaluated in the context of collaborative processing in WSNs in the work of Qi et al. [QXW03]. The authors

use the execution time and the energy consumption as metrics for evaluating the performance of the client/server-based and mobile agent-based models. In their simulations they found that even though both the execution time and the energy consumption grow as the number of nodes increases, the growth is much faster for the client/server model. They conclude that the mobile agent-based model is not consistently performing better than the client/server-based model, but it may be advantageous depending on the use case.

Intrusion Detection using Mobile Agents

Applying mobile agents for intrusion detection has been widely researched; several works exist. Helmer et al. [HWH+03] designed an intrusion detection system for traditional networks employing static as well as mobile agents. Stationary agents reside at each monitored component, gathering information, e.g., from system logs and providing this information in a common format. Mobile agents travel between monitored components, classify the data collected from the static agents as normal data and data signifying an intrusion, and pass this information to so-called *mediators*. Mediators manage the mobile agents and further use data mining techniques to relate single events to a specific attack.

Kachirski and Guha [KG02] proposed a mobile agent-based intrusion detection system for wireless ad hoc networks. They use different sensor types to perform specific functions. While few nodes have agents for network packet monitoring, every node's agent monitors the host itself for suspicious activities such as unusual user operations (e.g., invalid login attempts). On a host-level basis, decisions on the threat level of an intrusion are made individually. Certain nodes collaborate in order to make decisions about intrusions affecting the network level. For the purpose of responding and resolving an intrusion, each node is equipped with an action module.

Sparta is a system able to detect intrusions and security policy violations in a network [KT01]. A pattern language is introduced allowing the user to define intrusion patterns in a declarative manner. The approach to spot these patterns is fully distributed, utilizing mobile agents to correlate event data gathered on the single hosts.

All three approaches mentioned above were not designed for WSNs and create significant overhead.

Energy Consumption

Some authors have already used the energy consumption as a metric for intrusion detection. Nash et al. [NMHH05] presented an IDS for mobile computers that uses several parameters like CPU load and disk read and write access to estimate the power consumption. The linear regression they used is therefore quite complex, while our model only needs one variable: the energy status of a node. Moreover, their system determines the energy consumption on a per process basis. This renders the IDS vulnerable to attacks that distribute the workload to many different processes.

Buennemeyer et al. [BNC+08] developed an IDS that creates a power profile for mobile devices, generating an alert in case of abnormal current changes. The threshold value is adapted dynamically to account for false-positives and false-negatives. Battery readings are transmitted to a central point, which would cause significant overhead in WSNs. In order to create a reliable profile, a large amount of data has to be sent and

analyzed, whereas we require only the last three energy readings from each node for reliable attack detection. At the central server, attack traffic is correlated with Snort alerts. Thus, their system is very complex as it combines anomaly detection with a rule-based IDS. Another drawback of the last two approaches lies in the necessity to run an IDS agent on every node. In contrast, our system takes into account specific WSN requirements (typically, nodes run a single application, have severe resource restrictions, sleep most of the time, etc.) by developing a lightweight method for intrusion detection.

Shen et al. [SHS+12] proposed an intrusion detection scheme comparing the energy consumptions of different sensor nodes in clustered WSNs. It can differentiate the types of DoS attacks such as selective forwarding and wormhole attacks with the assistance of energy thresholds. Nodes are required to send messages containing their remaining energy to the base station. The energy consumption of all nodes is then predicted at the base station by using markov chains. The scheme looks for nodes which spend significantly more energy than the other nodes. In their work, they assume that the energy consumption is similar for all nodes, which is an unrealistic assumption.

6.5 SUMMARY

In this chapter we propose a novel lightweight IDS for wireless sensor networks. We neither require nodes to monitor their environment and collaborate with each other, nor do we need to transfer audit data to a central point. Instead, we use a mobile agent that collects energy readings and raises an alert if sudden changes occur. The feasibility of reducing the intrusion detection functionality using mobile agents in wireless sensor networks has been demonstrated.

7 CONCLUSIONS AND OUTLOOK

> You rarely achieve finality. If you did, life would be over, but as you strive new visions open before you.
>
> E. Roosevelt

7.1 SUMMARY AND CONCLUSIONS

Providing security in wireless sensor networks during operation involves addressing multiple challenges, especially the reduction of complexity and resource-requirements in intrusion detection. Throughout this thesis, we have contributed to solve this challenge by providing solutions along two key directions. In our first research direction, we have studied the practical effects of DoS attacks on wireless sensor networks. Albeit important for attack dection, this aspect has mainly been neglected by existing works. Moreover, in our second research direction, we have reduced the intrusion detection frequency and built extensible and lightweight systems that allow intrusion detection at a low cost.

Particulary, we have introduced a systematic approach for evaluating attack effects on the network behavior. Therefore, we have identified a large number of local node metrics, that can be easily obtained and calculated without incurring too much overhead. Next, we have statistically tested these metrics to assess whether they exhibit significantly different values when the network is attacked. The metrics we have analyzed look into different aspects of the motes and the network, for example, MCU and radio activities, network traffic statistics, and routing related information. In our experiments, we have varied several parameters to show that the metrics are applicable to different WSNs, such as traffic intensity and transmission power. Using the collection tree and the mesh protocol, we have considered two of the most common applications in wireless sensor networks, such as central data collection and meshed multi-hop networks. Finally, we have analyzed the metrics with regard to their capability of distinction. Our results show that certain metrics can be used solely to detect a jamming attack, while in some scenarios a combination of metrics needs to be analyzed. Even though we have focused on jamming and blackhole attacks, our methodology can be applied to other metrics and attacks as well. Besides, we have presented a fully localized IDS, which only analyzes node-specific metrics. In contrast to existing works, we do not require any form of collaboration.

Because of severe resource-restrictions, it is desirable to reduce the tasks of each mote to a minimum. We have proposed two intrusion detection systems that address the conflict between energy consumption and detection frequency. In detail, we have shown that even critical security functions, an example being intrusion detection, can be performed by means of randomizing the detection frequency at the cost of a slightly increased detection time. To this end, we have presented a system distributing the load

which is caused by various tasks across the network. This system utilizes tokens which are exchanged between nodes. Upon reception of such a token, a certain functionality, such as intrusion detection, is activated temporarily. As a proof-of-concept, we have designed and implemented a lightweight intrusion detection algorithm based on the energy consumption of the nodes. We have shown by experimentation in a real-world testbed that we can dectect flooding and blackhole attacks very fast also without constant intrusion detection.

We have finally proposed a second intrusion detection system, which is similar to the first one in the sense that we randomize the detection frequency. However, in this system we are exchanging the whole IDS routine in the network. The central building block is a mobile agent which migrates from node to node and contains code as well as data used for intrusion detection. It carries the energy status of the nodes and detects intrusions by analyzing the energy consumption with a linear regression model. Consequently, this approach exchanges the overhead of storing an IDS permanently with the communication overhead of transferring the mobile agent. We have shown in simulations that denial-of-service attacks such as flooding and blackhole can be detected with high accuracy, while keeping the number of false-positives very low.

In summary, this thesis contributes to the lightweight detection of denial-of-service attacks on wireless sensor networks. Our solutions are flexible, configurable, and extensible which allows them to be used in a large number of scenarios due to the relatively weak requirements. All contributions are motivated by the low power and low computational capabilities of state-of-the-art sensor nodes.

7.2 OUTLOOK

The contributions of this thesis lay the foundations for lightweight intrusion detection in wireless sensor networks. In what follows, we shed light on a variety of new research directions and challenges:

▷ POWERFUL SENSOR NODES

The development of nodes with more powerful processing capabilities, such as the ARM microcontroller, allows the usage of algorithms for intrusion detection that are very sophisticated. To give an example, the application of traditional machine learning operators such as decision trees or support vector machines might become feasible on sensor nodes. However, these microcontrollers consume much energy, thus energy-efficiency is still important.

▷ ATTACKERS EVERYWHERE

With the progress of the Internet of Things (IoT), security becomes even more an issue. IPv6 over Low-power Wireless Personal Area Network (6LoWPAN) [KMS07, HT11] enables the connection of sensor nodes with the untrusted Internet. Hence, an attacker can get access to the nodes from virtually everywhere; he no longer needs to be in physical proximity. In the same way, the number of potential attackers increases. To tackle this problem, new IDSs need to be developed taking into account the architecture in the IoT: (1) the edge node connecting 6LoWPAN networks with the Internet is assumed to be always acces-

sible, (2) end-to-end message security is required, and (3) sensor nodes have a globally unique IP address [RWV13].

▷ DETECTING FALSE DATA

A characteristic feature for many WSNs is the high density of deployed sensor nodes. Especially in industrial control scenarios, the number of sensors can reach 35.000 [SBR10]. This redundancy is necessary to account for the high criticality of the system and allows us to exploit this fact for detecting false data. Nodes in close proximity should exhibit highly correlated observations. Besides this spatial correlation, the measured physical parameters typically are temporally correlated. Measured processes are well-defined and executed repeatedly.

One possibility to exploit the spatio-temporal relationship between node readings is to perform statistical anomaly detection at the sink. This central point can leverage the global view it has on all nodes in the network and apply powerful machine learning algorithms to first build a model of normal readings, and then classify new observations based on historical data [NSBJ11].

Alternatively, the usage of decentralized algorithms to detect data anomalies requiring little memory and processing power is promising. First proposals to distributed data mining in WSNs have been made [BSG+06, BHL07, Rö7, FCG10]. However, their focus is rather on false data caused by measurement errors and node failures. Attackers that intentionally change the data to create a specific malfunctioning are not considered. In addition, their memory and communication overhead might still be too high in certain scenarios.

▷ INTRUSION RESPONSE

Once an attack has been detected, it is necessary to take corrective action. A challenge associated with this is how to inform the network operator while the network is under attack, e.g., no communication over the wireless links might be possible.

In conclusion, wireless sensors are widely used in the real-world, yet a number of open challenges especially in the domain of security persist. To the best of our knowledge, real WSN deployments are still missing intrusion detection functionality.

BIBLIOGRAPHY

[AIM10] L. Atzori, A. Iera, and G. Morabito: *The internet of things: A survey*. Computer Networks, 54:2787–2805, 2010.

[Aka72] H. Akaike: *Information theory and an extension of the maximum likelihood principle*. In *Proceedings of the 2nd International Symposium on Information Theory*, 1972.

[Alm15] L. Almon: *Practical decentralized intrusion detection in wireless sensor networks*. Master's thesis, Technische Universität Darmstadt, 2015.

[And80] J. P. Anderson: *Computer security threat monitoring and surveillance*. Technical report, James P. Anderson Company, 1980.

[ASSC02] I. Akyildiz, W. Su, Y. Sankarasubramaniam, and E. Cayirci: *Wireless sensor networks: a survey*. Computer Networks, 38:393–422, 2002.

[Ban14] M. E. Bansarkhani: *Statistische analyse der auswirkungen von denial-of-service angriffen auf drahtlose sensornetzwerke*. Master's thesis, Technische Universität Darmstadt, 2014.

[BCF08] Z. Benenson, P. M. Cholewinski, and F. Freiling: *Wireless Sensor Network Security*, chapter Vulnerabilities and Attacks in Wireless Sensor Networks, pages 22–43. IOS Press, 2008.

[Ber08] D. J. Bernstein: *The salsa20 family of stream ciphers*. In *New Stream Cipher Designs*. Springer Berlin / Heidelberg, 2008.

[BHL07] L. Bettencourt, A. Hagberg, and L. Larkey: *Separating the wheat from the chaff: Practical anomaly detection schemes in ecological applications of distributed sensor networks*. In *Proceedings of the 3rd IEEE International Conference on Distributed Computing in Sensor Systems (DCOSS)*. Springer Berlin / Heidelberg, 2007.

[BMS14] I. Butun, S. Morgera, and R. Sankar: *A survey of intrusion detection systems in wireless sensor networks*. IEEE Communications Surveys & Tutorials, 16:266–282, 2014.

[BNC+08] T. K. Buennemeyer, T. M. Nelson, L. M. Clagett, J. P. Dunning, R. C. Marchany, and J. G. Tront: *Mobile device profiling and intrusion detection using smart batteries*. In *Proceedings of the 41st Hawaii International Conference on System Sciences (HICSS)*, 2008.

[BSG+06] J. Branch, B. Szymanski, C. Giannella, R. Wolff, and H. Kargupta: *In-network outlier detection in wireless sensor networks*. In *Proceedings of the 26th International Conference on Distributed Computing Systems (ICDCS)*, 2006.

[BvKH+11] D. Bijwaard, W. van Kleunen, P. Havinga, L. Kleiboer, and M. Bijl: *Industry: Using dynamic wsns in smart logistics for fruits and pharmacy*. In *Proceedings of the 9th ACM Conference on Embedded Networked Sensor Systems (SenSys)*, 2011.

[BVN+11] C. Boano, T. Voigt, C. Noda, K. Römer, and M. Zuniga: *Jamlab: Augmenting sensornet testbeds with realistic and controlled interference generation*. In *Proceedings of the 10th International Conference on Information Processing in Sensor Networks (IPSN)*, 2011.

[BZV+10] C. Boano, M. Zuniga, T. Voigt, A. Willig, and K. Römer: *The triangle metric: Fast link quality estimation for mobile wireless sensor networks*. In *Proceedings of the 19th International Conference on Computer Communications and Networks (ICCCN)*, 2010.

[CA07] Y. Cheng and D. P. Agrawal: *An improved key distribution mechanism for large-scale hierarchical wireless sensor networks*. Ad Hoc Networks, 5:35–48, 2007.

[CCD+11] M. Ceriotti, M. Corra, L. D'Orazio, R. Doriguzzi, D. Facchin, S. Guna, G. Jesi, R. Lo Cigno, L. Mottola, A. Murphy, M. Pescalli, G. Picco, D. Pregnolato, and C. Torghele: *Is there light at the ends of the tunnel? wireless sensor networks for adaptive lighting in road tunnels*. In *Proceedings of the 10th International Conference on Information Processing in Sensor Networks (IPSN)*, 2011.

[CPMM11] M. Conti, R. D. Pietro, L. V. Mancini, and A. Mei: *Distributed detection of clone attacks in wireless sensor networks*. IEEE Transactions on Dependable and Secure Computing, 8(5):685–698, 2011.

[CS99] W. W. Cohen and Y. Singer: *A simple, fast, and effective rule learner*. In *Proceedings of the 16th National Conference on Artificial Intelligence (AAAI)*, pages 335–342, 1999.

[dC14] R. do Carmo: *Active Intrusion Detection for Wireless Multihop Networks*. PhD thesis, Technische Universität Darmstadt, 2014.

[Den87] D. Denning: *An intrusion-detection model*. IEEE Transactions on Software Engineering, SE-13:222–232, 1987.

[DG10] T. Dimitriou and A. Giannetsos: *Wormholes no more? localized wormhole detection and prevention in wireless networks*. In *Proceedings of the 6th IEEE International Conference on Distributed Computing in Sensor Systems (DCOSS)*, 2010.

[DGV04] A. Dunkels, B. Gronvall, and T. Voigt: *Contiki - a lightweight and flexible operating system for tiny networked sensors*. In *Proceedings of the 29th IEEE Conference on Local Computer Networks (LCN)*, 2004.

[DLHZ13] W. Dong, Y. Liu, Y. He, and T. Zhu: *Measurement and analysis on the packet delivery performance in a large scale sensor network*. In *Proceedings of the 32nd IEEE International Conference on Computer Communications (INFOCOM)*, 2013.

[dSMR+05] A. P. da Silva, M. Martins, B. Rocha, A. Loureiro, L. B. Ruiz, and H. C. Wong: *Decentralized intrusion detection in wireless sensor networks*. In *Proceedings of the 1st ACM International Workshop on Quality of Service & Security in Wireless and Mobile Networks (Q2SWinet)*, 2005.

[EG02] L. Eschenauer and V. D. Gligor: *A key-management scheme for distributed sensor networks*. In *Proceedings of the 9th ACM Computer and Communications Security Conference (CCS)*, 2002.

[FCG10] P. A. Forero, A. Cano, and G. B. Giannakis: *Consensus-based distributed linear support vector machines*. In *Proceedings of the 9th International Conference on Information Processing in Sensor Networks (IPSN)*, 2010.

[FRL05] C.-L. Fok, G.-C. Roman, and C. Lu: *Rapid development and flexible deployment of adaptive wireless sensor network applications*. In *Proceedings of the 25th IEEE International Conference on Distributed Computing Systems (ICDCS)*, 2005.

[GDMV09] P. Garcia-Teodoro, J. Diaz-Verdejo, G. Macia-Fernandez, and E. Vazquez: *Anomaly-based network intrusion detection: Techniques, systems and challenges*. Computers & Security, 28:18–28, 2009.

[GFJ+09] O. Gnawali, R. Fonseca, K. Jamieson, D. Moss, and P. Levis: *Collection tree protocol*. In *Proceedings of the 7th ACM Conference on Embedded Networked Sensor Systems (SenSys)*, 2009.

[GGSB13] P. E. Guerrero, I. Gurov, S. Santini, and A. Buchmann: *On the selection of testbeds for the evaluation of sensor network protocols and applications*. In *Proceedings of the 14th IEEE International Workshop on Signal Processing Advances in Wireless Communications (SPAWC)*, 2013.

[GKS05] G. Gaubatz, J.-P. Kaps, and B. Sunar: *Public key cryptography in sensor networks revisited*. In *Security in Ad-hoc and Sensor Networks*. Springer Berlin / Heidelberg, 2005.

[GZC07] S. Gupta, R. Zheng, and A. M. K. Cheng: *Andes: an anomaly detection system for wireless sensor networks*. In *Proceedings of the 4th IEEE International Conference on Mobile Ad-hoc and Sensor Systems (MASS)*, 2007.

[HC08] J. W. Hui and D. E. Culler: *Ip is dead, long live ip for wireless sensor networks*. In *Proceedings of the 6th ACM Conference on Embedded Networked Sensor Systems (SenSys)*, 2008.

[HHJ10] T. H. Hai, E.-N. Huh, and M. Jo: *A lightweight intrusion detection framework for wireless sensor networks*. Wirel. Commun. Mob. Comput., 10(4):559–572, 2010.

[HHW09] J.-H. Hauer, V. Handzinski, and A. Wolisz: *Experimental study of the impact of wlan interference on ieee 802.15.4 body area networks*. In *Proceedings of the 8th European Conference on Wireless Sensor Networks (EWSN)*, 2009.

[HR10] M. Hossain and V. Raghunathan: *Aegis: A lightweight firewall for wireless sensor networks*. In *Proceedings of the 6th IEEE International Conference on Distributed Computing in Sensor Systems (DCOSS)*, 2010.

[HSW+00] J. Hill, R. Szewczyk, A. Woo, S. Hollar, D. Culler, and K. Pister: *System architecture directions for networked sensors*. SIGPLAN Not., 35(11):93–104, 2000.

[HT11] J. Hui and P. Thubert: *Compression format for ipv6 datagrams over ieee 802.15.4-based networks*. In *RFC 6282*, September 2011.

[HWH+03] G. Helmer, J. S. K. Wong, V. Honavar, L. Miller, and Y. Wang: *Lightweight agents for intrusion detection*. Journal of Systems and Software, 67:109–122, 2003.

[IKP95] K. Ilgun, R. Kemmerer, and P. Porras: *State transition analysis: a rule-based intrusion detection approach*. IEEE Transactions on Software Engineering, 21:181–199, 1995.

[KBG+09] I. Krontiris, Z. Benenson, T. Giannetsos, F. C. Freiling, and T. Dimitriou: *Cooperative intrusion detection in wireless sensor networks*. In *Proceedings of the 6th European Conference on Wireless Sensor Networks (EWSN)*, 2009.

[KBT13] M. Keller, J. Beutel, and L. Thiele: *The problem bit*. In *Proceedings of the 9th IEEE International Conference on Distributed Computing in Sensor Systems (DCOSS)*, 2013.

[KDF07] I. Krontiris, T. Dimitriou, and F. C. Freiling: *Towards intrusion detection in wireless sensor networks*. In *Proceedings of the 13th European Wireless Conference (EW)*, 2007.

[KDGM08] I. Krontiris, T. Dimitriou, T. Giannetsos, and M. Mpasoukos: *Intrusion detection of sinkhole attacks in wireless sensor networks*. In *Algorithmic Aspects of Wireless Sensor Networks*, volume 4837, pages 150–161. Springer Berlin / Heidelberg, 2008.

[KE14] E. Karapistoli and A. A. Economides: *Adlu: a novel anomaly detection and location-attribution algorithm for uwb wireless sensor networks*. EURASIP Journal on Information Security, 3(1), 2014.

[KEW02] B. Krishnamachari, D. Estrin, and S. Wicker: *The impact of data aggregation in wireless sensor networks*. In *Proceedings of the 22nd International Conference on Distributed Computing Systems Workshops (ICDCSW)*, 2002.

[KG02] O. Kachirski and R. Guha: *Intrusion detection using mobile agents in wireless ad hoc networks*. In *Proceedings of the IEEE Workshop on Knowledge Media Networking (KMN)*, 2002.

[KMS07] N. Kushalnagar, G. Montenegro, and C. Schumacher: *Ipv6 over lowpower wireless personal area networks (6lowpans): Overview, assumptions, problem statement, and goals*. In *RFC 4919*, August 2007.

[KSBE07] C. Krauß, M. Schneider, K. Bayarou, and C. Eckert: *Stef: A secure ticket-based en-route filtering scheme for wireless sensor networks*. In *Proceedings of the 2nd International Conference on Availability, Reliability and Security (ARES)*, 2007.

[KT01] C. Krügel and T. Toth: *Sparta - a mobile agent based intrusion detection system*. In *Proceedings of the 1st IFIP Conference on Network Security (I-NetSec)*, 2001.

[KW03] C. Karlof and D. Wagner: *Secure routing in wireless sensor networks: attacks and countermeasures*. Ad Hoc Networks, 1:293–315, 2003.

[Lan05] M. Langheinrich: *Personal privacy in ubiquitous computing*. PhD thesis, ETH Zurich, 2005.

[LC11] T. Liu and A. Cerpa: *Foresee (4c): Wireless link prediction using link features*. In *Proceedings of the 10th International Conference on Information Processing in Sensor Networks (IPSN)*, 2011.

[LCC07] F. Liu, X. Cheng, and D. Chen: *Insider attacker detection in wireless sensor networks*. In *Proceedings of the 26th IEEE International Conference on Computer Communications (INFOCOM)*, 2007.

[LHL+11] Y. Liu, Y. He, M. Li, J. Wang, K. Liu, L. Mo, W. Dong, Z. Yang, M. Xi, J. Zhao, and X.-Y. Li: *Does wireless sensor network scale? A measurement study on greenorbs*. In *Proceedings of the 30th IEEE International Conference on Computer Communications (INFOCOM)*, 2011.

[LHS00] J. J. Louviere, D. A. Hensher, and J. D. Swait: *Stated Choice Methods: Analysis and Applications*. Cambridge University Press, 2000.

[LKP07] M. Li, I. Koutsopoulos, and R. Poovendran: *Optimal jamming attacks and network defense policies in wireless sensor networks*. In *Proceedings of the 26th IEEE International Conference on Computer Communications (INFOCOM)*, 2007.

[LMPG07] M. Luk, G. Mezzour, A. Perrig, and V. Gligor: *Minisec: A secure sensor network communication architecture*. In *Proceedings of the 6th International Conference on Information Processing in Sensor Networks (IPSN)*, 2007.

[LMZL11] K. Liu, Q. Ma, X. Zhao, and Y. Liu: *Self-diagnosis for large scale wireless sensor networks*. In *Proceedings of the 30th IEEE International Conference on Computer Communications (INFOCOM)*, 2011.

[LN08] A. Liu and P. Ning: *Tinyecc: A configurable library for elliptic curve cryptography in wireless sensor networks*. In *Proceedings of the 7th International Conference on Information Processing in Sensor Networks (IPSN)*, 2008.

[LNLP06] C. E. Loo, M. Y. Ng, C. Leckie, and M. Palaniswami: *Intrusion detection for routing attacks in sensor networks*. International Journal of Distributed Sensor Networks, 2:313–332, 2006.

[Lov96] L. Lovász: *Random walks on graphs: a survey*. In *Combinatorics, Paul Erdös is Eighty*. Janos Bolyai Mathematical Society, 1996.

[LSS+10] J. Lu, T. Sookoor, V. Srinivasan, G. Gao, B. Holben, J. Stankovic, E. Field, and K. Whitehouse: *The smart thermostat: Using occupancy sensors to save energy in homes*. In *Proceedings of the 8th ACM Conference on Embedded Networked Sensor Systems (SenSys)*, 2010.

[LTZ+13] G. Liu, R. Tan, R. Zhou, G. Xing, W.-Z. Song, and J. M. Lees: *Volcanic earthquake timing using wireless sensor networks*. In *Proceedings of the 12th International Conference on Information Processing in Sensor Networks (IPSN)*, 2013.

[LWW11] Z. Lu, W. Wang, and C. Wang: *From jammer to gambler: Modeling and detection of jamming attacks against time-critical traffic*. In *Proceedings of the 30th IEEE International Conference on Computer Communications (INFOCOM)*, 2011.

[Man97] S. Mann: *Wearable computing: a first step toward personal imaging*. Computer, 30:25–32, 1997.

[Men02] S. Menard: *Applied logistic regression analysis*. Sage, 2002.

[MHL94] B. Mukherjee, L. T. Heberlein, and K. N. Levitt: *Network intrusion detection*. IEEE Network, 8:26–41, 1994.

[MMH+12] X. Mao, X. Miao, Y. He, X.-Y. Li, and Y. Liu: *Citysee: Urban co2 monitoring with sensors*. In *Proceedings of the 31st IEEE International Conference on Computer Communications (INFOCOM)*, 2012.

[MMP+13] R. Marfievici, A. Murphy, G. Picco, F. Ossi, and F. Cagnacci: *How environmental factors impact outdoor wireless sensor networks: A case study*. In *Proceedings of the 10th IEEE International Conference on Mobile Ad hoc and Sensor Systems (MASS)*, 2013.

[MOV96] A. J. Menezes, P. C. V. Oorschot, and S. A. Vanstone: *Handbook of applied cryptography*. CRC Press, 1996.

[MPS09] I. Martinovic, P. Pichota, and J. B. Schmitt: *Jamming for good: A fresh approach to authentic communication in wsns*. In *Proceedings of the 2nd ACM Conference on Wireless Network Security (WiSec)*, 2009.

[NLL06] E. C. H. Ngai, J. Liu, and M. R. Lyu: *On the intruder detection for sinkhole attack in wireless sensor networks*. In *Proceedings of the 8th IEEE International Conference on Communications (ICC)*, 2006.

[NMHH05] D. C. Nash, T. L. Martin, D. S. Ha, and M. S. Hsiao: *Towards an intrusion detection system for battery exhaustion attacks on mobile computing devices*. In *Proceedings of the 3rd IEEE International Conference on Pervasive Computing and Communications Workshops (PerCom Workshops)*, 2005.

[NSBJ11] K. Nyalkalkar, S. Sinhay, M. Bailey, and F. Jahanian: *A comparative study of two network-based anomaly detection methods*. In *Proceedings of the 30th IEEE International Conference on Computer Communications (INFOCOM)*, 2011.

[OM05] I. Onat and A. Miri: *An intrusion detection system for wireless sensor networks*. In *Proceedings of the 3rd IEEE International Conference on Wireless And Mobile Computing, Networking And Communications (WiMob)*, 2005.

[PAS+14] O. Punal, I. Aktas, C.-J. Schnelke, G. Abidin, K. Wehrle, and J. Gross: *Machine learning-based jamming detection for ieee 802.11: Design and experimental evaluation*. In *Proceedings of the 15th IEEE International Symposium on A World of Wireless, Mobile and Multimedia Networks (WoWMoM)*, 2014.

[PIK11] K. Pelechrinis, M. Iliofotou, and S. V. Krishnamurthy: *Denial of service attacks in wireless networks: The case of jammers*. IEEE Communications Surveys & Tutorials, 13:245–257, 2011.

[PLP06] K. Piotrowski, P. Langendoerfer, and S. Peter: *How public key cryptography influences wireless sensor node lifetime*. In *Proceedings of the 4th ACM Workshop on Security of Ad hoc and Sensor Networks (SASN)*, 2006.

[PPG05] B. Parno, A. Perrig, and V. Gligor: *Distributed detection of node replication attacks in sensor networks*. In *Proceedings of the 26th IEEE Symposium on Security and Privacy (S&P)*, 2005.

[Pre14] S. Prentice: *The five smart technologies to watch*. http://www.gartner.com, 2014. Last access: December 3, 2014.

[PSC05] J. Polastre, R. Szewczyk, and D. Culler: *Telos: enabling ultra-low power wireless research*. In *Proceedings of the 4th International Symposium on Information Processing in Sensor Networks (IPSN)*, 2005.

[PSW04] A. Perrig, J. Stankovic, and D. Wagner: *Security in wireless sensor networks*. Communications of the ACM, 47:53–57, 2004.

[QXW03] H. Qi, Y. Xu, and X. Wang: *Mobile-agent-based collaborative signal and information processing in sensor networks*. Proceedings of the IEEE, 91:1172–1183, 2003.

[Rö7] K. Römer: *Distributed mining of spatio-temporal event patterns in sensor networks*. Technical report, ETH Zurich, 2007.

[RAH15] M. Riecker, L. Almon, and M. Hollick: *Lightweight detection of denial-of-service attacks on wireless sensor networks*. Technical report, Technische Universität Darmstadt, 2015.

[RAS08] C. Ramos, J. C. Augusto, and D. Shapiro: *Ambient intelligence - the next step for artificial intelligence*. IEEE Intelligent Systems, 23:15–18, 2008.

[RB06] S. Rost and H. Balakrishnan: *Memento: A health monitoring system for wireless sensor networks*. In *Proceedings of the 3rd Annual IEEE Communications Society Conference on Sensor, Mesh and Ad Hoc Communications and Networks (SECON)*, 2006.

[RBBH14] M. Riecker, S. Biedermann, R. E. Bansarkhani, and M. Hollick: *Lightweight energy consumption based intrusion detection system for wireless sensor networks*. International Journal of Information Security, 2014.

[RBH13] M. Riecker, S. Biedermann, and M. Hollick: *Lightweight energy consumption based intrusion detection system for wireless sensor networks*. In *Proceedings of the 28th ACM Symposium On Applied Computing (SAC)*, 2013.

[RH11] M. Riecker and M. Hollick: *A survey on intrusion detection in wireless sensor networks*. Technical report, Technische Universität Darmstadt, 2011.

[RM08] D. R. Raymond and S. F. Midkiff: *Denial-of-service in wireless sensor networks: Attacks and defenses*. IEEE Pervasive Computing, 7:74–81, 2008.

[RM09] K. Römer and J. Ma: *Pda: Passive distributed assertions for sensor network*. In *Proceedings of the 8th International Conference on Information Processing in Sensor Networks (IPSN)*, 2009.

[RRV07] M. Ringwald, K. Römer, and A. Vitaletti: *Passive inspection of sensor networks*. In *Proceedings of the 3rd IEEE International Conference on Distributed Computing in Sensor Systems (DCOSS)*, 2007.

[RTH14] M. Riecker, D. Thies, and M. Hollick: *Measuring the impact of denial-of-service attacks on wireless sensor networks*. In *Proceedings of the 39th IEEE Conference on Local Computer Networks (LCN)*, 2014.

[RWV13] S. Raza, L. Wallgren, and T. Voigt: *Svelte: Real-time intrusion detection in the internet of things*. Ad Hoc Networks, 11:2661 – 2674, 2013.

[RYBH14] M. Riecker, D. Yuan, R. E. Bansarkhani, and M. Hollick: *Patrolling wireless sensor networks: Randomized intrusion detection*. In *Proceedings of the 10th ACM International Symposium on QoS and Security for Wireless and Mobile Networks (Q2SWinet)*, 2014.

[RZL06] R. Roman, J. Zhou, and J. Lopez: *Applying intrusion detection systems to wireless sensor networks*. In *Proceedings of the 3rd IEEE Consumer Communications and Networking Conference (CCNC)*, 2006.

[SB12] W. Stallings and L. Brown: *Computer Security - Principles and Practice*. Pearson, 2012.

[SBR10] P. Suriyachai, J. Brown, and U. Roedig: *Time-critical data delivery in wireless sensor networks*. In *Proceedings of the 6th IEEE International Conference on Distributed Computing in Sensor Systems (DCOSS)*, 2010.

[SCK07] W.-T. Su, K.-M. Chang, and Y.-H. Kuo: *ehip: An energy-efficient hybrid intrusion prohibition system for cluster-based wireless sensor networks*. Computer Networks, 51:1151–1168, 2007.

[SE13] V. Sundaram and P. Eugster: *Lightweight message tracing for debugging wireless sensor networks*. In *Proceedings of the 43rd Annual IEEE/IFIP International Conference on Dependable Systems and Networks (DSN)*, 2013.

[SEZ10] V. Sundaram, P. Eugster, and X. Zhang: *Efficient diagnostic tracing for wireless sensor networks*. In *Proceedings of the 8th ACM Conference on Embedded Networked Sensor Systems (SenSys)*, 2010.

[SH06] L. Sachs and J. Hedderich: *Angewandte Statistik*. Springer Berlin / Heidelberg, 2006.

[SHS+12] W. Shen, G. Han, L. Shu, J. Rodrigues, and N. Chilamkurti: *A new energy prediction approach for intrusion detection in cluster-based wireless sensor networks*. In *Green Communications and Networking*, volume 51 of *Lecture Notes of the Institute for Computer Sciences, Social Informatics and Telecommunications Engineering*, pages 1–12. Springer Berlin / Heidelberg, 2012.

[SLX+09] K. Sun, A. Liu, R. Xu, P. Ning, and D. Maughan: *Securing network access in wireless sensor networks*. In *Proceedings of the 2nd ACM Conference on Wireless Network Security (WiSec)*, 2009.

[SMR+12] R. Sen, A. Maurya, B. Raman, R. Mehta, R. Kalyanaraman, N. Vankadhara, S. Roy, and P. Sharma: *Kyun queue: A sensor network system to monitor road traffic queues*. In *Proceedings of the 10th ACM Conference on Embedded Networked Sensor Systems (SenSys)*, 2012.

[SOS+08] P. Szczechowiak, L. Oliveira, M. Scott, M. Collier, and R. Dahab: *Nanoecc: Testing the limits of elliptic curve cryptography in sensor networks*. In *Wireless Sensor Networks*. Springer Berlin / Heidelberg, 2008.

[THBR11] M. Tancreti, M. S. Hossain, S. Bagchi, and V. Raghunathan: *Aveksha: A hardware-software approach for non-intrusive tracing and profiling of wireless embedded systems*. In *Proceedings of the 9th ACM Conference on Embedded Networked Sensor Systems (SenSys)*, 2011.

[Thi12] D. Thies: *Metrics for intrusion detection in wireless sensor networks*. Master's thesis, Technische Universität Darmstadt, 2012.

[Toh02] C.-K. Toh: *Ad hoc mobile wireless networks: protocols and systems*. Prentice Hall, 2002.

[TPS+05] G. Tolle, J. Polastre, R. Szewczyk, D. Culler, N. Turner, K. Tu, S. Burgess, T. Dawson, P. Buonadonna, D. Gay, and W. Hong: *A macroscope in the redwoods*. In *Proceedings of the 3rd ACM Conference on Embedded Networked Sensor Systems (SenSys)*, 2005.

[UKK+12] B. Ur, P. G. Kelley, S. Komanduri, J. Lee, M. Maass, M. L. Mazurek, T. Passaro, R. Shay, T. Vidas, L. Bauer, N. Christin, and L. F. Cranor: *How does your password measure up? the effect of strength meters on password creation*. In *Proceedings of the 21st USENIX Security Symposium (Security)*, 2012.

[VD10] J.-P. Vasseur and A. Dunkels: *Interconnecting Smart Objects with IP: The Next Internet*. Morgan Kaufmann, 2010.

[VJU+12] M. Valero, S. S. Jung, A. S. Uluagac, Y. Li, and R. Beyah: *Di-sec: A distributed security framework for heterogeneous wireless sensor networks*. In *Proceedings of the 33rd IEEE International Conference on Computer Communications (INFOCOM)*, 2012.

[VUV+12] M. Valero, S. Uluagac, S. Venkatachalam, K. Ramalingam, and R. Beyah: *The monitoring core: A framework for sensor security application development*.

In *Proceedings of the 9th IEEE International Conference on Mobile Ad hoc and Sensor Systems (MASS)*, 2012.

[Wal04] A. Wald: *Sequential Analysis*. Dover, 2004.

[WAL+14] D. Wang, M. T. Amin, S. Li, T. Abdelzaher, L. Kaplan, S. Gu, C. Pan, H. Liu, C. C. Aggarwal, R. Ganti, X. Wang, P. Mohapatra, B. Szymanski, and H. Le: *Using humans as sensors: An estimation-theoretic perspective*. In *Proceedings of the 13th International Conference on Information Processing in Sensor Networks (IPSN)*, 2014.

[WAR06] Y. Wang, G. Attebury, and B. Ramamurthy: *A survey of security issues in wireless sensor networks*. IEEE Communications Surveys & Tutorials, 8(2), 2006.

[WDN07] R. Wang, W. Du, and P. Ning: *Containing denial-of-service attacks in broadcast authentication in sensor networks*. In *Proceedings of the 8th ACM International Symposium on Mobile Ad Hoc Networking and Computing (MobiHoc)*, 2007.

[Wei91] M. Weiser: *The computer for the 21st century*. Scientific American, 265:94–104, 1991.

[WFK+09] C. Wang, T. Feng, J. Kim, G. Wang, and W. Zhang: *Catching packet droppers and modifiers in wireless sensor networks*. In *Proceedings of the 10th IEEE International Conference on Sensing, Communication, and Networking (SECON)*, 2009.

[WFSH06] A. D. Wood, L. Fang, J. A. Stankovic, and T. He: *Sigf: A family of configurable, secure routing protocols for wireless sensor networks*. In *Proceedings of the 4th ACM Workshop on Security of Ad Hoc and Sensor Networks (SASN)*, 2006.

[WGE+05] A. S. Wander, N. Gura, H. Eberle, V. Gupta, and S. C. Shantz: *Energy analysis of public-key cryptography for wireless sensor networks*. In *Proceedings of the 3rd IEEE International Conference on Pervasive Computing and Communications (PerCom)*, 2005.

[WHR+13] H. Wennerström, F. Hermans, O. Rensfelt, C. Rohner, and L.-A. Norden: *A long-term study of correlations between meteorological conditions and 802.15.4 link performance*. In *Proceedings of the 10th IEEE International Conference on Sensing, Communication, and Networking (SECON)*, 2013.

[Wol12] M. Wolf: *Computers as components: principles of embedded computing system design*. Morgan Kaufmann, 2012.

[WS02] D. Wagner and P. Soto: *Mimicry attacks on host-based intrusion detection systems*. In *Proceedings of the 9th ACM Conference on Computer and Communications Security (CCS)*, 2002.

[WS04] A. D. Wood and J. A. Stankovic: *A taxonomy for denial-of-service attacks in wireless sensor networks*. In *Handbook of Sensor Networks: Compact Wireless and Wired Sensing Systems*. CRC Press, 2004.

[WSS03] A. Wood, J. Stankovic, and S. Son: *Jam: a jammed-area mapping service for sensor networks*. In *Proceedings of the 24th IEEE Real-Time Systems Symposium (RTSS)*, 2003.

[WSZ07] A. Wood, J. Stankovic, and G. Zhou: *Deejam: Defeating energy-efficient jamming in ieee 802.15.4-based wireless networks*. In *Proceedings of the 4th IEEE International Conference on Sensing, Communication, and Networking (SECON)*, 2007.

[WTC03] A. Woo, T. Tong, and D. Culler: *Taming the underlying challenges of reliable multihop routing in sensor networks*. In *Proceedings of the 1st International Conference on Embedded Networked Sensor Systems (SenSys)*, 2003.

[WTt12] T. Winter, P. Thubert, and the ROLL Team: *Rpl: Ipv6 routing protocol for low-power and lossy networks*. http://www.rfc-editor.org/info/rfc6550, 2012.

[XTZ07] W. Xu, W. Trappe, and Y. Zhang: *Channel surfing: Defending wireless sensor networks from interference*. In *Proceedings of the 6th International Conference on Information Processing in Sensor Networks (IPSN)*, 2007.

[XTZW05] W. Xu, W. Trappe, Y. Zhang, and T. Wood: *The feasibility of launching and detecting jamming attacks in wireless networks*. In *Proceedings of the 6th ACM International Symposium on Mobile Ad Hoc Networking and Computing (MobiHoc)*, 2005.

[YL08] L. Yu and J. Li: *Spymon: Hidden network monitoring for security in wireless sensor networks*. In *Proceedings of the 5th IEEE International Conference on Mobile Ad hoc and Sensor Systems (MASS)*, 2008.

[YLLZ04] F. Ye, H. Luo, S. Lu, and L. Zhang: *Statistical en-route filtering of injected false data in sensor networks*. In *Proceedings of the 23rd IEEE International Conference on Computer Communications (INFOCOM)*, 2004.

[YT08] Z. Yu and J. J. Tsai: *A framework of machine learning based intrusion detection for wireless sensor networks*. In *Proceedings of the IEEE International Conference on Sensor Networks, Ubiquitous, and Trustworthy Computing (SUTC)*, 2008.

[ZG03] J. Zhao and R. Govindan: *Understanding packet delivery performance in dense wireless sensor networks*. In *Proceedings of the 1st International Conference on Embedded Networked Sensor Systems (SenSys)*, 2003.

[ZSJ06] S. Zhu, S. Setia, and S. Jajodia: *Leap+: Efficient security mechanisms for large-scale distributed sensor networks*. ACM Transactions on Sensor Networks, 2(4), 2006.

[ZSJN04] S. Zhu, S. Setia, S. Jajodia, and P. Ning: *An interleaved hop-by-hop authentication scheme for filtering of injected false data in sensor networks*. In *Proceedings of the 25th IEEE Symposium on Security and Privacy (S&P)*, 2004.

LIST OF ACRONYMS

CCA	Clear Channel Assessment
CTP	Collection Tree Protocol
DoS	Denial-of-Service
FN	False Negatives
FP	False Positives
IDS	Intrusion Detection System
IoT	Internet of Things
MCU	Microcontroller
PDR	Packet Delivery Rate
QoS	Quality-of-Service
WSN	Wireless Sensor Network

A

APPENDIX

A.1 SUPPLEMENTARY RESULTS FOR CHAPTER 4

A.1.1 *Logistic Regression Models for the Initial Testbeds*

CTP, Jamming, Initial Testbed 2

Table A.1: CTP, initial testbed 2, low power, low traffic, jamming

Node	**Factors**	**Analysis of variance**	**LR-test**	R^2
2	β_6, β_8	$8,60e-9 < 1222,76$	$794,91 > 5,99$	1
3	β_{26}	$6,70e-9 < 1222,76$	$794,24 > 3,84$	1
4	β_{26}	$9,25e-9 < 1222,76$	$794,24 > 3,84$	1
5	β_{15}, β_{17}	$3,11e-8 < 1223,80$	$795,62 > 5,99$	1
8	β_{26}	$8,79e-9 < 1224,83$	$795,65 > 3,84$	1
all nodes	$\beta_8, \beta_{17}, \beta_{26}$	$3,29e-7 < 5907,21$	$3974,66 > 7,81$	1

Table A.2: CTP, initial testbed 2, high power, low traffic, jamming

Node	**Factors**	**Analysis of variance**	**LR-test**	R^2
2	$\beta_7, \beta_8, \beta_{20}$	$7,85e-8 < 1253,79$	$816,44 > 7,81$	1
3	β_6, β_8	$2,84e-8 < 1257,93$	$818,45 > 5,99$	1
4	β_8	$1,09e-6 < 1254,82$	$815,74 > 3,84$	1
5	β_8	$4,74e-8 < 1252,76$	$814,40 > 3,84$	1
8	β_6, β_8	$3,01e-8 < 1254,82$	$816,39 > 5,99$	1
all nodes	β_6, β_8	$1,14e-5 < 6064,58$	$4081,44 > 5,99$	1

Table A.3: CTP, initial testbed 2, low power, high traffic, jamming

Node	**Factors**	**Analysis of variance**	**LR-test**	R^2
2	β_{26}	$2,00e-8 < 1223,80$	$794,97 > 3,84$	1
3	β_{26}	$6,71e-9 < 1221,73$	$793,56 > 3,84$	1
4	β_8	$2,07e-8 < 1221,73$	$793,58 > 3,84$	1
5	β_8	$4,43e-8 < 1223,80$	$794,94 > 3,84$	1
8	β_{26}, β_{28}	$1,06e-8 < 1224,83$	$796,33 > 5,99$	1
all nodes	β_{26}, β_8	$1,02e-6 < 5906,20$	$3973,37 > 5,99$	1

Table A.4: CTP, initial testbed 2, high power, high traffic, jamming

Node	**Factors**	**Analysis of variance**	**LR-test**	R^2
2	β_{15}	$1,35e-8 < 1193,80$	$774,85 > 3,84$	1
3	$\beta_3, \beta_6, \beta_7, \beta_{17}$	$6,32e-8 < 1201,04$	$781,61 > 9,49$	1
4	$\beta_8, \beta_{13}, \beta_{27}$	$5,66e-8 < 1201,04$	$780,94 > 7,81$	1
5	$\beta_3, \beta_{17}, \beta_{26}$	$1,32e-8 < 1195,87$	$777,57 > 7,81$	1
8	β_8	$2,08e-7 < 1203,11$	$780,94 > 3,84$	1
all nodes	$\beta_8, \beta_{13}, \beta_{27}$	$1,73e-6 < 5791,45$	$3895,95 > 9,49$	1

Mesh, Jamming, Initial Testbed 1

Table A.5: Mesh, initial testbed 1, high power, low traffic, jamming

Node	**Factors**	**Analysis of variance**	**LR-test**	R^2
11	$\beta_1, \beta_5, \beta_6, \beta_8,$ $\beta_{12} : \beta_{14}, \beta_{15}, \beta_{17}, \beta_{18}$	$118,53 < 1156,53$	$697,11 > 18,31$	0,92
13	$\beta_1, \beta_6 : \beta_8, \beta_{12} : \beta_{14}, \beta_{15} : \beta_{18}$	$31,90 < 1149,28$	$736,06 > 19,68$	0,98
14	$\beta_6 : \beta_8, \beta_{15}$	$7,64e-8 < 1171,03$	$761,77 > 9,49$	1
15	$\beta_1, \beta_3, \beta_5, \beta_6, \beta_8, \beta_{12}, \beta_{14} : \beta_{20}$	$3,55e-5 < 1155,50$	$758,30 > 23,68$	1
16	$\beta_6 : \beta_8$	$6,79e-8 < 1156,53$	$751,37 > 7,81$	1
17	$\beta_6 : \beta_8$	$4,52e-8 < 1157,57$	$752,05 > 7,81$	1
23	$\beta_6, \beta_8, \beta_{13}$	$1,60e-7 < 1158,60$	$752,05 > 7,81$	1
25	β_8, β_{14}	$1,03e-6 < 1161,71$	$754,14 > 5,99$	1
26	$\beta_3, \beta_6, \beta_{13}, \beta_{19}$	$1,64e-7 < 1165,85$	$758,30 > 9,49$	1
28	$\beta_6, \beta_8, \beta_{19}$	$6,61e-7 < 1183,45$	$769,36 > 7,81$	1
30	β_{13}	$8,44e-8 < 1161,71$	$753,45 > 3,84$	1
31	β_8	$6,84e-8 < 1161,71$	$753,45 > 3,84$	1
all nodes	$\beta_1 : \beta_6, \beta_8, \beta_{10} : \beta_{14} : \beta_{20}$	$996,59 < 14438,95$	$9331,22 > 28,87$	0,95

Table A.6: Mesh, initial testbed 1, low power, low traffic, jamming

Node	**Factors**	**Analysis of variance**	**LR-test**	R^2
11	$\beta_4, \beta_6, \beta_8, \beta_{13}, \beta_{14}, \beta_{17}, \beta_{20}$	$541,04 < 1175,17$	$413,51 > 14,07$	0,60
13	$\beta_1, \beta_3, \beta_6, \beta_7, \beta_9,$ $\beta_{12}, \beta_{14}, \beta_{15}, \beta_{17}, \beta_{18}$	$755,23 < 1178,27$	$309,00 > 19,68$	0,45
14	$\beta_3, \beta_7, \beta_8,$ $\beta_{12} : \beta_{14}, \beta_{15}, \beta_{16}, \beta_{19}, \beta_{20}$	$553,51 < 1177,24$	$409,12 > 18,31$	0,60
15	$\beta_6, \beta_8, \beta_{11}, \beta_{13}, \beta_{16}, \beta_{17}$	$662,04 < 1176,20$	$352,58 > 14,07$	0,52
16	$\beta_3, \beta_7, \beta_{12}, \beta_{14}, \beta_{17}, \beta_{19}, \beta_{20}$	$641,56 < 1181,38$	$365,02 > 15,51$	0,53
17	$\beta_1, \beta_2, \beta_4, \beta_6, \beta_7, \beta_{13}, \beta_{14}$	$378,22 < 1180,34$	$496,32 > 15,51$	0,72
23	$\beta_8, \beta_{12}, \beta_{13}, \beta_{16}, \beta_{17}, \beta_{20}$	$566,42 < 1175,17$	$400,02 > 14,07$	0,59
25	$\beta_8, \beta_{12}, \beta_{14}, \beta_{15}, \beta_{20}$	$641,07 < 1176,20$	$362,70 > 12,59$	0,53
26	$\beta_{13}, \beta_{16}, \beta_{17}, \beta_{19}$	$583,38 < 1180,34$	$391,38 > 11,07$	0,57
28	$\beta_1, \beta_8, \beta_{12}, \beta_{16}$	$570,05 < 1194,83$	$405,24 > 11,07$	0,59
30	$\beta_1, \beta_8, \beta_{14}, \beta_{15}, \beta_{17}$	$664,47 < 1181,38$	$352,46 > 11,07$	0,51
31	$\beta_1, \beta_{12}, \beta_{13}, \beta_{15} : \beta_{17}$	$652,33 < 1183,45$	$359,63 > 12,59$	0,52
all nodes	$\beta_1, \beta_6, \beta_8, \beta_{11} : \beta_{15}, \beta_{17} : \beta_{19}$	$9971,80 < 14705,52$	$3921,28 > 22,36$	0,44

Table A.7: (Mesh, initial testbed 1, low power, high traffic, jamming

Node	**Factors**	**Analysis of variance**	**LR-test**	R^2
11	$\beta_1, \beta_5, \beta_6, \beta_8, \beta_{12} : \beta_{14}, \beta_{17}, \beta_{20}$	$170,07 < 1195,87$	$697,53 > 18,31$	0,89
13	$\beta_3, \beta_6, \beta_8, \beta_{12} : \beta_{16}, \beta_{19}, \beta_{20}$	$147,75 < 1189,66$	$705,22 > 19,68$	0,91
14	β_8	$2,74e-8 < 1190,69$	$722,86 > 3,84$	1
15	$\beta_1, \beta_3 : \beta_8, \beta_{13} : \beta_{16}, \beta_{20}$	$45,55 < 1176,20$	$748,68 > 22,36$	0,97
16	$\beta_6, \beta_8, \beta_{12} : \beta_{14}$	$6,57e-5 < 1200,00$	$781,87 > 11,07$	1
17	β_8	$2,17e-8 < 1196,90$	$777,02 > 3,84$	1
23	β_8	$1,06e-8 < 1198,97$	$778,40 > 3,84$	1
25	β_6, β_8	$1,67e-8 < 1191,73$	$774,23 > 5,99$	1
26	β_8	$6,32e-8 < 1191,73$	$773,52 > 3,84$	1
28	β_6, β_8	$3,88e-8 < 1218,63$	$792,23 > 5,99$	1
30	β_8, β_{13}	$1,49e-7 < 1190,69$	$733,55 > 5,99$	1
31	β_6, β_8	$2,25e-8 < 1188,62$	$772,15 > 5,99$	1
all nodes	$\beta_1, \beta_4 : \beta_8, \beta_{11} : \beta_{20}$	$1167,10 < 14839,80$	$9520,46 > 27,59$	0,94

Table A.8: Mesh, initial testbed 1, high power, high traffic, jamming

Node	**Factors**	**Analysis of variance**	**LR-test**	R^2
11	β_8, β_{17}	$1,11e-7 < 1192,76$	$775,58 > 7,81$	1
13	$\beta_1, \beta_5, \beta_6, \beta_8,$ $\beta_{13}, \beta_{14}, \beta_{15}, \beta_{16}, \beta_{19}$	$8,95e-5 < 1167,92$	$763,10 > 16,92$	1
14	$\beta_6 : \beta_8$	$7,58e-8 < 1183,45$	$796,31 > 7,81$	1
15	$\beta_1, \beta_6, \beta_8, \beta_{12}, \beta_{14} : \beta_{16}, \beta_{18} : \beta_{20}$	$27,41 < 1173,10$	$754,24 > 19,68$	0,98
16	$\beta_7, \beta_8, \beta_{17}$	$6,63e-8 < 1188,62$	$773,46 > 9,49$	1
17	β_6, β_8	$2,27e-8 < 1172,06$	$761,07 > 5,99$	1
23	$\beta_6, \beta_{17}, \beta_{19}$	$7,07e-8 < 1188,62$	$772,76 > 7,81$	1
25	β_8, β_{15}	$1,10e-7 < 1182,41$	$767,86 > 5,99$	1
26	β_{14}, β_{19}	$1,50e-7 < 1185,52$	$769,99 > 5,99$	1
28	$\beta_5, \beta_6, \beta_8, \beta_{10}, \beta_{13}, \beta_{14}, \beta_{17}, \beta_{20}$	$98,75 < 1178,27$	$719,95 > 15,51$	0,94
30	β_1, β_{14}	$1,29e-7 < 1184,48$	$769,25 > 5,99$	1
31	β_8, β_{14}	$4,87e-8 < 1177,24$	$764,44 > 5,99$	1
all nodes	$\beta_1, \beta_6, \beta_8, \beta_{12} : \beta_{18}, \beta_{20}$	$877,89 < 15066,96$	$9816,13 > 21,03$	0,96

Mesh, Jamming, Initial Testbed 2

Table A.9: Mesh, initial testbed 2, low power, low traffic, jamming

Node	**Factors**	**Analysis of variance**	**LR-test**	R^2
2	β_2, β_{13}	$7,47e-8 < 1205,18$	$783,94 > 7,81$	1
3	β_8	$1,11e-6 < 1214,49$	$788,76 > 3,84$	1
4	β_8	$1,22e-8 < 1212,44$	$632,05 > 3,84$	1
5	$\beta_1, \beta_8, \beta_{14}$	$4,43e-8 < 1212,42$	$788,76 > 7,81$	1
8	β_8	$3,80e-8 < 1214,49$	$788,74 > 3,84$	1
all nodes	$\beta_1, \beta_2, \beta_{14}, \beta_{18}, \beta_{19}$	$4,68e-5 < 6807,35$	$4586,76 > 11,07$	1

Table A.10: Mesh, initial testbed 2, high power, low traffic, jamming

Node	**Factors**	**Analysis of variance**	**LR-test**	R^2
2	β_{13}, β_{16}	$2,08e-7 < 1188,62$	$771,22 > 5,99$	1
3	β_{14}	$1,88e-8 < 1190,69$	$771,87 > 3,84$	1
4	β_{13}	$2,91e-8 < 1190,69$	$771,95 > 3,84$	1
5	β_{14}	$3,42e-8 < 1192,76$	$773,34 > 3,84$	1
8	β_{14}	$3,33e-8 < 1188,62$	$770,56 > 3,84$	1
all nodes	$\beta_{14}, \beta_{16}, \beta_{18}$	$6,23e-6 < 6874,29$	$4360 > 7,81$	1

Table A.11: Mesh, initial testbed 2, low power, high traffic, jamming

Node	**Factors**	**Analysis of variance**	**LR-test**	R^2
2	β_{14}	$3,81e-8 < 1234,14$	$801,97 > 3,84$	1
3	β_{13}	$7,40e-8 < 1228,97$	$798,49 > 3,84$	1
4	β_{14}, β_{18}	$1,28e-7 < 1233,11$	$801,97 > 5,99$	1
5	β_{14}	$3,42e-8 < 1222,76$	$794,26 > 3,84$	1
8	β_{13}	$5,19e-8 < 1228,97$	$798,48 > 3,84$	1
all nodes	β_{14}, β_{18}	$1,67e-6 < 7107,54$	$4794,38 > 5,99$	1

Table A.12: Mesh, initial testbed 2, high power, high traffic, jamming

Node	**Factors**	**Analysis of variance**	**LR-test**	R^2
2	β_{13}	$5,59e-8 < 1206,21$	$783,26 > 3,84$	1
3	β_8	$9,68e-9 < 1206,21$	$783,26 > 3,84$	1
4	β_8	$5,16e-8 < 1020,74$	$642,24 > 3,84$	1
5	β_{13}, β_{14}	$4,86e-8 < 1204,14$	$782,56 > 5,99$	1
8	β_8	$7,48e-8 < 1205,18$	$782,56 > 3,84$	1
all nodes	$\beta_6, \beta_{14}, \beta_{19}$	$2,23e-6 < 6783,01$	$4571,04 > 7,81$	1

CTP, Blackhole, Both Initial Testbeds

Table A.13: CTP, initial testbed 1, high power, low traffic, blackhole

Node	Factors	Analysis of variance	LR-test	R^2
11	$\beta_6, \beta_9, \beta_{13}, \beta_{15}, \beta_{17}, \beta_{19}, \beta_{20}, \beta_{23}, \beta_{26} : \beta_{28}, \beta_{30}$	$941,12 < 1135,82$	$273,19 > 21,03$	0,37
13	$\beta_1 : \beta_5, \beta_7, \beta_{13}, \beta_{15}, \beta_{17}, \beta_{18}, \beta_{21}, \beta_{23}, \beta_{24}, \beta_{26} : \beta_{28}, \beta_{30}$	$71,38 < 1129,60$	$708,06 > 28,87$	0,95
14	$\beta_1 : \beta_4, \beta_6, \beta_8, \beta_{11}, \beta_{12}, \beta_{15}, \beta_{17}, \beta_{18}, \beta_{23}, \beta_{24}, \beta_{26}, \beta_{27}, \beta_{29}, \beta_{30}$	$1149,50 \not< 1129,60$	$168,98 > 28,87$	0,23
15	$\beta_3, \beta_6, \beta_8, \beta_{11}, \beta_{15}, \beta_{21}, \beta_{26},$	$968,30 < 1141,00$	$260,29 > 15,51$	0,34
16	$\beta_1, \beta_2, \beta_4, \beta_6 : \beta_8, \beta_{11}, \beta_{14}, \beta_{15}, \beta_{17}, \beta_{20}, \beta_{26}$	$1266,30 \not< 1133,75$	$109,91 > 22,36$	0,14
17	$\beta_2, \beta_5 : \beta_8, \beta_{15}, \beta_{17}, \beta_{18}, \beta_{20}, \beta_{26}, \beta_{27}, \beta_{30}$	$467,67 < 1132,71$	$508,53 > 22,36$	0,69
23	$\beta_1, \beta_5, \beta_7, \beta_8, \beta_{15}, \beta_{17} : \beta_{20}, \beta_{23}, \beta_{26}, \beta_{28}, \beta_{29}$	$766,15 < 1132,71$	$359,28 > 22,36$	0,48
25	$\beta_4 : \beta_7, \beta_{10}, \beta_{12}, \beta_{14}, \beta_{15}, \beta_{17}, \beta_{18}, \beta_{20}, \beta_{23}, \beta_{26}, \beta_{28}, \beta_{29}$	$825,34 < 1129,60$	$329,69 > 26,30$	0,44
26	$\beta_2, \beta_3, \beta_5 : \beta_8, \beta_{12}, \beta_{15}, \beta_{17} : \beta_{19}, \beta_{21}, \beta_{23}, \beta_{26}, \beta_{30}$	$965,53 < 1129,60$	$259,59 > 26,30$	0,35
28	$\beta_1, \beta_5, \beta_8, \beta_{10}, \beta_{12}, \beta_{13}, \beta_{15}, \beta_{19}, \beta_{24}, \beta_{26} : \beta_{29}$	$183,99 < 1130,64$	$648,98 > 22,36$	0,88
30	$\beta_1, \beta_2, \beta_5, \beta_8, \beta_{13} : \beta_{15}, \beta_{20}, \beta_{23}, \beta_{26}, \beta_{28}, \beta_{30}$	$763,30 < 1135,82$	$362,10 > 21,03$	0,49
31	$\beta_5 : \beta_7, \beta_9, \beta_{13}, \beta_{15}, \beta_{17}, \beta_{20}, \beta_{21}, \beta_{23}, \beta_{25}, \beta_{27} : \beta_{30}$	$791,80 < 1129,60$	$346,46 > 26,30$	0,47
all nodes	$\beta_1, \beta_4 : \beta_6, \beta_8, \beta_{11} : \beta_{15}, \beta_{17} : \beta_{19}, \beta_{23}, \beta_{25} : \beta_{30}$	$15409,00 \not< 13103,71$	$1210,58 > 32,67$	0,14

Table A.14: CTP, initial testbed 1, low power, high traffic, blackhole

Node	Factors	Analysis of variance	LR-test	R^2
11	$\beta_5, \beta_7, \beta_{13} : \beta_{15}, \beta_{17}, \beta_{18}, \beta_{21}, \beta_{27}, \beta_{30}$	$103,50 < 1134,78$	$690,61 > 19,68$	0,93
13	$\beta_1 : \beta_3, \beta_5 : \beta_8, \beta_{11}, \beta_{12}, \beta_{14}, \beta_{15}, \beta_{17}, \beta_{18}, \beta_{20}, \beta_{25} : \beta_{29}$	$300,28 < 1122,35$	$590,14 > 31,41$	0,80
14	β_{15}, β_{17}	$1,72e-7 < 1142,03$	$740,97 > 5,99$	1
15	$\beta_1 : \beta_3, \beta_7, \beta_{12}, \beta_{14}, \beta_{15}, \beta_{17} : \beta_{21}, \beta_{25}, \beta_{28}, \beta_{29}$	$413,43 < 1128,57$	$534,95 > 26,30$	0,72
16	$\beta_6 : \beta_8, \beta_{12}, \beta_{14}, \beta_{15}, \beta_{17}, \beta_{18}, \beta_{20}, \beta_{21}, \beta_{23}, \beta_{25} : \beta_{28}$	$147,32 < 1131,68$	$669,39 > 25$	0,90
17	$\beta_1 : \beta_3, \beta_5, \beta_7, \beta_8, \beta_{11}, \beta_{14}, \beta_{15}, \beta_{17}, \beta_{20}, \beta_{23} : \beta_{26}, \beta_{30}$	$224,10 < 1128,57$	$630,31 > 27,59$	0,85
23	$\beta_1, \beta_4, \beta_6, \beta_7, \beta_{11}, \beta_{14}, \beta_{15}, \beta_{17}, \beta_{18}, \beta_{20}, \beta_{24}, \beta_{26}, \beta_{27}$	$259,37 < 1135,82$	$641,76 > 22,36$	0,83
25	$\beta_1, \beta_6, \beta_7, \beta_{13} : \beta_{15}, \beta_{17}, \beta_{21}, \beta_{23}, \beta_{29}$	$97,79 < 1137,89$	$695,55 > 19,68$	0,93
26	$\beta_1, \beta_5, \beta_6, \beta_{11} : \beta_{15}, \beta_{17}, \beta_{19} : \beta_{21}, \beta_{23}, \beta_{28}, \beta_{29}$	$125,47 < 1131,68$	$681,01 > 26,30$	0,92
28	$\beta_1, \beta_5 : \beta_8, \beta_{15}, \beta_{17}, \beta_{21}, \beta_{23}, \beta_{26}, \beta_{27}, \beta_{29}$	$98,83 < 949,08$	$551,10 > 21,03$	0,92
30	$\beta_1, \beta_2, \beta_6, \beta_8, \beta_{14}, \beta_{15}, \beta_{20}, \beta_{23}, \beta_{24}, \beta_{28} : \beta_{30}$	$625,77 < 1134,78$	$430,86 > 22,36$	0,58
31	$\beta_1, \beta_5, \beta_8, \beta_{14}, \beta_{15}, \beta_{17}, \beta_{19}, \beta_{20}, \beta_{23}, \beta_{26}, \beta_{28}, \beta_{29}$	$469,80 < 1132,71$	$507,46 > 22,36$	0,68
all nodes	$\beta_1, \beta_5 : \beta_8, \beta_{11} : \beta_{15}, \beta_{17} : \beta_{21}, \beta_{23} : \beta_{25}, \beta_{27}, \beta_{29}, \beta_{30}$	$8733,00 < 12971,81$	$4420,62 > 33,92$	0,50

Table A.15: CTP, initial testbed 1, high power, high traffic, blackhole

Node	Factors	Analysis of variance	LR-test	R^2
11	$\beta_1, \beta_4, \beta_5, \beta_7, \beta_8, \beta_{12}, \beta_{13}, \beta_{15}, \beta_{17}, \beta_{18}, \beta_{20}, \beta_{23}, \beta_{26}$	$311,95 < 1133,75$	$587,77 > 23,68$	0,79
13	$\beta_1, \beta_5 : \beta_7, \beta_{13} : \beta_{15}, \beta_{17}, \beta_{20}, \beta_{21}, \beta_{23}, \beta_{26}, \beta_{27}$	$375,68 < 1135,82$	$556,60 > 22,36$	0,75
14	$\beta_1 : \beta_3, \beta_6, \beta_7, \beta_{13} : \beta_{15}, \beta_{17}, \beta_{18}, \beta_{20}, \beta_{23}, \beta_{27} : \beta_{29}$	$278,81 < 1132,71$	$604,34 > 25$	0,81
15	$\beta_2, \beta_5 : \beta_8, \beta_{10}, \beta_{14}, \beta_{15}, \beta_{17} : \beta_{19}, \beta_{23}, \beta_{26} : \beta_{28}$	$902,45 < 1132,71$	$293,22 > 26,30$	0,39
16	$\beta_1, \beta_6, \beta_8, \beta_{10}, \beta_{11}, \beta_{13}, \beta_{15}, \beta_{17} : \beta_{19}, \beta_{23}, \beta_{24}, \beta_{26}, \beta_{28}, \beta_{30}$	$702,53 < 1132,71$	$393,17 > 26,30$	0,52
17	β_{17}	$5,60e-8 < 1148,25$	$744,44 > 3,84$	1
23	$\beta_1, \beta_2, \beta_5 : \beta_8, \beta_{11}, \beta_{13} : \beta_{15}, \beta_{17}, \beta_{19}, \beta_{23}, \beta_{24}, \beta_{26}, \beta_{29}$	$207,34 < 1131,68$	$640,08 > 26,30$	0,86
25	$\beta_1, \beta_3, \beta_6, \beta_8, \beta_{15}, \beta_{17}, \beta_{20}, \beta_{21}, \beta_{26}, \beta_{28}$	$119,95 < 1136,86$	$683,08 > 18,31$	0,92
26	β_{17}	$6,35e-9 < 1147,21$	$743,75 > 3,84$	1
28	$\beta_1 : \beta_3, \beta_5, \beta_6, \beta_8, \beta_{11}, \beta_{12}, \beta_{13}, \beta_{15}, \beta_{17}, \beta_{20}, \beta_{21}, \beta_{23}, \beta_{26} : \beta_{29}$	$2,92e-5 < 1130,64$	$744,44 > 28,87$	1
30	$\beta_3, \beta_7, \beta_8, \beta_{14}, \beta_{15}, \beta_{17}, \beta_{20}, \beta_{21}, \beta_{23}, \beta_{24}, \beta_{27}, \beta_{28}, \beta_{30}$	$242,79 < 1134,78$	$622,35 > 22,36$	0,84
31	$\beta_1 : \beta_3, \beta_6, \beta_{13} : \beta_{15}, \beta_{17}, \beta_{20}, \beta_{22}, \beta_{28}, \beta_{30}$	$596,58 < 1135,82$	$445,45 > 21,03$	0,60
all nodes	$\beta_1 : \beta_4, \beta_6, \beta_7, \beta_{13}, \beta_{15}, \beta_{17} : \beta_{20}, \beta_{23} : \beta_{29}$	$11233,00 < 13122,90$	$3311,23 > 31,41$	0,37

Table A.16: CTP, initial testbed 2, high power, low traffic, blackhole

Node	Factors	Analysis of variance	LR-test	R^2
2	$\beta_1, \beta_2, \beta_6, \beta_7, \beta_{11}, \beta_{13} : \beta_{15}, \beta_{20}, \beta_{23}, \beta_{26} : \beta_{28}, \beta_{30}$	$755,37 < 1224,83$	$427,37 > 25$	0,53
3	β_{15}	$6,77e-9 < 1244,48$	$808,44 > 3,84$	1
4	$\beta_1, \beta_5, \beta_7, \beta_8, \beta_{13}, \beta_{15}, \beta_{20}, \beta_{21}, \beta_{23}, \beta_{28}, \beta_{29}$	$86,72 < 1228,97$	$761,69 > 19,68$	0,95
5	$\beta_1 : \beta_3, \beta_5, \beta_8, \beta_{13}, \beta_{15}, \beta_{19}, \beta_{21}, \beta_{23}, \beta_{28}$	$517,02 < 1225,87$	$545,25 > 21,03$	0,68
8	$\beta_1, \beta_5 : \beta_7, \beta_{11}, \beta_{13} : \beta_{15}, \beta_{17}, \beta_{19}, \beta_{20}, \beta_{23}, \beta_{26}, \beta_{28}, \beta_{29}$	$48,15 < 1226,90$	$782,31 > 25$	0,97
all nodes	$\beta_1, \beta_6 : \beta_8, \beta_{11} : \beta_{15}, \beta_{17}, \beta_{20}, \beta_{21}, \beta_{23}, \beta_{24}, \beta_{26} : \beta_{31}$	$3429,10 < 5571,18$	$2314,13 > 31,41$	0,57

Table A.17: CTP, initial testbed 2, low power, high traffic, blackhole

Node	Factors	Analysis of variance	LR-test	R^2
2	$\beta_6, \beta_8, \beta_{14}, \beta_{15}, \beta_{21}, \beta_{23}, \beta_{26}, \beta_{27}$	$59,34 < 1217,59$	$765,98 > 15,51$	0,96
3	$\beta_1, \beta_5, \beta_6, \beta_{13}, \beta_{15}, \beta_{26}$	$1,98e-5 < 1217,59$	$794,24 > 12,59$	1
4	$\beta_1 : \beta_3, \beta_5, \beta_6, \beta_{13} : \beta_{15}, \beta_{17}, \beta_{19}, \beta_{20}, \beta_{23}, \beta_{28}$	$193,76 < 1211,39$	$698,06 > 22,36$	0,88
5	$\beta_1, \beta_5 : \beta_7, \beta_{14}, \beta_{15}, \beta_{17}, \beta_{23}, \beta_{26}, \beta_{28}$	$156,58 < 1215,52$	$717,33 > 18,31$	0,90
8	$\beta_2, \beta_3, \beta_7, \beta_{13} : \beta_{15}, \beta_{17}, \beta_{19} : \beta_{21}, \beta_{23}, \beta_{24}, \beta_{26} : \beta_{28}$	$27,72 < 1209,32$	$781,11 > 25$	0,98
all nodes	$\beta_1 : \beta_3, \beta_5, \beta_6, \beta_8, \beta_{11}, \beta_{14}, \beta_{15}, \beta_{17} : \beta_{21}, \beta_{23}, \beta_{24}, \beta_{26}, \beta_{28}, \beta_{29}$	$2292,60 < 5890,97$	$2829,11 > 31,41$	0,71

Table A.18: CTP, initial testbed 2, high power, high traffic, blackhole

Node	Factors	Analysis of variance	LR-test	R^2
2	$\beta_1, \beta_2, \beta_6, \beta_7, \beta_{13} : \beta_{15}, \beta_{23}, \beta_{26}$	$671,71 < 1235,18$	$472,52 > 18,31$	0,58
3	$\beta_1, \beta_5 : \beta_8, \beta_{13}, \beta_{15}, \beta_{17}, \beta_{20}, \beta_{21}, \beta_{23}, \beta_{26}, \beta_{29}, \beta_{30}$	$328,84 < 1241,38$	$651,82 > 25$	0,80
4	$\beta_1, \beta_6, \beta_{13}, \beta_{15}, \beta_{20}, \beta_{23}, \beta_{26} : \beta_{28}$	$90,14 < 1246,55$	$770,45 > 16,92$	0,94
5	$\beta_2, \beta_3, \beta_6, \beta_{15}, \beta_{17}, \beta_{23}, \beta_{27}, \beta_{29}$	$31,32 < 1238,28$	$793,60 > 15,51$	0,98
8	$\beta_1 : \beta_{30}$	$2162,60 \not< 1226,90$	$-268,47 \not> 36,42$	$-0,33$
all nodes	$\beta_1 : \beta_3, \beta_5, \beta_6, \beta_8, \beta_{11}, \beta_{13}, \beta_{15}, \beta_{17}, \beta_{20}, \beta_{21}, \beta_{23}, \beta_{26} : \beta_{28}$	$4124,00 < 6022,96$	$2000,27 > 27,59$	0,49

Table A.19: CTP, initial testbed 2, low power, low traffic, blackhole

Node	Factors	Analysis of variance	LR-test	R^2
2	β_{15}	$1,37e-8 < 1223,80$	$794,91 > 3,84$	1
3	β_{15}, β_{17}	$3,13e-8 < 1220,70$	$793,56 > 5,99$	1
4	$\beta_1 : \beta_3, \beta_5, \beta_6, \beta_8, \beta_{14}, \beta_{15}, \beta_{17} : \beta_{21}, \beta_{23}, \beta_{24}, \beta_{28} : \beta_{30}$	$222,36 < 1203,11$	$681,70 > 28,87$	0,86
5	$\beta_{17}, \beta_{19}, \beta_{26}$	$2,60e-7 < 1221,73$	$794,94 > 7,81$	1
8	$\beta_1, \beta_2, \beta_5, \beta_6, \beta_{14}, \beta_{17}, \beta_{18}, \beta_{20}, \beta_{23}, \beta_{30}$	$45,63 < 1215,52$	$772,83 > 18,31$	0,97
all nodes	$\beta_1 : \beta_8, \beta_{11}, \beta_{13}, \beta_{15}, \beta_{17}, \beta_{18}, \beta_{20}, \beta_{21}, \beta_{23}, \beta_{24}, \beta_{26}, \beta_{28} : \beta_{30}$	$2566,70 < 5883,86$	$2688,59 > 33,92$	0,68

Mesh, Blackhole, Both Initial Testbeds

Table A.20: Mesh, initial testbed 1, high power, low traffic, blackhole

Node	Factors	Analysis of variance	LR-test	R^2
11	$\beta_4 : \beta_8, \beta_{10}, \beta_{13}, \beta_{16}, \beta_{17}, \beta_{18}, \beta_{19}$	$1437,70 \not< 1173,10$	$49,74 > 21,03$	0,06
13	$\beta_2, \beta_3, \beta_6, \beta_8, \beta_{13}, \beta_{15}, \beta_{17}$	$1475,00 \not< 1162,74$	$20,60 > 14,07$	0,03
14	$\beta_1, \beta_2, \beta_7, \beta_8, \beta_{10}$, $\beta_{12}, \beta_{13}, \beta_{15}, \beta_{16}, \beta_{19}$	$1484,10 \not< 1172,06$	$24,58 > 18,31$	0,03
15	$\beta_2, \beta_3, \beta_8, \beta_{11}, \beta_{13}, \beta_{17}, \beta_{18}$	$1510,10 \not< 1173,10$	$10,17 \not> 14,07$	0,01
16	$\beta_1 : \beta_3, \beta_6 : \beta_8, \beta_{12}, \beta_{13}, \beta_{15}, \beta_{18}$	$1441,90 \not< 1167,00$	$44,08 > 18,31$	0,06
17	$\beta_1, \beta_2, \beta_5, \beta_7, \beta_9$, $\beta_{13}, \beta_{14}, \beta_{15}, \beta_{16}, \beta_{18}$	$1366,90 \not< 1162,74$	$76,79 > 18,31$	0,1
23	$\beta_2, \beta_3, \beta_5 : \beta_7, \beta_{10}$, $\beta_{12}, \beta_{13}, \beta_{15}, \beta_{16}, \beta_{19}$	$1414,00 \not< 1161,71$	$53,30 > 19,68$	0,07
25	$\beta_4, \beta_5, \beta_7, \beta_8, \beta_{12} : \beta_{16}, \beta_{18}$	$1397,50 \not< 1171,03$	$67,78 > 19,68$	0,09
26	$\beta_2, \beta_5, \beta_7, \beta_8$, $\beta_{11}, \beta_{14} : \beta_{16}, \beta_{19}, \beta_{20}$	$1402,50 \not< 1171,17$	$68,00 > 19,68$	0,09
28	$\beta_1, \beta_6, \beta_7, \beta_{13} : \beta_{16}, \beta_{18}$	$1453,00 \not< 1196,90$	$56,03 > 16,92$	0,07
30	$\beta_1, \beta_2, \beta_4 : \beta_8, \beta_{13}, \beta_{14}, \beta_{16}, \beta_{19}$	$1378,50 \not< 1156,53$	$67,73 > 19,68$	0,09
31	$\beta_1, \beta_5 : \beta_8, \beta_{10}, \beta_{11}$, $\beta_{13}, \beta_{14}, \beta_{15}, \beta_{16}, \beta_{18}$	$1342,80 \not< 1150,32$	$82,04 > 21,03$	0,11
all nodes	$\beta_1, \beta_2, \beta_4 : \beta_8, \beta_{10} : \beta_{16}$	$19507,00 \not< 14606,56$	$187,73 > 25$	0,02

Table A.21: Mesh, initial testbed 1, low power, high traffic, blackhole

Node	Factors	Analysis of variance	LR-test	R^2
11	$\beta_2, \beta_3, \beta_{10} : \beta_{14}, \beta_{15} : \beta_{17}, \beta_{19}, \beta_{20}$	$1506,70 \not< 1191,73$	$27,80 > 21,03$	0,04
13	$\beta_6, \beta_{10}, \beta_{12}, \beta_{13}, \beta_{15}, \beta_{18}, \beta_{19}$	$1527,20 \not< 1184,48$	$9,22 \not> 14,07$	0,01
14	$\beta_2, \beta_3, \beta_5 : \beta_7, \beta_{10}, \beta_{15} : \beta_{20}$	$1483,10 \not< 1178,27$	$30,62 > 21,03$	0,04
15	$\beta_1 : \beta_3, \beta_6, \beta_7, \beta_{16}, \beta_{18}, \beta_{19}$	$1515,00 \not< 1185,52$	$17,43 > 16,92$	0,02
16	$\beta_1, \beta_2, \beta_6, \beta_{14}, \beta_{17} : \beta_{20}$	$1494,00 \not< 1195,87$	$34,20 > 15,51$	0,04
17	$\beta_5, \beta_6, \beta_8, \beta_{10}, \beta_{11}, \beta_{17} : \beta_{20}$	$1489,30 \not< 1185,52$	$30,27 > 16,92$	0,04
23	$\beta_1 : \beta_3, \beta_6 : \beta_8, \beta_{15}, \beta_{16}$	$1365,10 \not< 1189,66$	$94,45 > 15,51$	0,12
25	$\beta_1, \beta_5, \beta_8, \beta_{11}, \beta_{14} : \beta_{16}$	$1328,90 \not< 1183,45$	$108,42 > 15,51$	0,14
26	$\beta_1, \beta_5, \beta_7, \beta_8, \beta_{11}$, $\beta_{13}, \beta_{15}, \beta_{16}, \beta_{19}, \beta_{20}$	$1369,40 \not< 1180,34$	$88,13 > 19,68$	0,11
28	$\beta_1, \beta_4 : \beta_8, \beta_{10}, \beta_{11}, \beta_{13} : \beta_{16}, \beta_{19}$	$1395,70 \not< 1207,25$	$95,07 > 23,68$	0,12
30	$\beta_1 : \beta_3, \beta_5, \beta_6, \beta_8$, $\beta_{11}, \beta_{16}, \beta_{18} : \beta_{20}$	$1361,10 \not< 1181,38$	$93,70 > 21,03$	0,12
31	$\beta_2, \beta_5 : \beta_7, \beta_{11}, \beta_{13} : \beta_{16}, \beta_{19}, \beta_{20}$	$1347,00 \not< 1173,05$	$95,19 > 21,03$	0,12
all nodes	$\beta_1, \beta_5 : \beta_8, \beta_{10} : \beta_{17}, \beta_{19}$	$19510,00 \not< 14824,66$	$337,06 > 25$	0,03

Table A.22: Mesh, initial testbed 1, high power, high traffic, blackhole

Node	Factors	Analysis of variance	LR-test	R^2
11	$\beta_4, \beta_8, \beta_{13} : \beta_{16}$	$1485,30 \not< 1182,41$	$28,72 > 14,07$	0,04
13	$\beta_1, \beta_6, \beta_{13}, \beta_{14}, \beta_{15}, \beta_{16}, \beta_{19}$	$1457,90 \not< 1174,13$	$36,85 > 14,07$	0,05
14	$\beta_1, \beta_3, \beta_4, \beta_7, \beta_8,$ $\beta_{13}, \beta_{16}, \beta_{18}, \beta_{20}$	$1439,40 \not< 1173,10$	$47,54 > 18,31$	0,06
15	$\beta_1, \beta_3, \beta_4, \beta_6, \beta_7,$ $\beta_{13}, \beta_{14}, \beta_{15}, \beta_{16}, \beta_{19}$	$1436,80 \not< 1172,06$	$48,18 > 18,31$	0,06
16	$\beta_1, \beta_3, \beta_4, \beta_7,$ $\beta_{11}, \beta_{13}, \beta_{14}, \beta_{15}, \beta_{16}$	$1433,40 \not< 1180,34$	$54,72 > 16,92$	0,07
17	$\beta_1, \beta_6, \beta_8, \beta_{13}, \beta_{15}, \beta_{16}$	$1425,60 \not< 1179,31$	$55,83 > 18,31$	0,07
23	$\beta_5 : \beta_7, \beta_{10}, \beta_{11}, \beta_{13}, \beta_{15}, \beta_{16}, \beta_{19}$	$1437,70 \not< 1180,34$	$53,25 > 18,31$	0,07
25	$\beta_2, \beta_5 : \beta_8, \beta_{10}, \beta_{12}, \beta_{14} : \beta_{20}$	$1371,90 \not< 1162,74$	$77,84 > 25$	0,10
26	$\beta_2, \beta_5, \beta_7, \beta_8,$ $\beta_{10}, \beta_{13}, \beta_{15}, \beta_{16}, \beta_{18}$	$1449,60 \not< 1178,27$	$45,89 > 18,31$	0,06
28	$\beta_1 : \beta_5, \beta_7, \beta_8, \beta_{13}, \beta_{15}, \beta_{16}, \beta_{18}$	$1436,00 \not< 1185,52$	$58,97 > 21,03$	0,08
30	$\beta_1, \beta_2, \beta_7, \beta_8, \beta_{11}, \beta_{13} : \beta_{16}, \beta_{19}$	$1452,80 \not< 1174,13$	$42,15 > 15,68$	0,05
31	$\beta_2, \beta_3, \beta_5, \beta_7,$ $\beta_{13}, \beta_{15}, \beta_{16}, \beta_{18} : \beta_{20}$	$1374,60 \not< 1167,92$	$77,13 > 19,68$	0,1
all nodes	$\beta_1 : \beta_7, \beta_{11}, \beta_{12}, \beta_{14} : \beta_{19}$	$19863,00 \not< 15067,97$	$327,28 > 26,30$	0,03

Table A.23: Mesh, initial testbed 1, low power, low traffic, blackhole

Node	Factors	Analysis of variance	LR-test	R^2
11	$\beta_4, \beta_5, \beta_{13}, \beta_{14}, \beta_{17}, \beta_{18}, \beta_{20}$	$1456,30 \not< 1389,12$	$165,15 > 15,51$	0,18
13	$\beta_1 : \beta_3, \beta_7, \beta_{13} : \beta_{16}$	$1519,30 \not< 1393,25$	$135,68 > 16,92$	0,15
14	$\beta_1, \beta_6, \beta_8, \beta_{11}, \beta_{13} : \beta_{16}, \beta_{18}, \beta_{19}$	$1444,30 \not< 1389,12$	$172,10 > 19,67$	0,19
15	$\beta_2, \beta_4, \beta_6 : \beta_8, \beta_{14} : \beta_{16}, \beta_{18}$	$1509,80 \not< 1382,93$	$134,23 > 18,31$	0,15
16	$\beta_3 : \beta_8, \beta_{11} : \beta_{14}, \beta_{19}, \beta_{20}$	$1426,70 \not< 1393,25$	$154,24 > 21,03$	0,21
17	$\beta_1 : \beta_3, \beta_5, \beta_7,$ $\beta_8, \beta_{12} : \beta_{14}, \beta_{18}, \beta_{19}$	$1458,40 \not< 1392,22$	$166,99 > 19,68$	0,19
23	$\beta_1, \beta_5 : \beta_8, \beta_{13}, \beta_{14}, \beta_{16}$	$1315,10 < 13489,12$	$235,42 > 15,51$	0,26
25	$\beta_3 : \beta_6, \beta_8, \beta_{10},$ $\beta_{12} : \beta_{14}, \beta_{16}, \beta_{18}, \beta_{19}$	$1231,20 < 1380,86$	$273,88 > 21,03$	0,31
26	$\beta_1, \beta_5 : \beta_8, \beta_{12} : \beta_{14}, \beta_{16}, \beta_{18}, \beta_{19}$	$1326,30 < 1389,12$	$231,95 > 21,03$	0,26
28	$\beta_1 : \beta_3, \beta_5 : \beta_9,$ $\beta_{12} : \beta_{14}, \beta_{15}, \beta_{16}, \beta_{20}$	$1295,30 < 1401,51$	$255,68 > 23,68$	0,28
30	$\beta_1, \beta_3 : \beta_7, \beta_{10},$ $\beta_{13}, \beta_{14}, \beta_{16}, \beta_{18} : \beta_{20}$	$1157,50 < 1388,09$	$317,26 > 23,68$	0,35
31	$\beta_1, \beta_2, \beta_5 : \beta_8, \beta_{12} : \beta_{14}, \beta_{16}, \beta_{18}$	$1315,50 < 1387,06$	$233,72 > 19,67$	0,26
all nodes	$\beta_1, \beta_2, \beta_4 : \beta_8, \beta_{11} : \beta_{15}, \beta_{17}, \beta_{19}$	$19265,00 \not< 17418,44$	$1998,21 > 25$	0,17

Table A.24: Mesh, initial testbed 2, high power, low traffic, blackhole

Node	Factors	Analysis of variance	LR-test	R^2
2	$\beta_1 : \beta_3, \beta_5 : \beta_8, \beta_{13} : \beta_{16}, \beta_{18}$	$1212,10 \not< 1210,35$	$188,22 > 22,36$	0,24
3	$\beta_5 : \beta_8, \beta_{13} : \beta_{16}, \beta_{18}, \beta_{20}$	$1125,20 < 1211,39$	$230,94 > 19,67$	0,29
4	$\beta_2, \beta_3, \beta_5, \beta_7, \beta_8, \beta_{12} : \beta_{16}$	$1130,60 < 1210,35$	$227,55 > 19,67$	0,29
5	$\beta_1, \beta_2, \beta_5 : \beta_8, \beta_{13} : \beta_{16}, \beta_{18} : \beta_{20}$	$850,73 < 1208,28$	$368,16 > 23,68$	0,46
8	$\beta_1, \beta_5, \beta_6, \beta_8, \beta_{12} : \beta_{14}, \beta_{16}, \beta_{17}$	$1256,70 < 1210,35$	$163,79 > 18,31$	0,21
all nodes	$\beta_1 : \beta_7, \beta_{13}, \beta_{14}, \beta_{17} : \beta_{19}$	$8533,90 \not< 7047,71$	$493,66 > 22,36$	0,10

Table A.25: Mesh, initial testbed 2, low power, high traffic, blackhole

Node	Factors	Analysis of variance	LR-test	R^2
2	$\beta_1, \beta_3, \beta_8, \beta_{11}, \beta_{13}, \beta_{14}, \beta_{18}$	$2899,80 \not< 2411,66$	$150,52 > 15,51$	0,09
3	$\beta_1, \beta_5, \beta_6, \beta_8,$ $\beta_{13}, \beta_{14}, \beta_{16}, \beta_{18}, \beta_{19}$	$2799,50 \not< 2411,66$	$201,29 > 16,92$	0,13
4	$\beta_1 : \beta_3, \beta_5, \beta_8,$ $\beta_{13}, \beta_{14}, \beta_{16}, \beta_{18}, \beta_{19}$	$2776,00 \not< 2225,15$	$77,39 > 15,51$	0,05
5	$\beta_1, \beta_7, \beta_{11}, \beta_{13}, \beta_{14}, \beta_{17}, \beta_{18}, \beta_{20}$	$2890,30 \not< 2408,59$	$153,87 > 16,92$	0,10
8	$\beta_1, \beta_4, \beta_8, \beta_{13},$ $\beta_{14}, \beta_{15}, \beta_{16}, \beta_{18}, \beta_{19}$	$2915,00 \not< 2413,71$	$144,94 > 16,92$	0,09
all nodes	$\beta_1, \beta_{13} : \beta_{15}, \beta_{17}, \beta_{19}$	$18360,00 \not< 13941,09$	$297,14 > 14,07$	0,03

Table A.26: Mesh, initial testbed 2, high power, high traffic, blackhole

Node	Factors	Analysis of variance	LR-test	R^2
2	$\beta_3, \beta_5, \beta_{11}, \beta_{13}, \beta_{14}, \beta_{16} : \beta_{18}$	$1112,40 < 1228,97$	$247,48 > 16,92$	0,31
3	$\beta_1, \beta_5, \beta_8, \beta_{11},$ $\beta_{13}, \beta_{14}, \beta_{16}, \beta_{18}, \beta_{19}$	$1379,00 \not< 1228,97$	$114,19 > 16,92$	0,14
4	$\beta_5, \beta_7, \beta_8, \beta_{13} : \beta_{15}, \beta_{20}$	$1143,90 \not< 1044,61$	$85,60 > 15,51$	0,13
5	$\beta_1, \beta_3, \beta_6, \beta_8,$ $\beta_{11}, \beta_{13}, \beta_{14}, \beta_{17}, \beta_{18}$	$1283,30 \not< 1227,94$	$162,01 > 18,31$	0,20
8	$\beta_2, \beta_5, \beta_8, \beta_{13} : \beta_{16}, \beta_{19}$	$1175,60 < 1231,04$	$217,21 > 16,92$	0,27
all nodes	$\beta_1, \beta_3, \beta_5, \beta_7, \beta_{11}, \beta_{13},$ $\beta_{14}, \beta_{15} : \beta_{17}, \beta_{19}, \beta_{20}$	$8802,00 \not< 6962,53$	$291,67 > 21,03$	0,06

Table A.27: Mesh, initial testbed 2, low power, low traffic, blackhole

Node	Factors	Analysis of variance	LR-test	R^2
2	$\beta_1, \beta_2, \beta_4, \beta_5,$ $\beta_7, \beta_{13} : \beta_{15}, \beta_{17}, \beta_{20}$	$1257,80 \not< 1198,97$	$156,42 > 19,68$	0,20
3	$\beta_1, \beta_5 : \beta_7, \beta_{10}, \beta_{12},$ $\beta_{14}, \beta_{16}, \beta_{18}, \beta_{20}$	$1249,30 \not< 1205,18$	$164,81 > 19,68$	0,21
4	$\beta_1 : \beta_3, \beta_5 : \beta_7, \beta_{11},$ $\beta_{13}, \beta_{14}, \beta_{15} : \beta_{17}, \beta_{19}$	$881,93 < 1200,00$	$346,42 > 22,36$	0,44
5	$\beta_1 : \beta_3, \beta_6, \beta_7, \beta_{10}, \beta_{13} : \beta_{16}$	$1429,30 \not< 1206,21$	$75,52 > 19,68$	0,10
8	$\beta_5 : \beta_8, \beta_{12}, \beta_{14}, \beta_{18}, \beta_{19}$	$1280,40 \not< 1208,28$	$149,26 > 15,51$	0,19
all nodes	$\beta_1, \beta_5 : \beta_8, \beta_{10}, \beta_{12} : \beta_{15}, \beta_{17} : \beta_{20}$	$8533,60 \not< 7000,00$	$463,08 > 25$	0,10

A.1.2 *Wilcoxon-Mann-Whitney Results for the Final Testbeds*

Table A.28: Overall performance - basic + mesh metrics - final testbeds

Metric	**Detection rate**
B11 - Radio energy	0.85
B12 - Radio load	0.84
B07 - NET received pkts	0.84
B09 - MAC received pkts	0.84
M02 - No. of routing entries	0.83
B01 - RSSI	0.82
B13 - MCU energy	0.80
B08 - MAC sent pkts	0.80
M01 - No. of direct neighbors	0.79
B14 - MCU load	0.78
B04 - Transmit duty cycle	0.75
B05 - Listen duty cycle	0.75
B02 - Transmit time	0.68
B06 - NET sent pkts	0.54
B03 - Listen time	0.52
B10 - Invalid CRC	0.37
B15 - Contention drop	0.30
B16 - Pending pkts	0.23
B18 - Too long pkts	0.13
B17 - Too short pkts	0.00

Table A.29: Basic + mesh metrics with attack detection over 0.75 in the final testbeds

Metric	Constant jammer	Random jammer	Blackhole + Random jammer	Blackhole + Reactive jammer	Blackhole	Reactive jammer
B11 - Radio energy	✓	✓	✓	✓	✓	✓
B12 - Radio load	✓	✓	✓	✓	✓	✓
B07 - NET received pkts	✓	✓	✓	✓	✓	✓
B09 - MAC received pkts	✓	✓	✓	✓	✓	✓
M02 - No. of routing entries	✓	✓	✓	✓	✓	✓
B01 - RSSI	✓	✓	✓	✓	✓	✓
B08 - MAC sent pkts	✓	✓	✓	✓	✓	-
B13 - MCU energy	✓	✓	✓	✓	✓	-
M01 - No. of direct neighbors	✓	✓	-	✓	✓	-
B14 - MCU load	✓	✓	✓	✓	-	-
B05 - Listen duty cycle	✓	✓	✓	-	-	-
B04 - Transmit duty cycle	✓	✓	✓	-	-	-

Influence of the Testbed Location

Table A.30: Detection rates basic metrics - final testbed 1

Metric	Constant jammer	Random jammer	Reactive jammer	Blackhole	Blackhole + Random jammer	Blackhole + Reactive jammer
B09 - MAC received pkts	0.83	0.76	0.74	0.77	0.83	0.82
B11 - Radio energy	0.83	0.79	0.73	0.76	0.82	0.80
B01 - RSSI	0.80	0.76	0.75	0.76	0.83	0.81
B07 - NET received pkts	0.82	0.74	0.75	0.75	0.83	0.81
B12 - Radio load	0.82	0.77	0.71	0.74	0.81	0.79
B13 - MCU energy	0.78	0.74	0.72	0.74	0.79	0.77
B08 - MAC sent pkts	0.83	0.74	0.71	0.72	0.76	0.76
B14 - MCU load	0.78	0.73	0.71	0.72	0.77	0.77
B04 - Transmit duty cycle	0.79	0.70	0.69	0.71	0.78	0.76
B05 - Listen duty cycle	0.77	0.72	0.62	0.67	0.77	0.72
B02 - Transmit time	0.68	0.64	0.59	0.63	0.72	0.66
B06 - NET sent pkts	0.69	0.63	0.54	0.57	0.65	0.62
B03 - Listen time	0.61	0.56	0.42	0.46	0.54	0.49
B10 - Invalid CRC	0.41	0.29	0.31	0.31	0.36	0.37
B15 - Contention drop	0.28	0.17	0.28	0.26	0.28	0.25
B18 - Too long pkts	0.21	0.11	0.12	0.15	0.20	0.22
B16 - Pending pkts	0.40	0.19	0.08	0.03	0.10	0.03
B17 - Too short pkts	0.00	0.00	0.00	0.00	0.00	0.00

Table A.31: Detection rates basic metrics - final testbed 2

Metric	Constant jammer	Random jammer	Reactive jammer	Blackhole	Blackhole + Random jammer	Blackhole + Reactive jammer
B11 - Radio energy	0.92	0.85	0.78	0.77	0.91	0.77
B12 - Radio load	0.92	0.86	0.78	0.77	0.91	0.75
B09 - MAC received pkts	0.92	0.88	0.73	0.76	0.89	0.77
B07 - NET received pkts	0.92	0.88	0.73	0.76	0.89	0.75
B05 - Listen duty cycle	0.93	0.91	0.71	0.71	0.91	0.73
B08 - MAC sent pkts	0.93	0.83	0.74	0.71	0.84	0.75
B13 - MCU energy	0.89	0.78	0.76	0.76	0.82	0.76
B14 - MCU load	0.89	0.76	0.75	0.76	0.81	0.75
B04 - Transmit duty cycle	0.82	0.76	0.70	0.70	0.74	0.70
B01 - RSSI	0.87	0.74	0.68	0.72	0.73	0.66
B06 - NET sent pkts	0.84	0.83	0.48	0.51	0.80	0.56
B02 - Transmit time	0.68	0.67	0.61	0.60	0.66	0.64
B03 - Listen time	0.75	0.76	0.41	0.44	0.68	0.46
B15 - Contention drop	0.65	0.31	0.42	0.28	0.55	0.62
B10 - Invalid CRC	0.72	0.41	0.33	0.39	0.36	0.31
B16 - Pending pkts	0.80	0.38	0.09	0.05	0.38	0.07
B18 - Too long pkts	0.46	0.24	0.15	0.23	0.28	0.21
B17 - Too short pkts	0.01	0.00	0.00	0.00	0.01	0.00

Table A.32: Detection rates mesh metrics - final testbed 1

Metric	Constant jammer	Random jammer	Reactive jammer	Blackhole	Blackhole + Random jammer	Blackhole + Reactive jammer
M02 - No. of routing entries	0.85	0.80	0.76	0.78	0.82	0.80
M01 - No. of direct neighbors	0.86	0.77	0.76	0.80	0.78	0.78

Table A.33: Detection rates mesh metrics - final testbed 2

Metric	Constant jammer	Random jammer	Reactive jammer	Blackhole	Blackhole + Random jammer	Blackhole + Reactive jammer
M02 - No. of routing entries	0.93	0.86	0.71	0.79	0.88	0.74
M01 - No. of direct neighbors	0.92	0.75	0.69	0.71	0.66	0.68

Influence of the Density

Table A.34: Detection rates basic metrics - high power - final testbeds

Metric	Constant jammer	Random jammer	Reactive jammer	Blackhole	Blackhole + Random jammer	Blackhole + Reactive jammer
B11 - Radio energy	0.89	0.86	0.79	0.79	0.91	0.83
B09 - MAC received pkts	0.91	0.87	0.75	0.79	0.90	0.82
B07 - NET received pkts	0.91	0.86	0.76	0.78	0.88	0.81
B12 - Radio load	0.90	0.86	0.77	0.79	0.89	0.79
B13 - MCU energy	0.86	0.81	0.75	0.79	0.87	0.81
B14 - MCU load	0.86	0.80	0.75	0.78	0.84	0.80
B08 - MAC sent pkts	0.91	0.80	0.75	0.75	0.82	0.79
B05 - Listen duty cycle	0.87	0.84	0.66	0.69	0.87	0.76
B01 - RSSI	0.87	0.77	0.73	0.75	0.79	0.73
B04 - Transmit duty cycle	0.82	0.74	0.72	0.73	0.79	0.76
B06 - NET sent pkts	0.77	0.79	0.53	0.55	0.74	0.61
B02 - Transmit time	0.68	0.67	0.59	0.63	0.70	0.66
B03 - Listen time	0.69	0.69	0.40	0.44	0.63	0.47
B10 - Invalid CRC	0.62	0.38	0.33	0.36	0.37	0.39
B15 - Contention drop	0.48	0.24	0.34	0.30	0.43	0.43
B16 - Pending pkts	0.59	0.29	0.07	0.03	0.24	0.05
B18 - Too long pkts	0.33	0.17	0.12	0.18	0.21	0.22
B17 - Too short pkts	0.01	0.00	0.00	0.00	0.00	0.00

Table A.35: Detection rates basic metrics - low power - final testbeds

Metric	Constant jammer	Random jammer	Reactive jammer	Blackhole	Blackhole + Random jammer	Blackhole + Reactive jammer
B09 - MAC received pkts	0.89	0.82	0.76	0.79	0.87	0.83
B11 - Radio energy	0.91	0.83	0.77	0.78	0.87	0.79
B12 - Radio load	0.89	0.82	0.76	0.77	0.88	0.79
B07 - NET received pkts	0.89	0.80	0.76	0.78	0.89	0.81
B08 - MAC sent pkts	0.91	0.81	0.74	0.73	0.83	0.77
B01 - RSSI	0.86	0.77	0.74	0.78	0.81	0.79
B05 - Listen duty cycle	0.88	0.83	0.71	0.73	0.86	0.73
B13 - MCU energy	0.86	0.76	0.76	0.76	0.79	0.77
B14 - MCU load	0.86	0.73	0.75	0.75	0.79	0.77
B04 - Transmit duty cycle	0.84	0.76	0.71	0.72	0.78	0.75
B02 - Transmit time	0.73	0.68	0.64	0.64	0.73	0.68
B06 - NET sent pkts	0.80	0.71	0.52	0.56	0.76	0.60
B03 - Listen time	0.72	0.67	0.45	0.49	0.61	0.51
B10 - Invalid CRC	0.54	0.33	0.33	0.36	0.37	0.31
B15 - Contention drop	0.47	0.24	0.37	0.25	0.43	0.45
B18 - Too long pkts	0.36	0.19	0.16	0.20	0.28	0.21
B16 - Pending pkts	0.63	0.29	0.10	0.05	0.26	0.06
B17 - Too short pkts	0.00	0.00	0.00	0.00	0.00	0.00

Table A.36: Detection rates CTP metrics - high power - final testbeds

Metric	Constant jammer	Random jammer	Reactive jammer	Blackhole	Blackhole + Random jammer	Blackhole + Reactive jammer
CTP12 - Number of neighbors	0.96	0.88	0.83	0.87	0.88	0.90
CTP10 - Link estimation	0.89	0.82	0.82	0.83	0.91	0.87
CTP11 - Best neighbor	0.84	0.83	0.82	0.81	0.89	0.88
CTP07 - Packet delivery rate	0.94	0.81	0.85	0.79	0.81	0.84
CTP04 - Received ACK pkts	0.89	0.82	0.66	0.67	0.81	0.71
CTP09 - Parent congestion	0.78	0.72	0.71	0.72	0.81	0.81
CTP01 - Sent data pkts	0.90	0.80	0.60	0.63	0.78	0.71
CTP03 - Sent ACK pkts	0.75	0.72	0.69	0.70	0.75	0.74
CTP02 - Received data pkts	0.75	0.72	0.69	0.70	0.75	0.74
CTP06 - Dropped pkts	0.51	0.50	0.51	0.48	0.52	0.53
CTP08 - Changing parent	0.36	0.29	0.21	0.25	0.32	0.30
CTP05 - Received duplicates	0.38	0.23	0.19	0.24	0.28	0.24

Table A.37: Detection rates CTP metrics - low power - final testbeds

Metric	Constant jammer	Random jammer	Reactive jammer	Blackhole	Blackhole + Random jammer	Blackhole + Reactive jammer
CTP12 - Number of neighbors	0.96	0.89	0.84	0.90	0.94	0.85
CTP10 - Link estimation	0.83	0.82	0.83	0.84	0.88	0.88
CTP07 - Packet delivery rate	0.91	0.84	0.80	0.86	0.82	0.84
CTP11 - Best neighbor	0.86	0.82	0.80	0.82	0.86	0.82
CTP04 - Received ACK pkts	0.81	0.71	0.63	0.68	0.85	0.75
CTP01 - Sent data pkts	0.85	0.76	0.59	0.63	0.84	0.69
CTP09 - Parent congestion	0.70	0.68	0.70	0.69	0.75	0.72
CTP03 - Sent ACK pkts	0.67	0.65	0.66	0.62	0.69	0.68
CTP02 - Received data pkts	0.67	0.65	0.66	0.62	0.69	0.68
CTP06 - Dropped pkts	0.46	0.45	0.49	0.44	0.49	0.44
CTP05 - Received duplicates	0.32	0.19	0.19	0.24	0.27	0.25
CTP08 - Changing parent	0.26	0.20	0.13	0.14	0.20	0.14

Table A.38: Detection rates mesh metrics - high power - final testbeds

Metric	Constant jammer	Random jammer	Reactive jammer	Blackhole	Blackhole + Random jammer	Blackhole + Reactive jammer
M02 - No. of routing entries	0.92	0.87	0.71	0.81	0.91	0.78
M01 - No. of direct neighbors	0.91	0.80	0.74	0.78	0.74	0.76

Table A.39: Detection rates mesh metrics - low power - final testbeds

Metric	Constant jammer	Random jammer	Reactive jammer	Blackhole	Blackhole + Random jammer	Blackhole + Reactive jammer
M02 - No. of routing entries	0.92	0.84	0.79	0.81	0.84	0.81
M01 - No. of direct neighbors	0.93	0.76	0.76	0.78	0.75	0.75

Influence of the Traffic Intensity

Table A.40: Detection rates basic metrics - high traffic - final testbeds

Metric	Constant jammer	Random jammer	Reactive jammer	Blackhole	Blackhole + Random jammer	Blackhole + Reactive jammer
B09 - MAC received pkts	0.89	0.83	0.78	0.82	0.90	0.85
B11 - Radio energy	0.88	0.84	0.79	0.80	0.90	0.81
B07 - NET received pkts	0.87	0.80	0.79	0.81	0.90	0.84
B12 - Radio load	0.89	0.84	0.79	0.80	0.89	0.79
B01 - RSSI	0.87	0.82	0.78	0.81	0.87	0.82
B13 - MCU energy	0.88	0.80	0.79	0.81	0.83	0.82
B14 - MCU load	0.89	0.78	0.79	0.80	0.83	0.81
B08 - MAC sent pkts	0.91	0.80	0.77	0.75	0.84	0.80
B05 - Listen duty cycle	0.88	0.82	0.73	0.70	0.85	0.72
B04 - Transmit duty cycle	0.81	0.76	0.76	0.74	0.80	0.79
B06 - NET sent pkts	0.80	0.76	0.57	0.59	0.75	0.64
B02 - Transmit time	0.67	0.66	0.63	0.62	0.73	0.68
B03 - Listen time	0.69	0.69	0.45	0.52	0.64	0.55
B10 - Invalid CRC	0.56	0.32	0.35	0.38	0.35	0.40
B15 - Contention drop	0.48	0.25	0.36	0.30	0.47	0.46
B16 - Pending pkts	0.61	0.28	0.10	0.06	0.27	0.07
B18 - Too long pkts	0.28	0.14	0.13	0.22	0.24	0.26
B17 - Too short pkts	0.00	0.00	0.00	0.00	0.00	0.00

Table A.41: Detection rates basic metrics - low traffic - final testbeds

Metric	Constant jammer	Random jammer	Reactive jammer	Blackhole	Blackhole + Random jammer	Blackhole + Reactive jammer
B11 - Radio energy	0.92	0.84	0.76	0.76	0.88	0.81
B09 - MAC received pkts	0.92	0.87	0.73	0.75	0.87	0.79
B07 - NET received pkts	0.92	0.86	0.73	0.75	0.87	0.78
B12 - Radio load	0.90	0.84	0.74	0.76	0.88	0.79
B05 - Listen duty cycle	0.87	0.85	0.64	0.72	0.88	0.77
B08 - MAC sent pkts	0.91	0.82	0.72	0.72	0.81	0.76
B13 - MCU energy	0.84	0.77	0.73	0.74	0.83	0.76
B14 - MCU load	0.83	0.75	0.71	0.73	0.80	0.76
B04 - Transmit duty cycle	0.85	0.74	0.68	0.71	0.77	0.71
B01 - RSSI	0.85	0.73	0.69	0.72	0.74	0.71
B02 - Transmit time	0.74	0.69	0.60	0.65	0.69	0.66
B06 - NET sent pkts	0.77	0.74	0.48	0.52	0.74	0.58
B03 - Listen time	0.71	0.67	0.40	0.41	0.61	0.43
B10 - Invalid CRC	0.60	0.39	0.30	0.35	0.39	0.30
B15 - Contention drop	0.47	0.23	0.35	0.25	0.39	0.41
B18 - Too long pkts	0.40	0.22	0.14	0.17	0.25	0.18
B16 - Pending pkts	0.61	0.31	0.07	0.03	0.22	0.04
B17 - Too short pkts	0.00	0.00	0.00	0.00	0.00	0.00

Table A.42: Detection rates CTP metrics - high traffic - final testbeds

Metric	Constant jammer	Random jammer	Reactive jammer	Blackhole	Blackhole + Random jammer	Blackhole + Reactive jammer
CTP12 - Number of neighbors	0.95	0.88	0.82	0.86	0.89	0.88
CTP10 - Link estimation	0.84	0.81	0.83	0.84	0.86	0.86
CTP07 - Packet delivery rate	0.91	0.81	0.83	0.82	0.79	0.83
CTP11 - Best neighbor	0.82	0.79	0.80	0.81	0.85	0.83
CTP01 - Sent data pkts	0.88	0.79	0.67	0.70	0.88	0.78
CTP04 - Received ACK pkts	0.83	0.73	0.67	0.67	0.85	0.77
CTP09 - Parent congestion	0.73	0.68	0.71	0.71	0.74	0.79
CTP03 - Sent ACK pkts	0.56	0.63	0.65	0.61	0.63	0.62
CTP02 - Received data pkts	0.56	0.63	0.65	0.61	0.63	0.62
CTP06 - Dropped pkts	0.55	0.61	0.63	0.58	0.61	0.59
CTP05 - Received duplicates	0.10	0.06	0.05	0.07	0.09	0.10
CTP08 - Changing parent	0.01	0.02	0.02	0.03	0.02	0.02

Table A.43: Detection rates CTP metrics - low traffic - final testbeds

Metric	Constant jammer	Random jammer	Reactive jammer	Blackhole	Blackhole + Random jammer	Blackhole + Reactive jammer
CTP12 - Number of neighbors	0.96	0.89	0.85	0.91	0.94	0.87
CTP10 - Link estimation	0.88	0.83	0.81	0.83	0.93	0.88
CTP11 - Best neighbor	0.88	0.86	0.83	0.82	0.89	0.88
CTP07 - Packet delivery rate	0.94	0.83	0.83	0.83	0.84	0.85
CTP03 - Sent ACK pkts	0.85	0.74	0.69	0.72	0.81	0.80
CTP02 - Received data pkts	0.85	0.74	0.69	0.72	0.81	0.80
CTP04 - Received ACK pkts	0.87	0.80	0.62	0.68	0.81	0.69
CTP09 - Parent congestion	0.75	0.72	0.70	0.69	0.82	0.74
CTP01 - Sent data pkts	0.87	0.78	0.53	0.56	0.74	0.62
CTP08 - Changing parent	0.61	0.48	0.32	0.36	0.50	0.41
CTP05 - Received duplicates	0.60	0.36	0.34	0.41	0.46	0.39
CTP06 - Dropped pkts	0.42	0.34	0.37	0.35	0.40	0.38

Table A.44: Detection rates mesh metrics - high traffic - final testbeds

Metric	Constant jammer	Random jammer	Reactive jammer	Blackhole	Blackhole + Random jammer	Blackhole + Reactive jammer
M02 - No. of routing entries	0.95	0.90	0.79	0.86	0.93	0.82
M01 - No. of direct neighbors	0.92	0.79	0.77	0.78	0.75	0.79

Table A.45: Detection rates mesh metrics - low traffic - final testbeds

Metric	Constant jammer	Random jammer	Reactive jammer	Blackhole	Blackhole + Random jammer	Blackhole + Reactive jammer
M02 - No. of routing entries	0.89	0.80	0.72	0.77	0.82	0.77
M01 - No. of direct neighbors	0.92	0.78	0.73	0.78	0.74	0.72

Influence of the Attacker Location and Start

Table A.46: Detection rates basic metrics - inner attacker - final testbeds

Metric	Constant jammer	Random jammer	Reactive jammer	Blackhole
B11 - Radio energy	0.88	0.81	0.77	0.76
B09 - MAC received pkts	0.86	0.83	0.76	0.78
B12 - Radio load	0.87	0.81	0.76	0.75
B07 - NET received pkts	0.86	0.82	0.75	0.76
B13 - MCU energy	0.82	0.76	0.76	0.78
B01 - RSSI	0.83	0.78	0.74	0.76
B08 - MAC sent pkts	0.87	0.77	0.74	0.72
B14 - MCU load	0.82	0.74	0.75	0.75
B04 - Transmit duty cycle	0.80	0.73	0.72	0.71
B05 - Listen duty cycle	0.82	0.76	0.65	0.67
B02 - Transmit time	0.67	0.64	0.61	0.60
B06 - NET sent pkts	0.72	0.70	0.50	0.54
B03 - Listen time	0.62	0.63	0.42	0.46
B10 - Invalid CRC	0.53	0.36	0.33	0.33
B15 - Contention drop	0.46	0.24	0.29	0.24
B16 - Pending pkts	0.49	0.19	0.08	0.04
B18 - Too long pkts	0.31	0.17	0.14	0.16
B17 - Too short pkts	0.00	0.00	0.00	0.00

Table A.47: Detection rates basic metrics - both attackers - final testbeds

Metric	Constant jammer	Random jammer	Reactive jammer	Blackhole	Blackhole + Random jammer	Blackhole + Reactive jammer
B11 - Radio energy	0.92	0.87	0.79	0.81	0.89	0.81
B09 - MAC received pkts	0.95	0.86	0.76	0.80	0.89	0.82
B12 - Radio load	0.92	0.87	0.77	0.81	0.89	0.79
B07 - NET received pkts	0.94	0.85	0.77	0.80	0.89	0.81
B05 - Listen duty cycle	0.94	0.91	0.72	0.75	0.86	0.75
B08 - MAC sent pkts	0.94	0.85	0.74	0.76	0.82	0.78
B13 - MCU energy	0.89	0.81	0.76	0.78	0.83	0.79
B14 - MCU load	0.90	0.79	0.75	0.78	0.81	0.78
B01 - RSSI	0.89	0.77	0.73	0.77	0.80	0.76
B04 - Transmit duty cycle	0.86	0.77	0.72	0.74	0.79	0.75
B02 - Transmit time	0.74	0.71	0.63	0.67	0.71	0.67
B06 - NET sent pkts	0.85	0.80	0.54	0.57	0.75	0.61
B03 - Listen time	0.78	0.74	0.43	0.48	0.62	0.49
B10 - Invalid CRC	0.63	0.35	0.33	0.40	0.37	0.35
B15 - Contention drop	0.49	0.25	0.42	0.31	0.43	0.44
B16 - Pending pkts	0.73	0.40	0.09	0.05	0.25	0.05
B18 - Too long pkts	0.37	0.18	0.14	0.23	0.25	0.22
B17 - Too short pkts	0.00	0.00	0.00	0.00	0.00	0.00

Table A.48: Detection rates CTP metrics - inner attacker - final testbeds

Metric	Constant jammer	Random jammer	Reactive jammer	Blackhole
CTP12 - Number of neighbors	0.93	0.86	0.83	0.89
CTP07 - Packet delivery rate	0.90	0.82	0.84	0.83
CTP10 - Link estimation	0.85	0.80	0.82	0.82
CTP11 - Best neighbor	0.83	0.81	0.82	0.82
CTP04 - Received ACK pkts	0.82	0.74	0.64	0.66
CTP09 - Parent congestion	0.73	0.68	0.72	0.72
CTP01 - Sent data pkts	0.82	0.73	0.57	0.64
CTP03 - Sent ACK pkts	0.71	0.69	0.67	0.66
CTP02 - Received data pkts	0.71	0.69	0.67	0.66
CTP06 - Dropped pkts	0.49	0.47	0.51	0.47
CTP05 - Received duplicates	0.32	0.19	0.21	0.22
CTP08 - Changing parent	0.30	0.23	0.17	0.20

Table A.49: Detection rates CTP metrics - both attackers - final testbeds

Metric	Constant jammer	Random jammer	Reactive jammer	Blackhole	Blackhole + Random jammer	Blackhole + Reactive jammer
CTP12 - Number of neighbors	0.99	0.91	0.84	0.88	0.91	0.87
CTP10 - Link estimation	0.86	0.83	0.83	0.86	0.89	0.87
CTP07 - Packet delivery rate	0.95	0.83	0.82	0.82	0.81	0.84
CTP11 - Best neighbor	0.86	0.83	0.81	0.81	0.87	0.85
CTP04 - Received ACK pkts	0.88	0.79	0.65	0.69	0.83	0.73
CTP01 - Sent data pkts	0.93	0.83	0.62	0.61	0.81	0.70
CTP09 - Parent congestion	0.75	0.72	0.69	0.69	0.78	0.77
CTP03 - Sent ACK pkts	0.71	0.68	0.67	0.67	0.72	0.71
CTP02 - Received data pkts	0.71	0.68	0.67	0.67	0.72	0.71
CTP06 - Dropped pkts	0.48	0.49	0.49	0.46	0.51	0.49
CTP05 - Received duplicates	0.38	0.22	0.18	0.26	0.27	0.25
CTP08 - Changing parent	0.32	0.26	0.17	0.20	0.26	0.22

Table A.50: Detection rates mesh metrics - inner attacker - final testbeds

Metric	Constant jammer	Random jammer	Reactive jammer	Blackhole
M02 - No. of routing entries	0.87	0.85	0.76	0.81
M01 - No. of direct neighbors	0.90	0.76	0.75	0.77

Table A.51: Detection rates mesh metrics - both attackers - final testbeds

Metric	Constant jammer	Random jammer	Reactive jammer	Blackhole	Blackhole + Random jammer	Blackhole + Reactive jammer
M02 - No. of routing entries	0.97	0.86	0.75	0.81	0.87	0.79
M01 - No. of direct neighbors	0.93	0.80	0.75	0.79	0.74	0.76

Table A.52: Detection rates basic metrics - no delay attacker - final testbeds

Metric	Constant jammer	Random jammer	Reactive jammer	Blackhole	Blackhole + Random jammer	Blackhole + Reactive jammer
B11 - Radio energy	0.90	0.84	0.79	0.81	0.90	0.82
B09 - MAC received pkts	0.90	0.85	0.76	0.80	0.88	0.84
B12 - Radio load	0.89	0.85	0.79	0.79	0.90	0.80
B07 - NET received pkts	0.90	0.85	0.77	0.80	0.88	0.81
B13 - MCU energy	0.85	0.79	0.76	0.79	0.85	0.82
B08 - MAC sent pkts	0.91	0.81	0.75	0.75	0.84	0.79
B14 - MCU load	0.86	0.77	0.76	0.78	0.83	0.82
B05 - Listen duty cycle	0.89	0.84	0.71	0.72	0.88	0.76
B01 - RSSI	0.86	0.78	0.74	0.78	0.80	0.77
B04 - Transmit duty cycle	0.82	0.74	0.72	0.74	0.78	0.77
B02 - Transmit time	0.70	0.67	0.65	0.66	0.74	0.66
B06 - NET sent pkts	0.78	0.76	0.53	0.58	0.74	0.60
B03 - Listen time	0.71	0.68	0.46	0.50	0.63	0.49
B10 - Invalid CRC	0.59	0.38	0.34	0.40	0.37	0.39
B15 - Contention drop	0.49	0.23	0.40	0.29	0.44	0.43
B18 - Too long pkts	0.33	0.18	0.15	0.23	0.25	0.24
B16 - Pending pkts	0.62	0.29	0.10	0.04	0.24	0.04
B17 - Too short pkts	0.00	0.00	0.00	0.00	0.00	0.00

Table A.53: Detection rates basic metrics - delayed attacker - final testbeds

Metric	Constant jammer	Random jammer	Reactive jammer	Blackhole	Blackhole + Random jammer	Blackhole + Reactive jammer
B09 - MAC received pkts	0.91	0.85	0.75	0.78	0.90	0.81
B11 - Radio energy	0.90	0.84	0.76	0.76	0.88	0.79
B07 - NET received pkts	0.90	0.82	0.75	0.76	0.89	0.80
B12 - Radio load	0.90	0.83	0.75	0.76	0.87	0.79
B08 - MAC sent pkts	0.90	0.81	0.74	0.72	0.81	0.77
B13 - MCU energy	0.86	0.78	0.75	0.76	0.81	0.76
B01 - RSSI	0.86	0.77	0.74	0.75	0.81	0.76
B14 - MCU load	0.87	0.77	0.74	0.75	0.79	0.75
B05 - Listen duty cycle	0.86	0.83	0.66	0.69	0.85	0.74
B04 - Transmit duty cycle	0.84	0.76	0.71	0.72	0.79	0.73
B06 - NET sent pkts	0.79	0.74	0.51	0.54	0.76	0.61
B02 - Transmit time	0.70	0.68	0.59	0.61	0.68	0.67
B03 - Listen time	0.70	0.68	0.39	0.43	0.62	0.49
B10 - Invalid CRC	0.57	0.33	0.32	0.32	0.37	0.31
B15 - Contention drop	0.46	0.25	0.32	0.27	0.42	0.44
B16 - Pending pkts	0.60	0.30	0.07	0.05	0.25	0.07
B18 - Too long pkts	0.35	0.18	0.12	0.15	0.25	0.20
B17 - Too short pkts	0.00	0.00	0.00	0.00	0.01	0.00

Table A.54: Detection rates CTP metrics - no delay attacker - final testbeds

Metric	Constant jammer	Random jammer	Reactive jammer	Blackhole	Blackhole + Random jammer	Blackhole + Reactive jammer
CTP12 - Number of neighbors	0.97	0.89	0.83	0.87	0.91	0.90
CTP10 - Link estimation	0.87	0.82	0.86	0.86	0.91	0.90
CTP11 - Best neighbor	0.84	0.81	0.82	0.85	0.89	0.90
CTP07 - Packet delivery rate	0.91	0.84	0.84	0.81	0.83	0.83
CTP04 - Received ACK pkts	0.85	0.78	0.69	0.70	0.81	0.75
CTP01 - Sent data pkts	0.89	0.79	0.67	0.65	0.80	0.69
CTP09 - Parent congestion	0.74	0.70	0.75	0.71	0.77	0.78
CTP03 - Sent ACK pkts	0.71	0.69	0.67	0.67	0.73	0.70
CTP02 - Received data pkts	0.71	0.69	0.67	0.67	0.73	0.70
CTP06 - Dropped pkts	0.48	0.46	0.49	0.45	0.49	0.50
CTP05 - Received duplicates	0.36	0.21	0.19	0.29	0.28	0.26
CTP08 - Changing parent	0.31	0.25	0.16	0.23	0.27	0.25

Table A.55: Detection rates CTP metrics - delayed attacker - final testbeds

Metric	Constant jammer	Random jammer	Reactive jammer	Blackhole	Blackhole + Random jammer	Blackhole + Reactive jammer
CTP12 - Number of neighbors	0.95	0.88	0.84	0.90	0.92	0.85
CTP07 - Packet delivery rate	0.93	0.80	0.82	0.84	0.80	0.85
CTP10 - Link estimation	0.85	0.82	0.79	0.81	0.88	0.85
CTP11 - Best neighbor	0.85	0.84	0.80	0.78	0.85	0.81
CTP04 - Received ACK pkts	0.85	0.75	0.60	0.65	0.85	0.70
CTP09 - Parent congestion	0.74	0.70	0.66	0.70	0.79	0.75
CTP01 - Sent data pkts	0.87	0.78	0.53	0.61	0.82	0.71
CTP03 - Sent ACK pkts	0.71	0.68	0.67	0.65	0.71	0.71
CTP02 - Received data pkts	0.71	0.68	0.67	0.65	0.71	0.71
CTP06 - Dropped pkts	0.48	0.49	0.51	0.47	0.52	0.47
CTP05 - Received duplicates	0.34	0.21	0.19	0.20	0.27	0.23
CTP08 - Changing parent	0.31	0.24	0.18	0.16	0.25	0.18

Table A.56: Detection rates mesh metrics - no delay attacker - final testbeds

Metric	Constant jammer	Random jammer	Reactive jammer	Blackhole	Blackhole + Random jammer	Blackhole + Reactive jammer
M02 - No. of routing entries	0.90	0.87	0.77	0.82	0.87	0.85
M01 - No. of direct neighbors	0.92	0.78	0.71	0.81	0.76	0.79

Table A.57: Detection rates mesh metrics - delayed attacker - final testbeds

Metric	Constant jammer	Random jammer	Reactive jammer	Blackhole	Blackhole + Random jammer	Blackhole + Reactive jammer
M02 - No. of routing entries	0.93	0.84	0.74	0.80	0.88	0.74
M01 - No. of direct neighbors	0.92	0.78	0.79	0.76	0.73	0.72

A.1.3 *Logistic Regression Results for the Final Testbeds, All Nodes*

Table A.58: Most often used basic metrics in models created for all nodes in the final testbeds

Metric	Occurences (%)
B06 - NET sent pkts	91.9
B07 - NET received pkts	90.8
B01 - RSSI	83.9
B14 - MCU load	82.7
B08 - MAC sent pkts	82.4
B04 - Transmit duty cycle	81.6
B11 - Radio energy	80.4
B09 - MAC received pkts	78.1
B13 - MCU energy	77.0
B10 - Invalid CRC	75.8
B18 - Too long pkts	74.7
B05 - Listen duty cycle	74.3
B15 - Contention drop	73.5
B12 - Radio load	67.8
B16 - Pending pkts	67.4
B03 - Listen time	62.0
B02 - Transmit time	61.7
B17 - Too short pkts	31.0

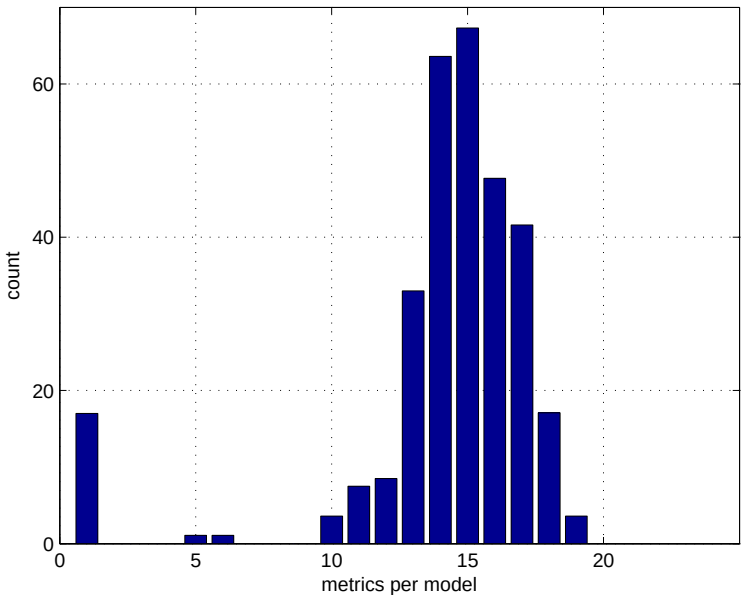

Figure A.1: Count of metrics used in each model created for all nodes using basic metrics in the final testbeds

Table A.59: Model quality - all nodes - basic metrics - final testbeds

		Mesh Count	Percent	CTP Count	Percent
JammingCnst	Bad model	6	0.188	8	0.250
	Acceptable model	2	0.063	5	0.156
	Perfect model	24	0.750	19	0.594
	Sum usable models	26	0.813	24	0.750
JammingRnd	Bad model	12	0.375	17	0.531
	Acceptable model	15	0.469	10	0.313
	Perfect model	5	0.156	5	0.156
	Sum usable models	20	0.625	15	0.469
JammingReact	Bad model	25	0.781	32	1.000
	Acceptable model	3	0.094	0	0.000
	Perfect model	4	0.125	0	0.000
	Sum usable models	7	0.219	0	0.000
SingleBlackhole	Bad model	28	0.875	31	0.969
	Acceptable model	0	0.000	1	0.031
	Perfect model	4	0.125	0	0.000
	Sum usable models	4	0.125	1	0.031
BlackholeReactJamming	Bad model	14	0.875	14	0.875
	Acceptable model	0	0.000	2	0.125
	Perfect model	2	0.125	0	0.000
	Sum usable models	2	0.125	2	0.125
BlackholeRndJamming	Bad model	6	0.375	11	0.688
	Acceptable model	0	0.000	5	0.313
	Perfect model	10	0.625	0	0.000
	Sum usable models	10	0.625	5	0.313

Table A.60: Most often used CTP metrics in models created for all nodes in the final testbeds

Metric	Occurences (%)
B07 - NET received pkts	91.4
B06 - NET sent pkts	91.4
B08 - MAC sent pkts	82.9
B01 - RSSI	81.7
B13 - MCU energy	78.0
B11 - Radio energy	77.8
B14 - MCU load	75.6
B04 - Transmit duty cycle	75.4
B09 - MAC received pkts	74.3
B05 - Listen duty cycle	73.1
B10 - Invalid CRC	70.7
B18 - Too long pkts	69.5
B15 - Contention drop	67.0
B12 - Radio load	67.0
B03 - Listen time	63.4
B16 - Pending pkts	60.9
B02 - Transmit time	59.7
CTP12 - Number of neighbors	46.3
CTP11 - Best neighbor	46.3
CTP07 - Packet delivery rate	45.1
CTP09 - Parent congestion	43.9
CTP10 - Link estimation	43.7
CTP04 - Received ACK pkts	41.4
CTP02 - Received data pkts	41.2
CTP01 - Sent data pkts	39.0
CTP06 - Dropped pkts	38.8
CTP05 - Received duplicates	31.7
B17 - Too short pkts	28.0
CTP08 - Changing parent	26.8
CTP03 - Sent ACK pkts	1.2

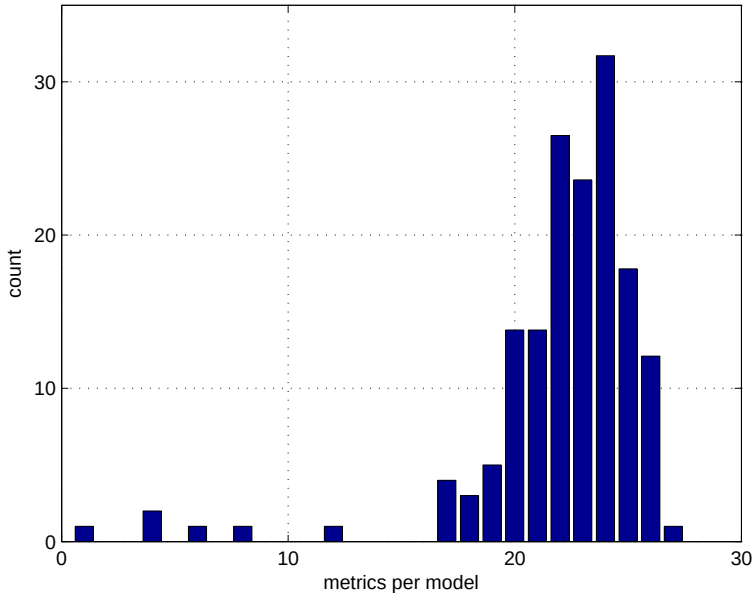

Figure A.2: Count of metrics used in each model created for all nodes using CTP metrics in the final testbeds

Table A.61: Most often used mesh metrics in models created for all nodes in the final testbeds

Metric	Occurences (%)
B07 - NET received pkts	91.5
B06 - NET sent pkts	91.5
B08 - MAC sent pkts	83.7
B01 - RSSI	81.9
B13 - MCU energy	79.5
B11 - Radio energy	79.3
B14 - MCU load	77.1
B04 - Transmit duty cycle	76.9
B09 - MAC received pkts	74.6
B05 - Listen duty cycle	73.4
B10 - Invalid CRC	72.2
B18 - Too long pkts	69.8
B15 - Contention drop	67.4
B12 - Radio load	67.4
B03 - Listen time	63.8
B16 - Pending pkts	61.4
B02 - Transmit time	60.2
M02 - No. of routing entries	42.1
M01 - No. of direct neighbors	41.9
B17 - Too short pkts	28.9

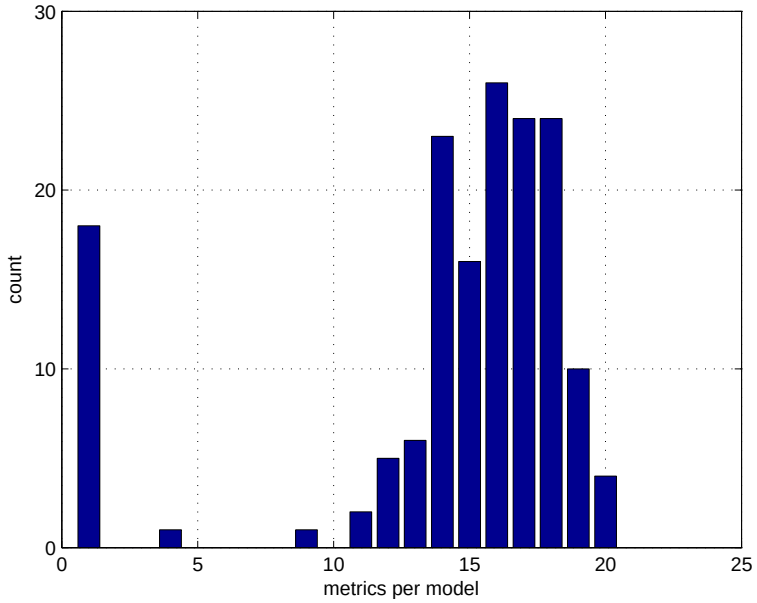

Figure A.3: Count of metrics used in each model created for all nodes using mesh metrics in the final testbeds

A.1.4 *Logistic Regression Results for the Final Testbeds, Neighboring Nodes*

Table A.62: Most often used basic metrics in all neighboring nodes models in the final testbeds

Metric	Occurences (%)
B06 - NET sent pkts	96.5
B07 - NET received pkts	96.0
B01 - RSSI	85.0
B08 - MAC sent pkts	83.9
B04 - Transmit duty cycle	79.3
B11 - Radio energy	78.1
B09 - MAC received pkts	77.0
B13 - MCU energy	75.8
B10 - Invalid CRC	71.2
B05 - Listen duty cycle	71.0
B15 - Contention drop	64.3
B18 - Too long pkts	64.0
B03 - Listen time	60.9
B14 - MCU load	56.8
B12 - Radio load	55.1
B02 - Transmit time	55.1
B16 - Pending pkts	51.7
B17 - Too short pkts	28.7

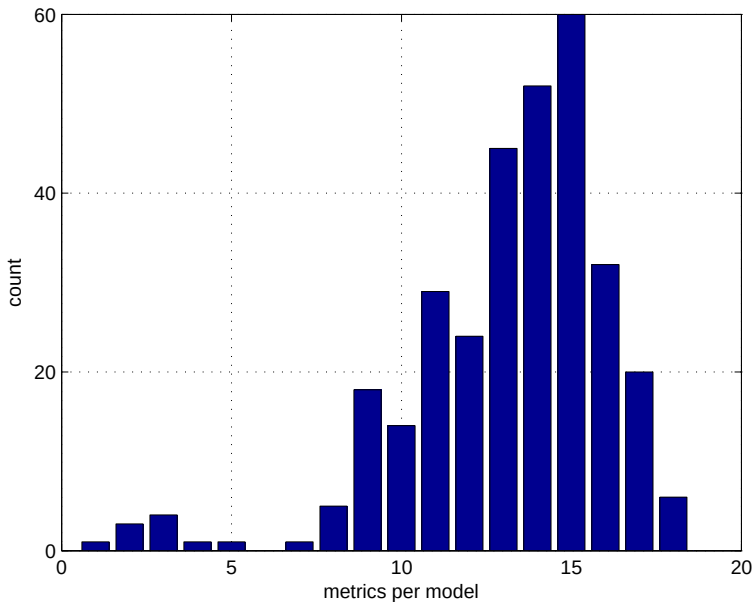

Figure A.4: Count of metrics used in each model created for all neighboring nodes using basic metrics in the final testbeds

Table A.63: Most often used CTP metrics in all neighboring nodes models in the final testbeds

Metric	Occurences (%)
B06 - NET sent pkts	89.5
B07 - NET received pkts	88.3
B08 - MAC sent pkts	78.5
B01 - RSSI	78.5
B04 - Transmit duty cycle	73.6
B11 - Radio energy	72.3
B09 - MAC received pkts	68.7
B13 - MCU energy	67.4
B05 - Listen duty cycle	66.2
B14 - MCU load	61.3
B10 - Invalid CRC	61.0
B18 - Too long pkts	58.8
B02 - Transmit time	55.2
B15 - Contention drop	53.9
B12 - Radio load	53.7
B03 - Listen time	53.5
CTP12 - Number of neighbors	44.1
B16 - Pending pkts	43.9
CTP11 - Best neighbor	42.9
CTP10 - Link estimation	42.9
CTP07 - Packet delivery rate	40.4
CTP09 - Parent congestion	38.0
CTP04 - Received ACK pkts	35.5
CTP02 - Received data pkts	33.1
CTP01 - Sent data pkts	29.4
CTP06 - Dropped pkts	29.1
B17 - Too short pkts	24.5
CTP05 - Received duplicates	23.3
CTP08 - Changing parent	18.4
CTP03 - Sent ACK pkts	0.1

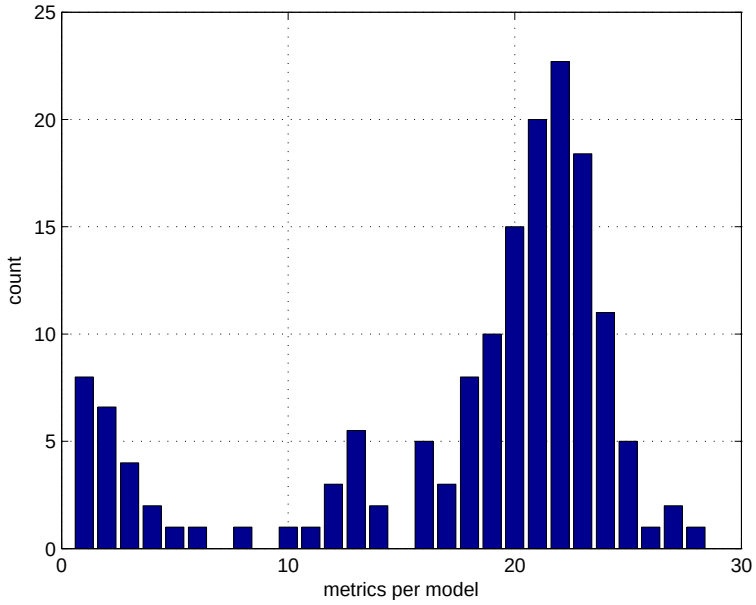

Figure A.5: Count of metrics used in each model created for all neighboring nodes using CTP metrics in the final testbeds

Table A.64: Most often used mesh metrics in all neighboring nodes models in the final testbeds

Metric	Occurences (%)
B06 - NET sent pkts	90.3
B07 - NET received pkts	87.9
B08 - MAC sent pkts	78.3
B01 - RSSI	78.3
B04 - Transmit duty cycle	73.4
B11 - Radio energy	73.0
B09 - MAC received pkts	68.6
B13 - MCU energy	67.4
B05 - Listen duty cycle	66.2
B14 - MCU load	61.4
B10 - Invalid CRC	61.2
B18 - Too long pkts	59.0
B02 - Transmit time	55.4
B15 - Contention drop	54.4
B12 - Radio load	54.2
B03 - Listen time	53.0
M02 - No. of routing entries	45.7
B16 - Pending pkts	43.3
M01 - No. of direct neighbors	43.1
B17 - Too short pkts	24.0

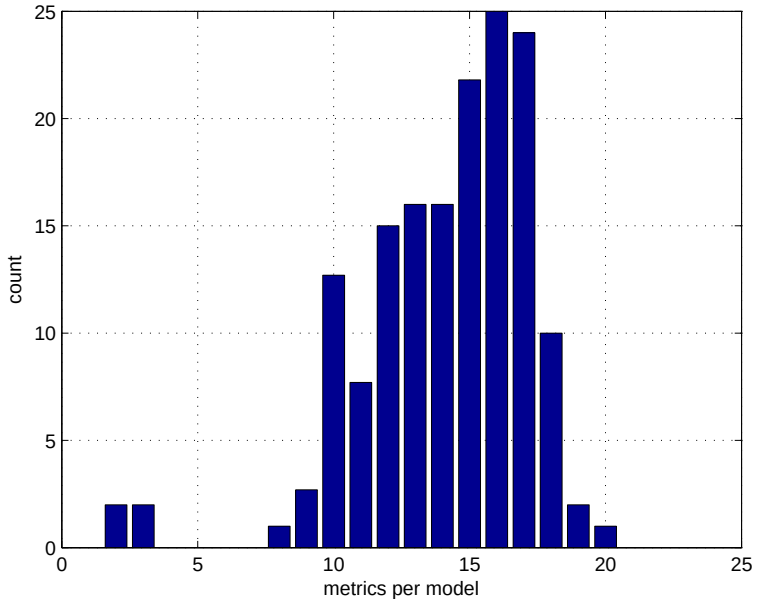

Figure A.6: Count of metrics used in each model created for all neighboring nodes using mesh metrics in the final testbeds

A.2 SUPPLEMENTARY RESULTS FOR CHAPTER 5

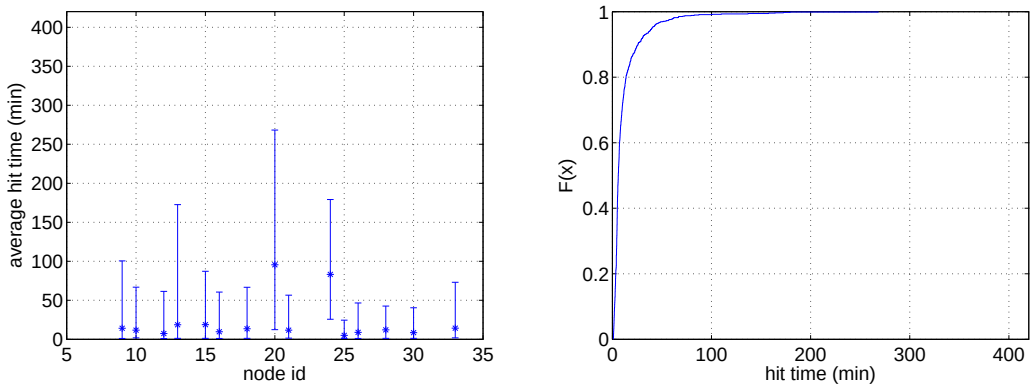

Figure A.7: Average hitting times and CDFs for the random sending (2 tokens)

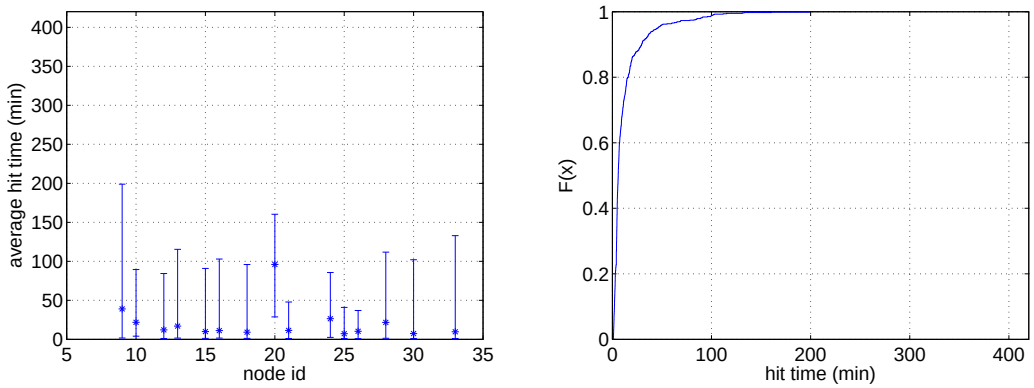

Figure A.8: Average hitting times and CDFs for the uniform sending (2 tokens)

B

CURRICULUM VITÆ

PERSONAL DETAILS

Name	Michael Riecker
Date of Birth	26 March 1982
Place of Birth	Heilbronn, Germany
Nationality	German

EDUCATION

since 07/2010	Technische Universität Darmstadt, Darmstadt, Germany Doctoral candidate at the Department of Computer Science
03/2007 – 08/2007	Eidgenössische Technische Hochschule Zürich, Switzerland Guest student with a focus on IT Security
10/2002 – 03/2009	University of Mannheim, Germany Studies of Business Informatics Degree: Diplom-Wirtschaftsinformatiker (Dipl.-Wirt.-Inf.), M. Sc. equivalent
08/1992 – 06/2001	Elly-Heuss-Knapp-Gymnasium Heilbronn, Germany Degree: Allgemeine Hochschulreife (Abitur)

WORK EXPERIENCE

since 07/2010	Technische Universität Darmstadt, Darmstadt, Germany Research associate at the Secure Mobile Networking Lab and at the Center for Advanced Security Research Darmstadt
04/2009 – 06/2010	Protiviti GmbH, Frankfurt, Germany IT Consultant
10/2007 – 07/2008	SAP Deutschland AG & Co. KG, Walldorf, Germany Working student in the area consulting public sector
09/2006 – 02/2007	PricewaterhouseCoopers AG WPG, Stuttgart, Germany Internship in the area process assurance
03/2004 – 09/2005	University of Mannheim, Germany Student assistant for computer and network administration
12/2001 – 09/2002	Klinikum Heilbronn, Germany Community service at the hospital of Heilbronn

TEACHING ACTIVITIES

since 07/2010	Technische Universität Darmstadt, Darmstadt, Germany Teaching assistant for the lecture “Network Security”

since 07/2010	Technische Universität Darmstadt, Darmstadt, Germany Coordinator of the seminar "Selected Topics in Network Security"
since 07/2010	Technische Universität Darmstadt, Darmstadt, Germany Tutor for various Bachelor and Master theses as well as seminars and lab exercises

Darmstadt, 11 May 2015

C

AUTHOR'S PUBLICATIONS

MAIN PUBLICATIONS

1. Michael Riecker, Dingwen Yuan, Rachid El Bansarkhani, Matthias Hollick. Patrolling Wireless Sensor Networks: Randomized Intrusion Detection. In *Proceedings of the 10th ACM International Symposium on QoS and Security for Wireless and Mobile Networks (Q2SWinet)*, 2014.

2. Michael Riecker, Daniel Thies, Matthias Hollick. Measuring the Impact of Denial-of-Service Attacks on Wireless Sensor Networks. In *Proceedings of the 39th IEEE Conference on Local Computer Networks (LCN)*, 2014.

3. Michael Riecker, Sebastian Biedermann, Rachid El Bansarkhani, Matthias Hollick. Lightweight Energy Consumption Based Intrusion Detection System for Wireless Sensor Networks (Extended version of ACM SAC 2013 paper). In *International Journal of Information Security, Volume 14, Issue 2, pages 155–167*, 2015.

4. Michael Riecker, Matthias Hollick. Weniger ist Mehr: Leichtgewichtige Metriken zur Erkennung von Denial-of-Service Angriffen in Drahtlosen Sensornetzen. In *Proceedings of the 12th GI/ITG KuVS Fachgespräch Drahtlose Sensornetze (FGSN)*, 2013.

5. Michael Riecker, Sebastian Biedermann, Matthias Hollick. Lightweight Energy Consumption Based Intrusion Detection System for Wireless Sensor Networks. In *Proceedings of the 28th ACM Symposium On Applied Computing (SAC)*, 2013.

6. Michael Riecker, Ana Barroso, Matthias Hollick, Sebastian Biedermann. On Data-centric Intrusion Detection in Wireless Sensor Networks. In *Proceedings of the IEEE International Conference on Cyber, Physical and Social Computing (CPSCom)*, 2012.

7. Michael Riecker, Rainer Thome, Dingwen Yuan, Matthias Hollick. A Secure Monitoring and Control System for Wireless Sensor Networks. In *Proceedings of the 37th IEEE Conference on Local Computer Networks (LCN)*, 2012.

8. Michael Riecker, Ana Barroso, Matthias Hollick. It's the Data that Matters! On the Detection of False Data in Wireless Sensor Networks. In *Proceedings of the 6th Essener Workshop "Neue Herausforderungen in der Netzsicherheit"*, 2012.

9. Michael Riecker, Walther Müller, Matthias Hollick, Karsten Saller. A Secure Monitoring and Control System for Wireless Sensor Networks. In *Proceedings of the 10th GI/ITG KuVS Fachgespräch Drahtlose Sensornetze (FGSN)*, 2011.

CO-AUTHORED PUBLICATIONS

1. Dingwen Yuan, Michael Riecker, Matthias Hollick. Making 'Glossy' Networks Sparkle: Exploiting Concurrent Transmissions for Energy Efficient, Reliable, Ultra-low Latency Communication in Wireless Control Networks. In *Proceedings of the 11th European Conference on Wireless Sensor Networks (EWSN)*, 2014.

2. Dingwen Yuan, Michael Riecker, Matthias Hollick. HOPSCOTCH: An Adaptive and Distributed Channel Hopping Technique for Interference Avoidance in Wireless Sensor Networks. In *Proceedings of the 37th IEEE Conference on Local Computer Networks (LCN)*, 2012.

D

ERKLÄRUNG LAUT §9 DER PROMOTIONSORDNUNG

Ich versichere hiermit, dass ich die vorliegende Dissertation selbständig und nur unter Verwendung der angegebenen Quellen und Hilfsmitteln verfasst habe. Alle Stellen, die aus Quellen entnommen wurden, sind als solche kenntlich gemacht. Die Arbeit hat in gleicher oder ähnlicher Form noch nicht zu Prüfungszwecken gedient.

Darmstadt, 11. Mai 2015

Dipl.-Wirt.-Inf. Michael Riecker